ADVANCES IN APPLIED MECHANICS

VOLUME I

ADVANCES IN APPLIED MECHANICS

EDITED BY

RICHARD VON MISES
Harvard University
Cambridge, Massachusetts

THEODORE VON KÁRMÁN
California Institute of Technology
Pasadena, California

VOLUME I

1948

ACADEMIC PRESS INC., PUBLISHERS
NEW YORK, N. Y.

ACADEMIC PRESS INC.
111 FIFTH AVENUE
NEW YORK, NEW YORK 10003

United Kingdom Edition
Published by
ACADEMIC PRESS INC. (LONDON) LTD.
BERKELEY SQUARE HOUSE, LONDON W. 1

First Printing, 1948
Second Printing, 1964

PREFACE

The plan of publishing "Advances in Applied Mechanics" was conceived as early as 1940. Wartime conditions, in particular the fact that most of the pertinent subjects were more or less connected with classified material, made it necessary to postpone the whole matter. When the war was over and declassification took place gradually, shortages in printing facilities caused further delay.

The book is intended for students, scholars, and engineers who are familiar with the contents of textbooks and handbooks but are unable to follow up all the research papers currently published in periodicals and institutional reports. Perhaps the research worker will not need our surveys in the proper field in which he is himself active, but he might be interested in summaries of related topics. It is a well-known fact that the more research in mechanics expands, the more interconnections of seemingly far distant fields become apparent.

The present volume might be considered as indicative of the topics to be dealt with in future issues and as an example for the diversified kinds of approach we wish to cultivate. In both respects, however, the Editors reserve a certain freedom of choice. Suggestions are invited and the offering of contributions will be appreciated.

TH. V. KÁRMÁN
R. V. MISES

CONTENTS

On Numerical Methods in Wave Interaction Problems

By Hilda Geiringer, *Wheaton College, Norton, Massachusetts*

On Bergman's Integration Method in Two-Dimensional Compressible Fluid Flow

By R. v. Mises and M. Schiffer, *Harvard University, Cambridge, Massachusetts*

Recent Advances in the Mechanics of Boundary Layer Flow

By HUGH L. DRYDEN[1]

National Bureau of Standards

CONTENTS

NOTATION

l = length
m = parameter in velocity distribution $U = kx^m$
p = static pressure
r = radius of curvature of surface
u = local mean velocity, always parallel to surface
u' = root mean square component of turbulent velocity fluctuation parallel to the surface and to the mean flow
v' = root mean square component of turbulent velocity fluctuation normal to the mean flow and to the surface
w' = root mean square component of turbulent velocity fluctuation normal to the mean flow but parallel to the surface
x = distance along surface from leading edge
x_t = distance from leading edge to transition point
y = distance normal to the surface

[1] Now Director of Aeronautical Research, National Advisory Committee for Aeronautics.

z = Mangler parameter $U\delta^2/\nu l$

$C_\tau = \tau/\frac{1}{2}\rho U^2$, coefficient of turbulent shearing stress based on U

$C_{\tau_0} = \tau/\frac{1}{2}\rho U_0^2$, coefficient of turbulent shearing stress based on U_0

D = reference dimension of body, diameter of sphere, minor axis of elliptical cylinder

$H = \delta^*/\theta$, a parameter describing turbulent velocity distribution in boundary layers with pressure gradient

L = scale of turbulence, defined as the integral of the correlation coefficient between longitudinal velocity fluctuations at points at distance y apart in a direction transverse to the flow for y varying from zero to infinity

$R = U\delta^*/\nu$, Reynolds number based on displacement thickness

R_c = critical Reynolds number below which all oscillations in a laminar boundary layer are damped

$R_{CRIT} = UD/\nu$, critical Reynolds number of a sphere, *i.e.* that for which the drag coefficient is 0.3

$R_\theta = \dfrac{U\theta}{\nu}$, Reynolds number based on momentum thickness

U = mean speed in free stream just outside boundary layer, usually varying with x

$U' = \dfrac{dU}{dx}$

U_0 = reference speed at fixed point; for National Bureau of Standards turbulent boundary layer at $x = 17$ ft

V_0 = suction velocity normal to wall in boundary layer suction through a porous wall

α = 2π times wave length of oscillation; also angle of principal axis of turbulent stress tensor to flow direction

β = Hartree parameter in velocity distribution $U = kx^m$, equal to $2m/(1 + m)$

β_r = 2π times frequency of oscillation

β_i = amplification coefficient

δ = boundary layer thickness; if otherwise unspecified, that of the Pohlhausen four-term approximation

δ^* = displacement thickness of boundary layer = $\displaystyle\int_0^\infty \left(1 - \frac{u}{U}\right) dy$

θ = momentum thickness of boundary layer = $\displaystyle\int_0^\infty \frac{u}{U}\left(1 - \frac{u}{U}\right) dy$

λ = Pohlhausen parameter $U'\delta^2/\nu$ for four-term approximation

λ_{P6} = Pohlhausen parameter λ for six-term approximation

μ = viscosity of fluid

ρ = density of fluid

$\nu = \mu/\rho$, kinematic viscosity of fluid

τ = turbulent shearing stress, at x, y

τ_w = turbulent shearing stress at the wall

I. Introduction

In 1904 L. Prandtl proposed the concept of a boundary layer near the surface of a body moving through a fluid, a region of comparatively small

thickness within which the viscous forces are comparable to the inertial forces and within which the relative speed between the body and the fluid decreases rapidly to zero. He derived the equations of flow in the boundary layer from the Navier-Stokes equations, and his pupil, Blasius, in 1908 obtained their solution for the special case of flow along a thin flat plate parallel to the direction of flow in an airstream of uniform speed. The theory gave both the skin friction and the velocity distribution within the layer. While experimental data on skin friction were available at that time, experimental observations on the velocity distribution were first made by Burgers and van der Hegge Zijnen in 1925.

Comparisons of skin friction data soon showed certain discrepancies and it became clear that the boundary layer flow did not always conform to the Prandtl equations. It had been known since the work of Osborne Reynolds that flow in a pipe did not always correspond to the usual solution of the Navier-Stokes equations, a type of flow usually designated *laminar flow*. The pipe flow was often turbulent. The flow in a boundary layer may likewise be laminar or turbulent; and although this was at first a mere hypothesis, it has since been abundantly confirmed.

This concept of Prandtl has been extraordinarily fruitful in the development of fluid mechanics. Many puzzling phenomena have been clarified by a study of the nature of the flow within the boundary layer and its effect on the general flow around the body. Scale effect in aerodynamic measurements, the effect of wind tunnel turbulence, flow separation phenomena, minimum drag and maximum lift, can be understood and treated, at least qualitatively if not always quantitatively, by consideration of the boundary layer flow. Even at high speeds near the speed of sound it appears that the general flow pattern and location of shock waves are dependent on the type of flow in the boundary layer.

The last extensive review of the mechanics of boundary layer flow published in the English language was contained in the book *Modern Developments in Fluid Dynamics* by S. Goldstein and others (Oxford, 1938). German periodicals now available refer to a series of lectures by H. Schlichting on boundary layer theory published in 1942 but this document of 279 pages with 116 figures is not yet generally available in this country. The present report is an attempt to summarize or give references to some of the more important papers published since 1936 that may contribute to a better understanding of the mechanics of boundary layer flow. Most of the work cited relates to incompressible flow although references are given to such papers as are available on compressible flow. Because of the current difficulties in covering the literature of the world, this survey is of necessity incomplete.

II. Laminar Flow in Boundary Layers

The problems of laminar flow in boundary layers are largely mathematical problems, since it is certain that the fundamental mechanical principles are fully understood and that the equations adequately describe the phenomena when the flow may be regarded as incompressible. A bibliography of papers on this subject during the decade 1936–1946 that have come to the author's attention is given at the end of this section. Only a few highlights will be discussed, since the developments follow the same general methods of attack as those described in *Modern Developments in Fluid Dynamics.*

H. Schmidt and K. Schröder (33,34) have attempted to clarify the boundary layer theory and make it more precise from the mathematical point of view. The discussion is limited to two-dimensional flow and does not attempt to deal with the question of proving the existence or uniqueness of the solution. The papers thus become descriptions of the boundary layer that are intellectually satisfying to the mathematician because they are stated in the language of limits and inequalities.

The principal problem of the theory of the laminar boundary layer is the calculation of the flow for a given pressure distribution and, as in the past, most of the work accomplished has been limited to two-dimensional flow. The problem becomes especially difficult in a region of adverse pressure gradient as the position of separation is approached. The method of expansion in series is not practicable, step-by-step methods are extremely laborious, and the results obtained from application of the momentum equation to assumed families of velocity distributions are unreliable. The method of Kármán and Millikan has been frequently used (6) but is known to be subject to some error.

The application of the momentum equation to assumed families of velocity distributions as first carried out by Pohlhausen remains popular, and many variations in detail have been proposed, in spite of the fact that von Mises demonstrated long ago that accurate values of laminar skin friction can not be determined by this method. The method is useful in giving at least a general picture of the variation of the thickness of the laminar boundary layer provided the point of separation is not approached too closely. As an example of one type of variation of procedure, Mangler (24) uses the momentum equation as an integral equation for the quantity $z = U\delta^2/\nu l$ rather than as a differential equation for the parameter $\lambda = U'\delta^2/\nu$. Many types of nomograms have been constructed to facilitate the solution by this general method.

Further study has been made of the so-called "similar" solutions (4,13,40,43) of the boundary layer equations for which the partial dif-

ferential equations reduce to a single ordinary differential equation. These solutions can occur only if the distribution of velocity outside the boundary layer is proportional to a power of the distance x along the wall or to c^x. Mangler (40) discusses these solutions at some length, giving the body shapes for which such distributions occur and investigating the asymptotic behavior of the solutions at the outer boundary. The physically meaningful solutions can be distinguished among the solutions satisfying the boundary conditions by the fact that the displacement thickness remains finite and the velocity in the boundary layer remains smaller than that outside.

Discussion of the work done on laminar boundary layers along porous or slotted walls with suction or pressure is postponed to a later section.

Very little additional work has been done during the last decade on three-dimensional problems. There are several papers on the axially symmetric problems for bodies of revolution (16,26,30,36), the paper of Burgers (20) on flows with a rotational component, and papers on flow toward a plane surface (37) and flow in a corner (45). It is understood that the Göttingen group have succeeded in showing that the differential equation for the axially symmetric case can be reduced to the differential equation of the two-dimensional boundary layer by a simple transformation but details are not available. The same group had in progress the behavior of a boundary layer under the influence of a pressure gradient transverse to the flow direction.

There are several papers listed on the effects of compressibility on laminar boundary layer flow (7,17,21,22,27,28). At supersonic speeds the aerodynamic and thermodynamic problems become intertwined and the thermal environment becomes of great importance. The papers of Ackeret, Feldmann, and Rott (42) and of Liepmann (44) are of great importance as demonstrating the influence of the state of the boundary layer flow on the general flow pattern and as indicating the breakdown of the usual assumption of the boundary layer theory that the pressure differences across the layer may be neglected.

Bibliography
on
Laminar Flow in Boundary Layers

1. Blaisdell, A. H., Boundary layer flow over flat and concave surfaces, *A.S.M.E. Trans.*, **58**, 343–348 (1936).
2. Homann, F., Der Einfluss grosser Zähigkeit bei der Strömung um den Zylinder und um die Kugel, *Z. angew. Math. Mech.*, **16**, 153–164 (1936).
3. Howarth, L., Velocity and temperature distribution for a flow along a flat plate, *Proc. Roy. Soc. (London)*, *A*, **154**, 364–377 (1936).

4. HARTREE, D. R., On an equation occurring in Falkner and Skan's approximate treatment of the equations of the boundary layer, *Proc. Cambridge Phil. Soc.*, **33**, 223–239 (1937).
5. SUTTON, W. G. L., Approximate solution of the boundary layer equation for a flat plate, *Phil. Mag.*, **23**, 1146–1152 (1937).
6. VON DOENHOFF, A. E., A method of rapidly estimating the position of the laminar separation point, *N.A.C.A. Tech. Note* **671** (1938).
7. VON KÁRMÁN, T., and TSIEN, H. S., Boundary layer in compressible fluids, *J. Aeronaut. Sci.*, **5**, 227–232 (1938).
8. HOWARTH, L., Solution of the laminar boundary layer equation, *Proc. Roy. Soc. (London), A*, **164**, 547–579 (1938).
9. MILLS, R. H., A note on some accelerated boundary layer velocity profiles, *J. Aeronaut. Sci.*, **5**, 325–327 (1938).
10. PRANDTL, L., Zur Berechnung der Grenzschichten, *Z. angew. Math. Mech.*, **18**, 77–82, 1938; also *N.A.C.A. Tech. Memo.* **959** (1940); also *J. Roy. Aeronaut. Soc.*, **44**, 795–801 (1940).
11. GÖRTLER, H., Weiterentwicklung eines Grenzschichtprofils bei gegebenem Druckverlauf, *Z. angew. Math. Mech.*, **19**, 129–140 (1939); also *J. Roy. Aeronaut. Soc.*, **45**, 35–40 (1941).
12. FALKNER, V. M., A further investigation of solutions of the boundary layer equations, *Brit. A.R.C., Repts. and Memo.* No. **1884** (1939).
13. GOLDSTEIN, S., A note on the boundary layer equations, *Proc. Cambridge Phil. Soc.*, **35**, 338–340 (1939).
14. SAKURAI, T., New method of evaluating the flow in boundary layer which varies with time, *Proc. Phys.-Math. Soc. Japan*, **21**, 632–637 (1939).
15. SAKURAI, T., Two-dimensional boundary layer equations for motion of viscous fluids near moving obstacles, *Proc. Phys.-Math. Soc. Japan*, **21**, 707–712 (1939).
16. FRÖSSLING, N., Verdunstung, Wärmeübergang und Geschwindigkeitsverteilung bei zweidimensionaler und rotationssymmetrischer laminarer Grenzschichtströmung, *Lunds Univ. Årsskr.* N.F. Avd 2, **36** (1940).
17. HANTZSCHE, W., and WENDT, H., Zum Kompressibilitäts-Einfluss bei der laminaren Grenzschicht der ebenen Platte. *Jahrb. deut. Luftfahrtforsch.*, **1940**, p. 517.
18. WADA, K., Theory of laminar boundary layer, *Rept. Aeronaut. Research Inst. Tokyo Imp. Univ.*, **196** (Sept. 1940).
19. FALKNER, V. M., Simplified calculation of the laminar boundary layer, *Brit. A.R.C., Repts. and Memo.* No. **1895** (1941).
20. BURGERS, J. M., Some considerations on the development of boundary layers in the case of flows having a rotational component, *Proc. Koninkl. Nederland. Akad. Wetensch.*, **44**, 13–25 (1941).
21. EMMONS, H. W., and BRAINERD, J. G., Temperature effects in a laminar compressible fluid boundary layer along a flat plate, *J. Applied Mechanics*, **8**, A105–A110 (1941).
22. HANTZSCHE, W., and WENDT, H., Die laminare Grenzschicht bei einem mit Überschallgeschwindigkeit angeströmten nichtangestellten Kreiskegel, *Jahrb. deut. Luftfahrtforsch.*, **1941**, Vol. I, 76.
23. LOITSIANSKII, L. G., Integral methods in the theory of the boundary layer, *Applied Math. and Mechanics U.R.S.S.*, **5**, 453–470 (1941); also *N.A.C.A. Tech. Memo.* No. **1070** (1944).
24. MANGLER, W., Eine Vereinfachung des Pohlhausen-Verfahrens zur Berechnung

der laminaren Reibungsschicht, *Jahrb. deut. Luftfahrtforsch.*, 1941, Vol. I, 18–20.

25. Preston, J. H., Note on the method of successive approximations for the solution of the boundary layer equations, *Phil. Mag.* [7] 31, 452–465 (1941).
26. Pretsch, Die laminare Reibungsschicht an elliptischen Zylindern und Rotationsellipsoiden bei symmetrischer Umströmung, *Luftfahrtforsch.*, 18, 397 (1941).
27. Brainerd, J. G., and Emmons, H. W., Effect of variable viscosity on boundary layers, with a discussion of drag measurements, *J. Applied Mechanics*, 9, A1–A6, (1942).
28. Dorodnitzyn, A., Laminar boundary layer in compressible fluids, *Compt. rend. acad. sci. U.R.S.S.*, 34, 213–219 (1942).
29. Loitsianskii, L. G., Approximate method for calculating the laminar boundary layer on an airfoil, *Compt. rend. acad. sci. U.R.S.S.*, 35, 227–232 (1942).
30. Loitsianskii, L. G., Laminar boundary layer on a body of revolution, *Compt. rend. acad. sci. U.R.S.S.*, 36, 166–168 (1942).
31. Kochin, N. E., and Loitsianskii, L. G., An approximate method of calculating the laminar boundary layer, *Compt. rend. acad. sci. U.R.S.S.*, 36, 262–266 (1942).
32. Piskunov, N. S., On the problem of flow separation in a viscous fluid, *Compt. rend. acad. sci. U.R.S.S.*, 37, 345 (1942).
33. Schmidt, H., and Schröder, K., Laminare Grenzschichte-Ein kritischer Literaturbericht, *Luftfahrtforsch.*, 19, 65–97 (1942).
34. Schmidt, H., and Schröder, K., Die Prandtlsche Grenzschichtgleichung als asymptotische Näherung der Navier-Stokesschen Differentialgleichungen bei unbegrenzt wachsender Reynoldscher Kennzahl, *Deut. Math.*, 6, 307–322 (1942).
35. Scherbarth, K., Grenzschichtmessungen hinter einer punktförmigen Störung in laminarer Strömung, *Jahrb. deut. Luftfahrtforsch.*, 1942, Vol. I, 51–53.
36. Stepanyantz, L. G., The calculation of laminar boundary layers around bodies of revolution, *Applied Math. and Mechanics U.R.S.S.*, 6, 317–326 (1942). (Russian text, English summary.)
37. Van Wijngaarden, A., Laminar flow in radial direction along a plane surface, *Proc. Koninkl. Nederland. Akad. Wetensch.*, 45, 269–275 (1942).
38. Weyl, H., On the differential equations of the simplest boundary layer problems, *Ann. Math.*, 43, 381–407 (1942).
39. Basin, A. M., A new approximate method for the calculation of laminar boundary layers, *Compt. rend. acad. sci. U.R.S.S.*, 40, 14–17 (1943).
40. Mangler, W., Die "ähnlichen" Lösungen der Prandtlschen Grenzschichtgleichungen, *Z. angew. Math. Mech.*, 23, 241–251 (1943).
41. Görtler, H., Verdrängungswirkung der laminaren Grenzschichten und Druckwiderstand, *Ing. Arch.*, 14, 286–305 (1944).
42. Ackeret, J., Feldmann, F., and Rott, N., Untersuchungen an Verdichtungsstössen und Grenzschichten in schnell bewegten Gasen, *Mitt. Inst. Aerodyn.*, E.T.H. Zürich, No. 10 (1946); also *N.A.C.A. Tech. Memo.* 1113 (1947).
43. Oldroyd, J. G., Calculations concerning theoretical values of boundary layer thickness and coefficients of friction and of heat transfer for steady two-dimensional laminar flow in an incompressible boundary layer with main stream velocity $U \sim x^m$ or $U \sim e^x$, *Phil. Mag.*, 36, 587–600 (1945).
44. Liepmann, H., The interaction between boundary layer and shock waves in transonic flow, *J. Aeronaut. Sci.*, 13, 623–638 (1946).

45. Carrier, G. F., The boundary layer in a corner, *Quart. Applied Math.*, **4**, 367 (1947).

III. Stability of Laminar Boundary Layer Flow

The circumstances surrounding the breakdown of laminar flow and the beginning, at least, of the process of transition to turbulent flow are now fully understood as a result of work completed during the last decade. It has been assumed from the time of Reynolds that the problem of the origin of turbulence is associated with or equivalent to the problem of the stability of the laminar flow. Reynolds' own experiments on flow in pipes showed that at low Reynolds numbers disturbances of any magnitude at the entrance were damped and the flow ultimately became steady. At higher Reynolds numbers the magnitude of the disturbance present at the entrance was an important factor and the flow remained steady to a Reynolds number that increased as the disturbance was reduced. In 1938 there were two schools of thought as to the nature of the instability. The one, exemplified by the theoretical workers of the Göttingen school, believed that the laminar flow was unstable for infinitesimal disturbances. The other, exemplified by experimental workers in England and America, believed that transition occurred as a result of external disturbances of finite magnitude.

1. Status of Problem in 1938

The theoretical problem of the stability of two-dimensional laminar flow was investigated by Heisenberg, Tietjens, Tollmien, and Schlichting of the Göttingen group during the period 1924–1935. The specific problem of the boundary layer near a thin flat plate without pressure gradient was attacked by Tollmien and Schlichting. The problem was idealized by assuming a layer of constant thickness within which the velocity distribution was given by an approximation to the Blasius distribution. Small periodic disturbances were assumed to be present and their subsequent history was computed. The mathematical discussion is complicated and involves a troublesome joining of solutions in the neighborhood of the point at which the wave velocity coincides with the local flow velocity. Tollmien found that unstable waves can exist if the Reynolds number formed from the free stream velocity and the displacement thickness of the boundary layer is greater than 420. Schlichting obtained a value 575 for this critical Reynolds number. At higher Reynolds numbers there is a definite locus of neutral disturbances which are neither amplified nor damped. For any given Reynolds number there are two such neutral disturbances, differing in wave length, frequency, and wave velocity. For intermediate values of wave length or frequency

or wave velocity the disturbances are amplified; for values outside these ranges, larger or smaller, the disturbances are damped.

Experimental workers could find no evidence in 1938 to support the Tollmien-Schlichting theory. Dryden and his colleagues had studied the fluctuations in the boundary layer near a plate and had not observed the unstable wave motion. They found slow fluctuations, which were interpreted as probable fluctuations in thickness of the layer forced by disturbances in the free stream. There was no evidence of shear stresses or effect of the fluctuations on the distribution of mean speed. Transition

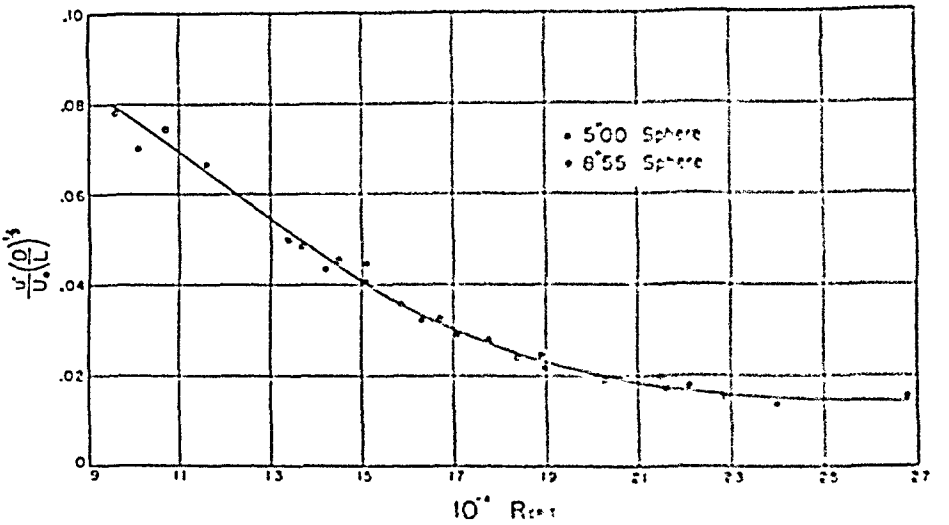

FIG. 1.—Critical Reynolds number of a sphere in air streams of different turbulence.

occurred intermittently and suddenly with no development of amplified disturbances. Experiments by the groups at the California Institute of Technology, Massachusetts Institute of Technology, and Cambridge University, England, likewise failed to show the amplified disturbances.

Not only did the experimental group obtain this negative result; their experiments confirmed a theory developed by G. I. Taylor, (84) which attributed transition to the presence of free stream turbulence. Taylor assumed that transition occurred as the result of momentary separation in regions of adverse pressure gradient associated with the free stream turbulence. The Reynolds number at transition was found to be a function of $(u'/U)(D/L)^{\frac{1}{2}}$, where u'/U is the intensity of the turbulence (u' being the root mean square speed fluctuation, U the mean speed), L is the scale of the turbulence (defined as the integral of the correlation coefficient between longitudinal velocity fluctuations at points distance y apart in a direction transverse to the flow for y varying from zero to infinity), and D is a reference dimension of the body. Figures 1 and 2

show experimental checks of this relation taken from *National Advisory Committee for Aeronautics, Technical Reports* **581** *and* **682.**

2. Observation of Tollmien-Schlichting Oscillations

These conflicting theoretical and experimental results have now been completely reconciled by the work of Schubauer and Skramstad, who first observed the Tollmien-Schlichting oscillations in 1940 in a wind tunnel at

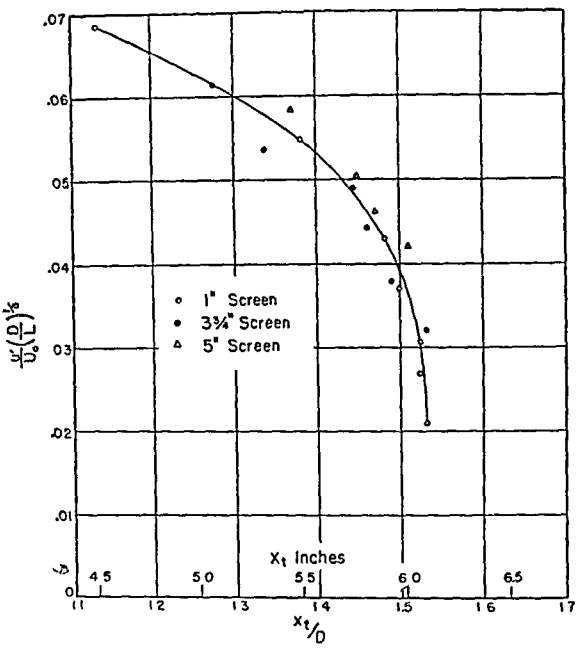

FIG. 2.—Location of transition in the boundary layer on an elliptic cylinder in air streams of different turbulence.

the National Bureau of Standards, for which the turbulence of the free stream was only 0.02 to 0.04 per cent of the mean speed. Their work is described in full in the *National Bureau of Standards Research Paper* **1772,** which is a reprint of the original N.A.C.A. advance confidential report issued in April 1943, now declassified and issued as N.A.C.A. Wartime Report W-8. When the free stream turbulence is less than about 0.1 per cent of the mean speed, transition is preceded by the Tollmien-Schlichting oscillations, and the theory is beautifully confirmed quantitatively as well as qualitatively. For ordinary wind tunnels the stream turbulence usually lies in the range 0.2 to 1.0 per cent. In these wind tunnels the turbulence is the controlling factor and the mechanism is that of the Taylor theory.

Fig. 3 shows the first record obtained by Schubauer and Skramstad

in August 1940 of the naturally occurring laminar boundary layer oscillations. After assuring themselves that the oscillations were not effects of vibration, acoustic phenomena, or other extraneous disturbance, and that the frequency did in fact agree with the value predicted by the theory, they devised an ingenious method for proceeding experimentally

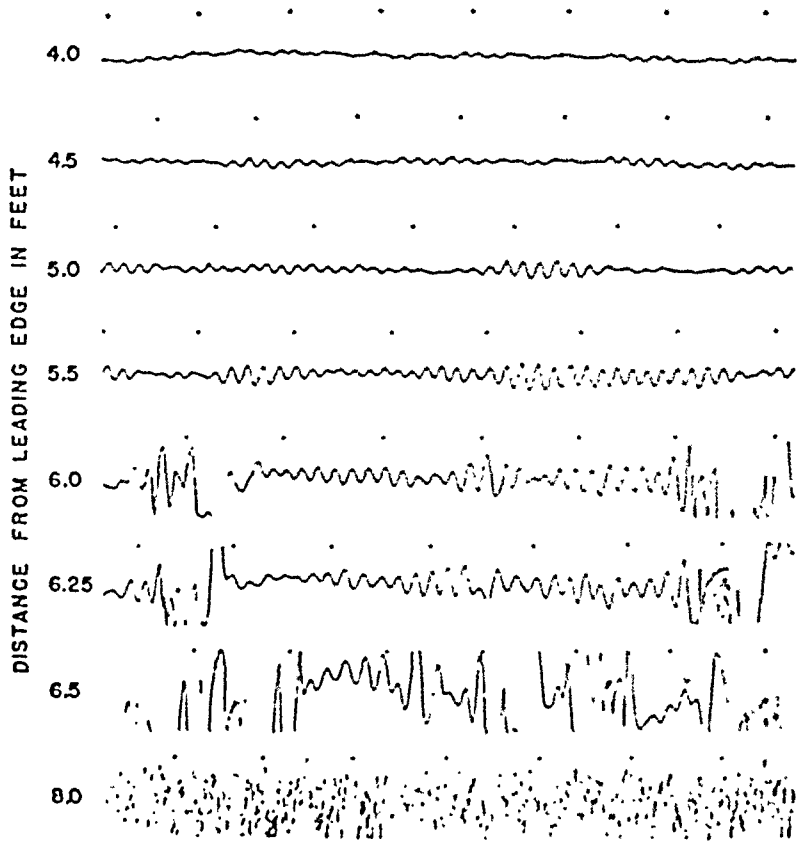

FIG. 3.—Laminar boundary layer oscillations in the boundary layer of a flat plate. Distance from surface = 0.025 inch, speed of free stream = 80 ft/sec, time interval between dots = $\frac{1}{10}$ sec.

exactly as Tollmien and Schlichting proceeded mathematically. They introduced small disturbances of known frequency by the arrangement shown in Fig. 4. An alternating current of the desired frequency was sent through a metal ribbon 0.002 inch thick placed in a magnetic field, causing it to vibrate about a mean position about 0.006 inch from the plate, the amplitude being controlled by the magnitude of the current. The resulting fluctuations in speed in the boundary layer at various distances were measured by means of a hot-wire anemometer. The procedure was repeated for several frequencies and wind speeds. From these data the damping and amplification coefficients could be determined

for disturbances of various frequencies over the range of Reynolds numbers covered, and the frequencies of the neutral oscillations, which are neither damped nor amplified, could be plotted against Reynolds number.

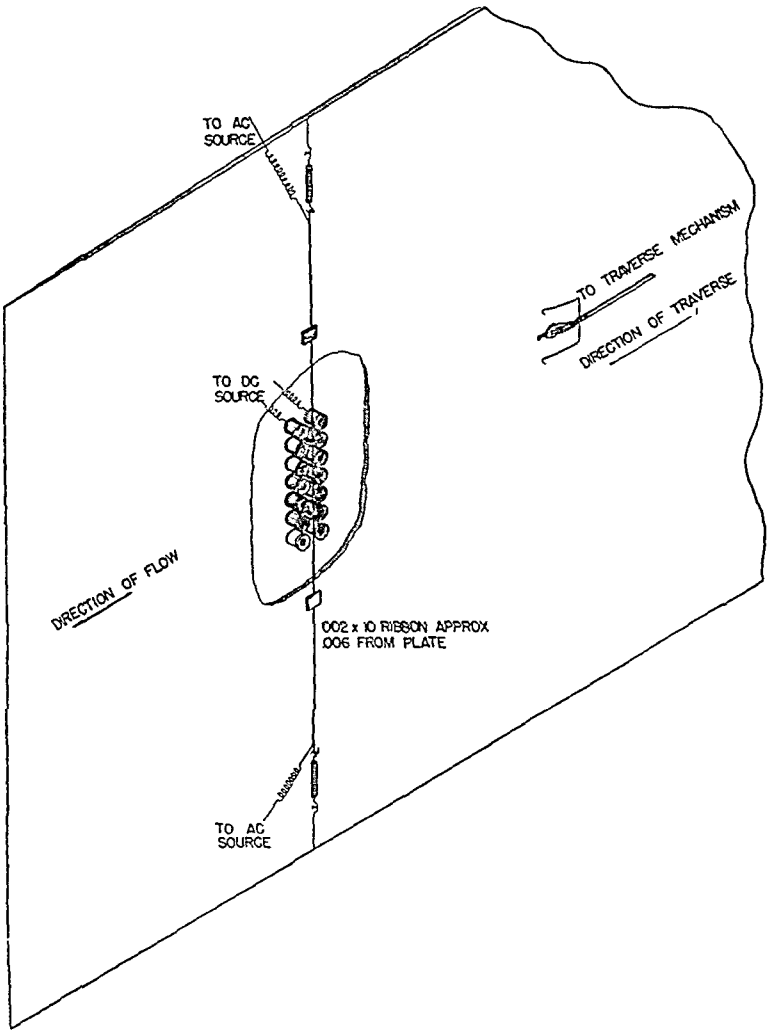

FIG. 4.—Method used by Schubauer and Skramstad to excite controlled disturbances in the laminar boundary layer of a flat plate.

The wave lengths were independently determined from the distance through which the hot-wire anemometer had to be moved to return to the same phase relationship between the observed wave and the current through the ribbon. The wave velocities were determined as the product of frequencies and corresponding wave lengths.

After the experimental work had been completed, C. C. Lin (66)

undertook a revision of the mathematical theory and a clarification of some features that had been adversely criticized. Lin's calculation gave a critical Reynolds number of 420 as compared with Tollmien's 420 and Schlichting's 575, and a slightly different locus for the neutral oscillations. Figs. 5 and 6 show the nondimensional wave length and frequency loci as observed by Schubauer and Skramstad compared with the theoretical results of Schlichting and Lin. The agreement is remarkable. Fig. 7 shows a comparison of the distribution of amplitude of the u-fluctuations

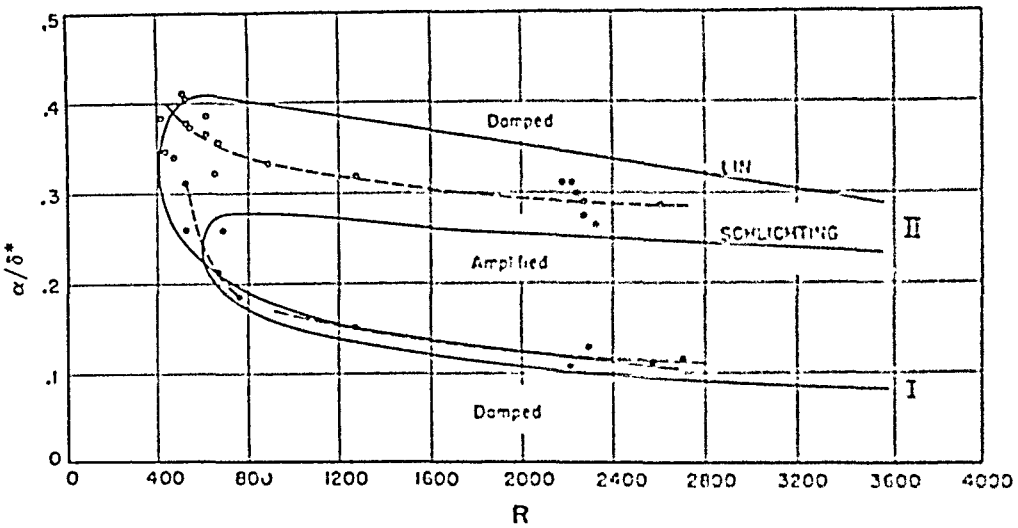

FIG. 5.—Experimentally determined wave lengths of neutral oscillations in the laminar boundary layer of a flat plate compared with the theoretical curves of Schlichting and Lin.

across the boundary layer for a particular case with the theoretical computations of Schlichting.

These experimental results were confirmed by Liepmann at the California Institute of Technology for the boundary layer on the convex side of a curved plate. Schlichting had computed the effect of convex curvature on the neutral curve and found a slightly stabilizing effect. Liepmann used the vibrating ribbon technique, acoustic excitation, and a method employing roughness elements uniformly spaced on the surface to give a disturbance of known wave length. The results were found to agree closely with those obtained at the National Bureau of Standards, the influence of convex curvature being extremely small.

An important factor in these observations is the reduction of the turbulence of the air stream to a value as low as practicable. This is accomplished by the use of damping screens as described by Dryden and Schubauer in *Journal Aeronautical Science*, 14, 221–228 (1947). At the

low levels obtained, the noise of the wind tunnel propeller produces the predominant speed fluctuation. In such a tunnel it is easy to demonstrate that sounds of the proper pitch cause an earlier breakdown of the laminar flow.

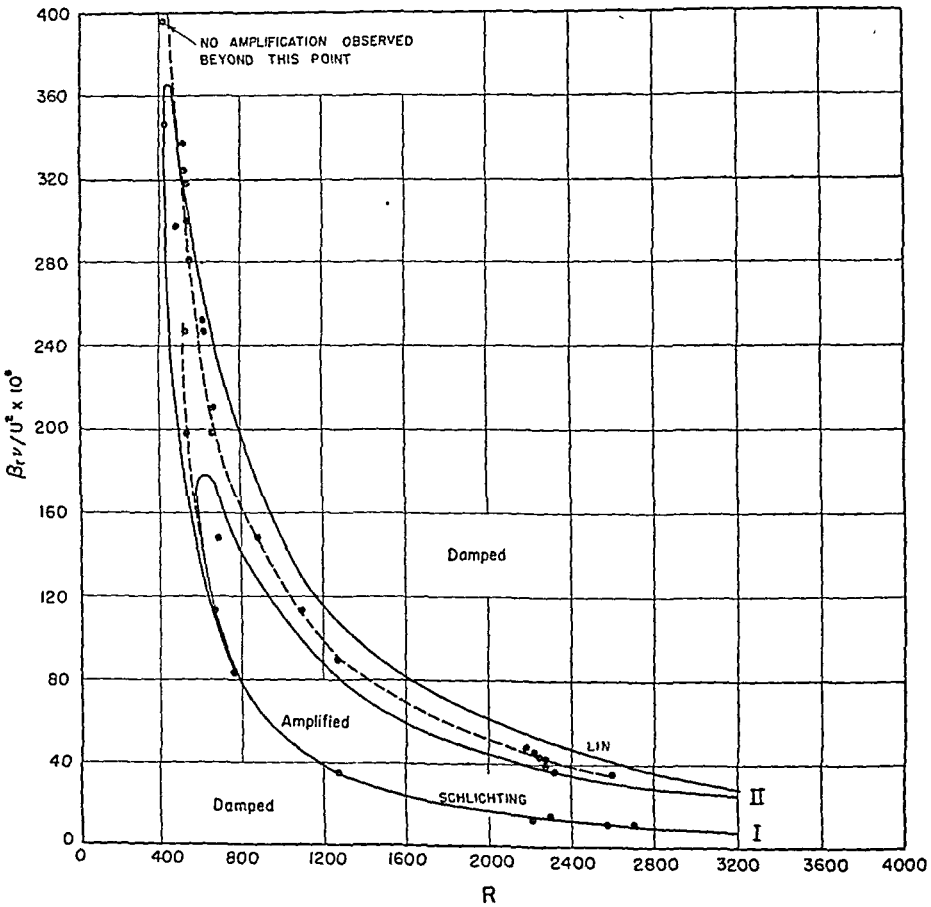

FIG. 6.—Experimentally determined frequencies of neutral oscillations in the laminar boundary layer of a flat plate compared with the theoretical curves of Schlichting and Lin.

3. *Relation of Tollmien-Schlichting Waves to Transition*

The Tollmien-Schlichting waves do not in themselves constitute turbulent flow. The regular waves grow in amplitude, become distorted, then exhibit intermittent bursts of high frequency fluctuations. At some distance from the surface the bursts usually appear in the low velocity part of the cycle and near the surface there is occasional evidence of intermittent separation. It is believed but not definitely proved that

intermittent separation produces dynamically unstable vortex sheets, which roll up into small eddies.

Thus the two originally conflicting pictures coalesce. If the free stream turbulence is greater than 0.2 per cent, intermittent separation

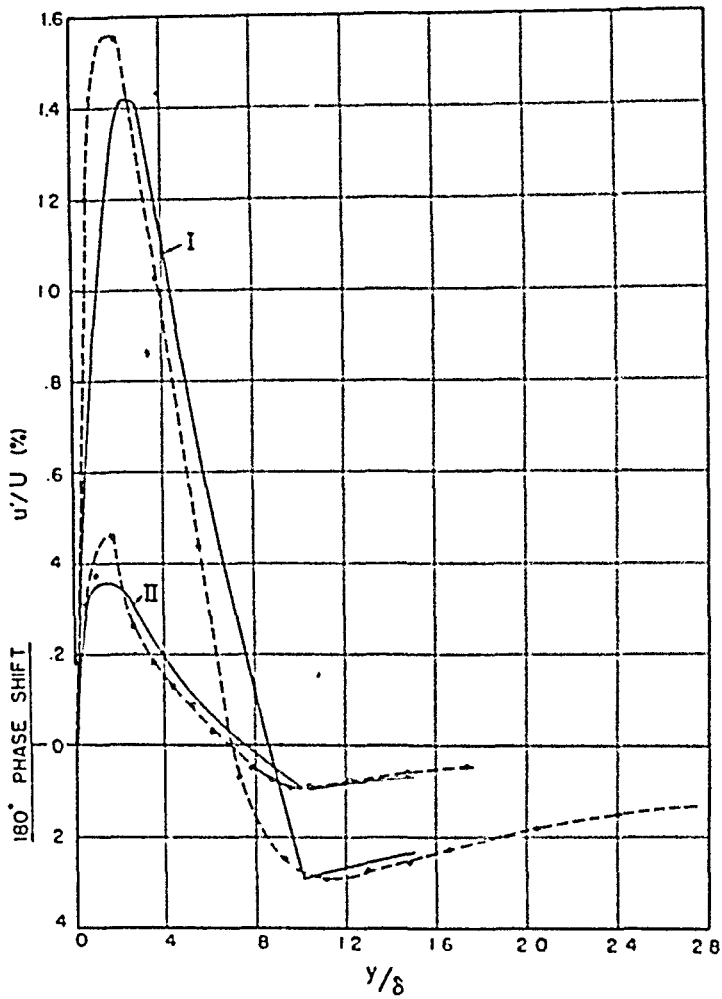

FIG. 7.—Experimental and theoretical distribution of amplitude across the boundary layer for two particular neutral oscillations computed by Schlichting. Solid curves are theoretical, broken curves with points are experimental.

occurs as soon as the Pohlhausen parameter $(\delta^2/\mu U)(dp/dx)$ reaches the appropriate value, δ being the thickness of the boundary layer, μ the viscosity of the fluid, U the free stream speed, and dp/dx the pressure gradient. For lower turbulence this step is preceded by the appearance of amplified waves. At the higher turbulence the intensity and scale of the turbulence determine transition; at the lower turbulence the spectrum of the disturbances originally present is of great importance.

Whether these disturbances are small free stream turbulence, noise, or surface roughness, they are selectively amplified until large sinusoidal oscillations are present. In free flight noise may well be the most important factor.

4. Effect of Curvature

Liepmann completed an extensive study of the effect of curvature on transition. The boundary layer on convex surfaces, at least up to values of momentum thickness equal to 0.001 time the radius of curvature, exhibits the same Tollmien-Schlichting instability as the flat plate, and the effect of curvature is so small as to lie within the precision of measurement. Transition on the upper surface of an airfoil will therefore not be noticeably influenced by the curvature.

The experimental work on concave surfaces was described by Liepmann in *N.A.C.A. Advance Confidential Report* No. **4J28** (now declassified and available as *N.A.C.A. Wartime Report* W-87). When the momentum thickness θ is greater than 0.0005 times the radius of curvature r, the laminar flow is dynamically unstable, owing to three-dimensional disturbances as studied theoretically by Görtler (50). In a stream of the lowest turbulence the Görtler parameter $R_\theta \sqrt{\theta/r}$, where R_θ is the Reynolds number based on momentum thickness, is equal to 9.0. This value decreases to about 6.0 at a turbulence level of 0.003 (value of u'/U).

If the value of θ/r is less than 0.00005 the flow is unstable because of Tollmien-Schlichting waves like the flat plate and the convex surface, and transition occurs at a constant Reynolds number whose value depends on the free stream turbulence. For values of θ/r between 0.00005 and 0.0005 there appears to be a more or less continuous change from transition due to Görtler vortices to transition caused by Tollmien-Schlichting waves.

5. Effect of Pressure Gradient

The theory of the instability of a laminar boundary layer subjected to a falling or rising pressure was investigated by Pretsch (58) at Göttingen and by Schlichting and Ulrich (62) at Braunschweig.

Pretsch considered the velocity distributions corresponding to the "similar" solutions for a free stream velocity U proportional to a power law of the distance x, *i.e.*, $U = kx^m$. A positive value of m corresponds to accelerated flow (falling pressure) and a negative value to decelerated flow (rising pressure). These solutions had previously been computed and tabulated by Hartree (4) in terms of a parameter β connected with m by the relation $m = \beta/(2 - \beta)$. For positive values of $m (0 < \beta < 2)$

Pretsch found it possible to approximate Hartree's tabulated values by the expression

$$\frac{u}{U} = 1 - \left(1 - \frac{y}{a}\right)^n$$

and for m negative or zero ($-0.198 < \beta < 0$) by the expression

$$\frac{u}{U} = \frac{u_s}{U} + \left(1 - \frac{u_s}{U}\right) \sin\left[\left(\frac{y}{s} - 1\right) \sin^{-1} \frac{u_s}{U - u_s}\right]$$

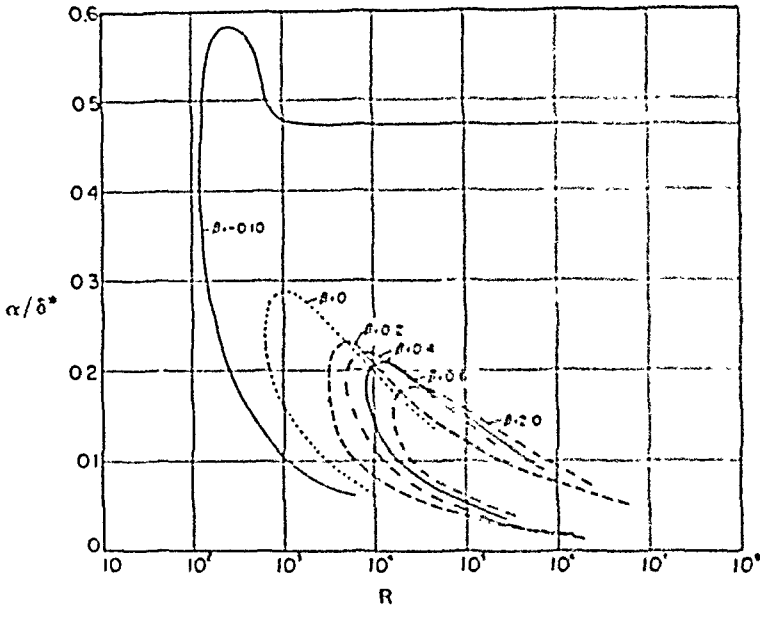

FIG. 8.—Wave lengths of neutral oscillations for flows with pressure gradient as computed by Pretsch.

where the quantities n, a, u_s, and s were selected to give the best possible approximations to Hartree's values. The stability of laminar flows represented by these approximations to Hartree's solutions was investigated, but for convenience the distributions were identified in terms of Hartree's parameter β.

The locus of the neutral oscillations for various values of β are shown in Fig. 8 as a plot of the nondimensional wavelengths against Reynolds number. The usual nondimensional parameter for the pressure gradient is Pohlhausen's parameter $\lambda = U'\delta^2/\nu$. Pohlhausen's four-term approximate solution for $U = kx^m$ is λ = constant where λ is the function of β shown in Fig. 9. Fig. 10 shows the critical Reynolds number, based on displacement thickness, as a function of λ. While the values of m, β, and λ are useful in giving a rough idea of the velocity profiles considered,

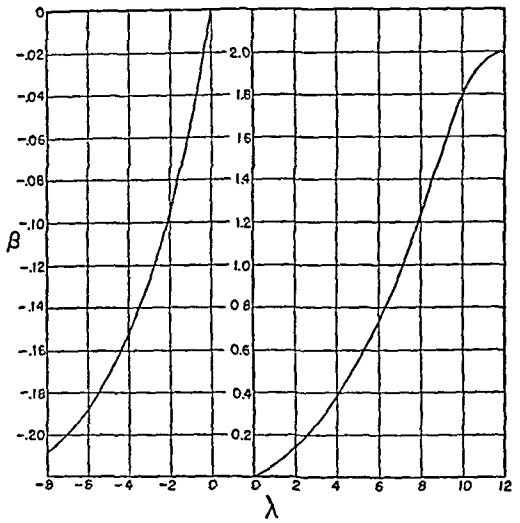

FIG. 9.—Relation between Hartree parameter β and the Pohlhausen parameter λ.

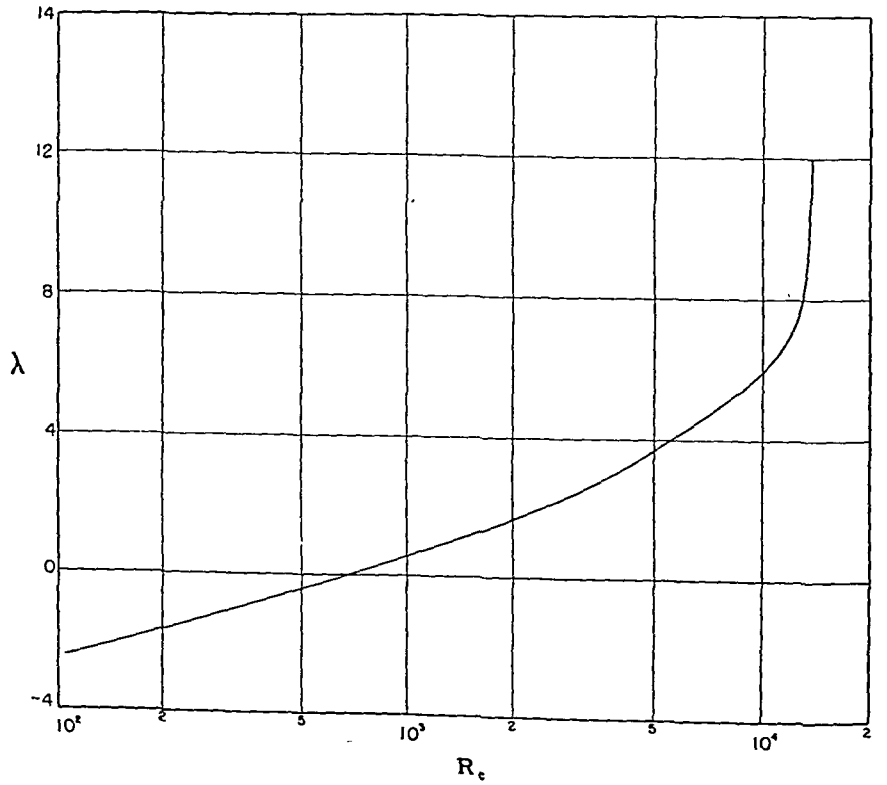

FIG. 10.—Effect of pressure gradient on stability of laminar flow.

the stability limits actually apply to the approximations previously referred to, for which the constants are tabulated in Pretsch's paper.

In a second paper Pretsch (61) computed the damping and amplification of disturbances other than the neutral one for the same pressure distributions. The maximum observed amplification coefficient as a function of λ is shown in Fig. 11. The values are always larger for

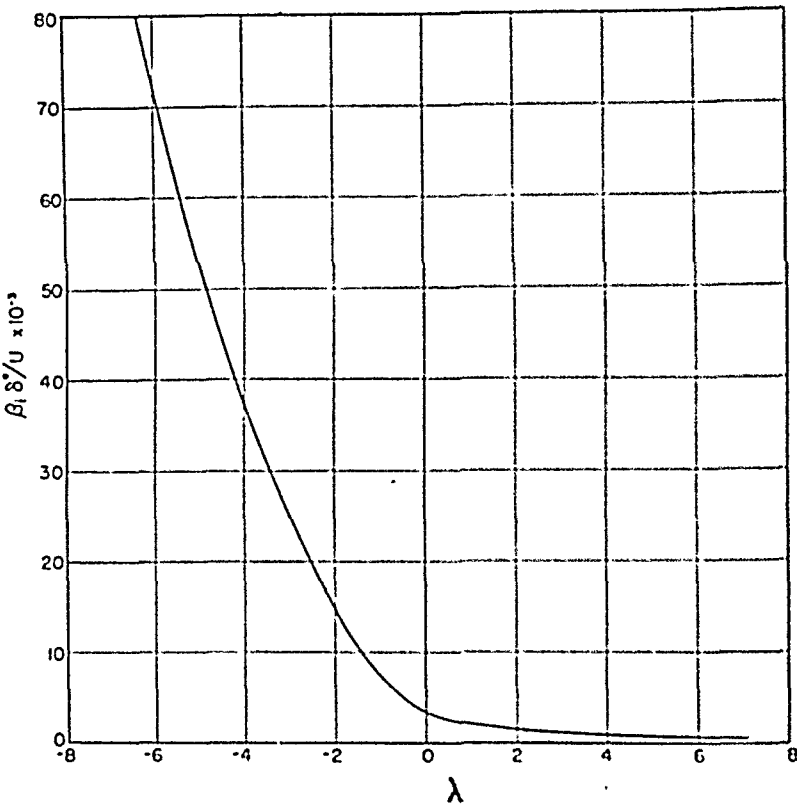

FIG. 11.—Maximum amplification coefficient in flows with pressure gradient as computed by Pretsch.

decelerating flow than for accelerating flow and become very large as λ approaches large negative values corresponding to separation of the flow.

At about the same time as Pretsch's investigation a similar study was carried out by Schlichting and Ulrich (62). They studied the velocity distributions given by a six-term power series of the Pohlhausen type, choosing as the additional boundary conditions the vanishing of d^3U/dy^3 at the wall and at the outer boundary. The resulting parameter λ_{Pe} characterizing a given pressure gradient differs somewhat from the parameter λ for the four-term series approximation. The relation between values giving the same momentum thickness is shown in Fig. 12. The accuracy of the stability computations was studied by computing the critical Reynolds number for the case of zero pressure gradient. The four-

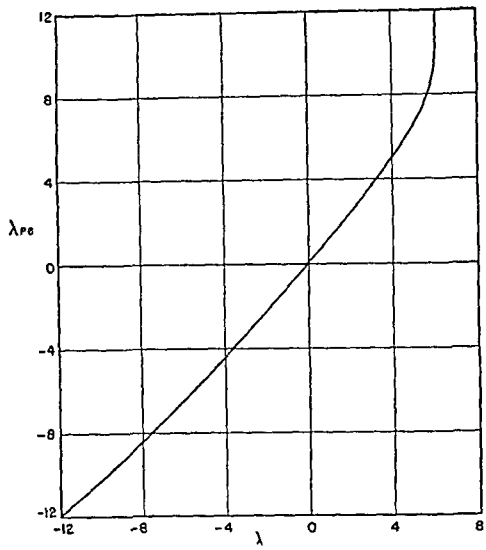

FIG. 12.—Relation between Pohlhausen parameters for six-term and four-term approximations giving same momentum thickness.

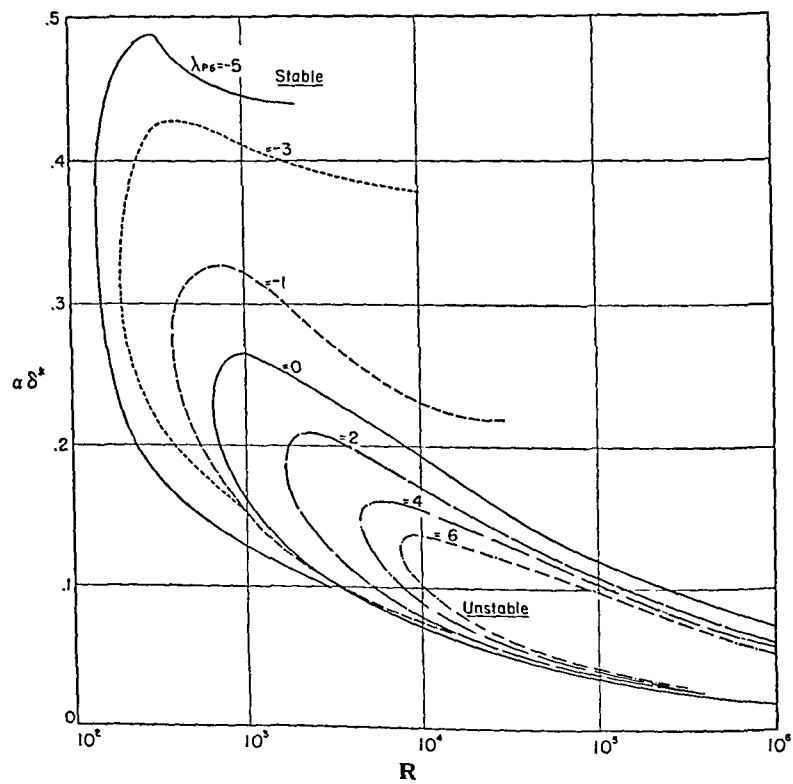

FIG. 13.—Wavelengths of neutral oscillations for flows with pressure gradient as computed by Schlichting and Ulrich.

term approximation gives 1150, the six-term approximation 645, as compared with Pretsch's value of 680 and Schlichting's "exact" value 575. The results obtained for several values of λ are shown in Fig. 13 in the form of loci of the neutral disturbances. The critical Reynolds number is plotted against λ in Fig. 14, in which Pretsch's result is also shown.

The accuracy of the computed values is open to some question since the values obtained for zero pressure gradient differ from Lin's more accurate value 420, which agrees with the experimentally determined

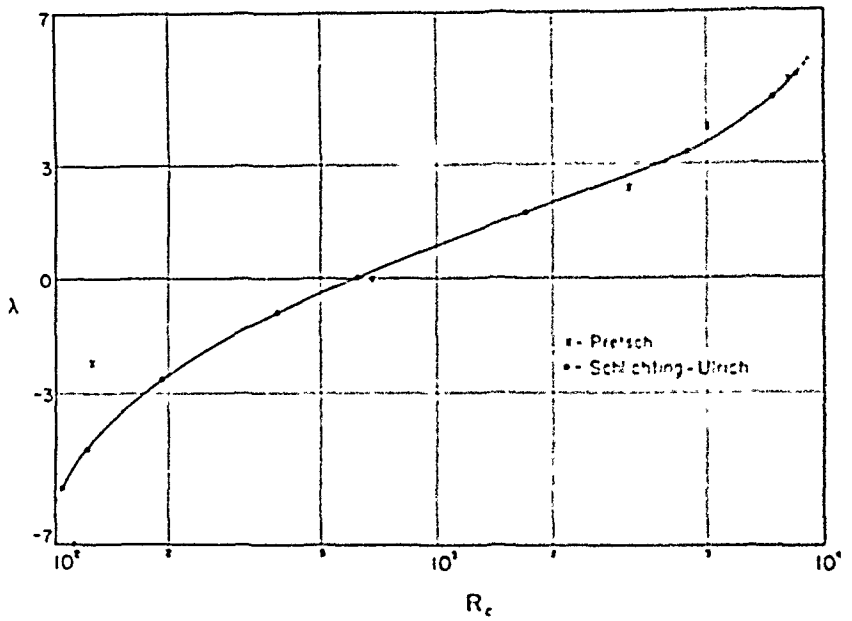

FIG. 14.—Comparison of results of Pretsch and those of Schlichting and Ulrich for effect of pressure gradient on stability of laminar flow.

value of Schubauer and Skramstad. Nevertheless the trend and general order of magnitude are probably correct. The effect of pressure gradient is very large; for $-3 < \lambda < 3$ the critical Reynolds number is approximately proportional to $e^{0.6\lambda}$. It is easy to understand why the observed critical Reynolds number for airfoils is so large; the effect of the acceleration of the flow over the upper surface is to increase greatly the critical Reynolds number.

In both papers computations were made of the parameter λ at various points along the surface of airfoils, and the point for which the critical Reynolds number corresponding to the prevailing value of λ was first reached was interpreted as the most forward possible position of the transition point. The experiments available indicated that transition did not occur until some distance further back even in the fairly turbulent wind tunnel available. It was recognized that the amplification of the disturbance must be considered.

In view of the good experimental check of the theoretical computations for the case of zero pressure gradient, it would seem worth while to devote considerable effort to refining the theoretical stability computations for flows with pressure gradient and to carrying on additional experimental investigation. Schubauer and Skramstad made only a few exploratory measurements.

6. Effect of Compressibility

A theoretical investigation of the stability of the laminar boundary layer in a compressible fluid has been carried out by Lees and Lin (68), although in their first report the investigation did not reach the stage of numerical computations. It was found that for Reynolds numbers of the order of those encountered in most aerodynamic problems the temperature disturbances have only a negligible effect on those particular solutions that depend primarily on the viscosity. The chief physical mechanism of the instability is essentially the same for compressible flow as for incompressible flow.

It was found that when the solid boundary is heated, the boundary layer flow is destabilized by the change in the distribution of the product of density and vorticity, but stabilized by the increase in kinematic viscosity near the boundary. When the boundary is cooled, the reverse is true. The detailed results are given in N.A.C.A. Tech. Note No. 1360 by Lester Lees, entitled *The Stability of the Laminar Boundary Layer in a Compressible Fluid.* The first effect was found to predominate.

Bibliography on Stability of Laminar Boundary Layer Flow and Transition

46. Clauser, M., and Clauser, F., The effect of curvature on the transition from laminar to turbulent boundary layer, *N.A.C.A. Tech. Note* No. **613** (1937).

47. Rosenbrook, G., Instabilität der Gleitschicht im schwach divergenten Kanal, *Z. angew. Math. Mech.*, **17**, 8–24 (1937).

48. Silverstein, A., and Becker, J. V., Determination of boundary layer transition on three symmetrical airfoils in the N.A.C.A. full-scale wind tunnel, *N.A.C.A. Tech. Rept.* No. **637** (1938).

49. Von Doenhoff, A. E., Preliminary investigation of boundary layer transition along a flat plate with adverse pressure gradient, *N.A.C.A. Tech. Note* No. **639** (1938).

50. Görtler, H., Über eine dreidimensionale Instabilität laminarer Grenzschichten an konkaven Wänden, *Nachr. Ges. Wiss. Göttingen*, Fachgruppe I (N.F.), **2**, 1–26 (1940).

51. Dryden, H. L., Turbulence and the boundary layer, *J. Aeronaut. Sci.*, **6**, 85-100 (1939).

52. Fage, A., Fluid motion transition from laminar to turbulent flow in a boundary layer, *Phys. Soc. Repts. on Progress in Physics*, **6**, 270–279 (1939).

53. Townend, H. C. H., Note on boundary layer transition, *Brit. A.R.C., Repts. and Memo.* No. **1873** (1939).

54. FAGE, A., Experiments on the breakdown of laminar flow, *J. Aeronaut. Sci.*, 7, 513–517 (1940).
55. LANGER, R. E., On the stability of the laminar flow of a viscous fluid, *Bull. Am. Math. Soc.*, 46, 257 (1940).
56. SCHLICHTING, H., Über die theoretische Berechnung der kritischen Reynoldsschen Zahl einer Reibungsschicht in beschleunigter und verzögerter Strömung, *Jahrb. deut. Luftfahrtforsch.*, 1940, Vol. I, 97.
57. FAGE, A., and PRESTON, J. H., Experiments on transition from laminar to turbulent flow in the boundary layer, *Proc. Roy. Soc. (London)*, *A*, 178, 201–227 (1941).
58. PRETSCH, J., Die Stabilität einer ebenen Laminarströmung bei Druckgefälle und Druckanstieg, *Jahrb. deut. Luftfahrtforsch.*, 1941, Vol. I, 58–75.
59. FAGE, A., Transition in the boundary layer caused by turbulence, *Brit. A.R.C., Repts. and Memo.* No. 1896 (1942).
60. PRANDTL, L., Bericht über neuere Untersuchungen über das Verhalten der laminaren Reibungsschicht, insbesondere den laminar-turbulenten Umschlag, *Mitt. deut. Akad. Luftfahrtforsch.*, 2, 141 (1942).
61. PRETSCH, J., Die Anfachung instabiler Störungen in einer laminaren Reibungsschicht, *Jahrb. deut. Luftfahrtforsch.*, 1942, Vol. I, 54–71.
62. SCHLICHTING, H., and ULRICH, A., Zur Berechnung des Umschlages laminar/turbulent, *Jahrb. deut. Luftfahrtforsch.*, 1942, Vol. I, 8–35.
63. BATCHELOR, G. K., The laminar flow characteristics of three related airfoils, *Australia, Council Sci. Ind. Research Div. Aeronaut., Rept.* No. A20 (1943).
64. CHARTERS, A. C., Transition between laminar and turbulent flow by transverse contamination, *N.A.C.A. Tech. Note* No. 891 (1943).
65. PILLOW, B. A., A review of hydrodynamic stability and its bearing on transition to turbulent flow in the boundary layer, *Australia, Council Sci. Ind. Research, Div. Aeronaut., Rept.* No. A35 (1945).
66. LIN, C. C., On the stability of two-dimensional parallel flows, *Quart. Applied Math.* 3 (No. 2), 117–142 (July 1945); 3 (No. 3), 218–234 (Oct. 1945); 3 (No. 4), 277–301 (Jan. 1946).
67. LOFTIN, L. K., JR., Effects of specific types of surface roughness on boundary-layer transition, *N.A.C.A. Wartime Rept.* L-48 (1946).
68. LEES, L., and LIN, C. C., Investigation of the stability of the laminar boundary layer in a compressible fluid, *N.A.C.A. Tech. Note* No. 1115 (1946).

(See also references under Boundary Layer Suction.)

IV. BOUNDARY LAYER SUCTION

During the war German investigators studied the effect of removing a part of the boundary layer air by suction through a homogeneous porous surface. At a considerable distance from the leading edge of a plate in a flow of uniform free stream velocity, the velocity distribution is given by $u/U = 1 - e^{-V_0 y/\nu}$ where u is the velocity at distance y from the surface, U is the free stream velocity, V_0 is the velocity of the air sucked through the surface, and ν is the kinematic viscosity. The boundary layer displacement thickness is constant and equal to $|\nu/V_0|$. Pretsch (77) obtained a critical Reynolds number of 55,200 and Bussmann

and Münz (76) 70,000 as compared with Schlichting's value of 575 for the plate without suction and Pretsch's values of 10,000 to 20,000 for the plate without suction but with a large favorable pressure gradient. The required suction velocity V_0 is of the order of 0.000014 time the free stream speed. The maximum amplification parameter $\beta_i\delta^*/U$ in the unstable region is 4.65×10^{-4} for the flow with suction as compared with 3.45×10^{-3} for the flow without suction. These results are extremely important as indicating a possible method of greatly increasing the stability of laminar flow and thus delaying transition.

Some experimental work has been carried out in Switzerland and England with attention given to the practical aspect of reducing drag. J. Ackeret (74,83) and his colleagues at the Aerodynamic Institute of the Federal Institute of Technology at Zürich, by removing a part of the boundary layer air by suction through a small number of slots, were in fact able to partially restore a turbulent boundary layer to the laminar condition. By careful attention to the detailed design of the internal ducting of the suction system they obtained extremely low drag coefficients.

Mr. E. F. Relf (82) has given a general account of work carried out in England during the war on boundary layer suction as applied to the maintenance of laminar flow and reduction of drag of rather thick airfoils. A single slot was used on each surface of an airfoil especially designed to suit the suction, an idea due to A. A. Griffith and followed up by S. Goldstein and by Lighthill on the theoretical side and presumably by Relf and his collaborators on the experimental side. Reference is also made to the use of distributed suction acting through a porous surface with theoretical work by J. H. Preston and a flight test by F. G. Miles. No experimental results are given and no references to detailed reports.

Bibliography on Boundary Layer Suction

69. Shenstone, B. S., Sucking off the boundary layer, *Aeroplane*, **52**, 98–100 (1937).
70. Gerber, A., Untersuchungen über Grenzschichtabsaugung, *Mitt. Inst. Aerodyn.*, E.T.H. Zürich, No. 6 (1938).
71. Richardson, E. C., Manipulating the boundary layer, *J. Roy. Aeronaut. Soc.*, **42**, 816–831 (1938).
72. Miles, F. G., Sucking away boundary layers, *Flight*, **35**, 180–184 (1939).
73. Weske, J. R., Reduction of skin friction on a flat plate through boundary layer control, *J. Aeronaut. Sci.*, **6**, 289–291 (1939).
74. Ras, M., and Ackeret, J., On prevention of boundary layer turbulence through removal by suction, *Helv. Phys. Acta*, **14**, 232 (1941).
75. Schrenk, O., Grenzschichtabsaugung, *Luftw.*, **7**, 409–414 (1940); also *N.A.C.A. Tech. Memo.* No. **974** (1941).
76. Bussmann, K., and Münz, H., Die Stabilität der laminaren Reibungsschicht mit Absaugung, *Jahrb. deut. Luftfahrtforsch.*, **1942**, Vol. I, 36–39.

77. Pretsch, J., Umschlagbeginn und Absaugung, *Jahrb. deut. Luftfahrtforsch.*, 1942, Vol. I, 1–7.
78. Schlichting, H., Berechnung der laminaren Grenzschicht mit Absaugung, *Luftfahrtforsch.*, 19, 179 (1942).
79. Schlichting, H., Die Grenzschicht an der ebenen Platte mit Absaugung und Ausblasen, *Luftfahrtforsch.*, 19, 293–301 (1942).
80. Schlichting, H., and Bussmann, K., Exakte Lösungen für die laminare Grenzschicht mit Absaugung und Ausblasen, *Schriften deut. Akad. Luftfahrtforsch.*, 7B, No. 2 (1943).
81. Freeman, H. B., Boundary layer tests in Langley propeller research tunnel, *N.A.C.A. Tech. Note* No. 1007 (1946).
82. Relf, E. F., Recent aerodynamic developments, *J. Roy. Aeronaut. Soc.*, 50, 421–449 (1946).
83. Pfenninger, W., Untersuchungen über Reibungsverminderungen an Tragflügeln, insbesondere mit Hilfe von Grenzschichtabsaugung, *Mitt. Inst. Aerodyn.*, E.T.H. Zürich, No. 13 (1946).

V. Turbulent Flow in Boundary Layers

There have been no notable advances in the theory of fully developed turbulent motion during the last decade, although the great advances in experimental techniques for studying the turbulent velocity fluctuations lead one to expect the early appearance of that long-awaited new idea that will permit further progress. In the period 1934–1938 Taylor developed his statistical theory of turbulence, which was so fruitful in treating the problem of isotropic turbulence. Von Kármán extended the theory, clothed it in more elegant mathematical form, and attempted, with incomplete success, to treat the problem of shear flow. The concepts and language of the statistical theory have been found most useful in guiding the experimental work.

At the Fifth International Congress for Applied Mechanics in 1938 von Kármán discussed some measurements of turbulent velocity fluctuations in a channel by Wattendorf and by Reichardt and suggested the existence of a kind of statistical similarity between the fluctuations at different points over the region not too close to the wall or to the channel center. He pointed out the difficulty of reconciling Reichardt's measurements of the plane stress tensor with the picture of momentum transfer by a mixing process involving only a scalar "mixing length." In the discussions Tollmien and Prandtl suggested that the turbulent fluctuations might consist of two components, one derivable from a harmonic function and the other satisfying an equation of the heat-conduction type, *i.e.*, a nondiffusive and a diffusive component or viscosity independent and viscosity-dependent type.

1. Development of Empirical Methods of the Buri-Gruschwitz Type

Since engineers have to make computations relating to turbulent skin friction and turbulent boundary layers, there has been some

development of empirical methods. These are of the "one-dimensional" type involving the application of the von Kármán integral equation for the momentum and the use of empirical relations obtained from a few experimental studies of flow in convergent and divergent passages. While the earliest procedure was suggested by Buri, the method proposed by Gruschwitz has been more widely used and apparently was used in substantially its original form by German engineers throughout the war. In the United States a modified procedure suggested by von Doenhoff and Tetervin (86) has been found useful.

In common with Buri and Gruschwitz, von Doenhoff and Tetervin assumed that the boundary layer at any section could be described by the momentum thickness $\theta = \int_0^\infty \left(1 - \frac{u}{U}\right)\left(\frac{u}{U}\right) dy$ and by a single parameter that fixes the shape of the velocity distribution curve. Buri had used as the parameter the quantity $(U'\theta/U)(U\theta/\nu)^{\frac{1}{4}}$. Gruschwitz had used $1 - (u/U)^2_{y=\theta}$ as primary parameter and the ratio of displacement thickness $\left[\int_0^\infty \left(1 - \frac{u}{U}\right) dy\right]$ to momentum thickness as secondary parameter. This ratio will be denoted H. Von Doenhoff and Tetervin selected H as an appropriate shape parameter. They give a comprehensive summary and analysis of available experimental data, plotting u/U versus H for a series of constant values of y/θ. The available data gave a reasonably close approximation to a single family of curves. The value of H for separation was found to lie between 1.8 and 2.6.

The particular velocity distribution curve corresponding to the single parameter adopted to describe it is of course dependent on the external forces acting on the boundary layer, that is, on the shear stress at the wall and the pressure gradient. Von Doenhoff and Tetervin adopt the ratio of the nondimensional pressure gradient to the shearing stress coefficient at the wall as a parameter characteristic of the external forces acting on the boundary layer. Calling the shearing stress at the wall τ_w, this parameter is $2\rho UU'\theta/\tau_w$ $\left(\text{in their notation } \frac{\theta}{q}\frac{dq}{dx}\frac{2q}{\tau_0}\right)$. It is then assumed that this parameter determines not H itself, *i.e.*, the particular velocity distribution curve of the one-parameter family, but the rate of change of H with x. Thus $\theta \frac{dH}{dx}$ is plotted against $2\rho UU'\theta/\tau_w$, τ_w being computed from the Squire-Young formula (88)

$$\frac{\rho U^2}{\tau_w} = \left[5.890 \log_{10}\left(4.075 \frac{U\theta}{\nu}\right)\right]^2.$$

The experimental data are fairly well represented by the empirical equation

$$\theta \frac{dH}{dx} = e^{4.680(H-2.975)} \left[\frac{2\rho U U' \theta}{\tau_w} - 2.035(H - 1.286) \right].$$

The momentum equation gives the relation

$$\frac{\tau_w}{\rho U^2} = \frac{d\theta}{dx} + \frac{U'\theta}{U}(2 + H).$$

Elimination of τ_w gives two simultaneous first-order differential equations, which can be solved by a step-by-step calculation to give θ and H.

Kalikhman (91) describes a still different empirical approach based also on the momentum relation and the Squire-Young formula.

All such methods rest on empirical assumptions and become more and more unsatisfactory as separation is approached. They do not contribute to the construction of a rational theory founded on knowledge of the underlying physical phenomena.

2. Developments Proceeding from Reynolds Theory of Turbulent Stresses

The fundamental equations of turbulent flow of an incompressible fluid developed by Reynolds are identical with the Navier-Stokes equations except for the addition of the six components of the turbulent stress tensor, *i.e.*, $-\rho\overline{u'^2}$, $-\rho\overline{v'^2}$, $-\rho\overline{w'^2}$, $-\rho\overline{u'v'}$, $-\rho\overline{v'w'}$, and $-\rho\overline{u'w'}$. With these six additional unknown functions, the number of unknowns exceeds the number of equations and there are insufficient data for a solution. All of the past procedures assume that the turbulent stress tensor at a point is determined by the mean flow in the neighborhood of the point. In the most general form it is assumed that the stress tensor is equal to the product of the deformation tensor by a mixing length tensor. The most widely used theory of Prandtl assumes the mixing length tensor to reduce to a scalar mixing length, that is, one number instead of six. Prandtl related this mixing length to the geometry of the flow field (distance from the wall) by a kind of dimensional reasoning but von Kármán related it to the derivatives of the mean velocity. As will be seen later, the available experimental data suggest re-examination of the assumption that the turbulent fluctuations at a point are determined by the mean flow in the neighborhood of that point, that is, whether the entire field must be considered, leading perhaps to an integral equation for the relation between the fluctuations at a point and the mean flow.

A recent paper by Nevzgljadov (94) is of interest in this connection. He writes down the Reynolds equations, the continuity equation, and the energy equation for the turbulent velocity fluctuations. The unknown functions are the mean velocity, the mean pressure, the turbulent pressure $\pi = \frac{1}{3}\rho(u'^2 + v'^2 + w'^2)$, the turbulent stress tensor, the current density of the kinetic energy of the turbulent fluctuations, the energy flux transferred by the pressure fluctuations, and the viscous dissipation. It is proposed to select the mean velocity, the mean pressure, and the turbulent pressure as independent fundamental quantities and to assume that the other unknowns can be related to these fundamental quantities by "equations of state."

Nevzgljadov discusses the question whether the shearing stress at a given point can be expressed in terms of the values of the fundamental quantities in the immediate neighborhood of the point. His theory differs from that of Prandtl in assuming that the turbulent shearing stress may depend on the turbulent pressure as well as on the mean motion. The relation proposed, that is, that the shearing stress is proportional to the product of the turbulent pressure by the mean velocity gradient, is not supported by the experiments to be described; the experiments in fact show a more direct relation between shear stress and turbulent pressure than between shear stress and local mean velocity gradient.

3. National Bureau of Standards Experiments

The only experimental work known during recent years on the turbulent stress tensor in a turbulent boundary layer is that carried out by the National Bureau of Standards for the National Advisory Committee for Aeronautics and reported by Dryden at the Sixth International Congress for Applied Mechanics. The paper will appear in the proceedings of the Congress and also as *N.A.C.A. Tech. Note* No. **1168.** It is a progress report on a long range study of the mechanics of a separating turbulent boundary layer.

The experiments were made in the boundary layer along a partition of airfoil-like section extending in a diametral plane across the 10-foot wind tunnel of the National Bureau of Standards. The partition was 27.9 ft long and had a maximum thickness of 2 ft. The leading edge radius was 1 in. and the leading edge was joined tangentially to cylindrical surfaces of 23-ft radius forming the nose. The downstream portion of the partition was flat on one side and in the form of a cylinder of 31-ft radius on the other. By various tricks two-dimensional flow was obtained over the central region with separation occurring along a line 25.7 ft from the leading edge. The variation of the velocity just outside the boundary layer is

shown in Fig. 15. The maximum velocity occurs at 17 ft from the leading edge, and was about 161 ft/sec in the measurements to be

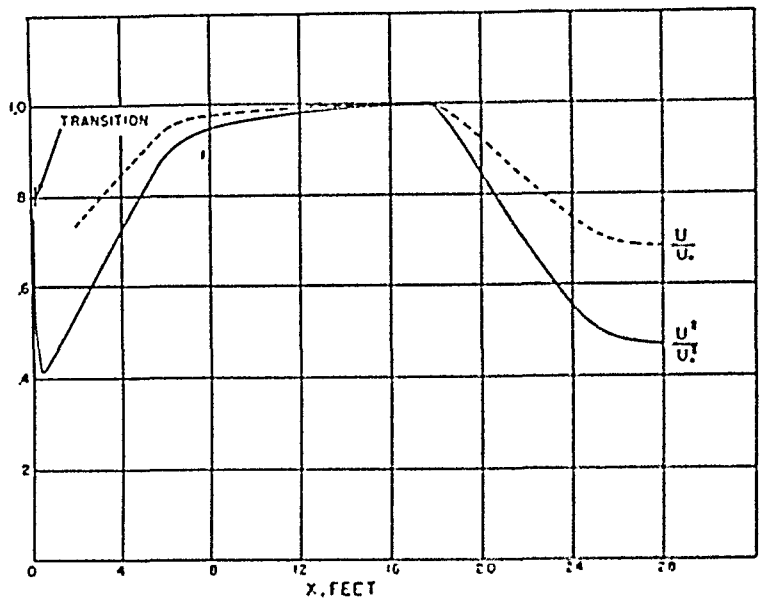

FIG. 15.—Velocity and pressure distribution just outside the turbulent boundary layer studied at National Bureau of Standards.

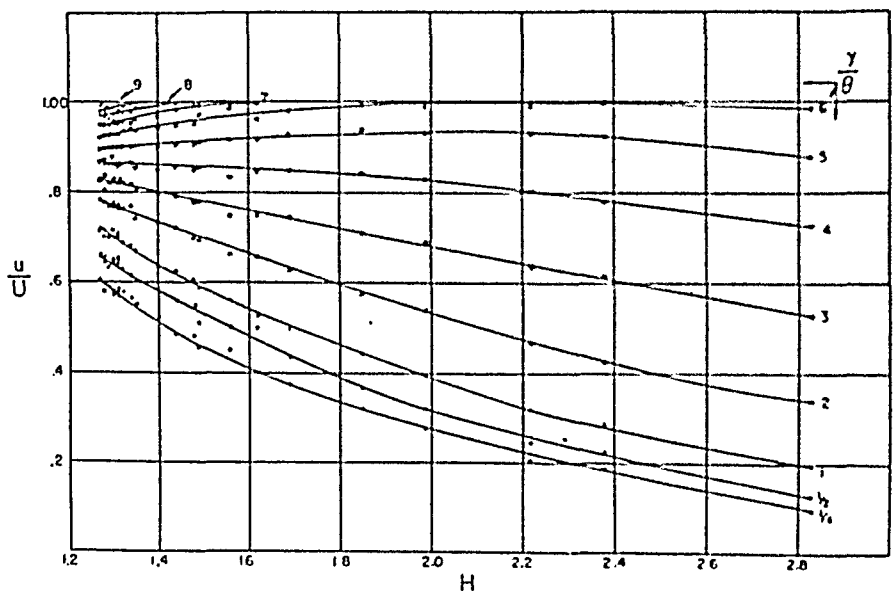

FIG. 16.—Velocity distribution within turbulent boundary layer studied at National Bureau of Standards.

described. Its exact value was adjusted to be proportional to the viscosity of the air, thus maintaining a constant Reynolds number.

At the 17-ft position the boundary layer was about 2.3 in. thick,

corresponding to that which would have prevailed on a flat plate 14.3 ft long with fully turbulent boundary layer and no pressure gradient, the equivalent flat-plate Reynolds number being about 14×10^6. The free stream turbulence was about 0.5 per cent and the boundary layer flow

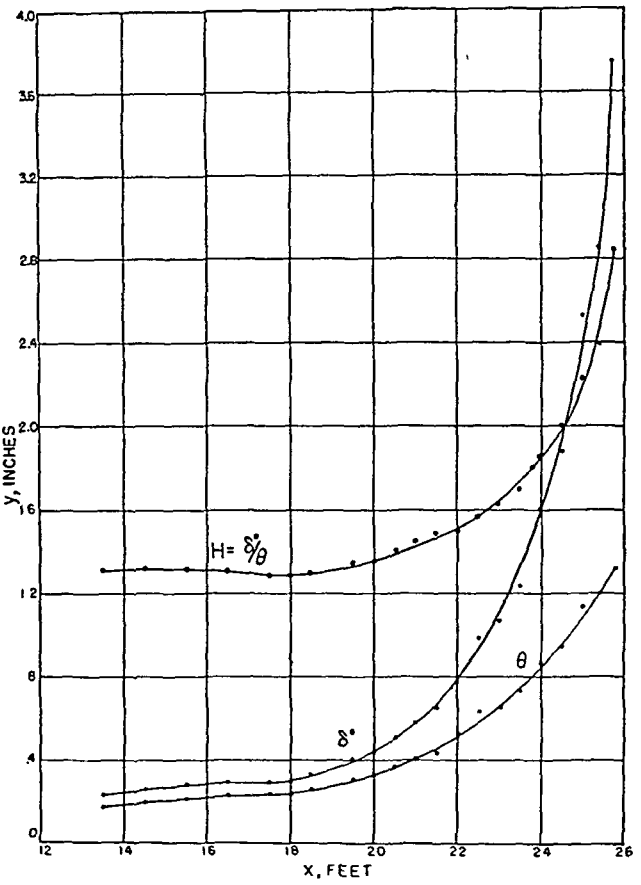

FIG. 17.—Displacement thickness, δ^*, momentum thickness, θ, and parameter, $H = \delta^*/\theta$, for NBS turbulent boundary layer.

was turbulent from the leading edge as desired because of the unsymmetrical form of the partition.

The experimental program has been directed principally at the measurement of the turbulent fluctuations and of the turbulent stress tensor by means of hot-wire anemometers and contemplates the development and application of such additional hot-wire measurements as will throw light on the underlying phenomena. The usual traverses of mean speed were also made. Unfortunately the hot-wire methods are not adaptable to the simultaneous measurements of a number of quantities at a large

number of points in the flow field. The measurements extend over months and are not suitable for analysis of differential changes from point to point with high accuracy.

The distribution of mean speed is plotted in the manner suggested by von Doenhoff and Tetervin (86) in Fig. 16, and the displacement thickness, momentum thickness, and their ratio, the parameter H, are shown

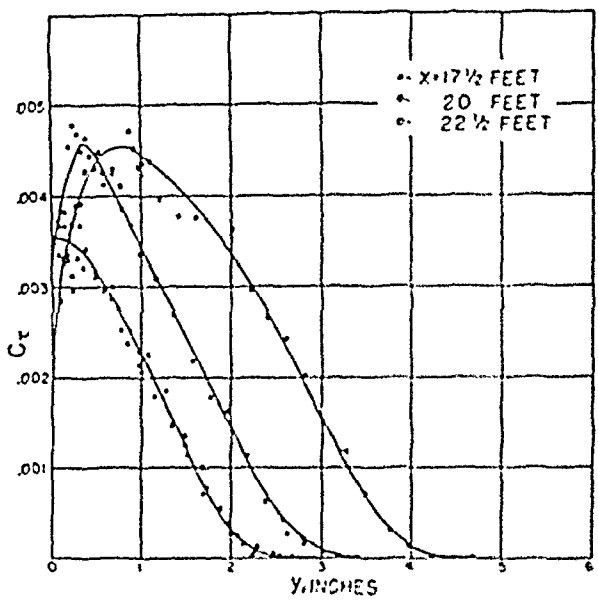

FIG. 18.—Typical distributions of turbulent shearing stress coefficient in NBS turbulent boundary layer.

in Fig. 17. The agreement with previous results is good, although there are systematic differences slightly greater than the experimental dispersion.

Typical distributions of the turbulent shearing stress are shown in Fig. 18 and a contour map for the whole region studied is shown in Fig. 19. The measurements were made by the procedure devised by Skramstad and described by Dryden at the Fifth International Congress for Applied Mechanics. The viscous shearing stresses are wholly negligible in the regions studied, because of the large Reynolds number, being less than ½ per cent of the turbulent shearing stress at 0.1 in. from the surface. The laminar sublayer is never approached in any of the measurements.

The stress coefficient used in Fig. 19 is based on the velocity at 17 ft as a constant reference velocity and hence the contours are those of equal absolute values of the stress. In the region of adverse pressure gradient, that begins at 17 ft the maximum value of the shearing stress gradually shifts from the wall on proceeding downstream until at separa-

tion it is located near the middle of the boundary layer. The maximum value slowly increases downstream.

In addition to the shearing stress, the root-mean-square values of the three components of the turbulent fluctuations were also measured, u'

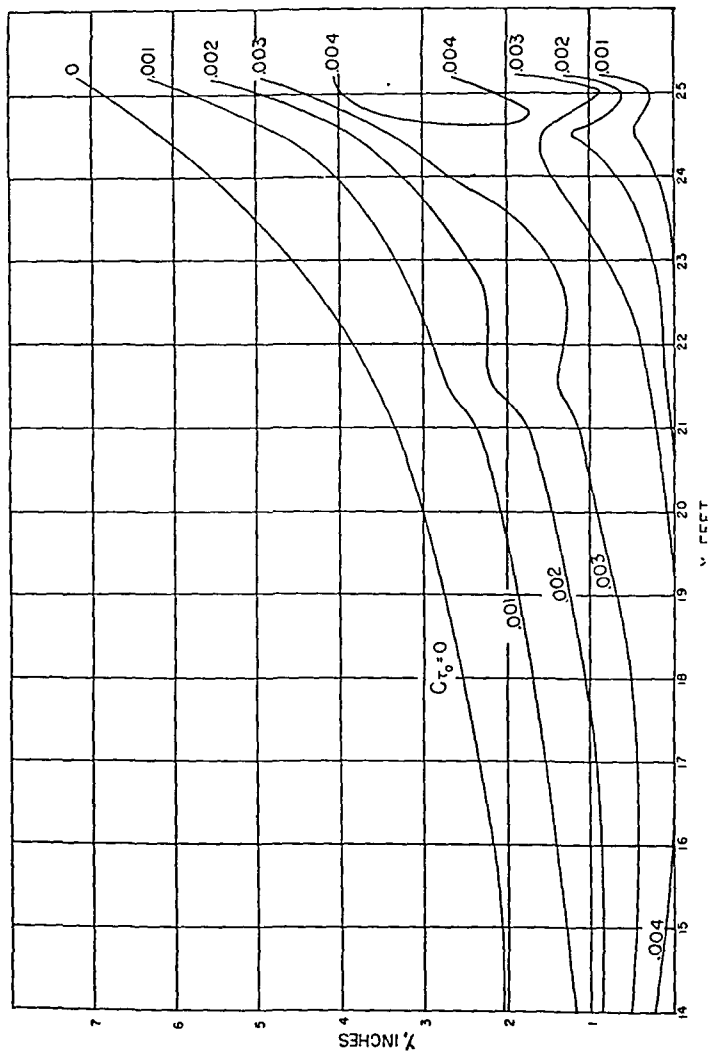

Fig. 19.—Contour map of distribution of turbulent shearing stress for NBS turbulent boundary layer.

parallel to the mean flow, v' perpendicular to the mean flow and to the surface, and w' perpendicular to the mean flow but parallel to the surface. Contours of their distributions are shown in Figs. 20, 21, and 22. The values are made nondimensional by dividing by the reference velocity just outside the boundary layer at 17 ft from the nose, but since the same reference value is used throughout, the contours are also contours of equal absolute values of u', v', and w'. The mean velocity just outside

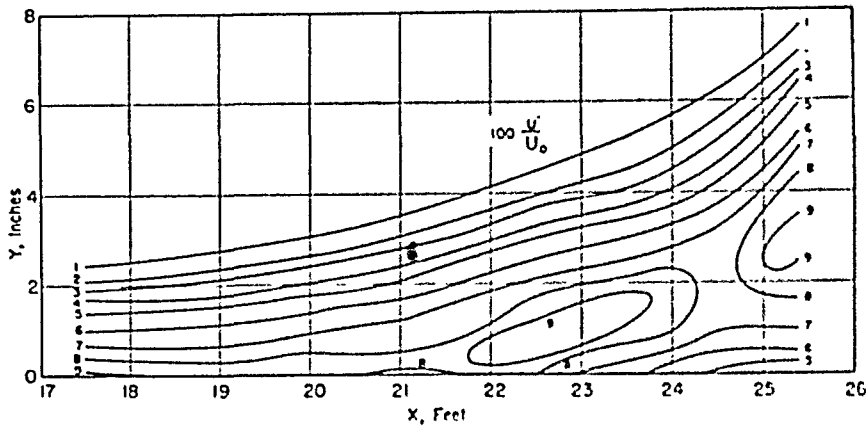

FIG. 20.—Contour map of u' for NBS turbulent boundary layer.

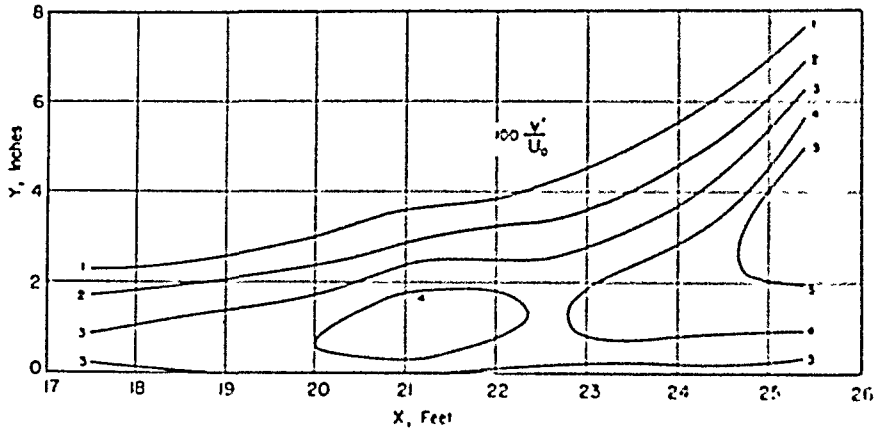

FIG. 21.—Contour map of v' for NBS turbulent boundary layer.

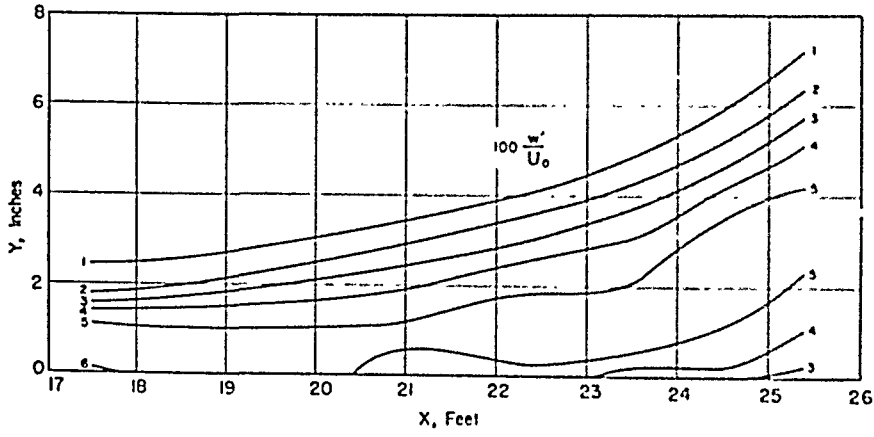

FIG. 22.—Contour map of w' for NBS turbulent boundary layer.

the boundary layer at each section varies from section to section as given in Fig. 15. The turbulence is three-dimensional even though the mean flow is two-dimensional. The turbulence is strongly nonisotropic, v' being considerably less than u' and w' being intermediate in value. Isotropy is reached in the free stream.

From these data the complete turbulent stress tensor can be computed and in particular the angle α between the direction of the principal axis

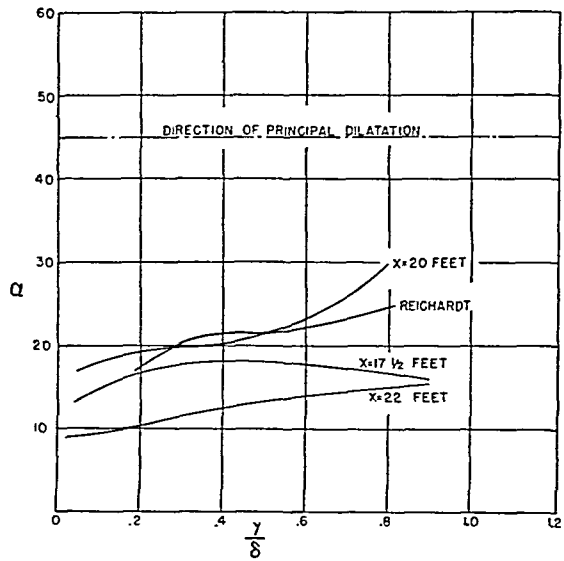

FIG. 23.—Angle α of the principal axis of the turbulent stress tensor to the mean direction of flow.

of the stress tensor and the mean flow. Typical results are shown in Fig. 23 along with Reichardt's results for two-dimensional flow under pressure between two plates as given by von Kármán. These results confirm the difficulty pointed out by von Kármán, namely, that the principal axis of dilatation is at 45° to the mean flow as compared with 10° to 30° for the principal axis of the turbulent shearing stress. There are directions for which there is a shearing stress but no rate of shear of the mean flow, and vice versa. This result cannot be reconciled with the concept of a scalar mixing length.

As further indication challenging the correctness of the assumption that there is a close relation between the turbulent fluctuations and the mean flow in the immediate neighborhood, consider Fig. 24, which shows the stress coefficient plotted against the mean velocity gradient. Over extended regions the velocity gradient is nearly constant; yet the shearing stress changes by a factor of 4 or 5.

In order to test Nevzgljadov's assumption that the shearing stress τ is proportional to $(u'^2 + v'^2 + w'^2)\frac{du}{dy}$, the ratio of τ to $(u'^2 + v'^2 + w'^2)$ was plotted against du/dy. The results are shown in Fig. 25. For the

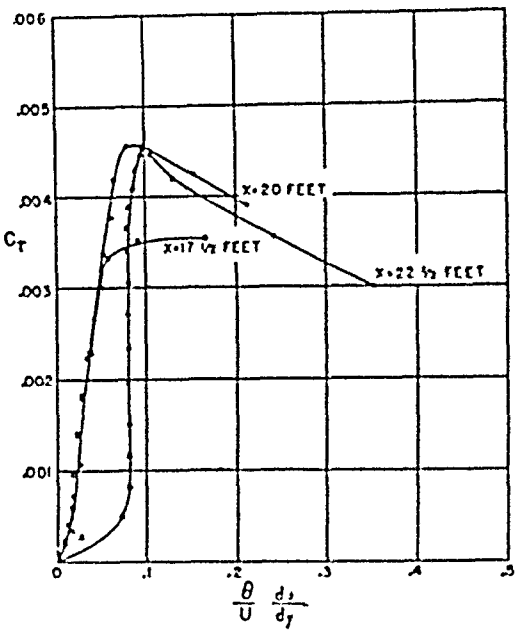

FIG. 24.—Relation between shearing stress coefficient and mean velocity gradient.

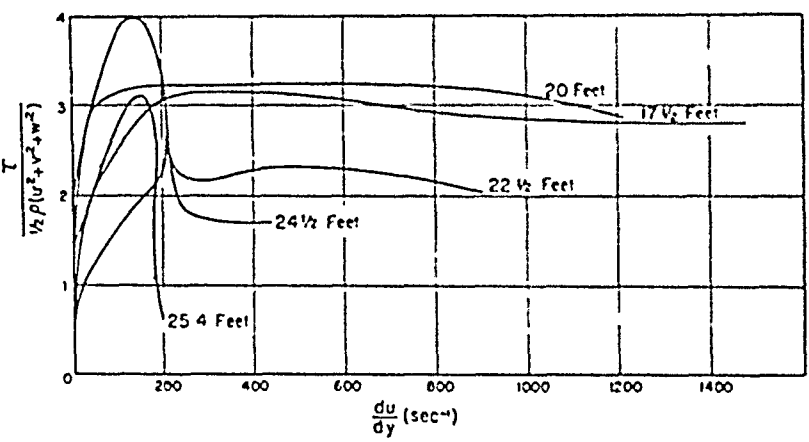

FIG. 25.—Ratio of shearing stress τ to mean energy of turbulence as a function of the mean velocity gradient.

17½- and 20-ft positions the ratio is almost independent of du/dy except in the outer part of the layer where τ falls to zero and the turbulence decreases to that of the free stream. Perhaps if the free stream were sufficiently free from turbulence, both quantities would fall to zero together, retaining a constant ratio. Nevzgljadov's assumption is not a

good approximation but confirmation is given to von Kármán's assumption of statistical similarity between the fluctuations at different points in the same cross section. However, for stations further downstream as the boundary layer proceeds further against the adverse pressure gradient, there is considerable variation in the ratio of τ to $(u'^2 + v'^2 + w'^2)$.

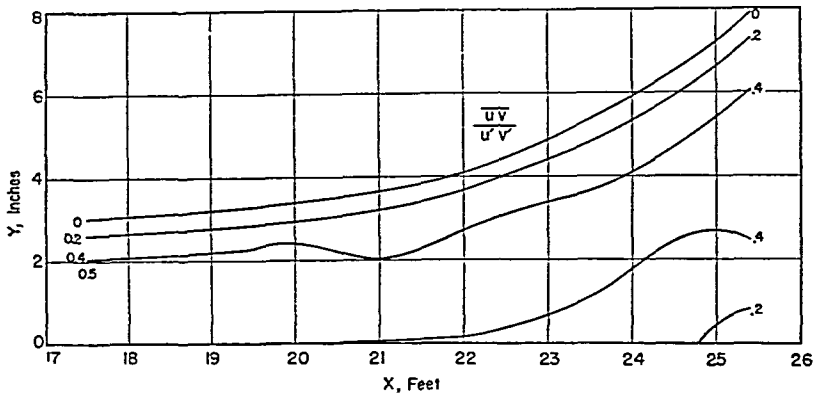

FIG. 26.—Contour map of uv correlation coefficient for NBS turbulent boundary layer.

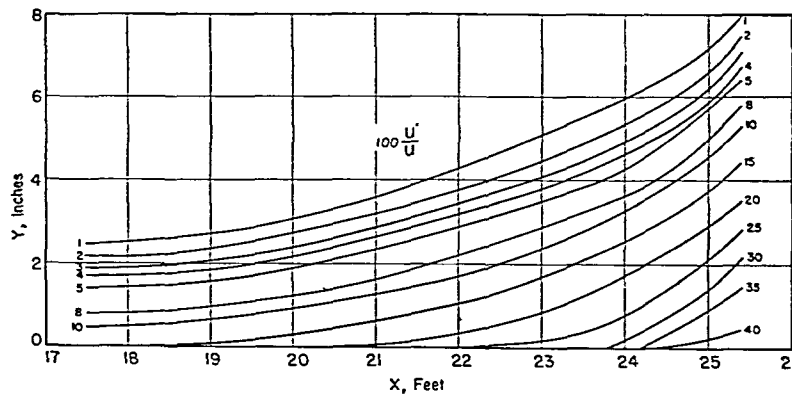

FIG. 27.—Contour map of u'/u for NBS turbulent boundary layer.

Contours of the uv correlation coefficient are shown in Fig. 26. Comparison of Figs. 19, 20, 21, 22 and 26 shows that the turbulent stress near the wall falls regularly and smoothly as separation is approached and that the decrease is caused by decreasing uv correlation and not by any marked diminution in u' or v'. The laminar sublayer apparently serves only as a medium for transferring the stress from the fluid to the wall and does not play any fundamental rôle in the phenomenon of turbulent separation.

Although the absolute values of u', v', and w' near the wall decrease slowly as separation is approached, they become continually increasing fractions of the mean speed because of the decreasing mean speed. At separation the u' fluctuation near the wall exceeds 40 per cent of the local mean speed as seen in Fig. 27. Hence there are probably extended areas of intermittent reverse flow just upstream from the mean separation point, since it is well known that momentary fluctuations of three times the root mean square value are quite frequent.

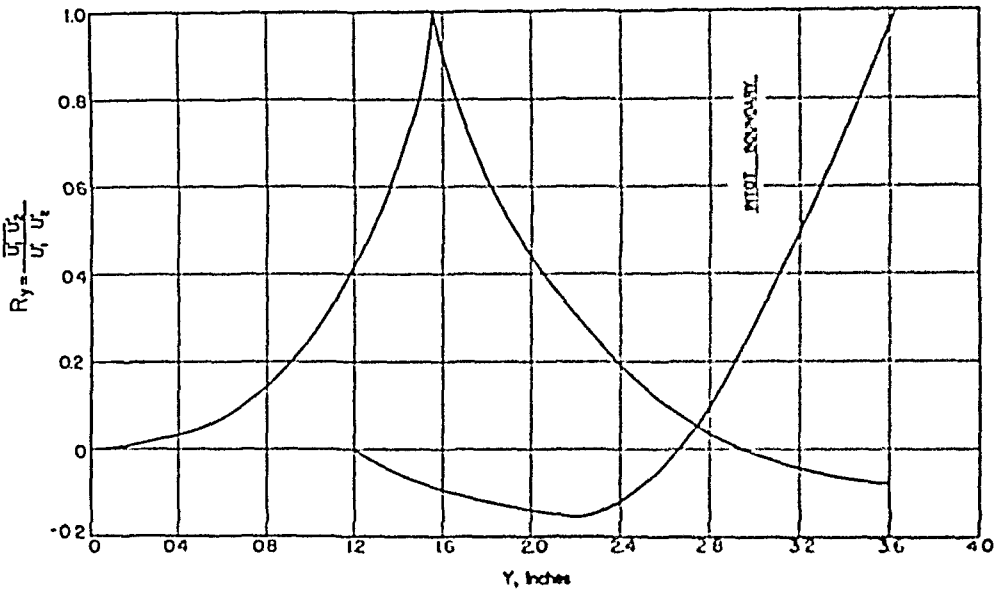

FIG. 28.—Correlation between velocity fluctuations at two points in the same cross section of the NBS turbulent boundary layer at $x = 20$ ft.

At left, one point is fixed at $y = 1.56$ inches, at right one point is fixed at $y = 3.62$ inches.

A few measurements have been made of the correlation between u fluctuations at two points in the same cross section of the boundary layer as function of location of one of the points and their distance apart. The cross section selected was at 20 ft from the leading edge. Two typical curves are shown in Fig. 28. The surprising result is that there is a positive correlation between the fluctuation at any point in the boundary layer and that at a point in the middle of the boundary layer, and a negative correlation between the fluctuations at a point just outside the boundary layer and that at the middle of the boundary layer. The spatial extent of the disturbance at any instant is large compared with the boundary layer thickness. Here again the mixing length concept seems wholly inadequate.

The negative correlation may be interpreted as the effect of the outer rough "edge" of the boundary layer on the external flow, an effect sug-

gested by G. I. Taylor in private discussion. If the disturbance is predominantly a slowing up of the boundary layer at any moment, the boundary layer will thicken by reason of the continuity of the flow. This presents a bump to the outer potential flow, and the outer flow will speed up in passing over the bump. Thus the two effects will be in opposite phase and there will be a negative correlation.

In terms of the kinetic theory analogy or the mixing length description, these results show that the "mean free path," mixing length, or scale of the turbulent processes is large compared with the thickness of the boundary layer. Considerable masses of fluid move as more or less coherent units. The process cannot be smoothed by averaging over a small volume because it is not possible to choose dimensions small compared with the boundary layer thickness and at the same time large compared with a single fluid element. The mixing-length idea and even the idea that the turbulent fluctuations and turbulent shear stress are directly related to the mean speed at a point and its derivatives at that point must be abandoned. Shall the flow then be regarded as a mean flow that merely transports and distorts large eddies superposed on the flow, these eddies being of varying size and intensity? Or shall the flow be regarded as a mean flow on which traveling wave systems are superposed, each wave extending across the entire boundary layer and traveling at a speed determined by the geometry of the whole boundary layer, the speed outside the boundary layer, and the physical properties of the fluid? It is hoped such questions will be answered by further experiment.

The rapidly developing theory of random functions (96) may possibly form the mathematical framework of an improved theory of turbulence. However it is necessary to separate the random processes from the non-random processes. It is not yet fully clear what the random elements are in turbulent flows. The experimental results described suggest that the ideas of Tollmien and Prandtl that the measured fluctuations include both random and non-random elements are correct, but as yet there is no known procedure either experimental or theoretical for separating them.

Bibliography
on
Turbulent Flow in Boundary Layers

84. Taylor, G. I., Statistical theory of turbulence, V. Effect of turbulence on boundary layers, *Proc. Roy. Soc. (London) A*, **156**, 307–317 (1936).

85. Taylor, G. I., Flow in pipes and between parallel planes, *Proc. Roy. Soc. (London) A*, **159**, 496–506 (1937).

86. Von Doenhoff, A. E., and Tetervin, N., Determination of general relations

for the behavior of turbulent boundary layers, *N.A.C.A. Wartime Report*, L-382 (1943).

87. Goldstein, S., The similarity theory of turbulence, and flow between parallel plates and through pipes, *Proc. Roy. Soc. (London) A*, 159, 473–496 (1937).
88. Squire, H. B., and Young, A. D., The calculation of the profile drag of aerofoils, *Brit. A.R.C., Repts. and Memo.* No. 1838 (1938).
89. Jacobs, W., Umformung eines turbulenten Geschwindigkeitsprofils, *Z. angew. Math. Mech.*, 19, 87–100 (1939); also *N.A.C.A. Tech. Memo.* No. 951 (1940).
90. Sasaki, T., On the theory of turbulent boundary layer on a flat plate, *Aeronaut. Research Lab. Rept., Tokyo Imp. Univ.*, 16 (No. 8), 483–492 (1941). (Japanese text, English summary.)
91. Kalikhman, L. E., A new method for calculating the turbulent boundary layer and determining the separation point, Compt. Rend. *Akad. Nauk U.S.S.R.* Leningrad, 38, 180–185 (1943).
92. Kehl, A., Untersuchungen über konvergente und divergente turbulente Reibungsschichten, *Ing. Arch.*, 13, 293–329 (1943).
93. Mohr, E., Laminare und turbulente Strömungen mit besonderer Berücksichtigung des Einflusses von festen Wänden, *Z. Physik*, 121, 301–350 (1943).
94. Nevzgljadov, V., A phenomenological theory of turbulence, *J. Phys. (U.S.S.R.)*, 9, 235–243 (1945).
95. Tetervin, N., Approximate formulas for the computation of turbulent boundary layer momentum thicknesses in compressible flows, *N.A.C.A. Wartime Rept.* L-119 (1946).
96. Bass, J., Les fonctions aléatoires et leur interpretation mécanique, *Revue sci.*, 83, 3–20 (1945).

Bibliography of Related Papers

Drag Calculations

97. Fage, A., Profile and skin friction airfoil drags, *Brit. A.R.C., Repts. and Memo.* No. 1852 (1938).
98. Piercy, N. A. V., Preston, J. H., and Whitehead, L. G., Approximate prediction of skin friction and lift, *Phil. Mag.* [7], 26, 791–815 (1938).
99. Squire, H. B., and Young, A. D., The calculation of the profile drag of airfoils, *Brit. A.R.C., Repts. and Memo.* No. 1838 (1938).
100. Pretsch, J., Zur theoretischen Berechnung des Profilwiderstandes, *Jahr. deut. Luftfahrtforsch.*, 1938, Vol. I, 60; also *N.A.C.A. Tech. Memo.* No. 1009 (1942).
101. Young, A. D., The calculation of the total and skin friction drags of bodies of revolution at 0° incidence, *Brit. A.R.C., Repts. and Memo.* No. 1874 (1939).
102. Tetervin, N., A method for the rapid estimation of turbulent boundary-layer thicknesses for calculating profile drag, *N.A.C.A. Wartime Rept.* L-16 (1944).
103. Jacobs, E. N., and von Doenhoff, A. E., Formulas for use in boundary-layer calculations on low-drag wings, *N.A.C.A. Wartime Rept.* L-319 (1941).
104. Schultz-Grunow, F., Neues Reibungswiderstandsgesetz für glatte Platten, *Luftfahrtforsch.*, 17, 239–246 (1940); also *N.A.C.A. Tech. Memo.* No. 986 (1941).
105. Falkner, V. M., A new law for calculating drag. The resistance of a smooth flat plate with turbulent boundary layer, *Aircraft Eng.*, 15, 65–69 (1943).

106. NITZBERG, G. E., A concise theoretical method of profile-drag calculations, *N.A.C.A. ACR* No. 4B05 (1944). (Now declassified.)

Flight Tests on Boundary Layers

107. JONES, B. N., Flight experiments on boundary layers, *J. Aeronaut. Sci.*, **5**, 81–101 (1938); also *Engineering*, **145**, 397 (1938); also *Aircraft Eng.*, **10**, 135–141 (1938).
108. STEPHENS, A. V., and HASLAM, J. A. V., Flight experiments on boundary layer transition in relation to profile drag, *Brit. A.R.C., Repts. and Memo.* No. **1800** (1938).
109. RUMPH, L. R., JR., and SCHAIRER, R., Boundary layer and wake survey measurements in flight and in the wind tunnel, *J. Aeronaut. Sci.*, **7**, 425–433 (1940).
110. YOUNG, A. D., and MORRIS, D. E., Note on flight tests on the effect of slipstream on boundary layer flow, *Brit. A.R.C. Repts. and Memo.* No. **1957** (1939).

Modern Trends in Nonlinear Mechanics

By N. MINORSKY

Stanford University

"Ce qui nous rend ces solutions périodiques
"si precieuses, c'est qu'elles sont, pour
"ainsi dire, la seule brèche par où nous
"puissions essayer de pénétrer dans une
"place jusqu'ici réputée inabordable"
Henri Poincaré

1. Introduction

During the decade preceding World War II there appeared numerous publications in the U.S.S.R. in connection with so-called nonlinear

mechanics, that is, a branch of mathematical physics amenable to nonlinear differential equations. An outline of this activity in its various phases is attempted in this review.

It may be useful to give a brief historical background of these studies. In its broad aspects the subject is not new, inasmuch as Euler, Lagrange, Pōinsot and other mathematicians of the nineteenth century came across nonlinear problems and succeeded in giving at least qualitative solutions in some special cases.

The development of the theory of linear differential equations in the middle of the last century resulted in a tendency to *linearize* the nonlinear problems so as to bring them within the scope of the linear theory. This trend resulted in the development of the well-known *method of small motions*, owing to which much was gained in the uniformity of treatment of the various problems. The drawback of the procedure was, however, in the restriction of problems to only *small motions* occurring in the neighborhood of equilibrium. In many applied problems this restriction is not serious and this is the principal reason why this method is so widely used in applications. It is apparent, however, that for the investigation of the phenomena in *the large* the method of small motions is inadequate.

At the end of the last century H. Poincaré undertook the analysis of solutions of certain nonlinear differential equations in the large (1). One important result of his analysis was the discovery of certain *closed characteristics*, which he calls the *limit cycles.* In another treatise devoted mainly to astronomical problems (2) Poincaré attacked the problem of integration of certain nonlinear differential equations by means of series expansions in terms of certain parameters. This method is sometimes designated as *the method of small parameters.* For a long time the work of Poincaré remained without any connection with applied problems except in astronomy.

Nearly a quarter century after these researches of Poincaré, the Dutch physicist B. van der Pol called attention (3) to certain nonlinear problems involved in the operation of the electron tube oscillators. It was pointed out that, inasmuch as the stationary oscillations observed in such oscillators take place with amplitudes far from the equilibrium point, it is obvious that one is confronted with a typical behavior of the system in the large so that the application of the method of small motions becomes meaningless under these conditions. Moreover, on purely physical grounds, it was also clear that what limits the amplitude in its stationary condition is the nonlinearity of the characteristic of the electron tube. In his search for the formulation of the problem, Van der

Pol succeeded in establishing a nonlinear differential equation bearing his name

$$\ddot{x} - \mu(1 - x^2)\dot{x} + x = 0 \tag{1}$$

where x is the coordinate and μ is a parameter. Van der Pol explored the field of solutions of his equation graphically by the method of isoclines and found that, in fact, in the plane of the variables $(x,\dot{x})$ all solutions approach a certain *closed solution.*

The discovery of van der Pol attracted universal attention, and a number of important papers (4,5) appeared shortly thereafter, although the connection with the theory of Poincaré was not noticed initially.

In 1929 Andronow (6) pointed out that the closed solution of the van der Pol equation is, in fact, the limit cycle of the theory of Poincaré.

From that moment the codification of nonlinear mechanics progressed along a definite theoretical pattern. At later stages there appeared two distinct trends: (a) the topological methods of qualitative integration and (b) the analytical methods leading to the quantitative solutions following the scope of the two treatises of Poincaré in the order mentioned. The theoretical researches conducted in the U.S.S.R. were closely coordinated with numerous experimental investigations and the whole program was directed by L. Mandelstam and N. Papalexi, who contributed much to the development of the theory of subharmonic resonance. Some of these theoretical researches departed eventually from the scope of the theory of Poincaré and followed, at least as far as the higher approximations are concerned, another astronomical method of Lindstedt; these modifications appear in the publications of Kryloff and Bogoliuboff (7).

This review deals only with the systems with one degree of freedom and is limited to the case when the parameter is a small number. A greater emphasis is laid on the equations of the first approximation as probably the only ones that are of interest in applications. A brief outline of the theory of the approximations of higher orders is given in section 13. Generalizations for systems with several degrees of freedom do not present any particular difficulty except in added complications in calculations. In view of the space limitation they could not find place here. Far more serious is the question of extending these methods for large values of the parameter that is outside the scope of the theory of Poincaré. Although some theoretical progress has been recently accomplished (8) the situation is far from being definitely settled. [The reader interested in additional details of the questions treated in this review is referred to N. Minorsky, *Introduction to Non-linear Mechanics* (Edwards

Bros., Ann Arbor, Mich., 1947), in which the whole subject is treated more fully.]

I. Topological Methods

2. *Phase Plane; Trajectories; Motions; Singular Points*

It is useful to review first a few fundamentals of the theory of differential equations in real domain referring the reader for a more complete information to the text books on this subject (9).

In what follows we shall deal with the differential equations of the form

$$\frac{dx}{dt} = P(x,y); \qquad \frac{dy}{dt} = Q(x,y). \tag{2.1}$$

A differential equation of the second order can always be reduced to the system (2.1) if one sets $y = dx/dt$. In applications (2.1) usually characterizes a system with one degree of freedom. The quantities x and y can be conveniently considered as cartesian coordinates in a certain (x,y) plane called *the phase plane.*

We shall call the curve specified by the equation

$$\frac{dy}{dx} = \frac{Q(x,y)}{P(x,y)} \tag{2.2}$$

the *phase trajectory** or, simply, trajectory. We shall define a point (x_0,y_0) for which $P(x_0,y_0) = Q(x_0,y_0) = 0$ a *singular point.* Any point that does not have this property will be called an *ordinary point.*

From these definitions it follows that an ordinary point is characterized by a definite slope of the tangent to the trajectory passing through that point; for a singular point, on the contrary, the direction of the tangent is indeterminate and the trajectory degenerates into one point, the singular point itself.

Using these definitions we can formulate the theorem of Cauchy as follows:

Through every ordinary point of the phase plane passes one, and only one, phase trajectory.

We can also consider equations (2.1) as defining a vector field with components dx/dt, dy/dt; for a singular point both components vanish. More specifically, if the vector field is a velocity field, it is clear that a singular point is a point at which the velocity vector vanishes.

* In mathematical texts the term *characteristic* is generally used. We prefer, however, to use the word *trajectory* inasmuch as we shall reserve the term *characteristic* as an engineering term (*e.g.*, characteristic of an electron tube).

We shall often speak of the point $R(x,y)$, *the representative point*, moving on a trajectory in accordance with equations (2.1), which thus define a certain *motion* on this trajectory. Since the time t does not enter explicitly on the right side of (2.1), the general solution can be written as

$$x = x(t - t_0, x_0, y_0) = x(t)$$
$$y = y(t - t_0, x_0, y_0) = y(t). \tag{2.3}$$

A trajectory is obtained by eliminating $(t - t_0)$ between these equations. Thus, equations (2.1) give the law of motion or, simply, *the motion*, while (2.2) determines a certain geometric curve passing through a given point. Since the time origin t_0 is arbitrary, it is clear that to a given trajectory corresponds an infinity of motions differing by the arbitrary selection of t_0. This can be stated differently: the solutions of the differential equations (2.1) form a two-parameter family while the trajectories defined by (2.2) form a one-parameter family. The topological methods studied here deal with the general topological aspects of trajectories defined by (2.2), while the analytical methods treated in part II deal with the differential equations (2.1).

In connection with dynamical problems an additional remark is noteworthy: A singular point for which dx/dt and dy/dt vanish simultaneously is clearly a point of equilibrium inasmuch as both the velocity and the acceleration of the system are zero at this point.

3. *Elementary Singular Points*

The consideration of a few simple differential equations will enable us to define the elementary singular points with which we shall be concerned in the discussion that follows.

a. Vortex Point. The differential equation of a harmonic oscillator $m\ddot{x} + cx = 0$ reduces to the form (2.1)

$$\frac{dy}{dt} = -\left(\frac{c}{m}\right)x = -\omega_0^2 x; \qquad \frac{dx}{dt} = y$$

and the equation of trajectories is

$$\frac{dy}{dx} = -\omega_0^2 \frac{x}{y}.$$

Integrating this equation we obtain $\frac{x^2}{\alpha^2} + \frac{y^2}{\beta^2} = \lambda$, where $\alpha^2 = \frac{2h}{\omega_0^2}$ and $\beta^2 = 2h$, h being the integration constant.

The trajectories thus form a family of homothethic ellipses with the ratio between the semi-axes equal to ω_0. The center of these ellipses $x = y = 0$ is a singular point called *the vortex point* (Fig. 1). The trajectories are thus closed curves enclosing the vortex point in their interior; none of trajectories approaches the vortex point.

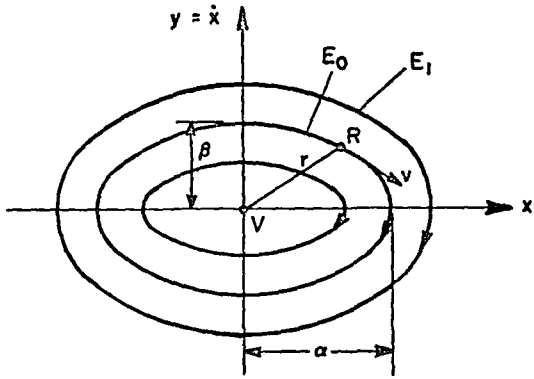

FIG. 1.

b. Saddle Point. The differential equation of an unstable motion (*e.g.*, a pendulum near its position of unstable equilibrium) $m\ddot{x} - cx = 0$ reduces to (2.1):

$$m\frac{dy}{dt} = cx; \qquad \frac{dx}{dt} = y$$

and (2.2) in this case is

$$\frac{dy}{dx} = \left(\frac{c}{m}\right)\frac{x}{y} = \omega_0^2\frac{x}{y}.$$

The integration gives

$$y^2 - \omega_0^2 x^2 = h$$

where h is an integration constant. The trajectories are thus hyperbolas, as shown in Fig. 2. The asymptotes are obtained by putting $h = 0$. The point $x = y = 0$ is a singular point called *the saddle point.* In this case there are two singular trajectories passing through the saddle point. The motions on these two trajectories are asymptotic, approaching the saddle point either for $t = +\infty$ or for $t = -\infty$, as indicated by the arrows. The field of trajectories in the neighborhood of a saddle point represents all possible motions occurring in the neighborhood of an unstable position of equilibrium.

c. Focal Point. The differential equation of a damped oscillator with unit mass is

$$\ddot{x} + 2b\dot{x} + \omega_0^2 x = 0 \qquad (3.1)$$

provided $b^2 - \omega_0^2 < 0$. The system (2.1) in this case is

$$\frac{dy}{dt} = -2by - \omega_0^2 x; \qquad \frac{dx}{dt} = y$$

and (2.2) gives

$$\frac{dy}{dx} = -\frac{(2by + \omega_0^2 x)}{y}.$$

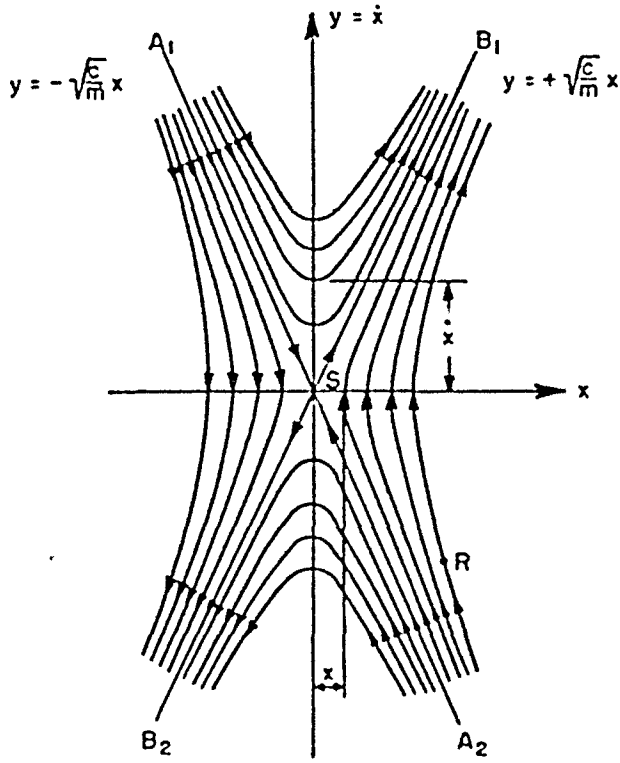

FIG. 2.

The origin $x = y = 0$ is again a singular point, *the focal point*. From the elementary theory it is known that the solution in the (x,t) plane is of the form

$$x = x_0 e^{-bt} \cos(\omega_1 t + \alpha)$$

where x_0 and α are constants of integration. Equation (2.2) in this case is a homogeneous equation of the first order and can be integrated by introducing a new variable u defined by equation $y = ux$. Transforming the general integral of this equation into polar coordinates, we obtain finally the equation of trajectories in the form

$$\rho = Ce^{\frac{b}{\omega_1}\psi}.$$

The trajectories are thus logarithmic spirals in a certain phase plane. It can be easily shown that for a normal *dissipative damping*, the motions on these spirals *approach* the focal point, as is obvious on physical grounds. The arrows on Fig. 3 show the direction of this approach. It is also clear that the trajectories approach the focal point without any definite direction inasmuch as the radius vector turns an infinite number of times as the motion on the trajectory approaches the focal point asymptotically.

d. Nodal Point. If $b^2 - \omega_0^2 > 0$ in (3.1) this equation, as is well known, has an aperiodically damped solution in the (x,t) plane that corresponds to the existence of two real roots r_1 and r_2 in the characteristic equation. Solutions in this case are of the form

$$x = Ae^{-r_1 t} + Be^{-r_2 t}$$

where A and B are constants of integration. If we eliminate t between x and $\dot{x}$ and change the variables, we find the following form of solutions in a (u,v) plane

$$v = Cu^a$$

where C is an integration constant and $a = r_1/r_2$. If one reverts to the original $(x,\dot{x})$ plane the trajectories have the appearance of certain parabolic curves shown in Fig. 4. The origin $x = y = 0$ is a singular point called *the nodal point.* For a positive (dissipative) damping the direction on trajectories is *toward* the nodal point, as shown by the arrows. It is observed that here the trajectories approach the nodal point from certain definite directions.

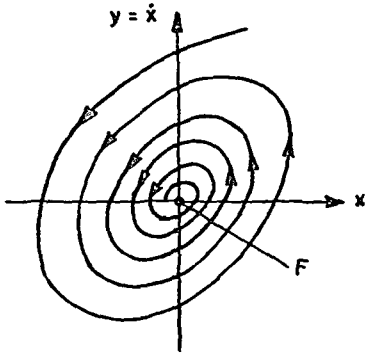

FIG. 3.

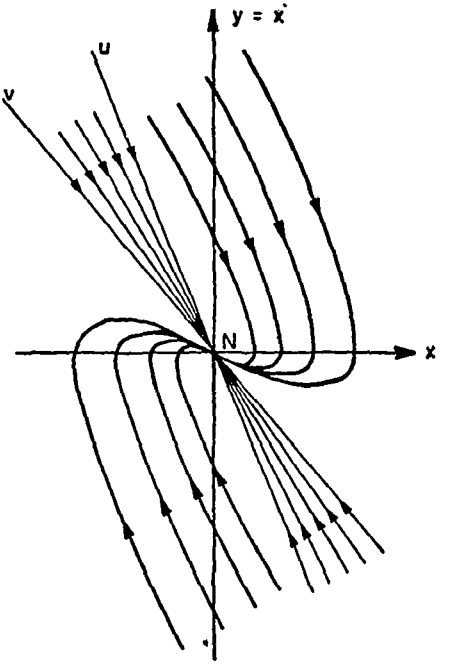

FIG. 4.

These properties can be summarized in the following self-explanatory table:

	Nature of motion	Neighborhood of	Approach
Vortex point..	Oscillatory undamped	Stable equilibrium	None
Saddle point..	Aperiodic	Unstable equilibrium	None, except on the asymptotes
Focal point...	Oscillatory damped	Stable equilibrium	Without any definite direction
Nodal point...	Aperiodic	Stable equilibrium	From some definite directions

It must be added that for a greater generality we have to include also the case of the so-called *negative damping* frequently encountered in engineering practice. The negative damping, or energy input according to the velocity law, formally means that b in the preceding equations is negative. The only change to be made in the preceding pictures of trajectories in the neighborhood of focal and nodal points is the reversed directions of the arrows. *Instead of approaching these singularities*, the trajectories in this case *depart* from them or, we may say, approach them for $t = -\infty$. In such a case the focal or nodal point are called *unstable.*

4. *Nonlinear Conservative Systems*

Consider a simple nonlinear conservative system with one degree of freedom represented by a differential equation of the form

$$\ddot{x} = f(x) \tag{4.1}$$

where $f(x)$ may be considered as a "nonlinear force." We can write this equation in form (2.1):

$$\frac{dy}{dt} = f(x); \qquad \frac{dx}{dt} = y$$

and the equation of trajectories (2.2) is here

$$\frac{dy}{dx} = \frac{f(x)}{y}. \tag{4.2}$$

From this equation it follows that a trajectory crosses the x-axis at right angles and has a horizontal tangent at such points x that are the roots of the equation $f(x) = 0$ provided $y \neq 0$ at these points which we exclude. Since the system is conservative by our assumption, the

integral of energy exists. If we assume for the sake of simplicity a system with unit mass, this integral is

$$\tfrac{1}{2}y^2 + V(x) = h \tag{4.3}$$

where the first term on the left side is the kinetic, and the second the potential energy and (4.3) expresses the fact that the sum of these energies remains constant. Since, by definition, $V(x) = -\int_0^x f(x)dx$, the

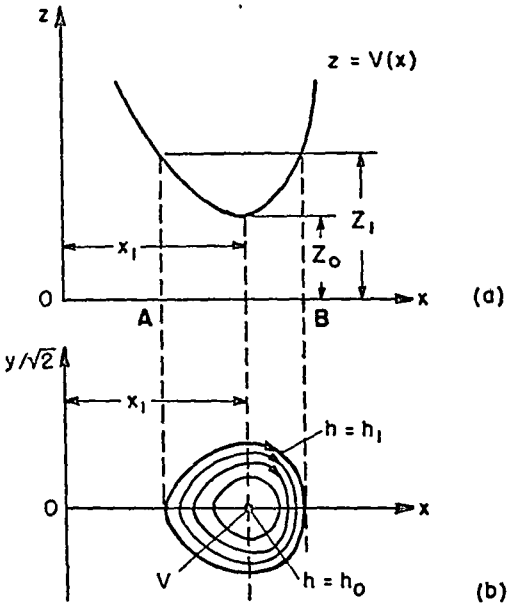

FIG. 5.

points of equilibrium correspond to the extremum values of $V(x)$, that is, to $f(x) = 0$. Trajectories are symmetrical with respect to the x-axis and the quantity $h - V(x)$ must be positive if y is to be real. The general qualitative aspect of trajectories can be readily obtained by the following graphical procedure, shown in Fig. 5. We assume that in a certain physical problem the potential energy has the form shown by curve $V(x)$ in Fig. 5(a) and let the constant of energy h have some value $h = z_1$. It is clear that no motion can exist outside the interval AB. We project the interval AB on the x-axis of the lower figure and for each point of the interval calculate the value $y/\sqrt{2}$ from (4.3), which gives a certain closed symmetrical curve. For some other value of h another curve is obtained. If we continue to decrease h we finally reach the value $h = z_0$, for which the straight line $h = z$ is tangent to $V(x)$. For this particular value of h the closed curve reduces to one point, the vortex point of the

family of closed trajectories. Clearly no closed trajectories can exist if $h < z_0$. This elementary argument can be applied to more complicated situations, such as the one depicted in Fig. 6. If we proceed in the manner just explained, we find two vortex points M and N surrounded by oval closed trajectories. If the constant of energy h is increased up to the value $h = z_p$, at which the horizontal line is tangent to $V(x)$ at its maximum point, a somewhat peculiar situation is encountered: the two

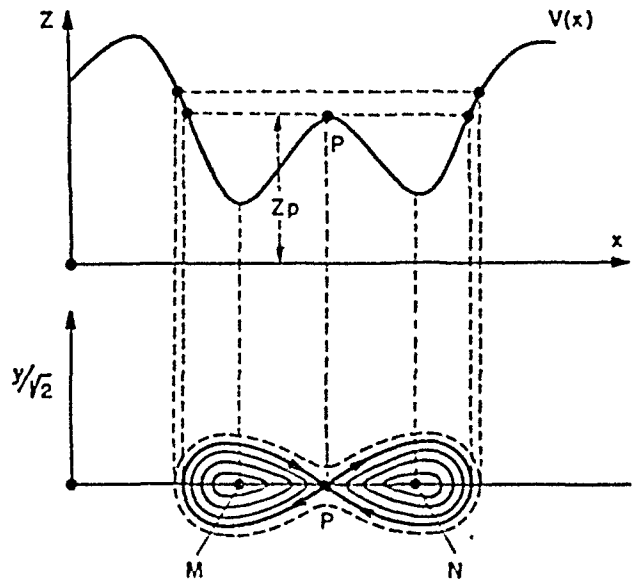

FIG. 6.

"islands" of closed trajectories touch at the point P; the singular trajectory obtained in this case is shown by a heavy line. On the other hand, from theoretical mechanics it is well known that the point P at which the potential energy is maximum is a point of *unstable equilibrium;* moreover, it is also known (10) that when the constant of energy is exactly equal to the potential energy of the unstable equilibrium point the motion becomes asymptotic toward that point. We conclude, therefore, that P is a saddle point. The closed curve in heavy line issuing from the saddle point is sometimes called the *separatrix*, inasmuch as it separates the motions of one type from motions of an entirely different type. In fact, if the constant of energy is just slightly increased, the motion is entirely different, and it is shown by a broken line enclosing two vortex points, M and N, and one saddle point, P.

This simple discussion shows that the topological aspect of trajectories may change at certain special values of a parameter appearing in the first integral of the dynamical problem.

It is more convenient, however, as was shown by Poincaré (11), to introduce the parameter into the differential equation itself.

Let us assume, for example, that the potential energy $V(x,\lambda)$ depends on a certain parameter λ. The nonlinear force, as before, is given by the expression

$$f(x,\lambda) = -\frac{\partial V(x,\lambda)}{\partial x}. \tag{4.4}$$

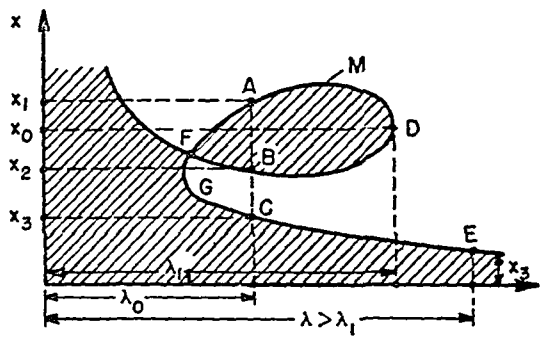

FIG. 7.

The positions of equilibrium are given by equating this expression to zero, which means a certain curve in the (x,λ) plane such as shown in Fig. 7. If the parameter λ is varied, there may be, for example, either three positions of equilibrium (*e.g.*, x_1, x_2, and x_3 corresponding to $\lambda = \lambda_0$) or only one, at the point E. The change from three positions of equilibrium to one occurs at the point D, corresponding to the *critical value* $\lambda = \lambda_1$ of the parameter. If we differentiate the equation $f(x,\lambda) = 0$ with respect to λ, we get

$$\frac{dx}{d\lambda} = -\frac{f_\lambda(x,\lambda)}{f_x(x,\lambda)}. \tag{4.5}$$

It is thus seen that the critical value of the parameter occurs when $f_x(x,\lambda) = 0$, which indicates that the tangent is vertical as at the point D. We shall not enter here into the consideration of a still more complicated case, when the expression (4.5) is indeterminate, but shall indicate the following theorem of Poincaré, which we shall have an occasion to use.

Theorem. If the region in which $f(x,\lambda) > 0$ is *below* the curve $f(x,\lambda) = 0$ (assuming $x > 0$; $\lambda > 0$), the equilibrium is stable; if it is above that curve, the equilibrium is unstable.

In fact, let us assume that the shaded area in Fig. 7 represents the region in which $f(x,\lambda) > 0$ and consider a point below the curve, proceed-

ing in the direction of increasing x with λ fixed. It is clear that $f(x,\lambda)$ decreases so that $f_x < 0$, which indicates the existence of a minimum of the potential energy and, hence, stability. The opposite conclusion is obtained if the region of $f(x,\lambda) > 0$ is above the curve $f(x,\lambda) = 0$. Thus the branches FAD and GCE are stable and GF and FBD unstable.

This can be summarized also as follows: *the points of equilibrium in conservative systems always appear and disappear in pairs*, for the critical values of the parameter. Everything happens as though a vortex point and a saddle point destroy each other upon their coalescence so that there remain no more equilibrium points thereafter.

As an example of the application of this method, let us consider a relative motion of a frictionless pendulum (12) of mass m, length a, rotating with angular velocity Ω about the vertical. An elementary calculation shows that the force $f(x,\lambda)$ of the preceding theory is here the moment

$$M(\theta,\lambda) = m\Omega^2a^2(\cos\theta - \lambda)\sin\theta$$

where $\lambda = g/(\Omega^2a^2)$. The differential equation of the relative motion is

$$I\ddot{\theta} - m\Omega^2a^2(\cos\theta - \lambda)\sin\theta = 0$$

where I is the moment of inertia of the pendulum and θ the angle of oscillation. The system (2.1) is

$$I\dot{\omega} - m\Omega^2a^2(\cos\theta - \lambda)\sin\theta = 0; \qquad \dot{\theta} = \omega$$

and (2.2) becomes

$$\frac{d\omega}{d\theta} = \frac{m\Omega^2a^2(\cos\theta - \lambda)\sin\theta}{I\omega}.$$

The singular points are: $\omega_1 = 0$, $\theta_1 = 0$; $\omega_2 = 0$, $\theta_2 = \pi$; $\omega_3 = 0$, $\theta_3 = \cos^{-1}\lambda$. The third singular point exists only for a sufficiently large angular velocity Ω. The points of equilibrium are given by the equation $M(\theta,\lambda) = 0$, that is, $\theta = 0, \pi, -\pi$, and $\theta = \cos^{-1}\lambda$.

Fig. 8 represents the (θ,λ) diagram for these values, with shaded regions corresponding to $M(\theta,\lambda) > 0$ and the non-shaded ones to $M(\theta,\lambda) < 0$. The application of the preceding theorem gives the stable branches (*i.e.*, vortex points) indicated by heavy points and the unstable ones (the saddle points) by circles. The points $\theta = 0, \lambda = 1$; $\theta = \pi, \lambda = -1$; $\theta = -\pi$, $\lambda = -1$ are the *branch points of equilibrium* and the values $\lambda = \pm 1$ are *the critical values* of the parameter λ at these points. The system being conservative, the integral of energy exists and is

$$(\tfrac{1}{2})I\dot{\theta}^2 - m\Omega^2a^2\left(\sin^2\frac{\theta}{2} + \lambda\cos\theta\right) = h.$$

We obtain the equation of the separatrix by writing that the constant h has particular values for which $\dot{\theta} = 0$ at the saddle point, viz., $\theta = \pm\pi$. In the (ω,θ) plane this separatrix (curve A in Fig. 9) is given by the equation

$$\omega^2 = \left(\frac{m\Omega^2a^2}{I}\right)[\sin^2\theta + 2\lambda(\cos\theta + 1)].$$

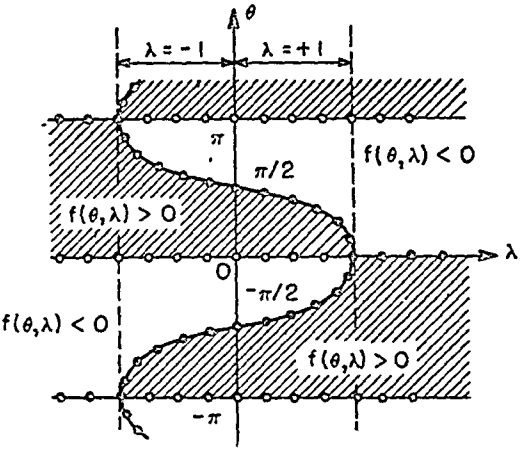

FIG. 8.

There exists also a second separatrix B passing through the saddle point $\theta = 0$, $\omega = 0$. Its equation is

$$\omega^2 = \left(\frac{m\Omega a^2}{I}\right)[\sin^2\theta + 2\lambda(\cos\theta - 1)]$$

Fig. 9 shows the topology of trajectories. It is interesting to note that the origin is a vortex point if $\Omega = 0$ and is a saddle point if $\Omega \neq 0$. In the latter case there appear also two vortex points V_1 and V_2; around each of these vortex points there exist closed asymmetrical trajectories. If the parameter is increased so that the separatrix B is crossed, the topological aspect of trajectories changes; there appear now symmetrical closed trajectories around the combination of the two vortex points and one saddle point. If the parameter goes through a second critical value for which the second separatrix A is crossed, the motion changes again and becomes rotatory (broken line).

For $\lambda = 0$, that is, for $\Omega \to \infty$, both separatrices coalesce and the vortex points move toward $\theta = \pm\pi/2$ positions. For $|\lambda| > 1$ there appear vortex points $\theta = 0$, π, $-\pi$, but the intermediate range disappears

entirely. Thus the values $\lambda = -1$; $\lambda = 0$; $\lambda = +1$ are the *critical values* of the parameter λ.

It may be useful to mention here another theorem of Poincaré, which we shall not prove here but which is apparent from the preceding:

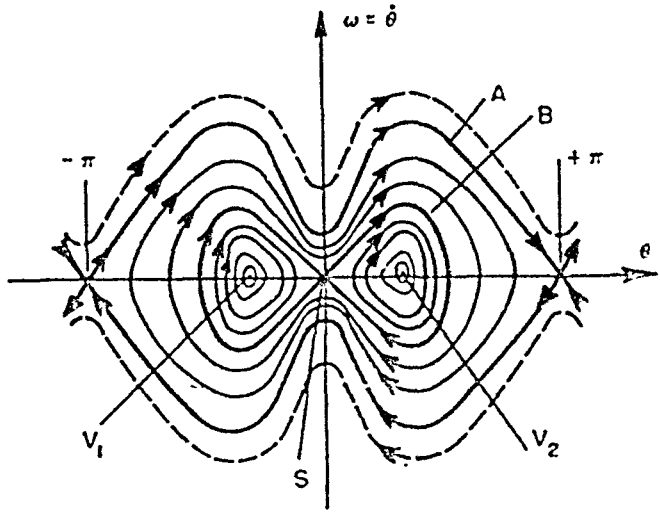

FIG. 9.

Closed trajectories may exist around an odd combination of singular points in which the number of vortex points is greater than the number of saddle points by one unit.

5. *Equilibrium*

We shall frequently encounter in the following discussion the questions of stability of equilibrium. At the end of the last century the question of equilibrium was generalized by Liapounoff (13) so as to absorb also the question of *stability of certain stationary motions*. It is clear that the stability of equilibrium may be considered as a particular case of stability of a stationary motion when the latter reduces to zero. Without entering into the details of this difficult subject we shall give here only a sufficiently broad intuitive definition of stability in the sense of Liapounoff and shall pass thereafter to a more restricted problem, in which we shall be primarily interested: the stability of equilibrium. Let us consider a periodic phenomenon indicated by a motion of the representative point R on a closed trajectory C (Fig. 10). Let us consider also a slightly *perturbed motion* depicted by the motion of R' on C'. If the initial distance R_0R_0',

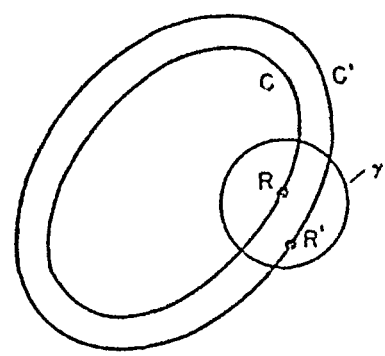

FIG. 10.

which we assume to be small, remains small for any value of time t, *we shall call such a motion stable in the sense of Liapounoff*. It is noted that the stability in this sense requires not only that C and C' be sufficiently close to each other but imposes also a condition that the motion of R on C and of R' on C' be strictly isochronous. We can now give a more precise definition, viz.:

Let $x = x(t,x_0,y_0)$ and $y = y(t,x_0,y_0)$ be the coordinates of a closed trajectory determining a periodic motion on C with period T. By this we mean that $x(0) = x(T)$ and $y(0) = y(T)$.

We shall call a motion *stable in the sense of Liapounoff* if for any given number $\epsilon > 0$ another number η can be found with the property that $|\bar{x}_0 - x_0| < \epsilon$; $|\bar{y}_0 - y_0| < \epsilon$ implies $|x(t,x_0,y_0) - x(t,\bar{x}_0,\bar{y}_0)| < \eta$; $|y(t,x_0,y_0) - y(t,\bar{x}_0,\bar{y}_0)| < \eta$ for all t, where $\bar{x}_0$, $\bar{y}_0$ are slightly modified initial conditions (point R_0').

We now assume that C reduces to a point; this brings us in contact with the important question of *stability of equilibrium.*

Let us consider a system of differential equations

$$\dot{x} = ax + by + P(x,y); \qquad \dot{y} = cx + dy + Q(x,y) \tag{5.1}$$

where P and Q are certain polynomials not having either constant or linear terms in x and y.

Liapounoff shows (14) that as far as the question of equilibrium is concerned we can drop P and Q and consider only the linear terms in these equations. Intuitively this means that inasmuch as the stability of equilibrium depends on what happens to the system if it departs very little from the equilibrium point, x and y are small quantities of the first order, so that P and Q, being of a higher order, can be neglected. Liapounoff's *equations of the first approximation*, therefore, are

$$\dot{x} = ax + by; \qquad \dot{y} = cx + dy. \tag{5.2}$$

It is well known that by a linear transformation of variables

$$\xi = \alpha x + \beta y; \qquad \eta = \gamma x + \delta y \tag{5.3}$$

equations (5.2) can be reduced to the *canonical form*

$$\dot{\xi} = S_1\xi; \qquad \dot{\eta} = S_2\eta \tag{5.4}$$

provided $\begin{vmatrix} \alpha & \beta \\ \gamma & \delta \end{vmatrix} \neq 0$, which we shall assume. Under these conditions the constants S_1 and S_2 are given by the roots of the *characteristic equation*

$$S^2 - (a + d)S + (ad - bc) = 0. \tag{5.5}$$

We shall also assume that $S_1 \neq S_2$, which is of interest in applications. We can now generalize the previous definitions of singular points.

(1) If S_1 and S_2 are real and of the same sign (5.2) has a nodal point. In fact from (5.4) upon the separation of variables and integration we get

$$\eta = C\xi^a \tag{5.6}$$

where $a = S_2/S_1 > 0$ and C is an integration constant. If S_1 and S_2 are negative the nodal point is stable; if they are positive, the nodal point is unstable.

(2) If S_1 and S_2 are of opposite signs and real, (5.2) has a saddle point at the origin $x = y = 0$. A similar procedure leads to the equation of trajectories

$$\eta = C\xi^{-a} \tag{5.7}$$

which represents a family of hyperbolic curves.

(3) If S_1 and S_2 are conjugate complex, (5.2) has a focal point at the origin. Since S_1 and S_2 are conjugate complex, so are ξ and η. If we set $\xi = u + iv$; $\eta = u - iv$, after simple calculations we obtain the system

$$\dot{u} = a_1 u - b_1 v; \qquad \dot{v} = a_1 v + b_1 u.$$

Transforming these equations into polar coordinates $u = r \cos \varphi$; $v = r \sin \phi$ we get finally

$$r = Ce^{\frac{a_1}{b_1}\phi} \tag{5.8}$$

which gives the familiar behavior of trajectories in the neighborhood of a focal point (Fig. 3).

It is convenient to represent the distribution of the various singularities directly from equation (5.5), in which we set $p = -(a + d)$ and $q = ad - bc$ so that (5.5) becomes

$$S^2 + pS + q = 0. \tag{5.9}$$

This representation is shown in Fig. 11 and is useful in practical problems.

As an example, we propose to investigate the nature of equilibrium of an electric circuit containing a nonlinear conductor, an electric arc, shown in Fig. 12. It is well known that the nonlinear function

$$V_a = \psi(i)$$

has the appearance shown in Fig. 13 and that the points of equilibrium are given by the intersection of this curve with a straight line

$$E - Ri = V$$

with notations indicated in Fig. 13. Applying the Kirchhoff laws we obtain the following equations

$$\frac{dV}{dt} = \frac{(E - V - Ri)}{RC}; \qquad \frac{di}{dt} = \frac{(V - \psi(i))}{L}.$$

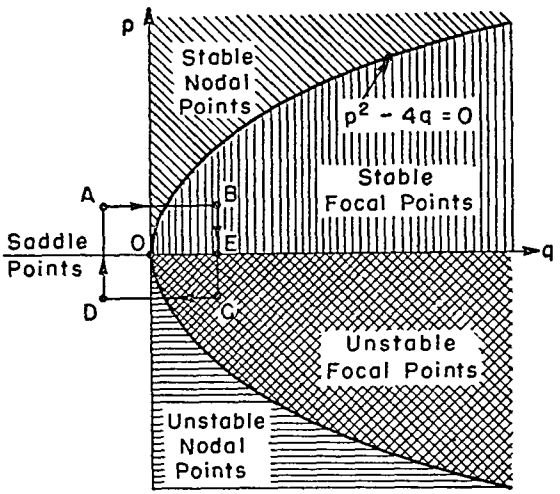

FIG. 11.

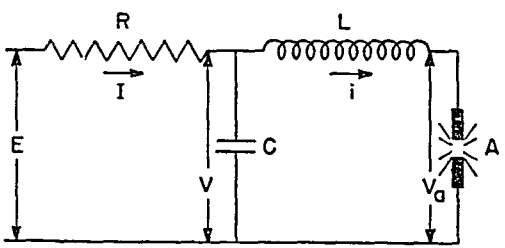

FIG. 12.

Depending on the position of the straight line, there are either three or one single position of equilibrium. We propose to investigate the stability of these various points of equilibrium. Applying the standard procedure of small perturbations v and j around a point (V_0, i_0) of equilibrium, that is replacing $V = V_0 + v$; $i = i_0 + j$ and developing $\psi(i)$ in Taylor's expansion to the first order, we get the following *variational equations*

$$\frac{dv}{dt} = -\frac{v}{RC} - \frac{j}{C}; \qquad \frac{dj}{dt} = \frac{v}{L} - \frac{j\rho}{L} \tag{5.10}$$

where $\rho = (d\psi/di)_{i=i_0}$:

The characteristic equation for (5.10) is

$$S^2 + \left(\frac{1}{RC} + \frac{\rho}{L}\right) S + \frac{1}{LC}\left(\frac{\rho}{R} + 1\right) = 0. \tag{5.11}$$

The rest of the analysis consists in exploring the distribution of singularities in the phase plane as was explained in connection with Fig. 11.

6. *Limit Cycles*

We have been concerned so far with the investigation of *local* properties of trajectories in the neighborhood of singular points, which requires only linear approximations. We shall attack now a more difficult problem of behavior of nonlinear systems in *the large*, which rules out any linear approximations. We shall begin this study with a brief qualitative outline of the theory of Poincaré concerning the properties of certain closed trajectories, *the limit cycles*.

First we shall give a few definitions and indicate examples in which such closed trajectories exist. Later we shall endeavor to establish a connection between these new concepts and certain physical phenomena.

Let us consider again a system (2.1) of two differential equations of the first order and assume that there exists a closed trajectory C in the phase plane; let us assume further that there exists also a non-closed trajectory C', represented by the equations $x = x(t)$, $y = y(t)$ such that either for $t = \infty$ or for $t = -\infty$ the representative point R' following C' approaches some point on C. By this we mean that for any number $\epsilon > 0$ one can find a value t_0 with the property that any point $x(t)$, $y(t)$ on C' is at a distance $\leqq \epsilon$ from some point on C either for $t > t_0$ or for $t < t_0$. Intuitively this means that C' winds around C either from the outside or from the inside like the spirals shown in Fig. 14. If the closed curve C is approached in this manner by a trajectory C', we call C a *limit cycle*.

We call a limit cycle C *stable* if it is approached by the spiral trajectories both from the inside and from the outside for $t = \infty$ and *unstable* if it is approached for $t = -\infty$.

There may be also a special case when C is approached by C' from the outside for $t = \infty$ and from the inside for $t = -\infty$ or vice versa; in such a case we call C a *semistable* limit cycle.

Limit cycles encountered in applications have the property that they are approached not by one spiral trajectory C' but by an infinite number of such trajectories passing through every ordinary point of the phase plane, at least within a certain region around C. If we recall that any

ordinary point (x_0,y_0) of the phase plane may be considered as a set of given initial conditions and that the motion on the limit cycle represents the ultimate stationary motion, we can also assert that the motion on the limit cycle is *independent of the initial conditions* in the sense that all trajectories passing through the various points of the phase plane approach eventually the same limit cycle.

An important difference between the closed trajectories of the conservative systems and closed trajectories of the limit-cycle type lies in the fact that the former always appear in continuous families whereas

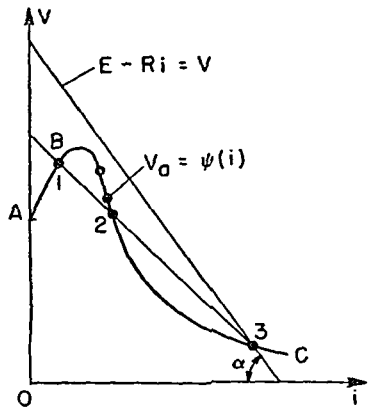

FIG. 13.

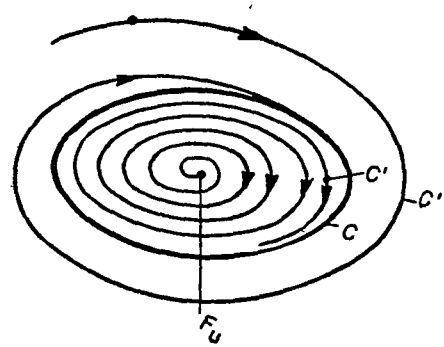

FIG. 14.

the latter are generally isolated. By this we mean that if C is such a closed trajectory of the limit-cycle type, there exists no other closed trajectory distinct from C and differing very little from it. This can be readily seen from the following comparison of a conservative system (*e.g.*, a pendulum) and a system of a limit-cycle type (*e.g.*, an electron tube oscillator or a clock).

The first system obviously executes motions entirely determined by the initial conditions and, by varying the latter, a continuum of closed trajectories can be obtained like those shown in Fig. 1. In an electron tube oscillator, on the other hand, the ultimate stationary oscillation is entirely independent of the initial conditions; in fact it is immaterial whether the self-excitation is started smoothly from rest or is produced by an initial impulse. Likewise a wound clock at standstill acquires its ultimate rhythm irrespectively of the fact whether it is started by a gentle shaking or by a violent impulse. In both cases the stationary motion depends only on the parameters of the system and has nothing to do with the initial conditions.

The determination of limit cycles in a given problem generally is very difficult, and besides the van der Pol equation and a few equations of a

similar type the situation remains practically unexplored. It is, however, relatively easy to form *synthetically*, so to speak, certain differential equations that possess limit cycles.

(a) Consider a system (2.1) of the form

$$\dot{x} = y + \frac{x}{\sqrt{x^2 + y^2}}[1 - (x^2 + y^2)]$$
$$\dot{y} = -x + \frac{y}{\sqrt{x^2 + y^2}}[1 - (x^2 + y^2)]. \tag{6.1}$$

Transforming into polar coordinates and making use of the relation $x\dot{x} + y\dot{y} = r\dot{r}$, we obtain finally the two equations

$$\dot{r} = 1 - r^2; \qquad \dot{\theta} = 1. \tag{6.2}$$

Integrating the first of these equations we get

$$r = \frac{(Ae^{2t} - 1)}{(Ae^{2t} + 1)} \tag{6.3}$$

where $A = (1 + r_0)/(1 - r_0)$ is the integration constant and $r_0 = \sqrt{x_0^2 + y_0^2}$ is the "initial condition." For $r_0 < 1$, as $t \to \infty$, r approaches from the inside the circle $r = 1$; for $r_0 > 1$, it approaches this circle from the outside. In view of the uniform rotation $\dot{\theta} = 1$ of the radius vector, it is clear that the trajectories C' are spirals winding onto the circle $r = 1$ both from the inside and the outside. Hence the system (6.1) admits a stable limit cycle $r = 1$ as a periodic solution.

(b) The system

$$\dot{x} = -y + x(x^2 + y^2 - 1)$$
$$\dot{y} = x + y(x^2 + y^2 - 1) \tag{6.4}$$

transformed into the polar coordinates becomes

$$\dot{r} = r(r^2 - 1); \qquad \dot{\theta} = -1.$$

By a similar argument we find that $r = 1/\sqrt{1 - Ae^{2t}}$ where $A = (r_0^2 - 1)/r_0^2$ is an integration constant. For $t = -\infty$, $r = 1$, that is, the spiral trajectories unwind from the circle $r = 1$ inward, if $r_0 < 1$, and approach $r = 0$ for $t = \infty$. For $r_0 > 1$, $A < 0$, so that for $t = -\infty$, again $r = 1$. This means that the spirals unwind outward from the circle $r = 1$, which is thus an unstable limit cycle.

In applications one encounters frequently systems possessing several limit cycles of a "concentric type." Since nothing is changed in the following argument, we can assume without any loss of generality that we

have a system of concentric circular limit cycles as shown in Fig. 15. Moreover, the singularity at the center may be considered as a limit cycle reduced to a point (cf. section 4). It can be shown (15)—we omit the proof—that in such a topological configuration the stable limit cycles alternate with the unstable ones; the latter are indicated by a broken line. Thus, for instance, if the singularity S is unstable, C is a stable limit cycle and C_1 an unstable one, etc. On the other hand, if S is stable (Fig. 16), C is unstable, C_1 stable, etc. Since the initial conditions

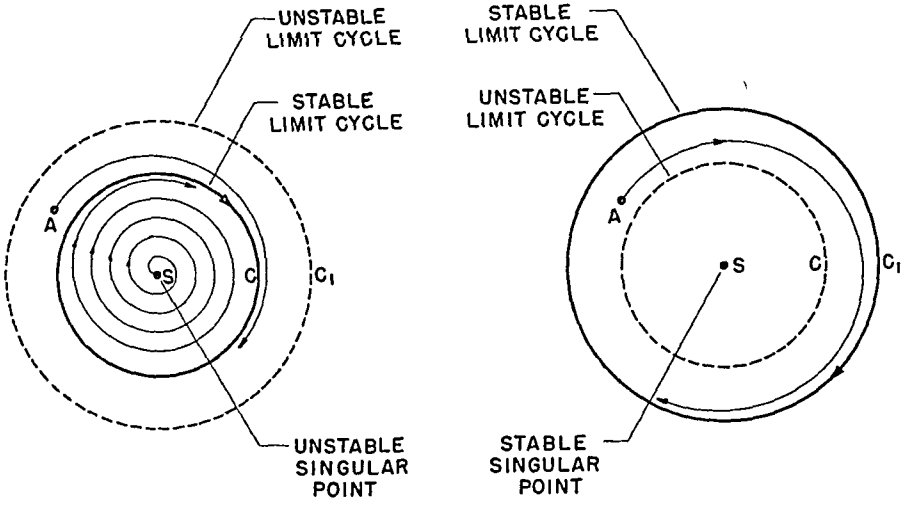

FIGS. 15 AND 16.

x_0, y_0 appear as points of the phase plane, several cases may appear. The case most frequently encountered in applications is that shown in Fig. 15, by S and C, namely, a trajectory unwinds from an unstable singularity and winds unto a stable limit cycle. This is the so-called *soft* self-excitation, usually observed, for example, in the electron tube oscillators starting from rest. If, however, the initial conditions are represented by a point A (Fig. 15) outside the stable limit cycle (*i.e.*, if the system is excited by an initial impulse), the stable limit cycle will be approached by the spiral trajectory. It is apparent that for the configuration shown in Fig. 16 no spontaneous self-excitation from rest is possible; in order to produce a self-excitation of such a system, an impulse bringing the initial condition to some point A outside the unstable limit cycle is required. Such a case of self-excitation is called *hard*. It is thus seen that the unstable limit cycles appear merely as *divides* separating the *field of attraction* of the stable limit cycles.

There are no dynamical systems known so far that possess several

stable limit cycles although, at least theoretically, they are possible for special forms of the nonlinear characteristics.

A convenient intuitive concept in grasping this situation is to consider *a flow of trajectories* in the phase plane. A trajectory in this mode of representation always "originates" in certain unstable elements of the phase plane (*e.g.*, unstable singularities, unstable limit cycles), which may be considered as *sources*, and "terminates" on the corresponding stable elements, the *sinks*. The trajectory considered from its beginning to its end (*i.e.*, from $t = -\infty$ to $t = \infty$) is called the *entire trajectory* or, simply, the trajectory. If, however, there is specified a certain instant $t = t_0$, which may be considered as the present instant, the *half trajectories* are obtained. One for $t < t_0$ describes the past history of the system and the other for $t > t_0$, its future history.

On the basis of this analogy many propositions which can be proved rigorously acquire an almost intuitive aspect. Thus, for example, the theorem of Poincaré that inside a closed trajectory there must be, at least, one unstable singularity becomes almost obvious.

It must be noted, however, that in the preceding argument we were using the expressions "stable" or "unstable singularity" only in connection with focal and nodal point, that is, the singularities that appear in essentially nonconservative dynamical systems. The real reason for this, as will appear later, is that stationary periodic motions of the limit-cycle type characterize essentially nonconservative and nonlinear dynamical systems. In conservative systems (both linear and nonlinear) on the contrary, the only singularities that may arise are the vortex and the saddle points.

In the following section we shall endeavor to develop certain inherent characteristics of singular points irrespectively of their physical significance.

7. *Indices of Poincaré. Theorems of Bendixson*

As has already been mentioned there exist no general rules for ascertaining the existence of closed trajectories in a given nonlinear differential equation. There exist, however, certain rules giving the *necessary* conditions for the existence of such trajectories based on the so-called *theory of indices* (16). There are also certain theorems due to Bendixson (17), of which we shall mention two that we shall have an occasion to use later. The first theorem gives both the necessary and sufficient conditions for the existence of a closed trajectory. Unfortunately its application is limited, as we are going to see later. The second theorem of Bendixson, the so-called *negative criterion*, permits ascertaining the *nonexistence* of closed trajectories. Although the application of the second theorem does

not present any difficulty, it is of lesser interest in applications because the principal effort of modern nonlinear mechanics centers precisely on the determination of closed trajectories in the various problems of mathematical physics.

a. Index of a Closed Trajectory. Let us consider a closed curve C in a vector field M, as shown in Fig. 17, and a positive direction (arrow) indicating the motion of the representative point R. We attach to R a frame of reference x', y' whose axes remain parallel to the axes of some fixed frame of reference. As R moves on C, the vector RM undergoes

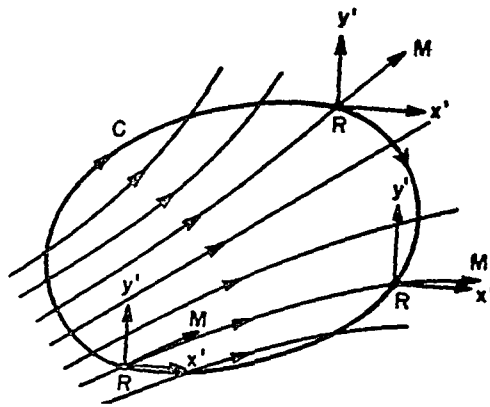

FIG. 17.

a certain rotation. It is clear that if R starting from a point R_0 on C comes back to the same point R_0 having completed one circuit on C, the vector RM will resume its original position in (x',y').

Poincaré calls the *index* j of a closed curve C relatively to the field M the algebraic number of complete revolutions of the vector RM in the positive direction in (x',y') when R completes one circuit on C.

From this definition it follows that the index j is always an integer. It is also clear that $j = 0$ if RM undergoes only an oscillation in (x',y') without any complete rotation.

By a slight extension of this definition we may also speak about the *index of a singular point.* It is sufficient for this purpose to surround the singularity by a small circle, to consider the trajectories approaching it as a vector field and to apply the procedure just stated. It is also possible to calculate the index by the equation

$$j = \oint_C d\left[\tan^{-1}\left(\frac{Q}{P}\right)\right] \tag{7.1}$$

as it follows from the very definition of P and Q in (2.1) as components of a vector field. Following one of these methods we ascertain that the

index of a vortex, a focal, or a nodal point is always $+1$; the index of a saddle point is -1.

We shall not enter into the theory of indices here but shall mention merely a few conclusions that are almost obvious from the preceding observations:

(1) The index of a closed curve not containing any singularities is zero.

(2) The index of a closed curve containing several singularities is equal to the algebraic sum of their indices.

(3) The index of a closed trajectory is always $+1$.

(4) The index of a closed curve C with respect to which the field vectors are directed either inward or outward at all points of C is $+1$.

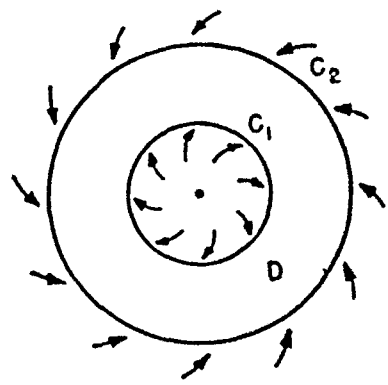

FIG. 18.

It is to be noted that the statement at the end of section 3 results directly from (2) and (3).

b. First Theorem of Bendixson. Let $x = x(t)$ and $y = y(t)$ be the parametric representation of a positive half trajectory C' $(t > t_0)$ and assume that for $t = \infty$, C' remains within a finite region D without approaching any singularity. The first theorem of Bendixson asserts that under these conditions *C' is either a closed trajectory C or approaches such a trajectory in D.*

As an example of the application of this theorem let us consider the following system of differential equations, which we shall encounter later:

$$\begin{aligned} \dot{x} &= -ay + x(1 - r^2) \\ \dot{y} &= A + ax + y(1 - r^2) \end{aligned} \tag{7.2}$$

where A is a constant and $r^2 = x^2 + y^2$. It is apparent that for a sufficiently large r the trajectories are directed inward. Transferring the origin to the singular point and changing the variables $x = x_0 + \xi$, $y = y_0 + \eta$ reduces (7.2) to the form

$$\begin{aligned} \dot{\xi} &= \xi - a\eta + \cdots \\ \dot{\eta} &= -a\xi + \eta + \cdots \end{aligned}$$

where nonwritten terms are of a higher degree in ξ and η. By Section 4, Part II, we conclude that the origin is an unstable focal point, which means that the trajectories departing from it enter the inner boundary of a domain D, as shown in Fig. 18. On the other hand, as was just mentioned, the trajectories enter also the external boundary of D from the

outside; moreover, no singular points exist inside the domain. Hence, there exists a stable limit cycle inside the domain.

Unfortunately, the application of the Bendixson theorem is not always possible, in view of the impossibility of determining D. The reader can easily ascertain this in the case of the van der Pol equation, in which it is impossible to determine the outward boundary of D without first integrating the differential equation, which, of course, defeats the very purpose for which the theorem is intended.

c. Second Theorem of Bendixson. We consider again the system (2.1). The second theorem of Bendixson states:

If the expression $\partial P/\partial x + \partial Q/\partial y$ does not change sign within a certain region D of the phase plane, no closed trajectories exist in D.

In fact, let us consider a closed circuit in D and apply Gauss' theorem

$$\oint_C (Pdy - Qdx) = \int\int \left(\frac{\partial P}{\partial x} + \frac{\partial Q}{\partial y}\right) dxdy. \tag{7.3}$$

If it is assumed that the circuit C is a trajectory satisfying (2.1), the line integral can be written $\int(\dot{x}\dot{y} - \dot{y}\dot{x})dt$ and is zero. On the other hand, the surface integral can be zero only when the integrand changes its sign in the domain of integration. This condition is contrary to the assumption. Therefore the theorem is proved.

As an example of the application of this theorem, one can consider a system of two series generators connected in parallel on an external load R. Designating by $\varphi(i)$ the electromotive force, by r the internal resistance and by L the inductance of each generator, the application of Kirchhoff's laws gives the following equations

$$\begin{aligned} \varphi(i_1) - (r + R)i_1 - Ri_2 - L\frac{di_1}{dt} &= 0 \\ \varphi(i_2) - (r + R)i_2 - Ri_1 - L\frac{di_2}{dt} &= 0 \end{aligned} \tag{7.4}$$

We take the quantities i_1 and i_2 as x and y of the general theory and obtain

$$\frac{\partial P}{\partial i_1} = \varphi_{i_1}(i_1) - (r + R); \qquad \frac{\partial Q}{\partial i_2} = \varphi_{i_2}(i_2) - (r + R) \tag{7.5}$$

where $\varphi_i(i)$ designates the derivative of $\varphi(i)$ with respect to i, that is, the tangent to the curve $\varphi(i) = e$, where e is the electromotive force. We know from the theory of electric machines that the self-excitation is possible only if $\varphi_i(i) - (r + R) > 0$. This means that the energy generated in the armatures of generators outweighs the energy dissipation.

In view of this the expressions (7.5) are positive and, by the second theorem of Bendixson, no sustained self-excited oscillations are possible in a system of this kind. In fact, it is a well-known fact that such a system behaves always aperiodically whether it is unstable (with a direct connection of the series fields) or stable (with a crossed connection).

8. Remarks

We shall not pursue further the outline of the topological methods but shall limit ourselves to a few observations of a general character. The principal advantage of these methods, as the reader may have observed, is in that they give a sufficiently broad, so to speak, bird's-eye view of the totality of all possible motions that may occur in a dynamical system under the various circumstances. In fact, once the singularities, separatrices, and limit cycles have been ascertained in a given problem, the phase plane becomes divided, or mapped, into certain domains with definite properties. A mere glance at such a mapping suffices to ascertain in which region periodic motions are to be expected, in which they are impossible, what the thresholds are at which the nature of the equilibrium changes, what the effect of certain parameters is on the behavior of the system in the large, etc. In an entirely new problem that a physicist or engineer may occasionally encounter these methods give a relatively simple means for appraising the situation.

These methods, however, possess definite limitations, which it is useful to mention.

First, these methods are limited to systems with one degree of freedom and, more specifically, to the systems of the form (2.1), in which the time t does not enter explicitly on the right-hand side of the differential equations. Systems of this kind are sometimes called *autonomous systems.* For that reason, a considerable number of nonlinear phenomena are outside the reach of these methods.

Finally, the most important problem of nonlinear mechanics, the determination of periodic motions, cannot be always solved by these methods, as we had an occasion to observe in the preceding section.

II. Analytical Methods

9. Introductory Remarks

There exists no general method yielding the exact solution of nonlinear differential equations, and the only methods available are those of approximations. At the end of the last century H. Poincaré came across certain nonlinear problems of celestial mechanics and developed the so-called *method of small parameters* (18), with which we shall be concerned here. This method deals with the so-called *quasi-linear equations*, that is,

such nonlinear equations as do not differ much from certain linear equations, the exact solutions of which are available. Thus, for example, the van der Pol equation

$$\ddot{x} - \mu(1 - x^2)\dot{x} + x = 0 \tag{9.1}$$

is a quasi-linear one if the parameter μ is small, in which case, it does not differ much from the corresponding linear equation $\ddot{x} + x = 0$, whose exact periodic solution is known. Hence when μ is small the van der Pol equation can be treated by the method of Poincaré. If, however, the parameter μ is a large number, the same equation offers considerable difficulties, which have not been completely overcome as yet although quite recently attempts were made (8) to attack this difficult problem.

The quasi-linear differential equations encountered in applications are generally of the form

$$\ddot{x} + x = \mu f(x,\dot{x}) \tag{9.2}$$

We shall frequently refer to this equation as *the quasi-linear equation* if we prefer not to specify any particular form.

The crux of the theory of Poincaré is the establishment of the existence of periodic solutions for quasi-linear differential equations. It is by no means apparent, at least intuitively, that even a slight change of the form of a differential equation would not change radically the qualitative nature of its solutions. In fact, as a trivial example, we can mention that the periodicity of solutions of the equation $\ddot{x} + x = 0$ is lost by adding a term $b\dot{x}$ where b may be as small as we please.

Poincaré shows, however, that, under certain conditions, a quasi-linear equation may possess certain periodic solutions, which will be identified later with closed trajectories of the limit-cycle type.

Attempts to apply the theory of Poincaré to the numerous nonlinear periodic phenomena did not meet with any particular difficulty as far as the first approximation is concerned. Certain difficulties appeared in the development of the theory of higher approximations. Although these difficulties due to the presence of the so-called *secular terms* in the solutions by series expansions were known long ago, in astronomical problems they did not present any serious objection, on account of the smallness of these secular terms. In problems of nonlinear mechanics, however, the presence of these terms appeared as a source of a considerable difficulty. For that reason in later years Kryloff and Bogoliuboff (19) departed from the original method of Poincaré and adopted an alternative method of Lindstedt (20) in which the secular terms are removed in each step of the recurrence procedure leading to the approximations of the higher orders, as will be shown in section 13.

In addition to these two methods, there exists also a third one, due to van der Pol (21). This method precedes historically the Kryloff-Bogoliuboff method although its theoretical justification appeared much later (22).

For applications the first approximation is generally sufficient, and in what follows we shall be mostly concerned with the first approximation. The results obtained by the first approximation are exactly the same in all three methods although the starting points are somewhat different.

10. Method of Poincaré

Consider a system of differential equations

$$\dot{x} = ax + by + \mu f_1(x,y); \qquad \dot{y} = cx + dy + \mu f_2(x,y) \tag{10.1}$$

where f_1 and f_2 are polynomials not containing either constant or linear terms in x and y and μ is a parameter; we shall assume that f_1 and f_2 are analytic in the domain under consideration. If $\mu = 0$ the system (10.1) is linear and we know that periodic solutions are possible under certain conditions, which we shall assume. Let $x = x_0(t,K)$ and $y = y_0(t,K)$ be such solutions where K is the amplitude.

If we assume that periodic solutions exist when $\mu \neq 0$ but small, we can write

$$x(0,\mu,K) = x_0(0,K) + \beta_1; \qquad y(0,\mu,K) = y_0(0,K) + \beta_2 \tag{10.2}$$

which expresses a relation between the initial conditions and where β_1 and β_2 are certain functions of μ such that $\beta_1(0) = \beta_2(0) = 0$.

In the general case when $\mu \neq 0$ but small, the solution of (10.1) can be written in the form

$$x = x(t,\mu,\beta_1,\beta_2,K); \qquad y = y(t,\mu,\beta_1,\beta_2,K).$$

Since we are looking for conditions for a periodic solution, it is natural to assume that, if it exists, its period will be $T + \tau$, T being the period of the neighboring linear solution and $\tau(\mu)$ is a small "correction for the period" when we pass from the linear problem ($\mu = 0$) to the nonlinear one ($\mu \neq 0$); clearly $\tau(0) = 0$. It is to be noted that one of the β's can always be made equal to zero by a proper selection of the time origin. The condition for the periodicity is then

$$\begin{aligned} x(T + \tau,\mu,0,\beta,K) - x(0,\mu,0,\beta,K) &= \varphi(\tau,\mu,\beta,K) = 0 \\ y(T + \tau,\mu,0,\beta,K) - y(0,\mu,0,\beta,K) &= \psi(\tau,\mu,\beta,K) = 0. \end{aligned} \tag{10.3}$$

Since when $\mu = 0$ and, hence, $\tau(0) = \beta(0) = 0$, there exists an infinity

of periodic trajectories corresponding to the different values of the integration constants, we can specify this by writing

$$\varphi(\tau,\mu,\beta,K) = \mu\varphi_1(\tau,\mu,\beta,K) = 0$$
$$\psi(\tau,\mu,\beta,K) = \mu\psi_1(\tau,\mu,\beta,K) = 0.$$

If, therefore, there are some *special periodic solutions* for $\mu \neq 0$, they must certainly be expressed by the equations

$$\varphi_1(\tau,\mu,\beta,K) = 0; \qquad \psi_1(\tau,\mu,\beta,K) = 0. \tag{10.4}$$

The functions $\tau(\mu)$ and $\beta(\mu)$ can always be expressed by a power series:

$$\tau(\mu) = d\mu + e\mu^2 + \cdots; \qquad \beta(\mu) = d_1\mu + e_1\mu^2 + \cdots. \tag{10.5}$$

The Taylor expansion of φ_1 and ψ_1 gives

$$\varphi_1 = \varphi_{10} + a\mu + b\tau + c\beta + \cdots$$
$$\psi_1 = \psi_{10} + a_1\mu + b_1\tau + c_1\beta + \cdots. \tag{10.6}$$

If we replace in these expressions $\tau(\mu)$ and $\beta(\mu)$ by their values (10.5) and keep only the quantities of the first order we get

$$\varphi_1 = \varphi_{10} + \mu(a + bd + cd_1) = 0$$
$$\psi_1 = \psi_{10} + \mu(a_1 + b_1d + c_1d_1) = 0. \tag{10.7}$$

This system of two equations with the unknowns d and d_1 must be solved for any arbitrary μ provided it is small. Hence, two conditions must be fulfilled:

$$\varphi_{10} = \varphi_{10}(K) = 0; \qquad \psi_{10} = \psi_{10}(K) = 0 \tag{10.8}$$
$$a + bd + cd_1 = 0; \qquad a_1 + b_1d + c_1d_1 = 0. \tag{10.9}$$

Hence, whenever the Jacobian $J = \partial(\varphi_1,\psi_1)/\partial(\tau_1\beta)$(*) is different from zero, it is possible to solve (10.9) for d and d_1 provided there are no terms free from μ, τ, and β in the expressions for φ_1 and ψ_1. In such a case one obtains the first order solution of the nonlinear problem provided μ is sufficiently small. Equations (10.8) give then the expression for the amplitude of the linear periodic solution in the neighborhood of which there exists a periodic solution of the nonlinear problem. This latter solution is called *the generating solution.*

Once the existence of periodic solutions of the quasi-linear problem has been ascertained we can proceed with the elaboration of certain details that will be useful later.

For this purpose instead of the system (10.1) we shall consider the quasi-linear equation in the form (9.2), in which it generally appears in applications.

* It is noted that $\partial\varphi_1/\partial\tau = b$; $\partial\varphi_1/\partial\beta = c$; $\partial\psi_1/\partial\tau = b_1$ and $\partial\psi_1/\partial\beta = c_1$ by (10.6).

Poincaré shows (18) that as a formal solution the following series can be taken:

$$x = \varphi_0(t) + A\beta_1 + B\beta_2 + C\mu + D\beta_1\mu + E\beta_2\mu + F\mu^2 + \cdots \quad (10.10)$$

where $\varphi_0, A, B, \cdots$ are functions of time t. Moreover, it is shown that this series converges for any arbitrary but finite time interval provided the quantities μ, β_1, β_2 are small. For this purpose it is necessary to substitute $\ddot{x}$ and x expressed in terms of (10.10) in the quasi-linear equation (9.2) and to develop the nonlinear function $f(x,\dot{x})$ into the Taylor series in the neighborhood of the generating solutions x_0 and $\dot{x}_0$. When all this is carried out, it is necessary to identify the coefficients of μ, β_1, β_2, $\beta_1\mu$, $\beta_2\mu$, $\cdots$ in these expressions. If the expansions are limited to the second order, nine differential equations are obtained as the result of this identification, of which three are satisfied identically, as it is easy to verify. The remaining six equations are

$$\ddot{A} + A = 0; \qquad \ddot{B} + B = 0; \qquad \ddot{C} + C = f(x_0,\dot{x}_0); \qquad \ddot{D} + D = \left(\frac{\partial f}{\partial x}\right)_0 A + \left(\frac{\partial f}{\partial \dot{x}}\right)_0 \dot{A}; \qquad \ddot{E} + E = \left(\frac{\partial f}{\partial x}\right)_0 B + \left(\frac{\partial f}{\partial \dot{x}}\right)_0 \dot{B};$$

$$\ddot{F} + F = \left(\frac{\partial f}{\partial x}\right)_0 C + \left(\frac{\partial f}{\partial \dot{x}}\right)_0 \dot{C} \quad (10.11)$$

where the symbols $(\partial f/\partial x)_0$ and $(\partial f/\partial \dot{x})_0$ designate the partial derivatives of f with respect to x and $\dot{x}$, in which the generating solutions $x_0 = \varphi_0(t)$ and $\dot{x}_0 = \dot{\varphi}_0(t)$ have been substituted after the differentiation. Recalling that $x - x_0 = \beta_1$; and $\dot{x} - \dot{x}_0 = \beta_2$, we find the following initial conditions

$$A(0) = 1; \qquad \dot{B}(0) = 1; \qquad B(0) = C(0) = D(0) = E(0) = F(0) = \dot{A}(0) = \dot{C}(0) = \dot{D}(0) = \dot{E}(0) = \dot{F}(0) = 0.$$

With these initial conditions the first two equations (10.11) give

$$A = \cos t; \qquad B = \sin t.$$

The other four are of the form: $\ddot{v} + v = V(t)$ with the initial conditions $v(0) = \dot{v}(0) = 0$; their solution is of the form

$$v = \int_0^t V(u) \sin (t - u)du. \quad (10.12)$$

Since for the establishment of conditions for periodicity it is important to know what happens after one period 2π, instead of (10.12) we calculate

$$v_{2\pi} = \int_0^{2\pi} V(u) \sin (t - u)du. \quad (10.3)$$

We shall omit here these calculations but shall merely mention that (10.13) leads finally to a number of expressions, $A(2\pi)$, $B(2\pi)\cdots$, $\dot{A}(2\pi)\cdots$, of which we shall indicate those that we shall need for the first approximation. It is clear that the explicit form of those functions depends on the form of the nonlinear function $f(x,\dot{x})$.

We are now in a position to formulate explicitly the conditions (10.3) for periodicity. Expanding the functions $x(2\pi+\tau)$ and $\dot{x}(2\pi+\tau)$ in the Taylor series and substituting the values of $A(2\pi)$, $B(2\pi)\cdots$ we obtain finally the following expressions

$$x(2\pi+\tau)-x(0) = -K\frac{\tau^2}{2}+\tau\beta_2+C(2\pi)\mu+\dot{C}(2\pi)\tau\mu+D(2\pi)\beta_1\mu + E(2\pi)\beta_2\mu+F(2\pi)\mu^2=0$$
$$\dot{x}(2\pi+\tau)-\dot{x}(0) = -K\tau-\tau\beta_1+\dot{C}(2\pi)\mu+\ddot{C}(2\pi)\tau\mu+\dot{D}(2\pi)\beta_1\mu + \dot{E}(2\pi)\beta_2\mu+\dot{F}(2\pi)\mu^2=0. \quad (10.14)$$

Since the quantities μ, β_1 and β_2 can be assumed as small of the first order, the terms containing their products are of the second order and can therefore be dropped in the first approximation. The first equation (10.14) gives then $C(2\pi)=0$ and the second $\tau=\dot{C}(2\pi)\mu/K$. Replacing now $C(2\pi)$ and $\dot{C}(2\pi)$ by their values we obtain the following *equations of the first approximation:*

$$C(2\pi) = -\int_0^{2\pi} f(K\cos\mu,\ -K\sin u)\sin u\,du = \Phi(K)=0$$
$$\tau=\frac{\dot{C}(2\pi)\mu}{K}=\frac{\mu}{K}\int_0^{2\pi} f(K\cos u,\ -K\sin u)\cos u\,du=\mu\Psi(K). \quad (10.15)$$

The first equation (10.15) gives the amplitude of the generating solution and the second, the correction for the period.

As an example we shall determine the first order solution of the van der Pol equation (1). The generating solutions are clearly $x=K\cos t$ and $\dot{x}=y=-K\sin t$ so that $f(x,\dot{x})=(1-x^2)\dot{x}$ with these generating solutions becomes

$$f(K\cos t,\ -K\sin t) = -(1-K^2\cos^2 t)K\sin t$$

and the first equation (10.15) gives

$$C(2\pi)=K\left(\int_0^{2\pi}\sin^2 t\,dt-K^2\int_0^{2\pi}\cos^2 t\sin^2 t\,dt\right)=K\pi\left(1-\frac{K^2}{4}\right)=0$$

which gives $K=0$ and $K=2$. The first value is clearly a singular point; it can be ascertained easily by forming the characteristics equation (5.5) that it is an unstable focal point. We have thus a familiar situation mentioned in connection with Fig. 15, namely, the trajectories depart

from an unstable focal point and approach a limit cycle in the neighborhood of the generating solution with radius $K = 2$.

The second equation (10.15) gives $\tau = 0$. Hence, to the first order, the period of the quasi-linear motion is the same as that of the generating solution.

11. Method of van der Pol

Let us consider again the quasi-linear equation and assume that for $\mu = 0$ the periodic solution is of the form

$$x = a \cos t + b \sin t \qquad \text{and} \qquad \dot{x} = -a \sin t + b \cos t. \tag{11.1}$$

We shall attempt to determine a and b as certain functions of time so as to have solutions of the form (11.1) satisfying the quasi linear equation ($\mu \neq 0$). It is clear that the procedure to follow is in all respects similar to the so-called method of variation of constants (Lagrange) although some special features of the problem will appear later.

We may consider (11.1) as a transformation defining x and $\dot{x}$ in terms of the new *variables a and b of van der Pol*. This transformation implies that

$$\left(\frac{da}{dt}\right) \cos t + \left(\frac{db}{dt}\right) \sin t = 0. \tag{11.2}$$

Replacing x, $\dot{x}$, and $\ddot{x}$ in the quasi-linear equation, we get

$$-\left(\frac{da}{dt}\right) \sin t + \left(\frac{db}{dt}\right) \cos t = \mu f(a \cos t + b \sin t, \; -a \sin t + b \cos t). \tag{11.3}$$

Solving (11.2) and (11.3) for da/dt and db/dt we have

$$\begin{aligned} \frac{da}{dt} &= -\mu f(a \cos t + b \sin t, \; -a \sin t + b \cos t) \sin t \\ \frac{db}{dt} &= \mu f(a \cos t + b \sin t, \; -a \sin t + b \cos t) \cos t. \end{aligned} \tag{11.4}$$

Since μ is small and f is bounded, da/dt and db/dt are small, so that during one period 2π of the trigonometric functions a and b vary very little. Since the right-hand term of (11.4) is a certain periodic function, we expand it in a Fourier series, viz.:

$$\begin{aligned} \frac{da}{dt} &= \mu \left[\frac{\varphi_0(a,b)}{2} + \varphi_1(a,b) \cos t + \bar{\varphi}_1(a,b) \sin t + \varphi_2(a,b) \cos 2t + \cdots \right] \\ \frac{db}{dt} &= \mu \left[\frac{\psi_0(a,b)}{2} + \psi_1(a,b) \cos t + \bar{\psi}_1(a,b) \sin t \right. \\ &\qquad \left. + \psi_2(a,b) \cos 2t + \cdots \right]. \end{aligned} \tag{11.5}$$

Van der Pol assumes that for the investigation of what happens during many periods of the trigonometric functions, it is sufficient to retain only the constant terms of these Fourier series. In this manner the so-called *abbreviated equations* of van der Pol are obtained:

$$\frac{da}{dt} = \mu \frac{\varphi_0(a,b)}{2}; \qquad \frac{db}{dt} = \mu \frac{\psi_0(a,b)}{2}. \tag{11.6}$$

On the other hand the Fourier procedure gives

$$\frac{\varphi_0(a,b)}{2} = -\frac{1}{2\pi}\int_0^{2\pi} f(a\cos\xi + b\sin\xi, -a\sin\xi + b\cos\xi)\sin\xi d\xi$$
$$\frac{\psi_0(a,b)}{2} = +\frac{1}{2\pi}\int_0^{2\pi} f(a\cos\xi + b\sin\xi, -a\sin\xi + b\cos\xi)\cos\xi d\xi. \tag{11.7}$$

Multiplying the first equation (11.6) by a, the second by b, adding and setting $a^2 + b^2 = K^2$, we get

$$\frac{1}{2}\frac{dK^2}{dt} = K\frac{dK}{dt} = \frac{\mu}{2\mu}\int_0^{2\pi} f(a\cos\xi + b\sin\xi, -a\sin\xi + b\cos\xi)$$
$$(-a\sin\xi + b\cos\xi)d\xi.$$

Setting

$$a\cos\xi + b\sin\xi = K\cos(\xi - \theta) = K\cos u;$$
$$-a\sin\xi + b\cos\xi = -K\sin(\xi - \theta) = -K\sin u$$

we obtain two equations

$$\frac{dK}{dt} = \mu\Phi(K) \qquad \text{and, by a similar procedure,} \qquad \frac{d\theta}{dt} = \mu\Psi(K) \tag{11.8}$$

where

$$\Phi(K) = -\frac{1}{2\pi}\int_0^{2\pi} f(K\cos u, -K\sin u)\sin u du$$
$$\Psi(K) = \frac{1}{2\pi K}\int_0^{2\pi} f(K\cos u, -K\sin u)\cos u du. \tag{11.9}$$

Equations (11.8) are the abbreviated equations written in terms of the amplitude and phase, and one observes that the functions (11.9) to a constant factor, are the same as the functions $C(2\pi)$ and $\dot{C}(2\pi)$ of the theory of Poincaré.

12. *Method of Kryloff and Bogoliuboff (K.B.)*

This method resembles the method of van der Pol, the only difference being that the K.B. method attempts to satisfy the quasi-linear equation by a solution of the form $x = a \sin \psi$.

We shall maintain the K.B. notations, which consist in writing the quasi-linear equation in the form

$$\ddot{x} + \omega^2 x + \mu f(x,\dot{x}) = 0. \tag{12.1}$$

This form is slightly more convenient for numerical calculations and reduces to (9.2) by changing the independent variable.

In these notations the quantity

$$\psi = \omega t + \varphi \tag{12.2}$$

is called the *total phase*. One looks, therefore, for the solutions of the form

$$x = a \sin (\omega t + \varphi); \qquad \dot{x} = a\omega \cos (\omega t + \phi). \tag{12.3}$$

Differentiating the first equation considering a and φ as unknown functions of t we have the condition

$$\dot{a} \sin (\omega t + \varphi) + a\dot{\varphi} \cos (\omega t + \varphi) = 0. \tag{12.4}$$

Differentiating the second equation (12.3) considering again a and φ as unknown functions of t so as to obtain $\ddot{x}$, the substitution of these values in the quasi-linear equation gives

$$\dot{a}\omega \cos (\omega t + \varphi) - a\omega\dot{\varphi} \sin (\omega t + \varphi) + \mu f[a \sin (\omega t + \varphi), a\omega \cos (\omega t + \varphi)] = 0 \tag{12.5}$$

Solving (12.4) and (12.5) for $\dot{a}$ and $\dot{\varphi}$ we get

$$\frac{da}{dt} = -\frac{\mu}{\omega} f[a \sin (\omega t + \varphi), a\omega \cos (\omega t + \varphi)] \cos (\omega t + \varphi)$$

$$\frac{d\varphi}{dt} = \frac{\mu}{a\omega} f[a \sin (\omega t + \varphi), a\omega \cos (\omega t + \varphi)] \sin (\omega t + \varphi). \tag{12.6}$$

The argument here is again similar to that used in the van der Pol method, viz., since μ is small and f is bounded, the quantities a and φ change very little during one period T. Likewise, the periodic nonlinear function written as a Fourier series is

$$f(a \sin \varphi, a\omega \cos \varphi) \cos \varphi = P_0(a) + \sum_{n=1}^{\infty} [P_n(a) \cos n\varphi + P_n'(a) \sin n\varphi]$$

$$f(a \sin \varphi, a\omega \cos \varphi) \sin \varphi = Q_0(a) + \sum_{n=1}^{\infty} [Q_n(a) \cos n\varphi + Q_n'(a) \sin n\varphi] \quad (12.7)$$

where $P_0, Q_0, P_n, \cdots$ are determined by the Fourier procedure. If one substitutes these Fourier series into (12.6) and integrates between t and $t + T$, all trigonometric terms drop out and we obtain the equations

$$\frac{a(t+T) - a(t)}{T} = -\frac{\mu}{\omega} P_0(a); \qquad \frac{\varphi(t+T) - \varphi(t)}{T} = \frac{\mu}{a\omega} Q_0(a).$$

Since a and φ do not change appreciably during one period, we can set $\Delta a = a(t+T) - a(t)$; $\Delta\varphi = \varphi(t+T) - \varphi(t)$ where Δa and $\Delta\varphi$ are small; moreover, one period T, say may also be considered as small, ΔT, in comparison with the total duration of the process extending over many periods. With these notations the preceding equations become

$$\frac{\Delta a}{\Delta T} = -\frac{\mu}{\omega} P_0(a); \qquad \frac{\Delta\varphi}{\Delta T} = \frac{\mu}{a\omega} Q_0(a).$$

At the limit we obtain the following *equations of the first approximation*

$$\frac{da}{dt} = -\frac{\mu}{\omega} P_0(a); \qquad \frac{d\varphi}{dt} = \frac{\mu}{a\omega} Q_0(a). \quad (12.8)$$

Comparing these equations with the exact equations (12.6), we observe that they are obtained from these exact equations by averaging over the period so that (12.8) do not describe the actual physical process in its instantaneous behavior but describes the behavior of the *envelope of modulation* if one uses a technical term.

Using the expressions (12.8) and substituting for P_0 and Q_0 their values we obtain the following equations of the first approximation of the K.B. theory:

$$\frac{da}{dt} = -\frac{\mu}{\omega} \frac{1}{2\pi} \int_0^{2\pi} f(a \sin \gamma, a\omega \cos \gamma) \cos \gamma d\gamma = \Phi(a)$$

$$\frac{d\psi}{dt} = \omega + \frac{\mu}{2a\omega\pi} \int_0^{2\pi} f(a \sin \gamma, a\omega \cos \gamma) \sin \gamma d\gamma = \Omega(a). \quad (12.9)$$

In this form the equations are convenient because the second term on the right-hand side of the second equation gives directly the nonlinear frequency correction $\Delta\omega$. These equations can be applied, for example, to the calculation of the first order solution of the Van der Pol equation, in which case one has to put $\omega = 1$.

An another example of the application of these equations we can consider a differential equation of a mechanical system with one degree of fredom having a quadratic dissipative damping, viz.,

$$m\ddot{x} + b\dot{x}^2 + cx + 0.$$

We assume that b is small so as to be able to remain within the limit of the quasi-linear theory. Dividing by m and setting $\omega^2 = c/m$; $\beta = b/m$ we have

$$\ddot{x} + \omega^2 x + \beta\dot{x}^2 = 0.$$

In this case $\mu f(x,\dot{x}) = \beta\dot{x}^2$. Since this function is even it is convenient to write it as $\beta|\dot{x}|\dot{x}$. Whence

$$\int_0^{2\pi} f(a\omega \cos\gamma) \cos\gamma d\gamma = \beta a^2\omega^2 \int_0^{2\pi} |\cos\gamma| \cos^2\gamma d\gamma = \tfrac{8}{3}\beta a^2\omega^2\pi.$$

The first equation (12.3) is then

$$\frac{da}{dt} = -\frac{4b\omega a^2}{3m}$$

and its integration yields

$$a = \frac{a_0}{\left(1 + \frac{(4b\omega a_0 t)}{3m}\right)}$$

where a_0 is the initial value of a.

Let us compare this result with the case of a linear damping corresponding to the equation

$$\ddot{x} + \omega^2 x + \beta\dot{x} = 0.$$

Proceeding as before we have

$$\int_0^{2\pi} f(a\omega \cos\gamma) \cos\gamma d\gamma = \beta a\omega \int_0^{2\pi} \cos^2\gamma d\gamma = \beta a\omega\pi.$$

Hence $da/dt = -ba/2m$ and, upon integration

$$a = a_0 e^{-\frac{b}{2m}t}$$

In this particular case the first approximation gives exactly the same result as the exact solution, which is known. It is easily verified that the frequency correction here is zero in the first approximation. The reason for that is sufficiently clear inasmuch it has been assumed that the damping is small so that the frequency correction is of the second order and does not appear in the first approxmation.

13. *Approximations of Higher Orders*

Although the equations of the first approximation with which we were concerned in Sections 10, 11, and 12 are generally sufficient for the great majority of applications, it may be of interest to mention also that the approximations of higher orders which may be useful whenever a greater accuracy of calculations is desired.

As was mentioned in Section 9, certain difficulties appear in the approximations of the higher orders, owing to the so-called *secular terms.* For that reason it is useful to explain first the origin of these terms.

Again let us consider the quasi-linear differential equation (12.1) in the Kryloff-Bogoliuboff form, viz.,

$$\ddot{x} + \omega^2 x + \mu f(x,\dot{x}) = 0. \tag{13.1}$$

Let us assume that we attempt to satisfy this equation by a solution of the form

$$x = x_0 + \mu x_1 + \mu^2 x_2 + \cdots \tag{13.2}$$

where x_0 is the known generating solution for $\mu = 0$. This particular form of solution (13.2) was first suggested by Poisson, and the method of Poincaré represents, to some extent, a further elaboration of this method. If we substitute (13.2) in (13.1) and limit (13.2) to a certain number of terms, we obtain a number of differential equations, viz.,

$$\begin{aligned} \ddot{x}_0 + \omega^2 x_0 &= 0 \\ \ddot{x}_1 + \omega^2 x_1 &= -f(x_0,\dot{x}_0) \\ \ddot{x}_2 + \omega^2 x_2 &= [-f_x(x_0,\dot{x}_0)x_1 + f_{\dot{x}}(x_0,\dot{x}_0)\dot{x}_1] \\ &\cdots\cdots\cdots\cdots\cdots\cdots\cdots \end{aligned} \tag{13.3}$$

which can be solved by a recurrence procedure that determines $x_1, x_2, \cdots$.

Let us apply this procedure to a simple case of a linear differential equation

$$\ddot{x} + \mu\omega\dot{x} + \omega^2 x = 0 \tag{13.4}$$

the exact solution of which is known, viz.,

$$x = Ae^{-\frac{\mu\omega t}{2}} \cos\left[\left(\omega\sqrt{1 - \frac{\mu^2}{4}}\right)t + \varphi\right] \tag{13.5}$$

where A and φ are the integration constants.

On the other hand, if we apply the method of approximations, the first equation (13.3) gives $x_0 = A\cos(\omega t + \varphi)$. Substituting this in the second equation (13.3) we get

$$\ddot{x}_1 + \omega^2 x_1 = -\dot{x}_0\omega = A\omega^2 \sin(\omega t + \varphi).$$

As is well known, this equation has the solution

$$x_1 = -\frac{A\omega t}{2}\cos(\omega t + \varphi). \tag{13.6}$$

Replacing x_0 and x_1 into (13.2), we get to the second order

$$x = x_0 + \mu x_1 = A\left(\frac{1 - \mu\omega t}{2}\right)\cos(\omega t + \varphi) \tag{13.7}$$

It is noted that the time t appears now outside the sign of the trigonometric functions. The term $(A\mu\omega t/2)\cos(\omega t + \varphi)$ in (13.7) is a *secular term*. The reason for this situation is sufficiently obvious. In fact, if we proceed with the calculation of $x_1, x_2, \cdots$, we find that the right-hand terms in (13.3), beginning with the second equation, are periodic functions of the same period as that of the general integral of these equations without the right-hand terms. Using engineering language we may say that we are here in the presence of the resonance when the periods of the free and the forced oscillations are equal and the system has no damping. This, clearly, leads to a cumulative phenomenon growing beyond any bounds.

From an offhand consideration, it may appear that the situation is not any better if we continue the procedure by calculating $x_2, x_3, \cdots$ by equations (13.2), inasmuch as all these terms will be also secular containing $t^2, t^3 \cdots$ outside the sign of the trigonometric functions. In reality the situation is somewhat different if we consider the following simple example:

$$\sin t = t - \frac{t^3}{3!} + \frac{t^5}{5!} - \cdots \tag{13.8}$$

representing the series expansion of the periodic function $\sin t$ in terms of an infinite series of "secular terms" $t, t^3/3!, \cdots$. It is clear that if one designates by $f_n(t)$ a finite sum of the first n terms of this series, this function f_n will represent $\sin t$ with a sufficient accuracy only for $t < t_0$, where t_0 is a fixed number depending on the accuracy of the approximation desired. If, however, t increases indefinitely, the function f_n will depart more and more from $\sin t$. Only when $n = \infty$ will the series of the "secular terms" represent *exactly* the periodic function $\sin t$ for all values of t.

It follows, therefore, that the formal solutions by series limited to a final number of terms inevitably will lead to the appearance of the secular terms. In astronomical problems for which Poincaré developed his method this circumstance does not present any serious difficulty

because it is always possible to determine the upper bound t_0 so that the effect of the secular terms is negligible from a practical standpoint.

In applied problems, however, this circumstance, results in a very serious difficulty. Thus, for example, an electron tube oscillator oscillating with a frequency of, say, several megacycles per second, in a few seconds will complete as many cycles as an astronomical system completes in many millions of years. The secular terms in this case will grow beyond any bound, so that the method becomes useless.

For that reason for the construction of the approximations of higher orders Kryloff and Bogoliuboff (7) adopted the alternative astronomical method of Lindstedt (20). The fundamental idea of this method consists in the elimination of secular terms in each step of the recurrence procedure. In order to be able to do this, one has to dispose of a certain number of additional parameters. In the Lindstedt method these parameters appear in the form of the coefficients of the power series representing the nonlinear frequency Ω as a function of μ.

Let us consider, for example, the quasi-linear differential equation of a conservative system

$$\ddot{x} + \omega^2 x + \mu f(x) = 0. \tag{13.9}$$

We shall look for a periodic solution of this equation with period T (frequency $\Omega = 2\pi/T$), which, for the time being, are unknown. Equation (13.9) becomes

$$\Omega^2 \ddot{z} - \omega^2 z + \mu f(z) = 0 \tag{13.10}$$

if we take as dependent variable $z(\tau)$, where $\tau = \Omega t + \varphi$. Differentiations in (13.10) are now with respect to τ. We shall look for the solutions of the form

$$z(\tau) = \sum_{n=0}^{\infty} \mu^n z_n(\tau) \tag{13.11}$$

where Ω^2 is given by

$$\Omega^2 = \sum_{n=0}^{\infty} \mu^n \alpha_n. \tag{13.12}$$

Since for $\mu = 0$, $\Omega^2 = \omega^2$, from (13.12) it follows that $\alpha_0 = \omega^2$. The nonlinear function $f(z)$ with the use of (13.11) becomes

$$f(z) = f(z_0 + \mu z_1 + \mu^2 z_2 + \cdots) = f(z_0) + \mu z_1 f'(z_0) + \mu^2 \left[z_2 f'(z_0) + \frac{z_1^2 f''(z_0)}{2} \right] + \cdots. \tag{13.13}$$

Substituting (13.11), (13.12), and (13.13) in (13.10) and equating the coefficients of like powers of μ, we obtain a number of differential equations:

$$\begin{aligned}
\omega^2\ddot{z}_0 + \omega^2 z_0 &= 0 \\
\omega^2\ddot{z}_1 + \omega^2 z_1 &= -f(z_0) - \alpha_1\ddot{z}_0 \\
\omega^2\ddot{z}_2 + \omega^2 z_2 &= -f'(z_0)z_1 - \alpha_2\ddot{z}_0 - \alpha_1\ddot{z}_1.
\end{aligned} \tag{13.14}$$

Comparing 13.14 with (13.3) we see that (13.14) has additional parameters $\alpha_1, \alpha_2, \cdots$, owing to (13.12).

Let $z_0, z_1, z_2, \cdots z_n$ and $\alpha_1, \alpha_2, \cdots \alpha_n$ be the solutions of the first n equations (13.14). They satisfy (13.9) to the order of n and, hence may be considered as the nth approximation. The first equation gives $z_0 = a \cos \tau$ where a is an arbitrary constant. The second constant, the phase angle, can be obviously assumed to be zero.

If we proceed now with the second equation, there will appear a certain arbitrariness in the determination of its solution, which we can now remove owing to the presence of the additional parameter α_1.

$$\omega^2(\ddot{z}_1 + z_1) = -f(a \cos \tau) + \alpha_1 a \cos \tau. \tag{13.15}$$

The nonlinear function $f(a \cos \tau)$ can be developed into a Fourier series containing only the cosine terms, namely,

$$f(a \cos \tau) = f_0(a) + f_1(a) \cos \tau + \sum_{n=2}^{\infty} f_n(a) \cos n\tau. \tag{13.16}$$

Substituting (13.16) in (13.15) we get

$$\omega^2(\ddot{z}_1 + z_1) = -\sum_{n=2}^{\infty} f_n(a) \cos n\tau + [\alpha_1 a - f_1(a)] \cos \tau - f_0(a). \tag{13.17}$$

It is clear that the term with $\cos \tau$ on the right side of this equation is a secular term. The *Lindstedt procedure consists in so determining* α_1 *as to remove this term, which gives*

$$\alpha_1 = \frac{f_1(a)}{a}. \tag{13.18}$$

The same procedure is applied to other equations (13.14). It is to be noted that the removal of the secular term in each subsequent approximation at the same time leads to the determination of the coefficients $\alpha_1, \alpha_2, \cdots$ entering in the expression (13.12), so that the expansions (13.11) and (13.12) are determined gradually by the same procedure.

As an example of the application of this method, let us consider the quasi-linear differential equation

$$\ddot{x} + x + \mu x^3 = 0. \tag{13.19}$$

Taking as generating solution $z_0(\tau) = a \cos \tau$, $\omega^2 = 1$ and $a_0 = 1$, we have

$$\ddot{z}_1 + z_1 = -z_0{}^3 - \alpha_1 \ddot{z}_0 = \left(\alpha_1 a - \frac{3}{4} a^3\right) \cos \tau - \frac{a^3}{4} \cos 3\tau.$$

The elimination of the secular term gives

$$\alpha_1 = (\tfrac{3}{4})a^2$$

and the solution z_1 is

$$z_1 = \tfrac{3}{32} a^3 \cos 3\tau.$$

Substituting these values α_1 and z_1 in the third equation (13.14) we get

$$\begin{aligned} \ddot{z} + z_2 &= -\tfrac{3}{32} a^5 \cos^2 \tau \cos 3\tau + \alpha_2 a \cos \tau + \tfrac{27}{128} \cos 3\tau \\ &= (\alpha_2 a - \tfrac{3}{128} a^5) \cos \tau + \tfrac{21}{128} a^5 \cos 3\tau - \tfrac{3}{128} a^5 \cos 5\tau. \end{aligned}$$

The elimination of the secular term determines $\alpha_2 = \tfrac{3}{128} a^4$ and gives

$$z_2 = -\frac{21}{1024} a^5 \cos 3\tau + \frac{a^5}{1024} \cos 5\tau.$$

The solution of (13.19) to the third order, therefore, is

$$x = a \cos(\omega t + \varphi) + \mu \frac{a^3}{32}\left(1 - \mu \frac{21}{32}\right) \cos.(3\omega t + \varphi) + \mu^2 \frac{a^5}{1024} \cos(5\omega t + \varphi)$$

where a and φ are the integration constants. The nonlinear frequency is

$$\Omega^2 = 1 + \tfrac{3}{4}\mu a^2 + \tfrac{3}{128}\mu^2 a^4.$$

There are certain difficulties regarding the convergence of the Lindstedt expansions (2) that limit its usefulness in astronomical calculations. In applied problems, however, this is less serious, inasmuch as the *physical existence* of a certain phenomenon frequently renders this question unnecessary and the method leads to the establishment of the approximations of higher orders without any difficulty except the length of calculations.

III. Nonlinear Resonance and Associated Phenomena

14. Introductory Remarks

The phenomena of resonance in nonlinear systems are far more diversified and complicated than the well-known effects of resonance in linear systems. From the mathematical viewpoint the difficulties are due to the fact that in this case the time t appears explicitly on the right-hand side of equations (2.1), which complicates considerably the situation, as we are going to see later. Furthermore, the simple intuitive concepts such as the coexistence of free and forced oscillations appearing in the theory of linear systems are not available in the nonlinear systems.

Very frequently one comes across rather paradoxical phenomena, at least from the standpoint of the familiar picture of the linear resonance. In some cases, for instance, one observes discontinuities or "jumps" in the resonance curve. Under some other conditions the application of an external periodic excitation to a nonlinear system may cause the appearance of an oscillation with a frequency different from that of the external excitation. In some other cases a nonlinear system begins to oscillate as the result of a periodic variation of one of its parameters without any external excitation and so on.

Among this variety of phenomena the one that seems to be best studied at present is the phenomenon of the so-called subharmonic resonance, to which a considerable part of what follows will be devoted. In spite of a relatively well-established theory of this phenomenon, the experimental confirmation of the various subharmonic resonances is still lacking in many respects. Thus, for instance, well explored is the resonance of the order $\frac{1}{2}$; there are experiments known in which a few other types of the subharmonic resonance have been observed but the picture is yet far from being complete. There are situations in which, on the other hand, the experimental evidence is sufficiently well established but the theory has not progressed sufficiently to be able to explain the observed facts. Thus, for example, we shall see in the theory of the so-called parametric excitation that the observed phenomena are apparently amenable to a nonlinear differential equation with periodic coefficients the theory of which is entirely unknown at present.

It must be admitted, therefore, that the present status of the theory of the nonlinear resonance with numerous associated phenomena is yet in an early stage of its development.

In spite of these handicaps the existing material on the subject is so extensive that an attempt to outline briefly what has been accomplished to date is worth while.

15. Subharmonics

It is useful to say a few words about the appearance of the so-called *subharmonics* in nonlinear problems in order to prepare the ground for the study of the resonance phenomena.

Helmholtz in his studies of the physiological acoustics discovered (24) that the ear receives sounds that are not contained in the emitted acoustic radiation and explained this on the basis of a slightly funnel-shaped form of the tympanic membrane, whose vibration is governed by a certain nonlinear differential equation. Without going into this matter here, it is sufficient to mention only the result of this analysis, namely, if the acoustic radiation possesses, say, two frequencies ω_1 and ω_2, in addition to these two frequencies the ear will hear also the so-called *combination tones* $\omega_1 + \omega_2$, $\omega_1 - \omega_2$.

Independently of this discovery of Helmholtz, Poincaré (25) in his studies of nonlinear differential equations established that in addition to certain fundamental frequencies ω_1 and ω_2 of a nonlinear system, there are also *solutions of the second kind*, as he calls them, that also satisfy the same differential equation and have the frequencies

$$\omega = m\omega_1 + n\omega_2 \tag{15.1}$$

where m and n are integers.

It is more convenient to reach these results from the theory of electron tubes, which may be considered as nonlinear conductors of electricity, whose nonlinear characteristic is of the form

$$i_a = f(v) \tag{15.2}$$

where i_a is the plate current and v is the grid potential; we shall be interested only in the alternating components of these quantities. Let us assume that we impress on the grid an alternating potential of the form

$$v = k(\cos \omega_1 t + \cos \omega_2 t).$$

Since the nonlinear function (15.2) can always be represented by a certain power series

$$i_a = a_1 v + a_2 v^2 + a_3 v^3 + \cdots \tag{15.3}$$

the oscillations of i_a will be clearly given by the expression

$$i_a = a_1 k(\cos \omega_1 t + \cos \omega_2 t) + a_2 k^2 (\cos \omega_1 t + \cos \omega_2 t)^2 + \cdots .$$

If one limits this expression, say, to the first three terms one finds easily

that there appear the following frequencies in the oscillation of the plate current:

$$\omega_1,\ \omega_2,\ 2\omega_1,\ 2\omega_2,\ 3\omega_1,\ 3\omega_2,\ \omega_1+\omega_2,\ \omega_1-\omega_2,\ 2\omega_1+\omega_2,$$
$$2\omega_1-\omega_2,\ 2\omega_2+\omega_1,\ 2\omega_2-\omega_1.$$

Thus, for instance, if $\omega_1 = 100$, $\omega_2 = 120$, the spectrum of the *combination frequencies* will be 20, 80, 100, 120, 140, 200, 220, 240, 300, 320, 360, and it is seen that this spectrum spreads both below (subharmonics) and above (superharmonics) the original frequencies 100 and 120. In applied problems the lower combination frequencies are of a greater importance and this is probably the reason why the term *subharmonic* replaced a more correct term *combination harmonic*.

16. Subharmonic Resonance of the Order 1/n

In the following analysis due to L. Mandelstam and N. Papalexi (26) we shall investigate a quasi-linear differential equation of the form

$$\ddot{x} + x = \mu f_1(t,x,\dot{x}). \tag{16.1}$$

We shall restrict the problem to an important practical case when the function f_1 is of the form

$$f_1(t,x,\dot{x}) = f(x,\dot{x}) + \lambda_0 \sin n\tau. \tag{16.2}$$

We have, therefore, the case when a quasi-linear system is subjected to an external periodic excitation $\lambda_0 \sin n\tau$ with amplitude λ_0 and period $T = 2\pi/n$.

Mandelstam and Papalexi show that the equation of a self-excited electron tube circuit to the grid of which is applied a voltage of the form $v \sin n\epsilon$ can be reduced to the form (16.2). We omit this reduction and shall pass directly to the analysis of (16.1), which will be here of the form

$$\ddot{x} + x = \mu f(x,\dot{x}) + \lambda_0 \sin n\tau. \tag{16.3}$$

It is clear that if $\mu = 0$, there exists an infinity of solutions of the form

$$x = a_0 \sin \tau + b_0 \cos \tau + \frac{\lambda_0}{(1-n^2)} \sin n\tau \tag{16.4}$$

where the first two terms represent the free oscillation and the third the forced one; a_0 and b_0 are the integration constants.

The principal part of the problem is to determine the functions $a(\mu)$ and $b(\mu)$ of the nonlinear problem so that $a(\mu) \to a_0$; $b(\mu) \to b_0$ when $\mu \to 0$. If one succeeds in so determining these functions, the solution so obtained will be called *the principal solution*.

If, in addition to this, one succeeds in showing that the principal solution is *stable*, this will mean that it actually exists, so that the problem is solved completely.

Introducing a new variable

$$z = x - \frac{\lambda_0}{1 - n^2} \sin n\tau \tag{16.5}$$

we find that equation (16.3) becomes

$$\ddot{z} + z = \mu f\left(z + \frac{\lambda_0}{1 - n^2} \sin n\tau,\ \dot{z} + \frac{n\lambda_0}{1 - n^2} \cos n\tau\right). \tag{16.6}$$

Changing the variables again, viz.,

$$\begin{aligned} u &= \dot{z} \cos \tau + z \sin \tau \\ v &= \dot{z} \sin \tau - z \cos \tau \end{aligned} \tag{16.7}$$

(16.6) is replaced by the system

$$\begin{aligned} \dot{u} &= (\ddot{z} + z) \cos \tau = \mu\psi(u,v,\tau) \cos \tau \\ \dot{v} &= (\ddot{z} + z) \sin \tau = \mu\psi(u,v,\tau) \sin \tau \end{aligned} \tag{16.8}$$

where

$$\psi(u,v,\tau) = f\left(u \sin \tau - v \cos \tau + \frac{\lambda_0}{1 - n^2} \sin n\tau,\right.$$
$$\left. u \cos \tau + v \sin \tau + \frac{n\lambda_0}{1 - n^2} \cos n\tau\right)$$

is periodic with period 2π. From (16.6) and (16.8) we get

$$x = u \sin \tau - v \cos \tau + \frac{\lambda_0}{1 - n^2} \sin n\tau$$

which is of the form (16.4). Hence, the principal solution will be obtained if $u \to a_0$, $v \to b_0$ when $\mu \to 0$. We apply now the argument of Poincaré and assume that for $\mu \neq 0$, u and v differ little from a_0 and b_0 when μ is small. This assumption is

$$u_{t=0} = a_0 + \alpha; \qquad v_{t=0} = b_0 + \beta \tag{16.9}$$

α and β being small numbers. From (16.8) we get

$$\begin{aligned} u &= u_{t=0} + \mu \int_0^\tau \psi(u,v,\tau) \cos \tau d\tau \\ v &= v_{t=0} + \mu \int_0^\tau \psi(u,v,\tau) \sin \tau d\tau. \end{aligned} \tag{16.10}$$

On the other hand, we know (cf. Eq. 10.10) that u and v can be expanded in a series in terms of α, β and μ, that is,

$$u = a_0 + \alpha + \mu C_1(\tau) + \mu\alpha D_1(\tau) + \mu\beta E_1(\tau) + \mu^2 G_1(\tau) + \cdots$$
$$v = b_0 + \beta + \mu C_2(\tau) + \mu\alpha D_2(\tau) + \mu\beta E_2(\tau) + \mu^2 G_2(\tau) + \cdots . \quad (16.11)$$

Comparison of (16.11) and (16.10) gives

$$C_1(\tau) = \int_0^\tau \psi(a_0,b_0,\tau)\cos\tau d\tau; \qquad C_2(\tau) = \int_0^\tau \psi(a_0,b_0,\tau)\sin\tau d\tau$$
$$D_1(\tau) = \int_0^\tau \left[\frac{\partial\psi}{\partial u}\right]\cos\tau d\tau; \qquad D_2(\tau) = \int_0^\tau \left[\frac{\partial\psi}{\partial u}\right]\sin\tau d\tau$$
$$E_1(\tau) = \int_0^\tau \left[\frac{\partial\psi}{\partial v}\right]\cos\tau d\tau; \qquad E_2(\tau) = \int_0^\tau \left[\frac{\partial\psi}{\partial v}\right]\sin\tau d\tau. \quad (16.12)$$

where [ ] designate the values of the partial derivatives for $\mu = \alpha = \beta = 0$. If u and v are periodic, that is $u(2\pi) = u(0)$; $v(2\pi) = v(0)$; (16.11) gives then

$$C_1(2\pi) + \alpha D_1(2\pi) + \beta E_1(2\pi) + \mu G_1(2\pi) = 0$$
$$C_2(2\pi) + \alpha D_2(2\pi) + \beta E_2(2\pi) + \mu G_2(2\pi) = 0 \quad (16.13)$$

to the second order. The procedure from now is similar to that encountered already. Clearly, since $\alpha(\mu)$ and $\beta(\mu)$ are small and approach zero as $\mu \to 0$, their determination is possible if

$$C_1(2\pi) = \int_0^{2\pi} \psi(a_0,b_0,\tau)\cos\tau d\tau = 0;$$
$$C_2(2\pi) = \int_0^{2\pi} \psi(a_0,b_0,\tau)\sin\tau d\tau = 0. \quad (16.14)$$

From these two equations are obtained a and b, to which approach u and v of the principal solution when $\mu \to 0$.

The functions $\alpha(\mu)$ and $\beta(\mu)$ are obtained from equations

$$\alpha D_1(2\pi) + \beta E_1(2\pi) + \mu G_1(2\pi) = 0$$
$$\alpha D_2(2\pi) + \beta E_2(2\pi) + \mu G_2(2\pi) = 0 \quad (16.15)$$

which must be satisfied for any arbitrary but small μ. It is clear that these equations yield nontrivial solutions for μ small if

$$\Delta = \begin{vmatrix} D_1(2\pi), & E_1(2\pi) \\ D_2(2\pi), & E_2(2\pi) \end{vmatrix} \neq 0. \quad (16.16)$$

If α and β can be determined in this manner, one obtains a nonlinear motion in the neighborhood of the linear one given by (16.4). It must be noted, however, that this nonlinear motion can exist physically only if it is stable.

The question of stability can be investigated by the standard procedure, which consists in setting $u = u_0 + \xi$, $v = v_0 + \eta$, and considering ξ and η as small quantities of the first order. Keeping only the first order terms we obtain

$$\frac{d\xi}{dt} = (\mu\psi_u \sin\tau)\eta + (\mu\psi_v \sin\tau)\xi$$
$$\frac{d\eta}{dt} = (\mu\psi_u \cos\tau)\eta + (\mu\psi_v \cos\tau)\xi. \qquad (16.17)$$

This is a system of differential equations with periodic coefficients, and the standard procedure can be applied (27). Let $\eta_1(\tau)$, $\xi_1(\tau)$; $\eta_2(\tau)$, $\xi_2(\tau)$ be two sets of solutions forming a fundamental system. The initial conditions $\eta_1(0) = 1$; $\xi_1(0) = 0$; $\eta_2(0) = 0$; $\xi_2(0) = 1$ can always be assumed. Since $\eta_1(\tau + 2\pi)$, $\xi(\tau + 2\pi)$, $\cdots$ are also solutions, we can write

$$\eta_1(\tau + 2\pi) = a\eta_1(\tau) + b\eta_2(\tau); \qquad \xi_1(\tau + 2\pi) = a\xi_1(\tau) + b\xi_2(\tau)$$
$$\eta_2(\tau + 2\pi) = c\eta_1(\tau) + d\eta_2(\tau); \qquad \xi_2(\tau + 2\pi) = c\xi_1(\tau) + d\xi_2(\tau). \qquad (16.18)$$

In view of the initial conditions we have

$$\eta_1(2\pi) = a; \qquad \xi_1(2\pi) = b; \qquad \eta_2(2\pi) = c; \qquad \xi_2(2\pi) = d. \qquad (16.19)$$

It is possible to reduce (16.18) to the canonical form $\eta_1(\tau + 2\pi) = S_1\eta_1(\tau) \cdots$ by determining the roots of the characteristic equation

$$S^2 + pS + q = 0$$

with

$$p = -[\eta_1(2\pi) + \xi_2(2\pi)] \qquad \text{and} \qquad q = [\eta_1(2\pi)\xi_2(2\pi) - \eta_2(2\pi)\xi_1(2\pi)]. \qquad (16.20)$$

If $\mu = 0$, η and ξ remain equal to their initial values $\eta_1(\tau) = \xi_2(\tau) = 1$; $\eta_2(\tau) = \xi_1(\tau) = 0$ and $p = -2$; $q = 1$. Hence when $\mu \neq 0$ but small, $p < 0$ and $q > 0$. Equation (16.20) has stable roots if their moduli are less than unity. This condition is fulfilled if

$$p > -2; \qquad 1 + p + q > 0$$

as it follows from the equations

$$1 + p + q = (S_1 - 1)(S_2 - 1); \qquad p = -(S_1 + S_2).$$

Hence, the conditions of stability are satisfied for $\mu \ll 1$ only when the first nonvanishing derivatives of p and $p + q$ with respect to μ are

positive for $\mu > 0$. Omitting the intermediate calculations, we obtain the following conditions for stability

$$D_1(2\pi) + E_2(2\pi) < 0; \qquad \begin{vmatrix} D_1(2\pi), & D_2(2\pi) \\ E_1(2\pi), & E_2(2\pi) \end{vmatrix} > 0. \tag{16.21}$$

17. Subharmonic Resonance of the Order One Half

We shall now investigate the important practical case when $n = 2$ in equation (16.3). It has been known for a long time that when a simple nonlinear system is acted on by an external periodic force with period T, there appears an oscillation with period $T/2$. Lord Rayleigh (28) investigated this case in detail, and we shall return to his results later. The school of Mandelstam and Papalexi carried out numerous theoretical and experimental researches on this subject and we shall review briefly this work. Most of these investigations was carried out with the electron tube circuits in which the nature of non-linearities can be easily ascertained. We shall not enter here to the question of reduction of the differential equations of the electron tube circuits to a standard form but shall proceed directly with the discussion of the reduced equation.

It can be shown (26) that the nonlinear function here is

$$\mu f(x,\dot{x}) = (k + 2x + A_3x^2 + A_4x^3 + A_5x^4)\dot{x} + \frac{\xi}{a_2}x$$

where

$$\mu = \frac{a_2}{1+\xi}; \qquad \theta = \frac{Rn}{2L\omega}; \qquad k = \frac{a_1 - 2\theta(1+\xi)}{a_2}; \qquad A_3 = \frac{3a_3}{a_2};$$

$$A_4 = \frac{4a_4}{a_2}; \qquad A_5 = \frac{5a^5}{a_2}; \qquad \xi = \frac{\omega^2}{\omega_0^2 n^2} - 1 \tag{17.1}$$

and $a_1, a_2, \cdots, a_5$ are the coefficients appearing in the approximation of the nonlinear function expressing the plate current I_a as a function of an auxiliary variable $x = V_g/V_0$, where V_g is the grid voltage and V_0 is the so-called *saturation voltage*, that is, a sufficiently high grid voltage for which the plate current does not change appreciably if V_g is varied. The nonlinear function is here

$$I_a = f_1(x) = I_{a_0} + a_1x + a_2x^2 + a_3x^3 + a_4x^4 + a_5x^5. \tag{17.2}$$

Some of these coefficients may be either positive or negatives according to the form of the characteristic of the electron tube. For $n = 2$, (16.4) is

$$x = a \sin \tau - b \cos \tau - \frac{\lambda_0}{3} \sin 2\tau = X \sin (\tau - \varphi) - \frac{\lambda_0}{3} \sin 2\tau. \tag{17.3}$$

In the case of the so-called soft self-excitation (section 5, part I) the characteristic has no inflection point, so that $a_4 = a_5 = 0$; we shall limit the following analysis to this particular case.

The problem consists in solving (16.14), in which $\psi(a,b,\tau)$ is $f(x,\dot{x})$ with x given by (17.3). We obtain thus the following expressions:

$$X^2 = a^2 + b^2 = -\frac{2}{9}\lambda_0^2 - \frac{4}{A_3}\left[k \pm \sqrt{\frac{\lambda_0^2}{9} - \frac{\xi^2}{a^2{}_2}}\right] \tag{17.4}$$

$$\varphi = \tan^{-1}\frac{b}{a} = \tan^{-1}\sqrt{\frac{\frac{\lambda_0}{3} + \frac{\xi}{a_2}}{\frac{\lambda_0}{3} - \frac{\xi}{a_2}}} \tag{17.5}$$

for the amplitude and phase of the principal solution. Since the amplitude X is a real quantity, the expression on the right-hand side of (17.4) must be positive. As the term $-(\frac{2}{9})\lambda_0^2$ is always negative, this condition is fulfilled if the second term on the right of (17.4) is positive and greater than $\frac{2}{9}\lambda_0^2$. If $A_3 < 0$, $k < 0$, the condition $X^2 > 0$ may be fulfilled for either sign before the square root. It is seen thus that in general the existence of the principal solution depends on the relative values of A_3, k and ξ/a_2 easy to discuss. It is interesting to note, however, that there may be conditions under which the principal solution does not exist.

The requirement for stability restricts further the existence of the principal solution. For this one has to calculate the explicit values of the functions $D_1(2\pi)$, $D_2(2\pi)$, $E_1(2\pi)$ and $E_2(2\pi)$ given by (16.12). We have

$$\left[\frac{\partial\psi}{\partial u}\right] = \frac{\partial f}{\partial x}\frac{\partial x}{\partial u} + \frac{\partial f}{\partial \dot{x}}\frac{\partial \dot{x}}{\partial u}; \qquad \left[\frac{\partial\psi}{\partial v}\right] = \frac{\partial f}{\partial x}\frac{\partial x}{\partial v} + \frac{\partial f}{\partial \dot{x}}\frac{\partial \dot{x}}{\partial v}$$

where $x = u\sin\tau - v\cos\tau - \frac{\lambda_0}{3}\sin 2\tau$; $\dot{x} = u\cos\tau + v\sin\tau - \frac{2\lambda_0}{3}\cos 2\tau$.

Hence

$$\frac{\partial x}{\partial u} = \sin\tau; \qquad \frac{\partial \dot{x}}{\partial u} = \cos\tau; \qquad \frac{\partial x}{\partial v} = -\cos\tau; \qquad \frac{\partial \dot{x}}{\partial v} = \sin\tau.$$

Substituting these expressions into (16.12) and noting that in this case

$$\frac{\partial f}{\partial x} = 2(1 + A_3 x)\dot{x} + \frac{\xi}{a_2}; \qquad \frac{\partial f}{\partial \dot{x}} = k + 2x + A_3 x^2$$

we obtain the conditions for stability (16.21) both for the principal solution and also the solution corresponding to the case when $a = b = 0$, which is called the *heteroperiodic solution*. Omitting the intermediate calculations, we find that for the principal solution

$$\frac{\xi^2}{a_2^2} \leq \frac{\lambda_0^2}{9} - \left(k - \frac{|A_3|\lambda_0^2}{18}\right)^2 \tag{17.6}$$

and for the heteroperiodic solution

$$\frac{\xi^2}{a_2^2} > \frac{\lambda_0^2}{9} - \left(k - \frac{|A_3|\lambda_0^2}{18}\right)^2. \tag{17.7}$$

Since $\xi = \dfrac{\omega^2}{\omega_0^2 n^2} - 1$ may be considered as a measure for the *discrepancy* between the impressed frequency ω and $n\omega_0 = n\sqrt{1/LC}$, it is clear that the solutions change with ξ. The essential point if this analysis is that the interval in which the two solutions exist *do not overlap*. In other words the principal solution exists in the interval of ξ in which the heteroperiodic one does not exist and vice versa. It is thus seen that these phenomena are of an entirely different nature from the well-known phenomena of the linear resonance in which both oscillations, the free and the forced ones, exist throughout the whole range of frequencies and coalesce only at the point of the resonance.

The equation

$$\frac{\xi^2}{a_2^2} = \frac{\lambda_0^2}{9} - \left(k - \frac{|A_3|\lambda_0^2}{18}\right)^2$$

gives two limit values ξ_1 and ξ_2 between which the stable principal solution exists. The interval is

$$\Delta\xi = \xi_2 - \xi_1 = 2a_2\sqrt{\frac{\lambda_0^2}{9}\left(1 - k_0 A_3 - \frac{A_3^2\lambda_0^2}{36}\right) - k_0^2}.$$

If all other parameters are fixed, $\Delta\xi$ is a function of λ_0. If λ_0 increases from zero, $\Delta\xi$ becomes real beginning with a certain value of λ_0, then goes through a maximum and disappears when

$$\frac{\lambda_0^2}{9} = \frac{2}{A_3^2}(1 - k_0 A_3 + \sqrt{1 - 2k_0 A_3}).$$

Here, again, we encounter a radical difference with the phenomenon of the linear resonance in which the interval of the existence of both free and

forced oscillations extends for all values of λ_0. Here, on the other hand, we come across a somewhat paradoxical fact that the principal oscillation disappears if the amplitude λ_0 of the external force becomes too large.

The phenomenon of the subharmonic resonance has been particularly well studied when the coefficient k in (17.1) is negative, that is, when the system (16.3) is stable for $x = 0$. With an electron tube oscillator this condition is obtained by adjusting the feed back coupling to a value at which the oscillator is just slightly below its point of self-excitation. If there is applied then to the grid of the tube a voltage of frequency ω in the

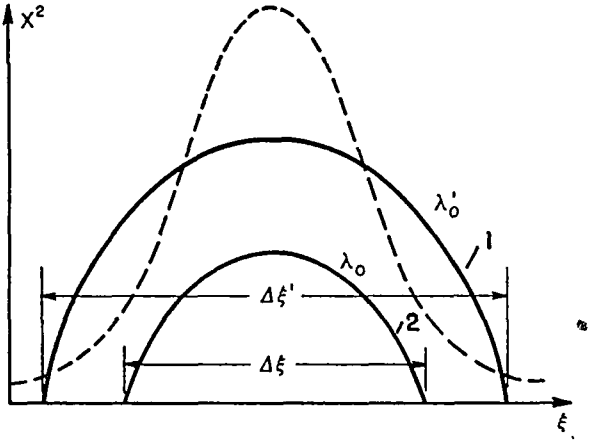

FIG. 19.

neighborhood of $2\omega_0$ where $\omega_0 = \sqrt{1/LC}$, the following phenomena are observed. If ω differs much from $2\omega_0$ only a small heteroperiodic oscillation is observed. If, however, ω approaches the value $2\omega_0$ so as to be within the above specified interval $\Delta\xi$, the principal oscillation suddenly appears with frequency $\omega/2$. It is to be observed that, since $\xi = (\omega^2 - 2\omega_0^2)/2\omega_0^2$ there are two possible ways for varying ξ, viz., to vary ω while keeping ω_0 constant, or to vary ω_0 keeping ω constant. In the first case, as just mentioned, the frequency of the principal oscillation will be exactly $\omega/2$, and therefore will be variable. In the second case, on the contrary, this frequency will be constant. In both cases, however, the zone in which the principal oscillation exists depends on both ω and ω_0 and not on each of these quantities separately. Curves 1 and 2 of Fig. 19 show the usual form of the subharmonic oscillation plotted against ξ. It is observed that these curves have an entirely different form as compared with the corresponding curve of the linear resonance, shown by the broken line.

If the nonlinear characteristic is of the *hard* type, that is, has an inflection point, the terms a_4x^4 and a_5x^5 have to be taken into account in

equation (17.2). If a similar argument is followed, it is found that the phenomenon of the subharmonic resonance in this case has the appearance shown in Fig. 20, namely, the principal oscillation suddenly jumps from zero up to a certain finite value and disappears in the same fashion. Calculations in this case are much longer than in the case of a "soft characteristic" and for that reason are omitted here. Numerous experimental researches have corroborated these theoretical predictions. It is also interesting to mention that attempts were made to explore other forms of the subharmonic resonance. More specifically, the resonance of the order *one third* was ascertained. In this case the existence of the principal oscillation is possible only when $k > 0$, that is, when the system is self-excited for $x = 0$.

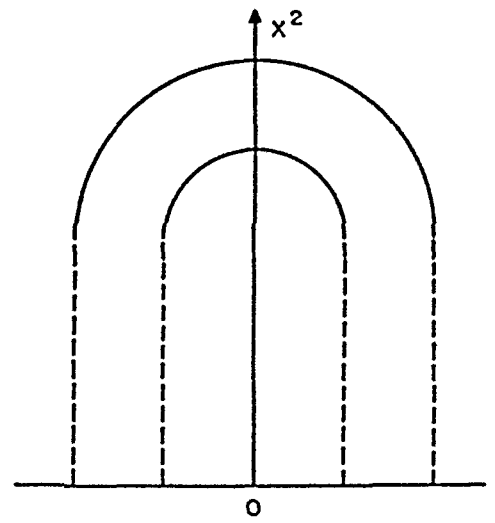

FIG. 20.

To complete this review, it must be also mentioned that in the case of a hard characteristic the intervals in which the principal and the heteroperiodic solutions exist generally overlap. This means that in the zone of overlapping both the principal and the heteroperiodic oscillations may occur at the same time.

18. Entrainment of Frequency

The reader might have noticed in the preceding section that the frequency of the principal oscillation is a subharmonic of one of the component frequencies ω and ω_0, whereas the amplitude depending on ξ depends on both ω and ω_0 simultaneously. Everything happens as though only one of the component frequencies is impressing its rhythm on the principal oscillation while the other is "entrained." In the theory of the subharmonic resonance this is merely incidental but the phenomenon of *entrainment of frequency* is sufficiently important to warrant its independent study.

It is likely that the phenomenon of entrainment has been known for a long time. Thus, for instance, Van der Pol (29) mentions that the tendency to a synchronization of two clocks fastened to a common support was already known to Huyghens.

The easiest way to observe this effect is to apply to the grid of an oscillator oscillating with frequency ω_0 a slightly different frequency ω

and to record the heterodyning, or beats, of both frequencies. As ω approaches ω_0, the beats become slower and, on the basis of the linear theory, one could expect that this process should continue indefinitely as ω approaches ω_0. In reality the beats disappear for a certain critical value of the difference $\Delta\omega = \omega - \omega_0$, after which there remains only one frequency ω as though the frequency ω_0 were suddenly pulled in, or *entrained* into synchronism with ω.

Vincent (30), Möller (31), Appleton (32) and others investigated this effect but it was van der Pol who gave a complete theory of the phenomenon (29). We shall outline here briefly this theory, supplementing it by certain topological considerations due to Andronow and Witt (33).

The differential equation of a heterodyne oscillator is

$$L\frac{di}{dt} + Ri + \frac{1}{C}\int idt - M\frac{di_a}{dt} = E_0 \sin \omega_1 t \tag{18.1}$$

where ω_1 is the extraneous frequency and $i_a = f(e_g)$ is a nonlinear function, the plate current versus the grid voltage.

As a first approximation van der Pol assumes

$$i_a = Se_g\left(1 - \frac{e_g^2}{3V_s^2}\right)$$

where V_s is the saturation voltage previously defined and S is the transconductance. If we introduce the notations

$$v = \frac{e_g}{V_s} = \frac{\int idt}{CV_s}; \qquad \alpha = \frac{MS}{LC} - \frac{R}{L}; \qquad \gamma = \frac{1}{3}\frac{MS}{LC}; \qquad B = \frac{E_0}{V_s};$$

$$\omega_0^2 = \frac{1}{LC}$$

(18.1) becomes

$$\ddot{v} - \alpha\dot{v} + \gamma\dot{v}^3 + \omega_0^2 v = B\omega_0^2 \sin \omega_1 t. \tag{18.2}$$

Taking as a solution of this equation the expression

$$v = b_1 \sin \omega_1 t + b_2 \cos \omega_1 t \tag{18.3}$$

and substituting it in (18.2) we obtain the following equations of the first approximation

$$\begin{aligned} 2\dot{b}_1 + zb_2 - \alpha b_1\left(1 - \frac{b^2}{a_0^2}\right) &= 0 \\ 2\dot{b}_2 - zb_1 - \alpha b_2\left(1 - \frac{b^2}{a_0^2}\right) &= -B\omega_0^2 \end{aligned} \tag{18.4}$$

with $z = 2(\omega_0 - \omega_1)$; $b^2 = b_1^2 + b_2^2$ and $a_0^2 = 4\alpha/3$. The quantities b_1 and b_2 are slowly varying functions of t since it is assumed that ω_0 and ω_1 are not far from each other. Incidentally, this circumstance permits neglecting the second derivatives of b_1 and b_2 in the first approximation. It is noted that (18.4) are of the form (2.1). It is apparent that when b_1 and b_2 are constant the solution corresponds to a singluar point of (18.4); on the other hand, in such a case there exists only one frequency ω_1. We are thus led to identify the singular points of the system (18.4) with the entrainment phenomenon. If, therefore, one succeeds in showing that there are certain regions of the phase plane in which the stable singular points of (18.4) exist, this region will be precisely *the zone of entrainment.*

If we set

$$x = \frac{b_1}{a_0}; \quad y = \frac{b_2}{a_0}; \quad a = \frac{z}{\alpha}; \quad A = -\frac{B\omega_0}{a_0\alpha}; \quad r^2 = x^2 + y^2; \quad \tau = \frac{t\alpha}{2}$$

the system (18.4) becomes

$$\begin{aligned} \frac{dx}{dt} &= x(1 - r^2) - ay \\ \frac{dy}{dt} &= ax + y(1 - r^2) + A. \end{aligned} \tag{18.5}$$

This system is identical with (7.2), which we have already discussed. As was shown, this system can be reduced to the following

$$\begin{aligned} \frac{d\xi}{dt} &= P(\xi,\eta) = m\xi + n\eta + \text{terms with } \xi^2,\eta^2 \cdots \\ \frac{d\eta}{dt} &= Q(\xi,\eta) = p\xi + q\eta + \cdots \end{aligned} \tag{18.6}$$

and where $x = x_0 + \xi$; $y = y_0 + \eta$.

The investigation of the distribution of singular points follows what was explained in Section 5, part I. The coordinates x_0 and y_0 of singular points are given by the equations

$$x_0 = -\frac{a\rho}{A}; \qquad y_0 = -\frac{\rho(1 - \rho)}{A} \tag{18.7}$$

where $\rho = r^2$ is given by

$$a^2\rho + \rho(1 - \rho^2) = A^2. \tag{18.8}$$

In the (ρ,a) plane the curve (18.8) of the third degree gives the "amplitudes" of singular points for any value of a; the quantity A is the

parameter of the family. It is clear that if the trajectories approach a singular point, b_1 and b_2 tend to become constant, which means that the ultimate oscillation will possess only one frequency.

If, however, the system (18.5) has a closed solution (limit cycle) b_1 and b_2 are certain periodic functions of t so that the oscillation occurs with two distinct frequencies.

Fig. 21 shows the family of curves (18.8) with A as parameter. For

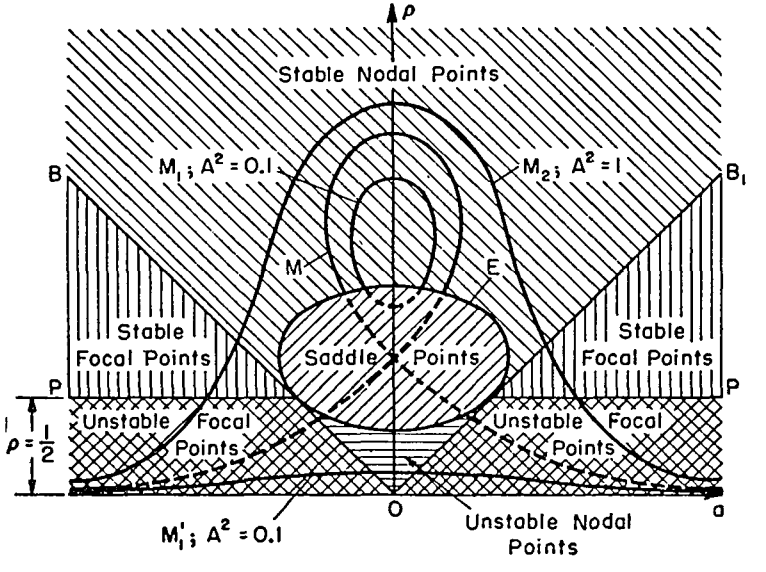

FIG. 21.

a sufficiently small A the curve consists of the two branches M_1 and M_1'. For an increasing A, the branch M_1 increases in size while M_1' rises until both branches join as shown by M. If A is further increased, there exists only one branch shown for $A^2 = 1$. The curves exist only above the a-axis and are symmetrical with respect to the ρ-axis. If we substitute the expressions $x = x_0 + \xi$; $y = y_0 + \eta$ into the equations of the first approximation, we get

$$\frac{d\xi}{dt} = \xi[(1 - \rho) - 2x_0^2] + \eta[-(a + 2x_0y_0)]$$

$$\frac{d\eta}{dt} = \xi(a - 2x_0y_0) + \eta[(1 - \rho) - 2y_0^2]. \qquad (18.9)$$

The characteristic equation of this system is

$$S^2 - 2(1 - 2\rho)S + [(1 - \rho)(1 - 3\rho) + a^2] = 0. \qquad (18.10)$$

We look now for the distribution of singularities in the (a,ρ) plane. It is clear that the saddle points are given by the inequality

$$(1 - \rho)(1 - 3\rho) + a^2 < 0$$

so that the saddle points are situated inside an ellipse E

$$(1 - \rho)(1 - 3\rho) + a^2 = 0$$

whose center is on the ρ axis. We verify that the quantity under the square root in the expression for the roots S_1 and S_2 changes its sign when $\rho^2 - a^2 = 0$. Hence, the straight lines B and B_1 given by $\rho + a = 0$ and $\rho - a = 0$ are the divides between the real roots and the complex ones. We find that B and B_1 are tangent to the ellipse E. We ascertain also from (18.10) that the stable roots are separated from the unstable ones by the line $\rho = \frac{1}{3}$; the stable roots lie above this line and the unstable roots below it. The analysis of the characteristic equation shows also that the region of nodal point lies inside the angle BOB_1, the area of the ellipse (saddle points) being excluded. In the region outside this angle lie focal points.

The condition that all three roots be real is $A^2 < \frac{4}{27}$. If $A^2 > \frac{4}{27}$, as is known, there is one real root and one pair of the complex conjugate roots, the latter being of no interest here. For $a^2 < a_1^2$, where a_1 is the abcissa of the point of intersection of the curve (18.8) with the ellipse E, there are three real roots, of which only one is stable. Hence, only in this interval the van der Pol solution (18.3) approaches a stationary periodic solution with frequency ω_1.

For $a^2 > a_1^2$ and still in the case of one real root, it is clear that this root is unstable and we saw in Section 7, part I that there exists a stable limit cycle. If the frequency on the latter is ω_0 it is clear that in this region the two frequencies ω_0 (the self-excited or autoperiodic) and ω_1, the heteroperiodic, coexist and form a regular heterodyning pattern, so that no entrainment occurs in that region. Thus the lines $a = \pm a_1$ determine a region, *the zone of entrainment*, in which the autoperiodic frequency ω_0 is *entrained* by the heteroperiodic one ω_1. Outside that region a regular heterodyne effect takes place.

In the zone of entrainment b_1 and b_2 are constant and (18.3) can be written as

$$v = b_1 \sin \omega_1 t + b_2 \cos \omega_1 t = b \sin (\omega_1 t + \varphi)$$

where

$$\tan \varphi = \frac{b_2}{b_1} = \frac{y_0}{x_0} = \frac{(1 - \rho)}{a} = \frac{(1 - r_0^2)\alpha}{2(\omega_0 - \omega_1)}$$

$$b = \sqrt{b_1^2 + b_2^2} = a_0 \sqrt{x_0^2 + y_0^2} = k \sqrt{\frac{4\alpha}{3\gamma}}$$

where

$$k = \frac{\rho}{a}\sqrt{a^2 + (1 - \rho)^2}. \tag{18.9}$$

In addition to the electrical form of entrainment investigated here, the entrainment phenomenon was discovered in acoustical and mechanical systems (34).

Successful attempts have been made in recent years to use the entrainment effect for an accurate control of speed of electric motors synchronized with an oscillating circuit whose frequency is maintained with great accuracy by a piezoelectric crystal (35).

19. Parametric Excitation

It has been known for a long time that it is possible to obtain a self-excitation of oscillations in a dynamical system by means of a periodic variation of some of its parameters. The classic experiment of this kind is due to Melde (36). Lord Rayleigh reproduced and further analyzed (37) the Melde experiment, which can be described as follows. If a stretched string is attached to a prong of a tuning fork and the latter is excited, there appears a lateral oscillation of the string with frequency equal to one half of that of the tuning fork. In later years Brillouin (38) and Poincaré (39) analyzed similar phenomena in electrical circuits. The usual explanation of the Melde-Rayleigh experiment is as follows: the oscillations of the tuning fork produce periodically varying tensions in the string. If a slight variation in the coefficient of elasticity of the string is assumed, it is clear that this periodically varying tension results in a differential equation with a periodic coefficient, describing the phenomenon. This question has been thoroughly explored as far as the *linear* differential equations with periodic coefficients are concerned (27). Unfortunately, there exists no theory whatever dealing with the nonlinear or, at least, quasi-linear equations of this kind. For that reason it is impossible at present to determine the stationary condition for such *parametrically excited oscillations;* it is possible only to ascertain under which conditions such oscillations may arise.

In spite of the present theoretical limitations, the phenomenon of *parametric excitation* presents a variety of possible applications. It is sufficient to mention as one such application the self-excitation of modern cavity resonators of the "klystron" type used extensively in high frequency technique (40). As another application the so-called parametric generator developed by Mandelstam and Papalexi (41) can be mentioned. There exists also a connection between this phenomenon and the theory of the subharmonic resonance, as will be mentioned below.

Before attacking the problem of parametric excitation it will be useful to say a few words about the differential equations with periodic coefficients. The simplest and most commonly encountered form of these equations is

$$\ddot{x} + M(t)x = 0 \tag{19.1}$$

where $M(t)$ is a periodic function. A special form of this equation is the so-called equation of Mathieu, in which $M(t) = a^2 + b^2 \cos t$, where a^2 and b^2 are constants. If $M(t)$ is a Fourier series, (19.1) is called the Hill equation. As the theory of these equations is practically the same, both equations can be studied together.

A differential equation of the form

$$\ddot{z} + 2p(t)\dot{z} + q(t)z = 0$$

where $p(t)$ and $q(t)$ are periodic, can be reduced to the form (19.1) by introducing a new variable x

$$z = xe^{-\int p dt} \qquad \text{so that} \qquad M(t) = q - p^2 - \dot{p}.$$

As is well known, the essential feature of the Mathieu equation is that, although $M(t)$ is periodic, its solutions are not necessarily periodic; under certain conditions they may be periodic, in which case the solutions are given in terms of the so-called *Mathieu functions*. One generally distinguishes between two kinds of solutions: the stable solutions and the unstable ones. Van der Pol and Strutt (42) investigated this question and calculated the stable and the unstable regions of the Mathieu equation in the (a^2,b^2) plane.

From the standpoint of the parametric excitation only the unstable solutions are of interest, inasmuch as in a physical problem of self-excitation from rest they represent cumulative phenomenon. It is easy to show that the phenomenon of parametric excitation is closely related to the phenomenon of the subharmonic resonance. In fact, let us consider again the fundamental equation (16.3) of the subhatmonic resonance in the neighborhood of its stationary solution $x_0(\tau)$ so that

$$x = x_0(\tau) + \rho \tag{19.2}$$

where ρ is a small perturbation. Substituting (19.2) in (16.3) we obtain after expanding $f(x,\dot{x})$ into a Taylor series the equation of the first approximation

$$\ddot{\rho} + \rho = \rho\mu f_{x_0}(x_0,\dot{x}_0) + \dot{\rho}\mu f_{\dot{x}_0}(x_0,\dot{x}_0) \tag{19.3}$$

where f_x and $f_{\dot{x}}$ are known periodic functions of time so that (19.3) is an equation with periodic coefficients. By introducing a new variable z related to ρ by the equation

$$\rho = ze^{\frac{\mu}{2}\int f_{\dot{x}_0}(x_0,\dot{x}_0)d\tau}$$

equation (19.3) becomes

$$\ddot{z} + \left[1 - \mu f_{\dot{z}_0} + \frac{\mu}{2}\frac{d}{d\tau}(f_{\dot{z}_0}) - \frac{\mu^2}{2} f^2_{\dot{z}_0}\right] z = 0 \tag{19.4}$$

that is, of the form (19.1). It must be noted, however, that we were able to establish this relation only because we know from the theory of Poincaré that the periodic subharmonic solution exists in this case.

In spite of the limitations just mentioned, this theory renders useful services in some special cases of parametric excitation as will appear from the following example due to Gorelik and Witt (43). These authors investigated the motion of a physical pendulum suspended on a spring and capable of oscillating in a plane. Let m be the mass of the pendulum, l_0 its length in the absence of the dynamical load, k the spring constant and g the acceleration of gravity. The system has, clearly, two degrees of freedom, viz., the angle φ of the pendulum and the elongation z of the spring. The kinetic energy of the pendulum is

$$T = \frac{m}{2}(\dot{r}^2 + r^2\dot{\varphi}^2)$$

and its potential energy

$$V = \frac{k}{2}(r - l_0)^2 - mgr\left(1 - \frac{\varphi^2}{2}\right)$$

where the first term corresponds to the elasticity and, the second, to gravity; moreover we assume $\cos\varphi \cong (1 - \varphi^2/2)$. If we introduce a new constant $l = r_0 + mg/k$ and a new variable $z = (r - l)/l$, these expressions become

$$T = \frac{ml^2}{2}(\dot{z}^2 + \dot{\varphi}^2 + 2z\dot{\varphi}^2); \qquad V = \frac{ml^2}{2}\left(\frac{k}{m}z^2 + \frac{g}{l}\varphi^2 + \frac{g}{l}z\varphi^2\right)$$

hence, the Lagrangian equations are

$$\begin{aligned} \ddot{z} + \frac{k}{m}z + \left(\frac{g}{2l}\varphi^2 - \dot{\varphi}^2\right) &= 0 \\ \ddot{\varphi} + \frac{g}{l}\varphi + \left(\frac{g}{l}z\varphi + 2\dot{z}\dot{\varphi} + 2z\ddot{\varphi}\right) &= 0. \end{aligned} \tag{19.5}$$

It is seen thus that there exists a nonlinear coupling between the two degrees of freedom. Nothing particularly interesting happens in the general case when

$$\omega_z \neq \left(\frac{p}{q}\right)\omega_\varphi$$

where p and q are integers. We consider the case when such a relation exists and assume that $\omega_z = 2\omega_\varphi$. Let us assume that for $t = 0$, $\varphi = 0$ and the spring, initially stretched, is released. The initial motion will be

$$z = z_0 \cos \omega_z t$$

Substituting this expression in the second equation (19.5) we get

$$(1 + 2z_0 \cos \omega_z t)\ddot{\varphi} - (2\omega_z \sin \omega_z t)\dot{\varphi} + \omega_\varphi^2(1 + z_0 \cos \omega_z t)\varphi = 0. \quad (19.6)$$

This is an equation with periodic coefficients and, if the conditions are such that initially there exists an unstable solution, the initial motion in the z-degree of freedom will result in the building up of oscillations in the φ-degree of freedom. At the same time, clearly, one is in the case of a subharmonic resonance, inasmuch as the force acting in the z-degree of freedom with frequency ω_z results in a motion in the φ-degree with frequency $\omega_\varphi = \omega_z/2$.

Since the system in this case is conservative, it is apparent that the building up of the oscillation in the φ-degree must be accompanied by a corresponding reduction of the oscillation in the z-degree of freedom, as was actually observed by Gorelik and Witt.

Similar phenomena can be produced electrically. Thus, for example, in a circuit containing a variable capacity and constant resistance and inductance, a parametric self-excitation of oscillations can be produced if the capacity is varied with a double frequency of that with which the circuit with constant parameters oscillates normally (44). Mandelstam and Papalexi developed an interesting electric machine, the *parametric generator*, in which one of the parameters (either L or C) is varies with a certain frequency. It is found that the generator produces self-excited oscillations with one-half frequency. If the circuit is linear, the oscillations build up indefinitely until the insulation is punctured. If, however, a nonlinear element is provided in the circuit, the oscillation reaches a stationary value and the generator performs in a stable manner.

An interesting application of the theory of parametric excitation was made by Goulayev (40) in connection with the operation of the so-called velocity modulation electron tubes of the "klystron" type. This author shows that the fluctuations in the number of electrons arriving in the "catcher" of these tubes produces a periodic variation in the dielectric constant of the condenser and, hence, results in a parametric excitation of the circuit.

It is likely that a number of other phenomena of self-excitation can be treated on the basis of the theory of the parametric excitation but the principal handicap of this method, as was mentioned, lies in the absence of a theory of the nonlinear differential equations with periodic coefficients.

References[1]

1. POINCARÉ, H., *J. Math.*, [3] **7**, 3, 5, 422 (1881); **8**, 251–296 (1882); also *Oeuvres*, Gauthier-Villars, Paris, 1928, pp. 1–222.
2. ———, *Les Méthodes nouvelles de la mécanique céleste.* Vol. 1, Paris, Gauthier Villars, 1892, pp. 79–232.
3. VAN DER POL, BALTH, *Phil. Mag.*, [7] **1926**, 978–992; *Radio Rev.* **1920**, 701.
4. CARTAN, E. and H., *Ann. P.T.T.*, Dec. 1925, pp. 1196–1207.
5. LIÉNARD, A., *Rev. Gen. Electric*, **23**, 901–953 (1928).
6. ANDRONOW, A., *Compt. rend.*, **189**, 559–561.
7. KRYLOFF, N., and BOGOLIUBOFF, N., *Introduction à la mécanique non-linéaire*, Kieff, 1937 (in Russian); also free translation of this book by S. Lefschetz, Princeton Univ. Press, Princeton, 1943. The same subject is outlined in the *Introduction to Non-linear Mechanics* by N. Minorsky, Edwards Bros., Ann Arbor, Michigan, 1947, Chapter XI.
8. SHOHAT, J. A., *J. Applied Phys.*, **15**, 568–574 (1944). M. L. CARTWRIGHT and J. E. LITTLEWOOD, *J. London Math. Soc.*, **20**, 180–189 (1945).
9. KAMKE, E., *Differentialgleichungen reeller Functionen.* Leipzig, 1930, Chapter VI
10. APPEL, P., *Traite de la mecanique rationnelle.* Vol. I, Gauthier-Villars, Paris, 1926, p. 452.
11. POINCARÉ, H., *Acta Math.*, **7**,

11a. ———, *Figures d'equilibre d'une masse fluide.* Paris, 1903.

12. ANDRONOW, A., and CHAIKIN, S., *Theory of Oscillations*, Moscow, 1937 (in Russian); also N. MINORSKY, ref. 7, pp. 32–39.
13. LIAPOUNOFF, M. A., *Ann. Faculté Sci. Toulouse*, Vol. 9, 203–469 (1907).
14. LIAPOUNOFF, loc. cit. 13; also S. LEFSCHETZ, *Lectures on Differential Equations*, Princeton Univ. Press, Princeton, 1946.
15. POINCARÉ, H., loc. cit. 1; BENDIXSON, I., *Acta. Math.*, **24**, 1–88 (1901).

15a. LEVINSON, N., and SMITH, O. K., *Duke Math. J.*, **9**, 382–403 (1942).

16. POINCARÉ, H., ref. 1, Chapter III.
17. BENDIXSON, J., ref. 15.
18. POINCARÉ, H., ref. 1, Chapters III and IV.
19. KRYLOFF, N., and BOGOLIUBOFF, N., ref. 7; also MINORSKY, N., ref. 7, pp. 209–229.
20. LINDSTEDT, A., *Mem. Acad. Sci. (St. Petersbourg)*, **31**, 1–20 (1883).
21. VAN DER POL, BALTH, ref. 3.
22. FATOU, P., *Bull. Soc. Math. France*, **66**, 98–180 (1928). MANDELSTAM, L., and PAPALEXI, N., *J. Exptl. Theoret. Phys. (U.S.S.R.)*, **4**, 117–122 (1934).
23. LINDSTEDT, A., ref. 20.
24. HELMHOLTZ, H., *Sensation of Tone.* London, 1895.
25. POINCARÉ, H., ref. 2, Vol. III, Chapter XXVIII.
26. MANDELSTAM, L., and PAPALEXI, N., *J. Tech. Phys. (U.S.S.R.)*, **2**, 775–811 (1932).
27. WHITTAKER, E. T., and WATSON, G. N., *Modern Analysis.* Cambridge Univ. Press, 1927, Chapter XIX.
28. LORD RAYLEIGH, *Collected Papers*, Vol. I, p. 409; Vol. V, p. 369.
29. VAN DER POL, BALTH, *Phil. Mag.*, [7] **3**, 65–80 (1927).
30. VINCENT, J. H., *Proc. Phys. Soc. (London)*, 84–90 (Feb., 1919).

[1] This list of references covers only the principal references concerning the topics treated in this review. For more complete references see the bibliography appended to references 7 (Minorsky), 12, 41 and also to the paper of Th. von Kármán, "Engineer grapples with non-linear problems," *Bull. Am. Math. Soc.*, **46**, 615–683 (1940).

31. Möller, H. G., *Z. Drahtl. Tel. u. Tel.*, 17, 256–287 (1921).
32. Appleton, E. H., *Proc. Cambridge Phil. Soc.*, 21, 231–248, (1922).
33. Andronow, A., and Witt, A., *Arch. Elektrech.*, 24, 99–110 (1930); also Minorsky, N., ref. 7, pp. 341–352.
34. Theodorchick, K., and Chaikin, S., *J. Tech. Phys.* (*U.S.S.R.*), 2, 111–118 (1932).
35. Kirschtein, F., *Elektrische Nachrichten Technik*, 20, 29–38 (1943).
36. Melde, F., *Pogg. Ann.*, 109 (1860).
37. Lord Rayleigh, *Phil. Mag.*, [5] 15, 229–235 (Apr. 1883).
38. Brillouin, M., *Ecl. Elect.*, 11, 49–59 (1897).
39. Poincaré, H., *Ecl. Elect.*, 50, 293–301 (1907).
40. Goulayev, V., *J. Phys.* (*U.S.S.R.*), 4, 143–150 (1941).
41. Mandelstam, L., and Papalexi, N., *J. Tech. Phys.* (*U.S.S.R.*), 4, (1934).
42. van der Pol, Balth, and Strutt, M. J. O., *Phil. Mag.*, [7] 5, 18–38 (1928).
43. Gorelik, G., and Witt, A., *J. Tech. Phys.* (*U.S.S.R.*), 3, 294 (1933).
44. Mandelstam, L., and Papalexi, N., ref. 41.

Survey of Papers on Elasticity Published in Holland 1940–1946.

By C. B. BIEZENO

Technical University, Delft, Holland

CONTENTS

The invitation of Professor von Mises to contribute to these "Advances" a survey of the work done in Holland during the war in the field of applied mechanics, in particular in the field of elasticity, has been met by the author with the greatest pleasure. After the sad years in which Holland suffered from the monstrous brutalities to which all western European peoples were subjected by a merciless occupant, it is generally felt as a duty to re-establish as soon as possible the manifold scientific connections by which our country was bound to its allies.

Since he has devoted a great deal of his endeavour to the international exchange of scientific advancement, the author enjoys the possibility of re-establishing contact with his American colleagues and hopes to profit as soon as possible from the enormous amount of knowledge and experience that has been heaped up during the past few years in the United States of America where the war did not stop—but even gave rise to—the creation of different scientific institutions, as for example, the Society for Experimental Stress Analysis.

It will not surprise the reader that—given the prevailing circumstances—Holland cannot claim to have contributed a great deal to the total number of newly issued publications. As a matter of fact in this country only two or three centers of specialized "mechanical" activity do exist: the Technische Hoogeschool (Technical University) at Delft, the recently founded department for experimental research of constructions of the Centrale Organisatie voor Toegepaste Natuurwetenschappelijk Onderzoek at the Hague (Central Institute for Technical Scientific Research), and the Nationaal Luchtvaartlaboratorium (the National Aeronautical laboratory) at Amsterdam. It is mainly the work of these three institutes that will be reviewed here.

Chronological order has been neglected in favor of a methodical treatment, but it must be emphasized that, in consequence of the diversity of the different subjects, coherence of this monograph as a whole could not be reached. Matters are divided according to their theoretical or experimental character, whereas publications in book form have been treated separately. The reader is referred to the index for further information about the topics of research.[1]

[1] Of nearly all treatises mentioned in this monograph, reprints are still available, and it will be a pleasure to the author to send them on application to the reader who may be interested in any of them; requests may be directed to him personally at the address: Laboratorium voor Toegepaste Mechanica, Nieuwe Laan 76, Delft, Holland.

I. Publications of the Laboratory for Applied Mechanics of the Technische Hoogeschool at Delft

A. Elastic Stability

1. *On the Stability of Elastic Equilibrium.* Hitherto the general theories of stability as developed by Bryan, Southwell, Biezeno and Hencky, Trefftz, Marguerre, Biot and others have been restricted to the investigation of neutral equilibrium; they aim particularly at the determination of the stability limit. The phenomena occurring on reaching and possibly on surpassing this limit were left out of account. This restriction as to the extent of the investigations is caused by two circumstances. First of all there must be mentioned the great mathematical difficulties that obstruct the theoretical treatment of elastic behavior after the stability limit is surpassed. Whereas the investigation of states of neutral equilibrium is still possible by means of linear differential equations, the equations describing elastic behavior after the stability limit is surpassed are no longer linear. Moreover engineering has long been satisfied with the knowledge of the stability limit (critical or buckling load). The recognized principle based on considerations of safety was that the load on a structure should always be kept below this limit, so that an investigation of the phenomena occurring above this limit seemed superfluous. However, it has been known for a long time that some structures (*e.g.* flat plates) are capable of sustaining considerably larger loads than the buckling one without exceeding the elastic limit at any point of the structure; in modern engineering, especially in aircraft engineering, where saving on structural weight is of the greatest importance, these higher loads are actually allowed. The theoretical treatment of this problem has been given by Marguerre and Trefftz, among others. On the other hand it has been noted that the experimentally determined buckling loads of some shell structures, *e.g.*, axially compressed thin-walled cylinders, lie considerably below the theoretical stability limit. Moreover the experimental results are widely divergent. (Cf. investigations by Flügge, Donnell, Cox, von Kármán and Tsien.)

From all this it appears that the general theories of stability framed so far do not suffice. They have to be completed in such a way that the divergent behavior of various structures in the case of loads in the neighborhood of the theoretical buckling load can be described as well. The present treatise aims at such an extension.

Chapter 1 gives a brief survey of the theory of elasticity for finite deformations, whereas the general equations of motion are derived by means of Hamilton's principle, using the potential or strain-energy func-

tion to describe the elasticity of the body. The equations of equilibrium are obtained by putting equal to zero all inertia forces.

In Chapter 2 the general theory of stability is dealt with. A precise definition is given by means of the energy criterion. In accordance with Trefftz it leads to two conditions of stability. The first condition is that the first variation of the potential energy is zero for any kinematically possible variation of displacement. The second condition requires that the second variation of the energy cannot be negative for any such possible variation of displacement. The stability *at* the stability limit is studied at full length.

In the next chapter the states of equilibrium at loads in the neighborhood of the buckling load are investigated. The approximate method used for this purpose naturally gives better results the less the load differs from the critical one. The character of these states actually appears to be governed by the stability at the buckling load. It must be said explicitly that the method exclusively enables to deal with buckling problems with a so-called point of bifurcation; so-called "oilcanning" problems are not taken into account. The most important result presented in Chapter 3 is that with stability of the equilibrium at the critical load neighboring states of equilibrium exist only for larger loads; these states are stable. Therefore larger loads than the buckling can be sustained. With an unstable buckling load, on the contrary, neighboring states of equilibrium do occur at loads smaller than the buckling load; these states are unstable.

The theory treated up to now does not give an explanation of the fact that for some structures the experimental buckling loads are considerably smaller than the theoretical buckling load. To arrive at such an explanation the influence of small deviations of a real structure from the simplified model, designed to represent the structure, is considered in Chapter 4. The most important result that this investigation shows is that with an unstable buckling state of the model the buckling load of the structure may be considerably lower in consequence of very small differences between structure and model. Hence the discrepancy between theoretical and experimental critical loads can be explained purely elastically by assuming small deviations of such a structure from the corresponding model; moreover the great sensibility of the buckling load of the structure for small variations in the magnitude of the deviations explains too the wide divergence of experimental results.

The most interesting example of the application of the theory developed here is the application to the axially compressed thin-walled cylinder; for in this technically important case the great discrepancy between the theoretical and experimental buckling loads has up to now not been

accounted for satisfactorily. To apply the general theory to this problem it is necessary to dispose of the knowledge of the elastic energy of the thin-walled cylindrical shell for finite displacements. With a view to the possibility of application to other shell structures as well, a general theory of thin shells for finite displacements is given in Chapter 5. Before passing to the rather complicated theory of the thin-walled cylinder it seemed advisable to deal first with some simpler applications, in order to elucidate the general theory (Chapter 6). The well-known problem of the elastica, Cox's problem, and the problem of equivalent width of compressed flat rectangular plates are considered in this connection.

Finally, Chapter 7 is concerned with the axially compressed cylindrical shell. Neglect of boundary conditions leads to the same result for the buckling load as known from existing literature. The same neglect leads to the conclusion that equilibrium in the buckling state is unstable. As to the neighboring states of equilibrium at loads in the neighborhood of the critical load, it is found that all existing neighboring states of equilibrium are unstable. The results are compared with those obtained by von Kármán and Tsien, and seem to be more satisfactory, at least for loads in the neighborhood of the critical load. Thereupon the influence of small deviations from the true cylindrical form is discussed. As the investigation is rather complicated the detailed calculations are restricted to one form of deviations. In this case a very marked decrease of buckling load is found already with very small deviations. This result is in striking contrast to that of Donnell and it may be stated indeed that the theory given here supplies an explanation of the large discrepancy between theoretical and experimental critical loads. The wide divergence of experimental results is likewise satisfactorily accounted for by the extreme sensibility of the critical load for small variations in the magnitude of the deviations.

2. *On the Buckling of a Thin-Walled Circular Tube Loaded by Pure Bending.* If a thin-walled circular tube (length l_1, radius a, thickness h) is loaded by two equal and opposite terminal bending moments M, its cross section alters its circular shape into an oval one, owing to the fact that apart from the normal bending stresses in the cross section of the tube, tangential bending stresses arise in its meridional sections. A closer examination of this fact reveals that the curvature of the "axis" of the tube does not increase proportionally with the loading moment M. The phenomenon has been studied at great length by Brazier. In the present paper another phenomenon is studied, which is characterized by the simultaneous appearance of longitudinal and circumferential waves in the cylindrical shape of the tube. It is assumed that—if unloaded—the tube possesses such initial curvature that under the action of the buckling

moment it is straight and—in cross section—circular and of constant thickness h. The coordinates used are cylinder coordinates r, φ, z; the corresponding displacements are denoted by u, v, w; the surface stresses by R, Φ, Z. It is well known that with the load system

$$R = a_{pq} \cos p\varphi \sin \lambda \frac{z}{a}; \qquad \Phi = b_{pq} \sin p\varphi \sin \lambda \frac{z}{a}; \qquad Z = 0 \quad (1)$$

(where p and q represent arbitrary positive integers and λ stands for $\lambda = \pi\, qa/l$), the following displacements are compatible:

$$u = u_{pq} \cos p\varphi \sin \lambda \frac{z}{a}; \qquad v = v_{pq} \sin \lambda \frac{z}{a}; \qquad w = w_{pq} \cos p\varphi \cos \lambda \frac{z}{a}. \quad (2)$$

As far as u and v are concerned u_{pq} and v_{pq} are represented by

$$u_{pq} = \alpha_{pq} a_{pq} + \beta_{pq} b_{pq}; \qquad v_{pq} = \beta_{pq} a_{pq} + \gamma_{pq} b_{pq} \quad (3)$$

α_{pq}, β_{pq} and γ_{pq} standing for

$$\alpha_{pq} = \left(\frac{T_1}{N}\right)_{pq} \frac{a^2}{B}; \qquad \beta_{pq} = -\left(\frac{T_2}{N}\right)_{pq} \frac{a^2}{B}; \qquad \gamma_{pq} = \left(\frac{T_3}{N}\right)_{pq} \frac{a^2}{B} \qquad \left(B = \frac{Eh}{1-\nu^2}\right) \quad (4)$$

T_1, T_2, T_3, N themselves standing for

$$T_1 = (1+k)p^4 + [2\lambda^2 + 2(1-\nu)\lambda^2 k]p^2 + (1+3k)\lambda^4$$

$$T_2 = p\{[1 + k(2\lambda^2 + 1)]p^2 + (\nu + 2)\lambda^2 + 2k\lambda^4\}$$

$$T_3 = kp^2(p^2-1)^2 + k\frac{2(2-\nu)}{1-\nu}\lambda^2 p^4 + \left[1 + \frac{5-\nu}{1-\nu}k\lambda^4 + \frac{2(\nu - \nu^2 - 2)}{1-\nu}k\lambda^2 + k\right]p^2 + 2(1+\nu)\lambda^2 + \frac{2}{1-\nu}k(\lambda^6 - 2\nu\lambda^4)$$

$$N = kp^8 + k[4\lambda^2 - 2]p^6 + k[6\lambda^4 - 2(4-\nu)\lambda^2 + 1]p^4 + k[4\lambda^6 - 6\lambda^4 + 2(2-\nu)\lambda^2]p^2 + (1-\nu^2)\lambda^4 + k\lambda^8 - 2\nu\lambda^6 k + (4 - 3\nu^2)\lambda^4 k.$$

It can be proved that two systems of so-called "elementary characteristic loads" B, with corresponding "elementary characteristic deformations" D, exist, for which the load components R_{pq}, Φ_{pq} are proportional to the corresponding displacements u_{pq}, v_{pq}, such that

$$\frac{R_{pq}}{u_{pq}} = \frac{\Phi_{pq}}{v_{pq}} = \omega. \quad (6)$$

These systems are defined except for a factor of proportionality, and possess certain properties of orthogonality. The factor of proportionality can be fixed by a suitable condition of standardization.

Returning to the buckling problem under consideration, we refer to the fact (cf., for instance, W. Flügge, *Statik und Dynamik der Schalen*, or C. B. Biezeno und R. Grammel, *Technische Dynamik*) that the differential equations for the *supplementary* displacements u, v, w (which transfer the cylinder from its state of "neutral" equilibrium into an infinitesimally neighboring state of equilibrium) agree with the differential equations for the displacements u, v, w of a cylinder, the loads R, Φ, Z of which are represented by

$$R = -Q\frac{\partial^2 u}{\partial z^2}, \qquad \Phi = -Q\frac{\partial^2 v}{\partial z^2}, \qquad Z = 0 \tag{7}$$

where $Q = Ma \cos \varphi/\pi a^3$ stands for the normal load per unit of circumferential length in the terminal cross sections of the cylinder, as exerted by the bending moment M.

Let (u,v,w) occurring under the critical load $M = \mu\bar{M}$ ($\bar{M}$ = unit moment) be named the "total" characteristic deformation T. Then T can be decomposed into a (infinite) series of elementary normal deformations D

$$T = \sum_{i=1}^{\infty} d_i D_i. \tag{8}$$

If the load system, derived from D_i with the aid of (7) be called $\bar{B}_i$, then the load system belonging to the "total characteristic deformation" T may be written as $\Sigma\, d_i\bar{B}_i$.

Each separate system $\bar{B}_i$ can be expanded into a (finite or infinite) series of "elementary characteristic loads" B_i, so that the load system corresponding with the "total characteristic deformation" finally can be looked upon as the sum of an infinite number of groups of a (finite or infinite) number of "elementary characteristic loads" B_i. In this reasoning it has been assumed that all deformations and load systems are connected with the *same* parameter λ, characteristic for the "total deformation" under consideration, so that all loads and deformations have the same number of longitudinal waves. All functions T, B, D can therefore be denoted by a single subscript p.

If artificially the tube be given the "elementary characteristic deformation" D_j, then we can, by the aid of (7), formally calculate the corresponding load system (R,Φ,Z) produced by two unit terminal moments $\bar{M}$. As stated before, this load system can be developed in a (finite or

infinite) series of "elementary characteristic" functions B. The coefficient α_{ij}, which in this expansion belongs to the elementary characteristic function B_i, is called the "influence number of the elementary characteristic deformation D_j with respect to the elementary characteristic load B_i."

This formal definition provides us with an expedient for obtaining a system of homogeneous linear equations for the coefficients d_i in the expansion (8), viz.,

$$d_i = \sum_j \mu d_j \alpha_{ij} \qquad (i = 1, 2 \cdots) \tag{9}$$

and therefore the problem of the buckling cylinder under bending is *formally reduced to the solution of the equation*

$$\begin{vmatrix} \alpha_{11} - \frac{1}{\mu} & \alpha_{12} & \cdots & \\ \alpha_{21} & \alpha_{22} - \frac{1}{\mu} & \cdots & \\ \cdot & \cdot & \cdot & \\ \cdot & \cdot & \cdot & \\ \cdot & \cdot & \cdot & \end{vmatrix} = 0. \tag{10}$$

It can be proved, that—if only the elementary characteristic functions are suitably numbered—$\alpha_{ij} = \alpha_{ji}$, so that equation (10) is a secular one possessing only real roots.

For the computation of the smallest root μ of this equation recourse is made to a generalization of an iterative method, which by the second author of this treatise has been established in his doctor's thesis, and which consists in deriving from an arbitrary set of quantities ϑ_{1i} another set ϑ_{2i}, defined by

$$\vartheta_{2i} = \Sigma \alpha_{ij} \vartheta_{1i} \qquad \text{etc.} \tag{11}$$

Two consecutive iterations ϑ_{si} and $\vartheta_{s+1,i}$ tend with increasing s to proportionality, the factor of which represents the smallest characteristic number. Its value μ_1 is fairly approximated by the expression given by Koch:

$$\mu_1 = \frac{\sum_i \vartheta_{1i} \vartheta_{2i}}{\sum_i \vartheta_{2i}^2} \tag{12}$$

so that only one iteration needs to be performed. The iteration process relates to a *fixed* value of λ, viz., to a fixed number of longitudinal waves in the buckling deformation. Therefore the iteration process has to be repeated for a great number of values λ if the absolute minimum of the critical buckling moment is required. This seems to be a rather tiresome technique, but means are provided to abbreviate considerably the numerical calculations.

3. *The Generalized Buckling Problem of the Circular Ring.* A circular ring, subjected to a uniform radial pressure q per unit of circumferential length, is apt to buckle under the action of one of the so-called "critical" loads $q = (n^2 - 1)EI/r^3$ (n integer and $\geqq 2$), EI representing the flexural rigidity of the ring and r its radius. This case of buckling is analogous to the buckling of a straight rod under the action of two compressive forces, as far as the cross sections of both ring and rod are loaded by a normal force of constant magnitude. If the straight rod is loaded by a prescribed system of axial forces, so that the normal force of the cross section varies with its coordinate, proportional increase of the load-system, say to the multiple λ, leads as well to critical buckling loads. The (positive or negative) value of the factor of magnification λ can best be found by a method of iteration. Obviously the analogous problem exists for the circular ring, if only it is subjected to an external load-system such that in every cross section the bending moment M and the shearing force D are zero, whereas the normal force of the section varies with its coordinate. Evidently the first of these conditions will not be fulfilled if the ring is loaded by an arbitrary system of radial and tangential forces, but it can be shown that every system can be split up into two components A and B, the first of which is called the "compressive" system because it is characterized by $M = D = 0$, whereas the second one is called the "bending" system characterized by $N = 0$.

The first system A, if suitably magnified, leads to the generalized buckling problem of the circular ring, which is the object of this treatise, but it is seen at once that an arbitrary load-system, consisting of both components A and B, gives rise to a problem, which again is analogous to a well-known problem, viz. the straight rod subjected to axial thrust and transverse bending loads. Just as with the straight rod the axial forces tend to increase the deflections caused by the transverse loads, the A-load-system of the circular ring will affect the deflections due to the B-system (cf. Section 4).

If the arbitrary load-system (q,t)—q = radial load, t = tangential load per unit of circumferential length—of the ring is expanded into Fourier series

$$q = a_0 + \sum_1^\infty a_k \cos k\varphi + \sum_1^\infty b_k \sin k\varphi; \qquad t = c_0 + \sum_1^\infty c_k \cos k\varphi + \sum_1^\infty d_k \sin k\varphi \quad (1)$$

the A- and B-components are represented by

$$A\left\{\begin{aligned} q^* &= a_0 + \frac{1}{2}a_1\cos\varphi + \sum_2^\infty\left[\frac{-1}{k^2-1}a_k + \frac{k}{k^2-1}d_k\right]\cos k\varphi \\ &\quad + \frac{1}{2}b_1\sin\varphi + \sum_2^\infty\left[-\frac{1}{k^2-1}b_k - \frac{k}{k^2-1}c_k\right]\sin k\varphi \\ t^* &= \frac{1}{2}b_1\cos\varphi + \sum_2^\infty\left[\frac{k}{k^2-1}b_k + \frac{k^2}{k^2-1}c_k\right]\cos k\varphi \\ &\quad + \frac{1}{2}a_1\sin\varphi + \sum_2^\infty\left[-\frac{k}{k^2-1}a_k + \frac{k^2}{k^2-1}d_k\right]\sin k\varphi \end{aligned}\right\} \quad (2)$$

$$B\left\{\begin{aligned} q^{**} &= \frac{1}{2}a_1\cos\varphi + \sum_2^\infty\left[\frac{k^2}{k^2-1}a_k - \frac{k}{k^2-1}d_k\right]\cos k\varphi \\ &\quad + \frac{1}{2}b_1\sin\varphi + \sum_2^\infty\left[\frac{k^2}{k^2-1}b_k + \frac{k}{k^2-1}c_k\right]\sin k\varphi \\ t^{**} &= -\frac{1}{2}b_1\cos\varphi + \sum_2^\infty\left[-\frac{k}{k^2-1}b_k - \frac{1}{k^2-1}c_k\right]\cos k\varphi \\ &\quad + \frac{1}{2}a_1\sin\varphi + \sum_2^\infty\left[\frac{k}{k^2+1}a_k - \frac{1}{k^2-1}d_k\right]\sin k\varphi. \end{aligned}\right\} \quad (3)$$

Here only attention will be paid to A-load systems from which it is presumed that the q^* and t^* components *keep their directions* with respect to the element of the ring on which they act. The differential equation of the problem is then given by

$$U'' + U = \frac{Nr^2}{EI}U + C \quad (4)$$

($U = u'' + u$,—u representing the increase of the radius vector r— N = prescribed normal force acting on the cross section, C = constant of integration to be found in the course of the investigation). Both N and U can be expanded into Fourier series

$$\left.\begin{aligned} N &= \lambda N_0 = \lambda\left[A_0 + \sum_{k=1}^{\infty} A_k \cos k\varphi + \sum_{k=1}^{\infty} B_k \sin k\varphi\right] \\ U &= a_0 + \sum_{l=1}^{\infty} a_l \cos l\varphi + \sum_{l=1}^{\infty} b_l \sin l\varphi \end{aligned}\right\} \tag{5}$$

and it can be proved that buckling of the ring can occur only if all multiples of φ in the Fourier series of N have a factor in common.

If the greatest factor in common be called p, all terms a_0, $a_1 \cos \varphi$, $b_1 \sin \varphi$, $\alpha_{\alpha p \pm 1} \cos (\alpha p \pm 1)\varphi$, and $b_{\alpha p \pm 1} \sin (\alpha p \pm 1)\varphi$, ($\alpha$ representing any positive integer $\neq 0$) have to be excluded from U.

Substitution of N and U in (4) would lead to an infinite system of recurrent relations between the coefficients a_l and b_l, and it would be seen that the system would break up into a number of minor systems, each of which is related to a distinct class of coefficients a_l, b_l, defined by

$$l = \pm q, \text{ (mod p)} \qquad \begin{aligned} q &= 0, 2, 3 \cdots \frac{p-1}{2} \quad (p = \text{odd}) \\ q &= 0, 2, 3 \cdots \frac{p}{2} \quad (p = \text{even}). \end{aligned} \tag{6}$$

With any prescribed p the buckling problem therefore is split up into $\frac{p-1}{2}$ or $\frac{p}{2}$ cases, in every one of which U is composed exclusively of terms relating to one of the congruences (6).

With respect to the constant C in (4) it must be observed that if the product NU in the right-hand side of the equations happens to miss a constant term after having been written as an ordinary Fourier series, then C must be suppressed; if not so, C serves to annul this term.

The practical solution of the problem is given in an iterative way, the justification of which is given by expressing the problem in terms of an integral equation.

Starting with an arbitrary function $V_1(\varphi)$, containing only cosine and sine terms of suitable multiples of φ, another function $V_2(\varphi)$ is derived, formally defined by the differential equation,

$$V_2'' + V_2 = \frac{N_0 r^2}{EI} V_1 + C$$

and the condition that it does not contain terms of the type $\alpha + \beta \cos \varphi +$

$\gamma \sin \varphi$ (C being again a constant to be determined *a posteriori*). From V_2 another function V_3 is deducted in the same way, etc.

It can be proved that the smallest characteristic value λ_1 is approximated by one of the following formulas:

$$\lambda_1 = \frac{\int_0^{2\pi} N_0 V_{m-1}^2 d\varphi}{\int_0^{2\pi} N_0 V_{m-1} V_m d\varphi}; \qquad \lambda_1 = \frac{\int_0^{2\pi} N_0 V_{m-1} V_m d\varphi}{\int_0^{2\pi} N_0 V_m^2};$$

the second of which exceeds in general the first in accuracy. The practical iteration scheme, along which the iteration has to be performed in fact, cannot be described here, but is elucidated at full length in the treatise itself.

The cases $N = \lambda N_0 = \lambda(1 + 2 \cos k\varphi)(k = 2, 3, \cdots 12)$ and $N = \lambda(1 + 2 \cos 2\varphi + \cos 4\varphi)$ are worked out numerically. Higher characteristic values can be calculated as well. In all such cases where the normal force N changes its sign, negative characteristic values are to be expected. A negative value of λ interchanges the compressed and the stretched parts of the construction, and a sufficiently great negative λ therefore causes the buckling of the initially stretched parts. As an example it can be stated that with a compressive force $N = \lambda(1 + 4 \cos 2\varphi)$ the second characteristic number proves to be negative $\lambda_2 = -2.1133 \frac{3EI}{r^2}$, whereas the first characteristic number is equal to $\lambda_1 = 0.6275 \frac{3EI}{r^2}$.

4. *The Circular Ring under the Combined Action of Compressive and Bending Loads.* In the previous section the problem treated here has already been announced. The ring is simultaneously subjected to an A- and B-system, but it is supposed that the A-system is small enough to guarantee the elastic stability of the ring. It is obvious that the deflections (and internal stresses) of the ring, due to the *single* action of the B-system, will be affected in a rather complicated way by the simultaneous action of the A-system, which, alone, would produce no deflections at all. The influence of the A-system upon the bending effect produced by the B-system can be expressed in terms of the characteristic numbers λ and the corresponding characteristic functions U of the A-system. To this end the so-called "reduced moment," $-\frac{r^2}{EI} M_B$, belonging to the B-system has to be expanded into a series

$$-\frac{r^2}{EI} M_B = \sum_{k=1}^{\infty} b_k U_k \qquad (1)$$

of the characteristic functions U_k of the A-system. The resultant bending moment M, resp. the resultant function U, due to the joint systems A and B, is then represented by

$$-\frac{r^2}{EI} M = U = \sum_{k=1}^{\infty} \frac{\lambda_k}{\lambda_k - 1} b_k U_k. \tag{2}$$

The resultant distortion of the ring is governed by the equation

$$u'' + u = U. \tag{3}$$

A numerical application is given for the ring compressed by two diametral forces P.

5. *On the Nonlinear Deflection of a Semicircular Ring, Clamped at Both Ends.* The aim of this paper is to deduce in a theoretical way the force-deflection relation (P,u) of a semicircular ring clamped at both ends and loaded (in its midpoint characterized by $\varphi = 0$) by a radial force P. The treatment of the problem (which finds its origin in a remarkable paper on the buckling of cylindrical shells by Th. von Kármán, L. G. Dunn, and Hue-Shen Tsien) is essentially based upon the methods developed in the two preceding papers. Instead of the semiring clamped at both ends, first a *complete* ring is considered loaded by two pairs of diametral forces P and Q, placed at right angled (P at $\varphi = 0$ and π, Q at $\pi/2$ and $3\pi/2$. For a number of values of the ratio P/Q, viz. $P/Q = 1$, 1,05, 1,10 and 1,2 and their reciprocals, the radial deflections u are calculated at $\varphi = 0$ and $\varphi = \pi/2$. From each of these results (relating to a distinct value of PQ), the absolute value of P can be deduced, for which the deflection u at $\varphi = \pi/2$ and $3\pi/2$ becomes zero, and by substituting the smallest of these values in the corresponding expression of u for $\varphi = 0$, the deflection of the point $\varphi = 0$ can be calculated. In a graph $\frac{P}{u}\frac{r^3}{EI}$ is plotted against u/r and the results are compared with the experimental ones of von Kármán l.c.

6. *On the Nonlinear Deflection of a Semicircular Ring, Clamped at Both Ends.* The method discussed in the preceding paper requires a considerable amount of computation. It therefore seemed desirable to investigate whether the results could be obtained in a simpler (be it approximative) way. Again the problem is attacked by considering a *complete* ring, loaded by two pairs of diametral forces P and Q. The simplification of the problem consists in replacing the rather complicated A-load-system (connected with these forces) by a radial *constant* pressure $(P + Q) : \pi r$ equally distributed along the circumference of the ring, giv-

ing rise to a *constant* normal force $(P + Q):\pi$ in the cross section. The approximative results obtained in this way are quite satisfactory.

7. *Large Distortions of Circular Rings and Straight Rods.* The present paper is closely-connected with the foregoing three papers, and provides the reader with a valuable extension. Indeed the authors of these previous treatises use the differential equation of the slightly curved beam to describe the distortions, an approximation, which can be made only if the difference in slope of the elastic line in its deformed and its undeformed shape is small. So their solution is limited to distortions not too large. Moreover, the distortions, as calculated by their method, appear as an infinite series of terms. As the calculation of the separate terms is rather tedious, one has for practical reasons to confine oneself to a small number of terms. The authors, for instance, use only two terms.

It therefore is of interest to give an exact treatment of the same problem, partly to have the exact results for themselves, partly to provide a check to the approximate results. The method used in this paper is principally based on the ideas used by some authors in the classical period of elasticity and consists in the use of a system of natural coordinates (s,φ) where s is the length of the arc measured from an arbitrary zero point, and φ the angle included by the normal of the distorted ring and a fixed direction. The method is not restricted to closed circular rings: many other problems of large distortions (as for instance the one referred to in section C2) can be solved by the same means. As may be expected, it calls for a knowledge of elliptic integrals. Four particular problems, one dealing with a closed circular ring, one with a semicircular ring, and two with straight beams admitting large deflections, have been numerically calculated, and the results have been plotted in diagrams. Comparisons are made with approximate results of other authors and with own experiments.

8. *On the Buckling and the Lateral Rigidity of Helical Compression Springs.* The buckling of helical springs was first studied by R. Grammel in a paper read before the first International Congress for Applied Mechanics. Later on C. B. Biezeno and J. J. Koch pointed out that the results obtained did not agree with the experiments and that the reason for this discrepancy was to be sought in the neglect of the "shear elasticity" of the spring. Unfortunately a partial misinterpretation of this shear effect leads Biezeno and Koch to an overestimation, which makes itself clearly perceptible in the end results. In this paper the correction is given, and it is proved that now full agreement between theory and experiment exists. The theory is not restricted to the determination of the buckling load of helical springs under compression but can be applied as well to springs subjected to an axial force combined with a bending

moment and a lateral force, as to springs under the combined action of compression and torsion. Apart from the fact that the normal and shear elasticity of the spring have to be brought into account if the latter (as a whole) is expected to behave like a very elastical rod, it must be remembered that the compression of the spring results in an increase of the number of coils per unit of axial length, and therefore leads to a decrease of all coefficients of rigidity as compared with those in the unloaded state.

If n is the number of active coils, D the mean spring diameter, I the linear moment of inertia of the circular wire section, l_0 the length of the unloaded spring, l the length of the loaded spring, E Young's modulus of elasticity, m Poisson's ratio, then the various coefficients of elastic rigidity per unit of length of the unloaded spring are (in succession of bending, shear, compression, and torsion)

$$\frac{1}{\alpha_0} = \frac{n}{l_0}\frac{\pi D}{EI}\frac{2m+1}{2m}; \qquad \frac{1}{\beta_0} = \frac{n}{l_0}\frac{\pi D^3}{8EI}; \qquad \frac{1}{\gamma_0} = \frac{n}{l_0}\frac{\pi D^3}{EI}\frac{m+1}{4m};$$

$$\frac{1}{\delta_0} = \frac{n}{l_0}\frac{\pi D}{EI} \tag{1}$$

those defined per unit of length of the loaded spring are represented by

$$\alpha = \frac{l}{l_0}\alpha_0; \qquad \beta = \frac{l}{l_0}\beta_0; \qquad \gamma = \frac{l}{l_0}\gamma_0; \qquad \delta = \frac{l}{l_0}\delta_0. \tag{2}$$

The differential equation of the problem is

$$y'' + \frac{P}{\alpha}\left(1 + \frac{P}{\beta}\right)y = 0 \tag{3}$$

(in contrast to the equation

$$y'' + \frac{\beta}{\alpha}\frac{P}{(\beta - P)}y = 0 \tag{4}$$

given by Biezeno and Koch), and it is an easy matter to deduce from this equation the required buckling load, taking due regard to the boundary conditions. The relative compressions ξ [defined by $l = (1 - \xi)l_0$] at which the spring buckles can be plotted against the ratio l_0/D and be compared with experimental results; this leads to the agreement already mentioned. Most interesting is the behavior of a spring the length of which is about 2.7 times its diameter. If the length exceeds this amount by some 5 per cent, the spring buckles under a compression of about 50 per cent, whereas no instability at all occurs if the length is some 5 per cent smaller. Similar results hold for other end conditions of the spring.

With the aim in view to use his results in the construction of so-called "vibration" tables, the author pursues his treatise in examining a spring clamped at one end and loaded at its free end by an axial force P, a lateral force L, and a bending moment M_0, and calculates the lateral displacement y_l and the slope ψ_l of the free end in terms of these loads. P being prescribed, the lateral force and the moment required to produce a given y_l and ψ_l can be written as

$$L = c_1 y_l - c_2 \psi_l; \qquad M_0 = -c_2 y_l + c_3 \psi_l. \tag{5}$$

The coefficients c_1, c_2, c_3, which are of the greatest importance to the designer, can be derived from graphs (for different values of ξ resp. P) as function from l_0/D.

Finally the author considers the buckling of the spring under combined compression (P) and torsion (W), but the treatment of this problem is far more intricate so that no details can be given here. The results are given in graphs, in which for various values of the "angle of twist" curves are drawn the ordinate of which represents the critical relative compression ξ of the spring as function of the ratio l_0/D. Theoretical and experimental data are again in full agreement.

B. Plates and Shells

1. *On the State of Stress in Perforated Plates.* This important monograph deals with the stress distribution occurring in plates perforated by an arbitrary number of circular holes of arbitrary size and arbitrary situation (though the author restricts himself to holes of a fixed radius a).

The starting point of all calculations is the well-known stress function F of Airy, satisfying the equation:

$$\Delta\Delta F = 0 \left(\Delta = \frac{\partial^2}{\partial y^2} + \frac{\partial^2}{\partial z^2} \text{ resp. } \frac{\partial^2}{\partial r^2} + \frac{1}{r}\frac{\partial}{\partial r} + \frac{1}{r^2}\frac{\partial^2}{\partial \varphi^2} \right). \tag{1}$$

Every solution of this equation—if only satisfying certain conditions of continuity—gives rise to a realizable distribution of stress $(\sigma_y, \sigma_z, \tau_{yz})$ resp. $(\sigma_r, \sigma_\varphi, \tau_{r\varphi})$, represented by

$$\sigma_y = \frac{\partial^2 F}{\partial z^2}; \qquad \sigma_z = \frac{\partial^2 F}{\partial y^2}; \qquad \tau_{yz} = -\frac{\partial^2 F}{\partial y \partial z} \text{ resp.} \tag{2}$$

$$\sigma_r = \frac{1}{r}\frac{\partial F}{\partial r} + \frac{1}{r^2}\frac{\partial^2 F}{\partial \varphi^2}; \qquad \sigma_\varphi = \frac{\partial^2 F}{\partial r^2}; \qquad \tau_{r\varphi} = -\frac{\partial}{\partial r}\left(\frac{1}{r}\frac{\partial F}{\partial r}\right). \tag{3}$$

If we restrict ourselves to stress functions the corresponding displacements of which are zero at infinity and unambiguous throughout the field the most general F useful in our problem is given by

$$F = A_0F_0 + A_1F_1 + \bar{A}_1\bar{F}_1 + \sum_{n=2}^{\infty} (A_nF_n + B_nF_n^* + \bar{A}_n\bar{F}_n + \bar{B}_nF_n^*) \quad (4)$$

with

$$\left.\begin{aligned} F_0 &= lnr, \qquad F_1 = r^{-1}\cos\varphi, \\ &\qquad\qquad \bar{F}_1 = r^{-1}\sin\varphi, \qquad F_n = r^{-n}\cos n\varphi \\ F_n^* &= r^{-n+2}\cos n\varphi, \qquad \bar{F}_n = r^{-n}\sin n\varphi, \\ &\qquad\qquad \bar{F}_n^* = r^{-n+2}\sin n\varphi \qquad (n \geqq 2). \end{aligned}\right\} \quad (5)$$

Evidently every function F_s, F_s^*, $\bar{F}_s$, $\bar{F}_s^*$, gives rise to stresses σ_r, σ_φ and $\tau_{r\varphi}$ in the points of the circle $r = a$ (afterwards to be considered as the boundary of a circular hole I). But it is an easy matter to construct such linear combinations $F_{\sigma s}$, $F_{\tau s}$, $\bar{F}_{\sigma s}$, $\bar{F}_{\tau s}$ of these elementary functions that apart from tangential stresses σ_φ all along the circle $r = a$ only cosinusoidal or sinusoidal radial stresses σ_r resp. only cosinusoidal or sinusoidal shearing stresses $\tau_{r\varphi}$ occur. It can easily be checked, for instance, that with the stress function

$$F_{\sigma s} = \frac{a^{s+2}}{2(s+1)}F_s - \frac{a^s}{2(s-1)}F_s^* \quad (6)$$

the stresses $\sigma_r = \cos s\varphi$ and $\tau_{r\varphi} = 0$ do correspond in points of the circle $r = a$. In many cases it is recommended that the function F be developed into a series of the arguments $F_{\sigma s}$, $F_{\tau s}$, $\bar{F}_{\sigma s}$, $\bar{F}_{\tau s}$. It takes the form

$$F = C_0F_{\sigma 0} + C_1(F_{\sigma 1} + F_{\tau 1}) + \bar{C}_1(\bar{F}_{\sigma 1} - \bar{F}_{\tau 1}) + \sum_{s=2}^{\infty} (C_sF_{\sigma s} + D_sF_{\tau s} + \bar{C}_s\bar{F}_{\sigma s} + \bar{D}_s\bar{F}_{\tau s}). \quad (7)$$

If now a second circle (radius a) is considered (later on to be regarded as the boundary of a second hole II), a second system of polar coordinates $(r'\varphi')$ may be introduced in the center of this circle. The polar axis coincides with the polar axis of the first system but has the inverse positive direction, whereas the azimuthal positive directions are opposite as well. Under these conditions the stresses σ_r and $\tau_{r\varphi}$ occurring in the points of circle I as produced by the stress functions $F'_{\sigma s}$, $F'_{\tau s}$, $\bar{F}_{\sigma s}$, $\bar{F}'_{\tau s}$ connected with the center of circle II can be expanded into a Fourier series of the argument φ by the aid of a simple complex transformation.

This being stated we draw our attention to an infinite plate with two circular holes I and II (of equal radius) at infinity subjected to uniform tension perpendicularly directed to the centerline of the holes. If for a moment the plate is thought to be unperforated, the stresses $\sigma_r{}^0$ and $\tau_{r\varphi}{}^0$ occurring along the boundaries I and II can be calculated and brought into the form

$$-\sigma_r{}^0 = C_0{}^0 + \sum_{n=1}^{\infty} C_n{}^0 \cos n\varphi, \qquad -\tau_{r\varphi} = \sum_{n=1}^{\infty} D_n{}^0 \sin n\varphi. \tag{8}$$

Thereupon a stress function F is introduced into each of the centers I and II, represented by

$$F = C_0 F_{\sigma 0} + C_1(F_{\sigma 1} + F_{\tau 1}) + \sum_{n=2}^{\infty} (C_n F_{\sigma n} + D_n F_{\tau n}). \tag{9}$$

The stress function F connected with the center I gives rise to stresses along the boundary I of the magnitude

$$\sigma_{r1} = C_0 + \sum_{n=1}^{\infty} C_n \cos n\varphi, \qquad \tau_{r\varphi 1} = \sum_{n=1}^{\infty} D_n \sin n\varphi. \tag{10}$$

The stress function F connected with the center II gives rise to stresses along the boundary I, which can be written as

$$\left.\begin{aligned} \sigma_{r2} &= C_0 h_0{}^0 + \sum_{s=1}^{\infty} (C_s h_0{}^s + D_s i_0{}^s) + \sum_{n=1}^{\infty} \Big[C_0 h_n{}^0 + \sum_{s=1}^{\infty} (C_s h_n{}^s \\ &\qquad + D_s i_n{}^s) \Big] \cos n\varphi \\ \tau_{r\varphi 2} &= \sum_{n=1}^{\infty} \Big[C_0 j_n{}^0 + \sum_{s=1}^{\infty} (C_s j_n{}^s + D_s k_n{}^s) \Big] \sin n\varphi. \end{aligned}\right\} \tag{11}$$

The requirement that σ_r and $\tau_{r\varphi}$ shall be zero along the boundary I (and consequently along the boundary II also) leads to the following infinite system of linear equations for the constants C_n and D_n:

$$\left.\begin{aligned} C_n &= C_n{}^0 - \Big[C_0 h_n{}^0 + \sum_{s=1}^{\infty} (C_s h_n{}^s + D_s i_n{}^s) \Big] \qquad (n = 1, 2, \cdots) \\ D_n &= D_n{}^0 - \Big[C_0 j_n{}^0 + \sum_{s=1}^{\infty} (C_s j_n{}^s + D_s k_n{}^s) \Big] \qquad (n = 1, 2, \cdots). \end{aligned}\right\} \tag{12}$$

The solution of this system can be found by iteration. By putting

$$\left.\begin{aligned} C_n^i &= -\left[C_0^{(i-1)}h_n^0 + \sum_{s=1}^{\infty}\left(C_s^{(i-1)}h_n^s + D_s^{(i-1)}i_n^s\right)\right] \\ D_n^i &= -\left[C_0^{(i-1)}j_n^0 + \sum_{s=1}^{\infty}\left(C_s^{(i-1)}j_n^s + D_s^{(i-1)}k_n^s\right)\right] \end{aligned}\right\} \tag{13}$$

C_n and D_n are represented by

$$C_n = \sum_{i=0}^{\infty} C_n^i \qquad D_n = \sum_{i=0}^{\infty} D_n^i \tag{14}$$

provided that the convergence of the iteration process be guaranteed. The process itself can be interpreted by the following mechanical direction:

a. Calculate (expressed in Fourier series) the stresses σ_r^0 and $\tau_{r\varphi}^0$ occurring along the boundaries I and II in the unperforated plate.

b. Introduce in the centers I and II (identical) stress functions F_{I}^0 and F_{II}^0 such that F_{I}^0 annuls the stresses σ_r^0 and $\tau_{r\varphi}^0$ along the boundary I and that F_{II}^0 annuls the stresses σ_r^0 and $\tau_{r\varphi}^0$ along the boundary II.

c. Calculate the stress systems σ_r^1 $\tau_{r\varphi}^1$ (expressed in Fourier-series) called into existence by F_{I}^0 and F_{II}^0 along the boundaries of the *non*-corresponding holes.

d. Introduce in the centers I and II new stress functions F^1, which annul these stresses along their *corresponding* boundaries, etc.

The convergence of the iteration process is brought into relation with the "Eigenwert" problem, defined by the system

$$\mu C_n = -\left[C_0 h_n^0 + \sum_{s=1}^{\infty}\left(C_s h_n^s + D_s i_n^s\right)\right]; \quad \mu D_n = -\left[C_0 j_n^0 + \sum_{s=1}^{\infty}\left(C_s j_n^s + D_s k_n^s\right)\right] \tag{15}$$

but it is impossible to go into further details.

The exposition given here contains (in principle) all data, required for the treatment of the following cases (all of which in the original treatise are considered in full detail, and calculated numerically):

Three holes (the centers of which are collinear)

An infinite row of holes

Three holes (the centers of which are not collinear)

Two infinite parallel rows of holes (shifted or not).

In the last two paragraphs of the treatise the plate with one or two rows is reconsidered, now under the assumption that each hole is loaded

by a resultant force P, adequately distributed along the boundary of the hole. All forces P are equal and perpendicular to the row (or rows) as may be expected to occur in a riveted joint. The new element in the treatment of these problems consists in the starting function of the iteration. It is shown that the maximum stress is smallest for two nonshifted rows. It is proved that the least maximum stress occurring in a plate with shifted rows exceeds the maximum stress occurring in a plate with one row of holes (the total load of the plate being equal in both cases).

2. *On the State of Stress in Perforated Strips and Plates.* The preceding treatise restricted itself exclusively to infinite plates. In a subsequent series of papers the same author draws attention to the strip of finite width (and infinite length) with one or more rows of holes (pitch = b). The calculations are performed only for a strip with one row of holes, though an extensive program of further investigation was projected, which unfortunately could not be executed; the Jewish author, who lived in Holland, was arrested and marched off to Germany or Poland, which meant his destruction.

The system of coordinates $0(yz)$ used now is rectangular; the y-axis coincides with the center line of the holes. Consequently the stress functions F_0, F_n, $\bar{F}_n$, F_n^*, $\bar{F}_n^*$ introduced in the preceding treatise are written now as

$$F_0 = Re \ln x, \qquad F_n = Re\, x^{-n}, \qquad \bar{F}_n = -Im\, x^{-n} \qquad (n \geqq 1)$$
$$(x = y + iz) \quad (1)$$
$$F_n = Re\, \bar{x}\, x^{-n+1}, \qquad \bar{F}_n^* = -Im\, \bar{x}\, x^{-n+1} \qquad (n \geqq 2).$$

Furthermore stress functions F_0^k, F_n^k, $\bar{F}_n^k$, F_n^{*k}, $\bar{F}_n^{*k}$ are introduced, identical with the preceding ones, every set related however to a point $0'$ of the y-axis, having the abscissa $y = kb$. Finally these functions are expressed in terms of the coordinates (yz) of the point 0, so that, for instance, $F_n^k = Re(x - kb)^{-n}$. The total system of identical stress functions F_n, related to the infinity of centers $y = kb$, can with the aid of this transformation be represented by one single stress function $U_n = F_n + \sum_k^{\infty} (F_n^k + F_n^{-k})$, related to the system of coordinates $0(yz)$. It can readily be understood that the generalized stress function

$$F = A_0 U_0 + A_1 U_1 + \bar{A}_1 \bar{U}_1 + \sum_{n=1}^{\infty} (A_n U_n + B_n U_n^* + \bar{A}_n \bar{U}_n + \bar{B}_n \bar{U}_n^*) \quad (2)$$

produces the same set of stresses σ_r, $\tau_{r\varphi}$ along the boundaries of *all* holes.

Just in the same way as in the preceding treatise the functions F_s,

F_s^*, $\bar{F}_s$, $\bar{F}_s^*$ were linearly combined, here the functions U_s, U_s^*, $\bar{U}_s$, $\bar{U}_s^*$ are combined by introducing functions $U_{\sigma s}$, $U_{\tau s}$, $\bar{U}_{\sigma s}$, $\bar{U}_{\tau s}$, the first of which, for instance, is defined by

$$U_{\sigma s} = \frac{a^{s+2}}{2(s+1)} U_s - \frac{a^s}{2(s-1)} U_s^*. \tag{3}$$

Each of these functions produces a radial stress σ_r *and* a shearing stress $\tau_{r\varphi}$ along the boundary I of all circular holes, on the understanding however that these stresses are composed of a main term and an infinite series of minor terms; the main term corresponds with the stress that would have been produced by the corresponding functions $F_{\sigma s}$, $F_{\tau s}$, $\bar{F}_{\sigma s}$, $\bar{F}_{\tau s}$.

If restriction is made to such functions that satisfy the conditions of symmetry inherent to the strip under tension, the most general stress function that can be brought into play is given by

$$F = C_0 U_{\sigma 0} + \sum_{s=1}^{\infty} (C_{2s} U_{\sigma,2s} + D_{2s} U_{\tau,2s}) + \sum_{s=0}^{\infty} (\bar{C}_{2s} \bar{U}_{\sigma,2s+1} + \bar{D}_{2s+1} \bar{U}_{\tau,2s+1}). \tag{4}$$

It produces along the boundaries II and III of the strip ($z = \pm c$) stresses σ_z and τ_{yz}, for which a Fourier series (as functions of y, and with the period b) can be developed.

On the other hand it is required to construct a stress function F' having reference to the infinite half-plane such that along the straight boundary of the stress field *prescribed* stresses of the type

$$\sigma_z = \sum_{n=1}^{\infty} C_n' \cos 2\pi n \frac{y}{b} \qquad \tau_{yz} = \sum_{n=1}^{\infty} D_n' \sin 2\pi n \frac{y}{b} \tag{5}$$

come into existence.

This function has the form

$$F' = \sum_{s=1}^{\infty} (C_s' F_{\sigma s}' + D_s' F_{\tau s}') \tag{6}$$

with

$$\left.\begin{aligned} F'_{\sigma s} &= \frac{b^2}{4\pi^2 s^2} (s\zeta - 1) e^{s\zeta} \cos s\eta, \qquad F'_{\tau s} = \frac{b^2}{4\pi^2 s^2} s\zeta e^{s\zeta} \cos s\eta \\ &\qquad\qquad\qquad\qquad\qquad\qquad\qquad\qquad (s \geqq 1) \\ \eta &= \frac{2\pi y}{b}; \zeta = \frac{2\pi z}{b}. \end{aligned}\right\} \tag{7}$$

It is defined with respect to a system of coordinates, the y-axis of which coincides with the straight boundary of the half plane, the z-axis of which points to the inner region of the field). The stresses occurring along the boundaries I of circular holes, the centers of which have a mutual distance b and a distance c to the boundary can be expanded into a Fourier series of the arguments to φ of the holes.

Now the *unperforated* infinite plate may be considered covered with the contours I of the holes afterward to be introduced, and the boundaries II and III of the strip, afterward to be cut out of the plate; and a state of stress may be introduced as belonging to:

α. a stress function F_{I} (4) with respect to the center of one of the holes

β. a stress function F'_{II} (6) with respect to the boundary II

γ. a stress function F'_{III} (6) with respect to the boundary III

δ. a uniform tension p' in the direction y.

Then all means are available to calculate the stresses σ_z and τ_{yz} along the boundaries II and III and σ_r and $\tau_{r\varphi}$ along the boundaries I for each of the cases separately. The requirement that the total stresses along these boundaries be zero provides an infinite system of linear equations for the unknown constants C_{2n}, D_{2n}, C_n', and D_n', viz.:

$$C_{2n} = C_{2n}{}^0 - \Big[C_0 h_{2n}{}^0 + \sum_{s=1}^{\infty} (C_{2s} h_{2n}{}^{2s} + D_{2s} i_{2n}{}^{2s}) + \sum_{s=1}^{\infty} (C_s' p_{2n}{}^s + D_s' q_{2n}{}^s) \Big] \qquad n \geqq 0$$

$$D_{2n} = D_{2n}{}^0 - \Big[C_0 j_{2n}{}^0 + \sum_{s=1}^{\infty} (C_{2s} j_{2n}{}^{2s} + D_{2s} k_{2n}{}^{2s}) + \sum_{s=1}^{\infty} (C_s' r_{2n}{}^s + D_s' t_{2n}{}^s) \Big] \qquad n \geqq 1$$

$$C_n' = C_n'{}^0 - \Big[C_0 h_n'{}^0 + \sum_{s=1}^{\infty} (C_{2s} h_n'{}^{2s} + D_{2s} i_n'{}^{2s}) + C_n' p_n' + D_n' q_n' \Big] \qquad n \geqq 1$$

$$D_n' = D_n'{}^0 - \Big[C_0 j_n'{}^0 + \sum_{s=1}^{\infty} (C_{2s} j_n'{}^{2s} + D_{2s} k_n'{}^{2s}) + C_n' r_n' + D_n' t_n' \Big] \qquad n \geqq 1 \qquad (8)$$

in which the quantities h, i, j, k, p, q, r, t, C^0 etc. are known.

This system is resolved in an iterative way, for which a mechanical interpretation can readily be given.

Three quantities are of outstanding practical importance: (1) The magnitude of the total tensional force $P = 2cp$, to which the strip is subjected; (2) the maximal stress occurring in the strip; (3) the mean elongation of the strip.

The answers to these three questions are:

1. $$\frac{p}{p'} = \frac{P}{2cp'} = 1 + \pi \frac{a^2}{bc} \frac{C_0 + C_2 - D_2}{p'}.$$

2. The maximal stress occurs at the boundaries I, and can for different values $\lambda = a/b$ and $\mu = a/c$ be read from Table 1:

TABLE 1
Maximum Stress: p

λ \ μ	0	0.20	0.40	0.60
0	3.0000			
0.10	2.7677	3.0905	3.7510	
0.20	2.3261	2.7121	3.5210	5.3256*
0.30	1.9956	2.3936	3.0741	4.8310

* Belongs to $\lambda = 0.15$.

3. $$\frac{\Delta b}{b} = \frac{p'}{p} \frac{P}{2Ec}.$$

All calculations mentioned before are repeated for the bent strip and all required numerical data are put at the disposal of the reader. The same holds for the problem connected with a row of rivet holes, in the neighborhood of a straight boundary, which is solved under the condition that the boundary stresses of every hole give rise to a resultant force P perpendicular to (and directed toward) the straight boundary, whereas the reaction of these resultant forces consists of a continuous constant tension $p = P/b$ acting at infinity at the "opposite edge" of the infinite plate. The resultant force P is supposed to be exerted by a normal pressure $\sigma_r = (2P/\pi a) \sin \varphi$ acting on the upper half of the circular boundary of the hole; no other stresses on this boundary are present.

It will be clear that only the principal features of the work could be outlined and that a tremendous amount of computation hides itself behind the theoretical deductions.

3. *Some Explicit Formulas of Use in the Calculation of Arbitrary Loaded Thin-Walled Cylinders.*[1]

[1] For the notation used here refer to section 2.

An arbitrary load system (R,Φ,Z) acting upon a thin-walled cylinder can be expanded into a double Fourier series:

$$R = \sum_{p=0}^{\infty}\sum_{q=0}^{\infty} a'_{pq} \cos p\varphi \sin \lambda \frac{z}{a} + \sum_{p=0}^{\infty}\sum_{q=0}^{\infty} b'_{pq} \cos p\varphi \cos \lambda \frac{z}{a}$$
$$+ \sum_{p=0}^{\infty}\sum_{q=0}^{\infty} c'_{pq} \sin p\varphi \sin \lambda \frac{z}{a} + \sum_{p=0}^{\infty}\sum_{q=0}^{\infty} d'_{pq} \sin p\varphi \cos \lambda \frac{z}{a} \quad (1)$$

and two other expansions for Φ and Z, which can be derived from (1) by replacing the coefficients $a'b'c'd'$ by a'', b'', c'', d'', and a''', b''', c''', d''', respectively (p and q integers, $\lambda = \pi qa/l$, a = radius, l = length of the cylinder).

It is the aim of this treatise to give *explicit* formulas for *all* internal forces and moments $k_{\varphi\varphi}$, $k_{\varphi z}$, $k_{z\varphi}$, k_{zz}, $m_{\varphi\varphi}$, $m_{\varphi z}$, $m_{z\varphi}$, m_{zz} occurring in the cylinder if it is loaded by any of the elementary loads contained in series (1) or by any of the elementary loads of which Φ and Z are built up. The derivation of the formulas called for a good deal of laborious computation, which, however, needed only to be done once forever, and can be avoided now by others.

4. *The Effective Width of Cylinders, Periodically Stiffened by Circular Rings.* The purpose of this treatise is to provide the reader with a simple rule for the computation of the greatest tangential stress occurring in a thin-walled cylinder which in itself possesses only a slight flexural rigidity against alteration of its circular cross section and which therefore in constant distances ($=2l$) has been stiffened by circular rings. The load system of the cylinder is subject to the condition of periodicity in the axial direction, the period being identical with that of the rings; moreover the load is supposed to be symmetrical with respect to the plane of symmetry of two consecutive rings and to consist of radial and tangential components only. A specialization of this load system presents itself if all loads are concentrated in the planes of the rings, and as a matter of fact in this paper attention is drawn only to such a special system. The justification of this restriction is mainly to be sought in its agreement with actual practice but also in the fact that the stress problem raised by a general load system can always be decomposed into two other problems, one of which refers to a cylinder of length $2l$ loaded in the prescribed way, but clamped at both ends, while the other one relates to the actual cylinder exclusively loaded in the planes of its stiffening rings. The orthodox method of solving this latter stress problem consists in the separate treatment of the rings and the cylinder, the first ones under the

action of unknown radial and tangential load components, the last one under the action of their reaction components and the prescribed load system. The unknown load components can then be found by equalizing the radial and tangential displacements of the corresponding points of the cylindrical shell and the stiffening rings. The authors used this method in solving a certain mineshaft problem and had thereby full opportunity to take note of the laborious computation that it involves. It was this very problem that led them to the approximate method developed in this paper.

If the cylinder, stripped of its stiffening rings, is subject to an arbitrary load system L in each of its former ring planes, it shows—if thin—a high degree of flexibility, characterized by large radial displacements. There exists, however, an infinite class of "characteristic" load systems L_p ($p = 1, 2, \cdots$) with radial and tangential components $r_p = B_p' \cos p\varphi$, $t_p = B_p'' \sin p\varphi$ (φ designing the azimuthal coordinate), which, in their planes of application produce no radial displacements u_p but solely tangential displacements v_p, so that in these planes the cylinder seems to lack any flexibility; the amplitudes B_p' and B_p'' of these characteristic components have a well-defined ratio. The circumferential elasticity of the cylinder can be measured by the quotient $v_p : t_p$, which for all points of the circumference appears to be a constant.

We now examine a circular ring of the same radius a and the same thickness h as the cylinder, and of the width $l' = \mu a$. This ring too can be loaded by "characteristic" loads $\bar{r}_p = \bar{B}_p' \cos p\varphi$, $\bar{t}_p = \bar{B}_p'' \sin p\varphi$ (but now uniformly distributed along the width l', so that the cross sections of this ring remain plane), such that no radial displacements $\bar{u}_p$ occur and only tangential displacements $\bar{v}_p$ are present. Again it can be stated that this ring (which does not bend in its plane) possesses a tangential elasticity to be measured by the quotient $\bar{v}_p : \bar{t}_p$, which for all points of the circumference proves to be constant. The width $\bar{l} = \mu a$ is said to represent the effective width $\bar{l}_p = \mu_p a$ of the cylinder (and the ring is said to be equivalent to the cylinder with respect to its tangential elasticity), if $\bar{v}_p : \bar{t}_p = v_p : t_p$. Consequently the cylinder and its equivalent ring of effective width $\bar{l}_p = \mu_p a$ will have the same tangential displacements if loaded by characteristic loads (r_p, t_p), $(\bar{r}_p, \bar{t}_p)$ resp. the t-components of which are equal. It can be shown that the equality $t = \bar{t}_p$ involves —with a high degree of approximation—the equality $r_p = \bar{r}_p$, and therefore it can be said that the cylinder and its equivalent ring of effective width $\bar{l}_p = \mu_p \cdot a$ behave similarly (with respect to the displacements u_p ($=0$) and v_p occurring in their midplanes) under the action of equal characteristic loads (r_p, t_p).

By comparing a section of the stiffened cylinder with an equally

stiffened ring of effective width $\bar{l}_p = \mu_p a$ and loaded by a system $r = A_p' \cos p\varphi$, $t = A_p'' \sin p\varphi$, which differs from the characteristic load system $r_p = B_p' \cos p\varphi$, $t_p = B_p'' \sin p\varphi$ (so that the ratio of the coefficients A_p' and A_p'' differs from the ratio $B_p' : B_p''$), it can be proved that both constructions are elastically identical, in so far as the transverse rings are similarly loaded at their joints with the cylinderical shell.

All this taken for granted, it is easily understood that the maximum stress occurring in the cylinder, which in the planes of its stiffening girders is loaded by an *arbitrary* system L, can be found by expanding L into a Fourier series, computing for every component ($r = A_p' \cos p\varphi$, $t = A_p'' \sin p\varphi$) the maximal tangential stress that occurs in the T-shaped ring of corresponding effective width $\bar{l}_p = \mu_p a$, and summing up the results obtained in this way.

It goes without saying that the computation of the coefficients μ_p is a rather tedious matter, in which the theory of cylindrical shells is fully involved. It has been the aim of the authors to do the computation once and for all, and the result of their attempt is laid down in tables and graphs, in which μ_p can be found up to $p = 50$ for four values of $k = h^2/12a^2$, viz. $k = 10^{-4}$, 10^{-5}, 10^{-6} and 10^{-7}. Obviously any particular case occurring in practice is related to another value of k. In such a case the procedure recommended is to calculate (eventually by suitable interpolation) the required effective width corresponding to the four values of $k = 10^{-4}, 10^{-5}, 10^{-6}, 10^{-7}$; to represent these values as ordinates in a graph, the abscissa of which indicates $lg\, k$, to join by a smooth curve the four points so obtained and to read from this curve the ordinate corresponding to the value of k under consideration.

5. *On Circular Plates, Supported in a Number of Points* ($\geqq 3$) *Regularly Distributed Along Its Boundary and Rotatory-Symmetrically Loaded.* The problem is governed by the differential equation

$$\Delta\Delta u = Ap; \qquad \Delta = \frac{\partial^2}{\partial r^2} + \frac{1}{r}\frac{\partial}{\partial r} + \frac{1}{r^2}\frac{\partial^2}{\partial \varphi^2}; \qquad A = \frac{12(m^2-1)}{m^2 E h^3} \tag{1}$$

(u = deflection; p = local load; h = thickness of the plate). The displacement u is decomposed into two components u^* and u^{**} ($u = u^* + u^{**}$) such that:

(1) u^* satisfies the differential equation (1) without satisfying the boundary conditions of the problem.

(2) $(u^* + u^{**})$ satisfies both the differential equation and the boundary conditions.

Hereby one is free to choose the boundary conditions for u^*, which in

the case under consideration is done in such a way that at the boundary $r = R \rightarrow u^*$ and $\sigma_r = 0$.

The differential equation for u^{**} obviously is

$$\Delta\Delta u^{**} = 0. \tag{2}$$

The boundary conditions are: (a) $u^{**} = 0$ in the points of support. (b) $\sigma_r = 0$ at $r = R$; (c) shear force (proportional to $u^* + u^{**}$) zero in all points $r = R$, except in the points of support, where it has a prescribed value, viz. one k^{th} of the total load, if k designs the total number of supports. To cover the most general case of loading, u^* is calculated under the assumption that the plate is loaded over the annular surface $2\pi r_0 dr_0$ only ($0 < r_0 < R$) by a constant pressure p; it is found that the (infinitesimal) deflection is given by

$$du^* = \frac{3(m^2-1)}{m^2}\frac{pr_0R^2}{Eh^3}\left[\frac{m-1}{2(m+1)}\left(\frac{r_0^2}{R^2}-1\right)\frac{r^2}{R^2}+\left(\frac{r^2}{R^2}+\frac{r_0^2}{R^2}\right)\ln\frac{r_0}{R}\right.$$
$$\left.-\frac{(3m+1)}{2(m+1)}\left(\frac{r_0^2}{R^2}-1\right)\right]dr_0.$$

if $0 \leqq r \leqq r_0$, and

$$du^* = \frac{3(m^2-1)}{m^2}\frac{pr_0R^2}{Eh^3}\left[\frac{m-1}{2(m+1)}\left(\frac{r^2}{R^2}-1\right)\frac{r_0^2}{R^2}+\left(\frac{r^2}{R^2}+\frac{r_0^2}{R^2}\right)\ln\frac{r_0}{R}\right.$$
$$\left.-\frac{3m+1}{2(m+1)}\left(\frac{r^2}{R^2}-1\right)\right]dr_0$$

if $r_0 \leqq r \leqq R$.

If the constant boundary shear force corresponding with u^* be denoted by q^*, then u^{**} consistent with u^* can be represented by

$$u^{**} = \frac{q^*Ar^3m}{(3m+1)(m-1)}\left[2\sum_{n=k}^{\infty}{}'\frac{(2n+1)m+1}{n^2(n^2-1)}+\right.$$
$$\left.\sum_{n=k}^{\infty}{}'\left\{-\frac{m(n^2+3n+2)-n^2+n+2}{n^2(n^2-1)}\left(\frac{r}{R}\right)^n+\frac{m-1}{n^2+n}\left(\frac{r}{R}\right)^{n+2}\right\}\cos n\varphi\right]$$

(where the suffix $'$ added to the Σ sign means that summation takes place over multiples of k only).

Numerical results are given for a plate with three supports loaded in its center by a concentrated force P, with respect to the deflection in the center as well as to the deflection at the boundary. A simple instruction is given to calculate the central deflection of a plate with k supports ($k = 3, 4$, up to 12), subject to an arbitrary rotatory load.

C. *Miscellaneous Papers*

1. *On Elastically Supported Beams.* The elastically supported beam has been treated by several authors. It has, for instance, been discussed at great length in *Technische Dynamik* by C. B. Biezeno and R. Grammel, where special attention is drawn to iterative methods developed by the first author and J. J. Koch. The points of support of the beam under consideration in this paper may be indicated by 0, 1, 2, $\cdots$ n; the shear force, the bending moment, and the spring reaction at the support i by D_i, M_i, and P_i (the shear force and the moment at the left of a support by D_{il}, and M_{il}, at the right of a support by D_{ir} and M_{ir}). The quantities D_{0l}, M_{0l}, D_{nr}, M_{nr} are supposed to be known and are denoted by $\bar{D}_{0l}$, $\bar{M}_{0l}$, etc. The deflection of the beam is denoted by y. The method starts with the assumption of arbitrary values for y_0 and y_0'. Then the first reaction of support P_0 can be calculated with the aid of the spring constant k_0 ($P_0 = k_0 y_0$) and consequently D_{1l} and M_{1l} can be statically determined. The deflection and slope y_1 and y_1' of the end point of the beam (01) clamped at (0) under prescribed y_0 and y_0' can easily be calculated by the aid of elementary deflection formulas, and consequently the reaction $P_1 (= k_1 y_1)$ (and if required D_{1r}) are known. From y_1, y_1', D_{1r} (and the external loads) M_2, D_{2l}, y_2, y_2' can be derived in the same way, and finally D_{nr} and M_{nr} are calculated, which naturally will not agree with the prescribed values $\bar{D}_{nr}$ and $\bar{M}_{nr}$.

The same process is repeated for two other sets of arbitrarily chosen values, y_0^*, $y_0'^*$ and y_0^{**}, $y_0'^{**}$ (not simultaneously zero, under the understanding that all external loads of the beam are put equal to zero, inclusive D_{0l} and M_{0l}). The end result of these computations may be represented by the sets D_{nr}^*, M_n^* and D_{nr}^{**}, M_n^{**}. It is readily understood that the real values $\bar{y}_0$, $\bar{y}_0'$ can be written as

$$\bar{y}_0 = y_0 + t_1 y_0^* + t_2 y_0^{**}, \qquad \bar{y}_0' = y_0' + t_1 y_0'^* + y_0'^{**} \tag{1}$$

and that consequently also the following equations must hold:

$$\begin{aligned} \bar{D}_{nr} &= D_{nr} + t_1 D_{nr}^* + t_2 D_{nr}^{**} \\ \bar{M}_{nr} &= M_{nr} + t_1 M_{nr}^* + t_2 M_{nr}^{**} \end{aligned} \tag{2}$$

from which t_1 and t_2 can be calculated. These constants being known, all other required data can easily be found. The practical applicability of the method lies in the fact that a simple schedule is put at the disposal of the reader, which enables him indeed to leave the whole computation to a calculator who may lack all mechanical knowledge.

2. *On a Special Case of Bending.* In a paper, published in the *Ingenieur Archiv* (Vol. XII, 1941), R. Sonntag draws attention to a special

case of bending, which occurs if a highly elastic beam freely supported in two points of prescribed distance l is subjected to a transverse load P, acting in the middle of the span. The beam is supposed to slide freely—and without friction—over its supports so that great deflections are to be expected even under relatively small loads. In an ingenious but rather artificial way the author of the present paper succeeds in deducing the relations between the load P, the corresponding deflection f, and the length of the deflected beam as far as it lies between the supports. The artificiality lies in the linearization of the problem, which—at the expense of a rather laborious control—is proved to hold within well-defined limits. In the Biezeno paper it is shown that the problem admits of a quite natural solution, which for all beams of constant flexural rigidity requires the construction of one single graph, from which Sonntag's conclusions—inclusive the interesting remark about the stability of the beam—can all be derived. The construction admits of some generalizations. First it can be extended without difficulty to symmetrical girders of varying flexural rigidity. But it can as well be extended to cases where friction comes into being during the gliding motion of the girder over its supports. Finally it can be stated that, whereas Sonntag's deductions hold true only as far as the central line of the beam can be approximated by a suitably chosen circular arc, the method proposed in the present paper admits of the investigation of much more complicated deflections. For another (analytical) treatment of the same problem refer to section A7.

3. *Critical Speeds of Rotating Shafts.* It is well known that a rotating shaft, supported either in a statically determined or a statically undetermined way and bearing n centered and concentrated masses m_1, $m_2, \cdots m_n$ (in comparison of which the mass of the shaft itself may be neglected), may whirl at most at n angular speeds. The reciprocal squares of these critical angular speeds are roots of a so-called secular equation of such particular structure that the reality and positiveness of these roots is recognized by the use of well-known mathematical results. But no guarantee is given for the fact—tacitly assumed by all engineers—that these roots are *different* ones. The paper under consideration deals with this unequality and gives the proof of it.

The proof is rather intricate and depends on deep-seated mechanical properties of the shaft, which find their expression in certain relations between the influence coefficients α_{ij} of Maxwell that are connected with the problem. It must be remarked that it is a fundamental feature of the proof that all supports are rigid and that at these supports no zero slope can occur if the shaft is loaded by a single force. Therefore supports—terminal ones eventually excepted—that should have a "clamp-

ing" effect must be excluded. Elastic supports too must be excluded. Examples are given to show that these restrictions are essential.

4. *On the Elastic Behaviour of the So-Called "Bourdon" Pressure Gage.* The Bourdon pressure gage consists of annular tube of an elliptic or oval cross section and of constant thickness, closed by two meridional planes, which, as a result, include an angle lying between 240° and 300°. The major axis of symmetry of the cross section is parallel, the minor axis of symmetry perpendicular to the axis of revolution of the pressure gage. An internal pressure p (as has initially been discovered by mere change) will change the angular distance of the terminal planes, and consequently the amount of this change can be considered as a measure of this pressure. The phenomenon has been studied by H. Lorenz (Zeitsch. Ver. Deutsch. Ingen. 54, 1890) but serious objections must be made against his mode of deduction: on the one hand, the flexural stiffness of the wall is neglected in one part of the calculations, so that there the wall is assumed to act solely as a membrane; on the other hand, in another part of the treatise in which the flexural rigidity of the wall is brought into account, another phenomenon—occurring with initially curved tubes—is neglected. A recent study by G. Schubert accounts for this latter phenomenon but since it touches on the pressure gage only indirectly it does not bring the subject to a conclusion. The present authors meet the objections just mentioned and develop a method that in a rather simple way leads to numerical calculation of both the deformation and the stresses of the gage. It is proved that exceedingly high stresses are caused by relatively low pressures, and that as a rule the limit of proportionality is greatly surpassed by those pressures for which the pressure gage is meant to be designed. It therefore is no longer surprising that manifold ruptures occur and that elastic hysteresis and nonproportionality between pressure and reading are frequently observed.

The calculations are based on the assumption that the displacements and stresses are the same for all meridional cross sections of the gage. It goes without saying that the similarity of all distorted cross sections, which is a consequence of this assumption, would occur only if the gage were closed by two oval flat pistons lacking all elastic stiffness in their planes. It must, however, be emphasized that the disturbance caused by the compressive stiffness of the actual closing ends will be restricted to their immediate neighborhood, and if necessary, may be taken into account by introducing a smaller effective length of the gage.

The crucial point of the problem lies in the calculation of the normal stresses, acting in a meridional plane; the corresponding system of normal forces (which as a whole represents an equilibrium system) obviously has to fulfill the requirement that the meridional section remains plane,

under consideration of the fact that the deformation of the cross section of the gage is influenced by this system. The solution is found in an iterative way.

The situation of the dangerous point of the structure, determined after the theory of rupture of Guest, is found to be in full agreement with the experiment. Directions are given for performing the required calculations for any given form of cross section.

5. *On the Torsion of Prismatic Beams the Cross Section of Which Is Bounded by Two Pairs of Orthogonal Circular Arcs.* The cross section is defined with respect to a rectangular system of coordinates (y,z), the origin of which is the center of two limiting arcs (radius R); the radius of the two other arcs (having their center on the y-axis and their convex side to the z-axis) is designed by ρ and is unambiguously fixed by the polar angle φ of one of the "angular" points of the cross section.

It is evident that the problem is solved with the aid of the equations

$$\Delta\Phi = -2G\omega, \qquad \tau_{xz} = -\frac{\partial\Phi}{\partial y}, \qquad \tau_{xy} = \frac{\partial\Phi}{\partial z} \tag{1}$$

and by the use of bipolar coordinates.

Beforehand the required function Φ is split up into two components Φ^* and Φ^{**} defined by

$$\Delta\Phi^* = -2G\omega \qquad \Phi_R{}^* = 0 \qquad \Phi_\rho{}^* \neq 0 \tag{2}$$

$$\Delta\Phi^{**} = 0 \qquad \Phi_R{}^{**} = 0 \qquad \Phi_\rho{}^{**} = -\Phi^* \tag{3}$$

whereby boundary values of Φ, Φ^*, or Φ^{**} in a point of the circles R and ρ are indicated by subscripts R and ρ respectively.

The function Φ^* is chosen as

$$\Phi^* = \frac{G\omega}{2}(R^2 - y^2 - z^2). \tag{4}$$

The bipolar coordinates used henceforth are defined by the complex transformation

$$u = R \operatorname{tgh}\frac{v}{2} \qquad (u = y + iz,\ v = \eta + i\zeta) \tag{5}$$

which gives rise to the following set of transformation formulas:

$$y = R\frac{\sinh\eta}{\cosh\eta + \cos\zeta} \qquad z = R\frac{\sin\zeta}{\cosh\eta + \cos\zeta} \tag{6}$$

The differential equation (3) is invariant with respect to this transformation.

nately by two statically equivalent load systems S_1 and S_2 (such that $S_1 - S_2$ is an equilibrium system), then the greater the distance of a given point P from the loaded surface the less the state of stress and strain occurring in P as produced by S_1 will differ from those produced by S_2.

O. Zanaboni (*Atti Accad. Lincei*, 1937) gives a remarkable set of theses with respect to the theorem, which, however ingenious their deduction may be, give nevertheless no satisfaction to the engineer, who is far more interested in the numerical question of what difference will occur in the stresses in the neighborhood of the field of application of the two statically equivalent force systems.

Restricting himself to the half plane and the half space, the author of this treatise indicates the narrowest possible limits between which the local stresses in a prescribed point can vary for all possible statically equivalent loads S.

The plane problem is related to a system of rectangular coordinates (x,y,z), the x-axis of which coincides with the boundary of the stress field, and the y-axis of which points to the inner stress field. The general solution is given by the stress function F:

$$F = \int_0^\infty [\{(f_1 + ytf_2)\cos xt + (f_3 + ytf_4)\sin xt\}e^{-xt} + f_5 x + f_6 y + f_7]\,dt \quad (1)$$

in which the f_i stand for unknown functions of t.

The corresponding stresses σ_x, τ_{xy}, σ_y are:

$$\left.\begin{aligned}
\sigma_x &= \int_0^\infty \{(f_1 - 2f_2 + ytf_2)\cos xt + (f_3 - 2f_4 + ytf_4)\sin x\,t\}e^{-yt}t^2dt \\
\tau_{xy} &= \int_0^\infty \{(f_3 - f_4 + ytf_4)\cos xt + (-f_1 + f_2 - ytf_2)\sin xt\}e^{-yt}t^2dt \\
\sigma_y &= \int_0^\infty \{(-f_1 - ytf_2)\cos xt + (-f_3 - ytf_4)\sin xt\}e^{-yt}t^2dt
\end{aligned}\right\} \quad (2)$$

so that at the boundary $y = 0$

$$\left.\begin{aligned}
\tau_{xy}(x,0) &= \int_0^\infty \{(f_3 - f_4)\cos xt + (-f_1 + f_2)\sin xt\}t^2dt \\
\sigma_y(x,0) &= \int_0^\infty \{-f_1\cos xt - f_3\sin xt\}t^2dt.
\end{aligned}\right\} \quad (3)$$

On the other hand the prescribed boundary stresses as far as τ_{yx} and σ_y are concerned can be written as:

$$\left.\begin{aligned}
\tau_{xy} = p_x(x) &= \frac{2}{\pi}\int_0^\infty \{P_{x1}(t)\cos xt + P_{x2}(t)\sin xt\}dt \\
\sigma_y = p_y(x) &= \frac{2}{\pi}\int_0^\infty \{P_{y1}(t)\cos xt + P_{y2}(t)\sin xt\}dt
\end{aligned}\right\} \quad (4)$$

with

$$\left.\begin{aligned} P_{x1} &= \int_0^\infty p_{x1}(u)\cos tu\,du, & P_{y1} &= \int_0^\infty p_{y1}(u)\cos tu\,du \\ P_{x2} &= \int_0^\infty p_{x2}(u)\sin tu\,du, & P_{y2} &= \int_0^\infty p_{y2}(u)\sin tu\,du \\ p_{x1}(x) &= \tfrac{1}{2}\{p_x(x)+p_x(-x)\} & p_{y1}(x) &= \tfrac{1}{2}\{p_y(x)+p_y(-x)\} \\ p_{x2}(x) &= \tfrac{1}{2}\{p_x(x)-p_x(-x)\} & p_{y2}(x) &= \tfrac{1}{2}\{p_y(x)-p_y(-x)\} \end{aligned}\right\} \quad (5)$$

Comparison of (3) and (4) leads to:

$$t^2 f_1 = \frac{2}{\pi}P_{y1}(t); \qquad t^2 f_2 = \frac{2}{\pi}\{-P_{x2}(t)+P_{y1}(t)\}; \qquad t^2 f_3 = \frac{2}{\pi}P_{y2};$$

$$t^2 f_4 = \frac{2}{\pi}\{P_{x1}(t)+P_{y2}(t)\}. \quad (6)$$

Herewith all data are formally at hand for the calculation of the stress field produced by the prescribed boundary stresses τ_{xy} and σ_y.

For the sake of comparison several special cases are treated first: (a) a constant pressure $p_{y1}(x)$ over the interval $-a \leqq x \leqq a$; (b) the concentrated force P at $x = 0$; (c) a constant shear p_{x1} over the interval $-a \leqq x \leqq a$; (d) the concentrated shearing force P_x at $x = 0$; (e) the load p_{y2}, constant in the interval $0 \leqq x \leqq a$, and $-a \leqq x \leqq 0$, but of different sign; (f) the statically equivalent "double-force" of moment M_z; (g) the shearing load p_{x2}, constant over the interval $0 \leqq x \leqq a$ and $-a \leqq x \leqq 0$, but of different sign; (h) the statically equivalent "double" force at $x = 0$ (clearly not exerting a moment now).

After having finished this preliminary work the author continues to examine the general case of loading in the interval $-a \leqq x \leqq +a$. To give an idea of his trend of thought the results of his computations may be reproduced for the specialized case for which the loading consists of normal pressures p_{y1d} only, symmetrical with respect to $x = 0$, and subjected to the restriction (indicated by the subscript d) that the system be definitely positive. (To the case in which this restriction is not fulfilled due attention is given later on by the author.) In this case the stress components can be written as:

$$\left.\begin{aligned} \sigma_x &= -\frac{4}{\pi}\frac{x^2 y}{r^4}\int_0^a p_{y1d}(u)F_1\,du; & \tau_{xy} &= -\frac{4}{\pi}\frac{xy^2}{r^4}\int_0^a p_{y1d}(u)F_2\,du \\ \sigma_y &= -\frac{4}{\pi}\frac{y^3}{r^4}\int_0^a p_{y1d}(u)F_3\,du; & r^2 &= x^2+y^2. \end{aligned}\right\} \quad (6)$$

In these formulas the factors before the integrals represent the stress components of σ_x', τ_{xy}', σ_y' produced by a statically equivalent concentrated load P_y at $x = 0$; and therefore the integrals themselves can be

looked upon as the "correction" factors of the stresses under consideration. They converge properly to unity if r increases indefinitely and are represented by:

$$\left.\begin{aligned} F_1(\alpha,\xi) &= \frac{(1+\alpha^2)^2\{1+(\alpha/\xi)^2\} - 4\alpha^2(2+\alpha^2-\xi^2)}{\{(1+\alpha^2)^2 - 4\alpha^2\xi^2\}^2} \\ F_2(\alpha,\xi) &= \frac{(1-\alpha^2)^2 + 4\alpha^2\xi^2 - 4\alpha^4}{\{(1+\alpha^2)^2 - 4\alpha^2\xi^2\}^2}; \qquad F_3 = \frac{(1+\alpha^2)^2 + 4\alpha^2\xi^2}{\{(1+\alpha^2)^2 - 4\alpha^2\xi^2\}^2} \\ F_3(\alpha,\xi) &= \frac{(1+\alpha^2)^2 + 4\alpha^2\xi^2}{\{(1+\alpha^2)^2 - 4\alpha^2\xi^2\}^2}; \qquad \alpha = \frac{u}{r}; \qquad \xi = \frac{x}{r} \end{aligned}\right\} \quad (7)$$

By introducing new indeterminate functions F_i', limited by the inequalities:

$$\min F_i \leqq F_i' \leqq \max F_i,$$

the stresses can be written as

$$\sigma_x = \sigma_x' F_1', \qquad \tau_{xy} = \tau_{xy}' F_2', \qquad \sigma_y = \sigma_y' F_3' \quad (8)$$

which represent the closest estimation to be made. The results are brought into numerical and graphical form, both for the special case that has served as an example here and for all other possible cases of loading.

The same problem is brought to a successful end for the symmetrically loaded half space (loaded over the surface $r \leqq a$) with the aid of Fourier-Bessel integrals of the type

$$f(r) = \int_0^\infty J_n(rt)tdt \int_0^\infty f(u)J_n(tu) \cdot udu. \quad (9)$$

It is not possible to go into further details here but it may be emphasized that the solution of the problem requires a considerable amount of analytical skill. (The reader will find the answers and the method of solution of a great number of important integrals at the end of the treatise.)

The second object treated with the same expedients concerns the torsion of prismatic rods, the cross section of which is limited by two circular arcs. All possible modifications (without exception) are considered; and all special cases already treated by other authors are found again as specializations of the general question put forward here, so that the results are checked in several ways. Extensive use is made of conformal transformation, viz:

$$\left.\begin{aligned} x + iy &= c \operatorname{cotg} \tfrac{1}{2}(u - iv) \\ x = c\frac{\sinh u}{\cosh u - \cos v} \qquad & y = c\frac{\sin v}{\cosh u - \cos v} \\ \tanh u = \frac{2cx}{x^2+y^2+c^2} \qquad & \operatorname{tg} v = \frac{2cy}{x^2+y^2-c^2}. \end{aligned}\right\} \quad (9)$$

It goes without saying that the transformation is chosen such that the points of intersection of the two boundary circles coincide with the singular points of the transformation.

All questions that relate to the maximum stress, the torsional rigidity, and the torsional moment are answered in detail but here too mathematical skill is required on the part of the reader if he wishes to follow all computations in detail (Bessel functions, elliptic functions, Γ functions, Ψ functions, conformal transformation, etc. are used). The treatise concludes with some practical applications.

7. *The Convergence of a Specialized Iterative Process in Use in Structural Analysis.* In recent years so-called "relaxation" methods have been developed that have completely altered the treatment of a great number of technically important structures, such as redundant girders, redundant frame-works, trusses of "Vierendeel" construction, etc.

These methods originate from an article by Hardy Cross, Analysis of continuous frames by distributing fixed-end moments, *Proc. Amer. Soc. C.E.* 96, 1–156 (1932), and have been developed mainly by R. V. Southwell and his disciples (cf. R. V. Southwell, Relaxation methods in engineering science, a treatise on approximate computation. Oxford University Press, New York, 1940).

All of them are iterative methods, the convergence of which—if considered at all—is generally discussed from the energetic point of view. The iterative method, under consideration here, is investigated in a different way. It is restricted to two-dimensional frameworks the joints of which are only liable to rotations, and for the rest are fixed in space. The joints of the framework may be denoted by A_i ($i = 1, 2, \cdots n$); the length of the member joining the points A_i and A_j may be indicated by $l_{ij} = l_{ji}$, and it may be prearranged by definition that $l_{ij} = 0$ if the A_i and A_j are unconnected and that, in agreement with this definition, $l_{ii} = 0$.

If the structure is loaded it will be brought into its "natural" state of stress and all joints A_i will rotate. If the rotations are prevented by suitable moments M_i applied in the joints A_i, the construction will be said to be "locked." It is supposed that the state of stress can easily be calculated for this fully "locked" structure. Then the problem to be solved consists in calculating all stresses that occur if the structure is "unlocked." It is this unlocking of the structure that is effectuated in degrees and in an iterative way. The locking moments, which prevail after the k'th iteration will be designated by $M_i(k)$. The procedure of iteration having once been fixed, it must be shown that all locking moments $M_i(k)$ ($i = 1, 2, \cdots n$) tend to zero if k tends to infinity. Obviously it must be guaranteed for the sake of practical applicability that this procedure of iteration be such that the change in state of stress, brought about by one single iteration, can easily be calculated.

The iterative method. Let the iteration be carried out k times, so that the locking moments are $M_i(k)$ $(i = 1, 2, \cdots n)$ and let the joint A_i alone be unlocked. Then A_i must be loaded with $-M_i(k)$. All joints connected with A_i will be influenced by this unloading in a way that depends upon the distribution of $-M_i(k)$ over all members by which A_i is connected with other joints A_j. This distribution can be described by attributing to every member A_iA_j a certain "elastic weight" α_{ij}. The portion of $-M_i(k)$ for which the member A_iA_j stands, will then be represented by

$$\frac{\alpha_{ij}}{\sum_h \alpha_{ih}} M_i(k) \tag{1}$$

(where the summation over h may be extended over all values $h = 1, 2, \cdots n$, if only α_{ih} is put equal to zero for every h for which $l_{ih} = 0$).

The "extra" locking moment, caused by the unlocking of A_i, depends solely on the elastic properties of the member A_iA_j and can be calculated by introducing the so-called "coefficient of transition" β_{ij}; it then becomes

$$-\frac{\beta_{ij}\alpha_{ij}}{\sum_h \alpha_{ih}} M_i(k). \tag{2}$$

If the liquidation of the moments $M_i(k)$ is supposed to take place simultaneously for all joints A_i, it is evident that at the point A_i the moment $M_i(k)$ vanished, but is replaced by a moment $M_i(k+1)$ represented by

$$M_i(k+1) = -\sum_j \frac{\beta_{ji}\alpha_{ji}}{\sum_h \alpha_{jh}} M_j(k) \qquad (1 = 1, 2, \cdots n) \tag{3}$$

The system (3) is the analytical representation of the iterative method proposed in this paper.

By putting

$$N_i(k) = \frac{M_i(k)}{\sum_h \alpha_{ih}} \tag{4}$$

it is reduced to the system:

$$N_i(k+1) \cdot \sum_j \alpha_{ij} = -\sum_j \beta_{ji}\alpha_{ji} N_j(k) \qquad (i = 1, 2, \cdots n). \tag{5}$$

The convergence of the iteration defined by these equations depends upon a secular equation, of which all the roots ought to be smaller than 1

(in absolute magnitude). The proof that this condition is fulfilled under all circumstances is given in two distinct ways. The first proof is based on well-known properties of quadratic definite positive polynomials; the second one requires the introduction of so-called reciprocal (or conjugated) influence numbers of Maxwell. The interconnection of both trends of thought leads to remarkable inequalities for the latter numbers.

A simplification of the problem, bearing only on an elastic beam of uniform cross section supported in n distinct points, found its treatment in the Dutch periodical *De Ingenieur* (1946).

8. *A Draft of Nomenclature for Deformations.* At the meeting of the Executive Committee of the International Council of Scientific Unions in 1932 in London Dr. G. E. Hale proposed that there be established a committee for "instruments and methods of research" with the purpose of accumulating data on the use of instruments and methods developed in special branches of science in order to make them known also in other branches. The Committee for International Scientific Relations of the Royal Academy of Sciences at Amsterdam received this proposal with much interest, and since Dr. Hale had also stimulated the formation of national committees that should be related to the international committee, it was considered that in this connection the subject of viscous and plastic deformation seemed particularly well suited to provide a theme that could bring together scientists from the rather different domains of physics, chemistry, and biology. The object of the committee was formulated as follows:

1. to gather information regarding the phenomena of viscous and plastic deformation as they present themselves in various domains of physics, chemistry, technology, and biology.

2. to investigate the relations existing between these phenomena.

3. to make proposals for a nomenclature that should eliminate existing uncertainties in the various denominations.

4. to study the methods used for the measurement of viscosity and of related properties of matter, to interpret the meaning of the results given by various technical instruments, and where possible to indicate instruments that allow an unambiguous measurement of scientifically well-defined quantities.

The first report of the Committee (256 pages) appeared in 1935 and contained six chapters, viz.: I. Mechanical considerations; model systems, phenomenological theories of relaxation and of viscosity. II. Remarks in connection with the experimental investigation of self-restoring substances. III. Viscosity measurements with special reference to their application in colloid chemistry. IV. Viscosity and plasticity from a technical point of view. V. Plasticity of crystalline substances, in par-

ticular of metals. VI. Viscosity effects in the living protoplasm and in muscles.

The second report (287 pages) appeared in 1938 and contains the following six chapters: I. Introductory remarks on recent investigations concerning the structure of liquids. II. Viscosity of liquids in connection with their chemical and physical constitution. III. On the motion of small particles of elongated form, suspended in a viscous liquid. IV. The yield value. V. Recent plastometers. VI. Technical capillary viscometers.

These two elaborate reports, which may already have found their way to the United States of America, cover items 1 and 2 and partly item 4 of the program mentioned before, whereas the treatise mentioned in the heading fulfills requirement 3. In contrast with the two reports this treatise is provisionally written in Dutch, but it is meant to be translated into English as well, in order that it can meet the criticism of countries abroad. Up to now no serious objections have been made by the scientific workers in the field of mechanics in Holland to whose judgment it has been subjected. It is impossible to go into details here, because nearly every one of them would call for some nearer explanation, but it seems to be worth while to draw attention to this important attempt in the furtherance of unity of expression in a field that up to now excells in diversity of expressions. The monograph is subdivided into 5 chapters: I. Fundamental views and definitions. II. Classification of all different possibilities of deformation of a homogeneous material subject to simple shear. III. On the applicability of the nomenclature introduced in the preceding chapter to states of stress differing from pure shear. IV. Complementary definitions. V. Denominations for the distinguishing of different classes of materials.

The treatise concludes with a conveniently arranged table of all possible deformations and their names.

D. *Experimental Work*

1. *The "Reduced" Length of (Cylindrical) Twisted Shafts of Variable Cross Section.* For shafts of variable cross section the customary standard formulas with respect to the maximum stress and the angle of twist (or the torsional rigidity) can be used only if the change in section is not too rapid. In the case of sharp variation of cross section (frequently occurring in practice) not only may high concentrations of stresses occur, but also the torsional rigidity may be perceptibly influenced. It was the aim of the investigation to provide the reader with experimental data that would enable him to calculate this torsional rigidity, by altering the lengths of the different parts of the shaft in such a way that no influence

of fillets needs to be brought into account and no other formula has to be used than $\varphi = Wl/GI_p$ (W = torsional moment, G = shear modulus, I_p = polar moment of inertia). The results, which are united in conveniently arranged graphs, are of great use in the calculation of the torsional frequency of shafts of the type in view.

2. *Some Experimental Data Concerning Flange Couplings.* This article is closely connected with the preceding one. The experiments described here are performed with the aim of comparing the reduced length of a normally constructed flange coupling with that of a "blind" flange the length of which has been reduced according to the directions indicated in Section 1. It appears that the last one has to be increased by about 50 per cent to yield the first one. A very accurate calculation of the reduced length of the coupling, however, is possible if the flanges are only pressed together along a small circular (circumferential) ring of their plane of separation. Another important series of experiments has been undertaken to answer the question whether it is useful or not to insist on fitting bolts and to investigate whether or not the usual number of bolts is necessary. Three series of 10.10^6 cycles of stress variations performed on the model of the coupling demonstrated that fitting of the bolts is entirely superfluous, and that even an absolutely reliable joint is possible with two bolts only. As far as can be seen no "scale" effects are to be feared, so that it may be expected that all conclusions arrived at in this paper are valid for full-scale constructions. It goes without saying that the last word in all these matters is to be spoken by engineering practice. The gain in labor and costs that is to be expected from the proposed alterations in the construction of flange connections make it, however, desirable that such engineering practice be pursued.

3. *Strength and Stiffness of a Twisted Cross Section Weakened by a Deep Key Way with Sharp Corners.* The direct cause of this investigation was given by the desirability of exactly knowing the stress concentrations in the ground of the key way, as occurring in the neighborhood of the fillets and the need for reliable directions for the choice of the radius r of such fillets. The method used was that of the well-known soap-film theory. For all measurements a brass model plate was used, the circular hole of which had a radius $R = 5.0$ cm; the width (b) of the key way amounted to $b = 1.5$ cm. Three series of tests were made corresponding with a depth l of the key way: $l = 0.5R$, $l = R$, and $l = 1.5R$. Every series was performed for a number of different values of r.

It appeared that for any prescribed value of r the greatest stress concentrations occur with $l = R$. With a prescribed value of l the stress concentration naturally decreases with increasing r, but it is noteworthy that for great and small values of l no perceptible improvement occurs if r

surpasses 2 mm; if $l = R$, however, it is recommended that r be enlarged to $r = 5$ mm. Denoting the angle of twist per unit of length by ω, the factor of rigidity by S_w ($= M:\omega$; M = torsional moment), the "moment of resistance" W_w by $W_w = M:\tau_{max}$, two characteristic numbers μ and λ, standing for the torsional rigidity and the moment of resistance can be introduced by putting $\mu = S_w:GR^4$ and $\lambda = W_w:R^3$.

For all cross sections under consideration, λ and μ have been calculated from the measured soap films, expressed in terms of the two parameters $\alpha = l:2R$ and $\beta = r:b$. Thanks to the theoretical deductions referred to in Section C6, many experimental results could be checked and reliable extrapolations could be made so that full information is available for the whole field (α,β) as far as it is of practical importance. It must be admitted that all results are restricted to those cases in which $b:R$ has the fixed value 1.5:5.0. Since this ratio represents the value that nearly always occurs in machine practice, it seemed inappropriate to waste a considerable amount of work on other cases.

4. *Experimental Determination of the Stresses Occurring in a Ship Propeller.* The object of this investigation is the same as that taken in view by the American authors E. S. Carmick and H. B. Dodge, who in the *Journal of the Society of Naval Engineers*, **52**, 1940, described the results of "the use of an electrical strain gage in investigating stresses (in a ship propeller)." It has also been treated in a Dutch periodical, *Schip en Werf* (1944–45) by W. H. C. E. Rösingh. The present treatise is restricted to the static load of the propeller as furnished by the water pressure, which of course could be only roughly imitated by a statically equivalent system of concentrated forces. No efforts are made to reproduce stresses as caused by the centrifugal forces. Stresses occurring at the root of the blades are considered only qualitatively, in order to compare them with estimated results obtained by the method of photoelasticity. No attention was given to problems as presented by the coupled bending and torsional vibrations of the blades, which in the future certainly will become of great importance. The measurements were performed with the aid of the Huggenberger extensometer, mounted in a newly designed frame, such that measurements in different directions (as required for the determination of the total state of stress) could easily be executed. This total state of stress was computed for a great number of circumferential points of four cross sections. The analysis of the results obtained led to the result that the maximum normal stress σ occurring in such a cross section can be represented with fair approximation by a formula of the classical form $\sigma = M/W$, in which M represents the bending moment with respect to a well-defined axis of the cross section and W a well-defined geometrical quantity depending on the shape of the cross

section and the position of the axis just mentioned. The maximum stress occurring in the fillet of the propeller can be estimated by using an experimental formula that will be mentioned in Section 5.

5. *Optical Determination of Stress Concentrations in Fillets of Flat Bars of Constant Thickness and Sharp Varying Width.* If the smallest width of the bar is denoted by h, the greatest width by H, and the radius of the fillets by r, the so-called factor of stress concentration α is a function of the two variables h/H and h/r. From the experimental data acquired by the author a formula for α has been deduced that may be considered as accurate for the range $h/H = 0 \cdots 1$, and $h/r = 1 \cdots 10$, viz.,

$$\alpha = 1 + 0.17 \left(\frac{h}{r}\right)^{0.6} \sqrt{1 - \left(\frac{h}{H}\right)^2}.$$

The factor α relates to the case of bending so that the maximum bending stress can be calculated by aid of the formula:

$$\sigma_{max} = \alpha M : W.$$

6. *Effect of Change in Section of Rotating Shafts on Fatigue Properties.* The treatise under consideration arose from a question put to the authors by the Dutch Central Bureau of Normalization and bearing on the effect of fillets in rotating shafts of variable cross section on the endurance limit of the bending moment. The German and Swiss rules with respect to this problem diverged largely: on the one hand the radius r of the fillet was made dependent on the smallest (d) of the two diameters only, on the other hand it was made dependent solely on the difference ($D - d$) of both diameters. Renewed examination of the question seemed desirable, and, as was to be expected, the result was that the dynamical concentration factor β proved to be dependent on both quantities d/r and d/D. (If M denotes the limiting moment that can be endured by the shaft under 10^7 revolutions, and M^* the limiting moment that under the same conditions can be endured by a smooth shaft of diameter d, then β is defined by: $\beta = M : M^*$.) The way in which this factor β can be determined in a satisfactorily short time will be described in the next section. The experiments mentioned in this paper lead to the result that the dynamical factor β can be represented in a reliable way by the formula referred to in the preceding section if only h and H be replaced by d and D, so that

$$\beta = 1 + 0.17 \left(\frac{d}{r}\right)^{0.6} \sqrt{1 - \left(\frac{d}{D}\right)^2}.$$

In structural design β will be prescribed, and after having calculated d on the base of strength requirements and D on the base of structural

considerations, the designer will have to determine the radius r of the fillet. For this reason a graph is given in which for different given values of β the ratio d/r is plotted against the ratio d/D.

7. *An Abbreviated Method for the Determination of the Factor β Mentioned in the Preceding Section, for Torsional Stress Cycles as Well as for Bending Ones.* It is well-known that the experimental determination of the factor β, defined in the preceding section takes up much time and is in addition very expensive. It therefore is worth while to seek for an abbreviated method, perhaps lacking to some extent in accuracy, but saving much time and cost.

An effort in this direction is made in this paper; it can be summarized as follows. Starting with a bending moment (of such magnitude that the bending stress is perceptibly smaller than the endurance stress σ_e belonging to 10^7 cycles) the load is regularly increased by 10 per cent after a period in which 10^6 revolutions are made. The experiment is performed not only with the shaft under consideration but also with a smooth shaft the diameter of which is equal to the smaller diameter of the first one. For both shafts the bending moment for which breakdown occurs can be determined to a high degree of approximation, and the factor β can be represented by the ratio β' of *these* two bending moments. The conclusion to be drawn from laborious experiments, performed in the Laboratory of the Technical University at Delft, is that results of the abbreviated method may be expected that deviate ± 5 per cent from the required value.

8. *A Highly Sensitive Electrical Apparatus for the Magnification, Reproduction, and Measurement of Mechanical Quantities Occurring with Vibratory Phenomena.* The apparatus under consideration is of the "capacity" type, so that the phenomenon to be registered always governs some displacement to be measured by the change of capacity of a condenser. The requirements to be fulfilled are:

(1) The apparatus must not influence the phenomenon to be measured; accordingly the displacement must be held between very narrow limits, and consequently the apparatus must have a great sensitivity.

(2) The phenomenon must be truly reproduced. This requirement can be divided into two other ones:

(a) Rapid and slow-passing phenomena (including static phenomena) must be reproduced with the same sensitivity. (If this requirement is fulfilled the apparatus admits of being statically gaged, which is of great practical importance.)

(b) The amplitude of the reproduction must depend linearly upon the amplitude of the mechanical quantity to be measured.

(c) On account of the manifold problems to be investigated it is

required that it be possible to regulate the sensitivity of the apparatus between wide limits.

In broad lines the apparatus operates as follows: In a so-called detector the quantity to be measured is converted into the relative displacement of the two plates of a condenser which itself is placed in a capacity Wheatstone bridge, subjected to an alternating tension of such high frequency (1 $M \cdot Hz$) that the period is negligibly small in comparison with the period of the phenomena to be measured. The modulated high-frequency tension in the measuring branch of the bridge is magnified in a high-frequency amplifier and this amplified tension is rectified; the result is a low frequency tension varying in accordance with the modulation. After a tension of constant magnitude is superposed, this low-frequency tension can be led into a dead-tension amplifier, where it is magnified. This magnified tension controls an electron ray tube, by which finally the phenomenon is made visible.

The apparatus satisfies all conditions mentioned before and has already been used with great success in different cases. Magnifications of 200,000 can be reached.

II. Publications of the Nederlandsche Centrale Organisatie voor Toegepast Natuurwetenschappelijk Onderzoek (T.N.O.), the Hague—Dutch Central Institute for Technical Scientific Research; Vibrations and Photoelasticity

1. *Experimental Determination of the Time Integral of an Impact with the Aid of a Vibrating System.* The theory of measuring the time integral of a mathematical impact S (defined by $S = \lim_{T_e \to 0} \int_0^{T_e} P dt$, where P tends to infinity in such a way that the integral tends to a finite value if $T_e \to 0$) with the aid of a simple vibrating system, consisting of an elastically suspended mass, is well known. The theory is equally known in case the vibrating system is subject to viscous damping. This treatise deals with the same problem, but now related to a real physical impact. In the time integral $S = \int_0^{T_e} P dt$, the duration of the impact will now be small though not negligible compared with the period T_e of the free vibration of the undamped system. With respect to P it is supposed that during the impact time it does not change its sign, but no other conditions are to be fulfilled. The vibrating system may have a small viscous damping. The question to be solved is: what error can be made when the formula that holds for the mathematical impact is used for the physical one? The answer given is the following:

When a mathematical impact S acting on an undamped system gives a characteristic indication $x_m = S/\omega M$ (x_m designating the first amplitude

of the undamped vibrating system, ω the natural frequency of the undamped system, and M the vibrating mass), then a physical impact acting on the damped vibrating system gives a characteristic indication

$$x_m = \frac{S}{\omega M}(1 + \alpha - \beta). \tag{1}$$

In this formula α depends on the damping only, whereas β depends on the ratio $T_s : T_e$ and on the functional character of P during the period of impact. If in the (P,t)-graph, the unit of time is represented by T_e, and the unit of force is chosen such that $\int_0^{T_e} P dt = 1$, if furthermore I represents the moment of inertia of the surface covered by the (P,t)-diagram with respect to the line $t = c$, passing through its center of gravity, then $\beta = 2\pi^2 I$. It is readily seen that no greater β can occur, whatever the time dependency of P may be, than

$$\beta_{\max} = \frac{\pi^2}{2}\left(\frac{T_s}{T_e}\right)^2 \tag{2}$$

Therefore the correction β provided by formula (1) is in most cases negligible.

2. *The Infinite, Elastically Supported Beam, Subject to an Impact Load.* It is well known that railway wheels locally flattened by abrasion occasionally give rise to such strong impacts that rail rupture occurs. Only a detail of the complex of problems related to this phenomenon is treated here. The elastic support of the beam is considered as obeying Zimmermann's hypothesis (after which the local deflection $\bar{Y}$ is proportional to the local pressure $\bar{p}, \bar{Y} = \bar{p} : \bar{\alpha}$). The damping resistance acting on the vibrating beam is supposed to be proportional to the local velocity of the beam (damping coefficient $= \bar{\beta}$). Up to the moment $t = 0$ the beam is unloaded and at that time a concentrated load $\bar{K}(t)$ comes into action at the fixed point $\bar{x} = 0$. The deflection and the bending moment at the point of application are represented by definite integrals

$$Y(0,t) = \frac{2^{-\frac{7}{4}}\sqrt{\pi}}{\Gamma(\frac{3}{4})}\int_0^t K(t-\tau)e^{-\beta\tau}\tau^{\frac{1}{4}} J_{\frac{1}{4}}(\tau)d\tau \tag{1}$$

$$M(0,t) = -\frac{2^{-\frac{3}{4}}\sqrt{\pi}}{\Gamma(\frac{1}{4})}\int_0^t K(t-\tau)e^{-\beta\tau}\tau^{-\frac{1}{4}} J_{-\frac{1}{4}}(\tau)d\tau. \tag{2}$$

The quantities occurring in these integrals are defined by EI = coefficient of rigidity of the beam, F = surface of its cross section; γ = specific weight:

$$\alpha^* = \frac{\bar{\alpha}}{EI}\ \text{cm}^{-4} \qquad a = \sqrt{\frac{gE}{\gamma}}\ \text{cm sec}^{-1} \qquad 2\beta^* = \bar{\beta}\frac{a}{EI}\sqrt{\frac{\bar{I}}{F}}\ \text{cm}^{-2}$$

$$\epsilon = \sqrt[4]{\alpha^* - \beta^{*2}}\ \text{cm}^{-1} \qquad (\beta^{*2} < \alpha^*)$$

$\alpha = \frac{\alpha^*}{\epsilon^4}$, $\beta = \frac{\beta^*}{\epsilon^2}$ $(\alpha - \beta^2 = 1)$, $Y = \epsilon\bar{Y}$, $x = \epsilon\bar{x}$, $M = \frac{\bar{M}}{EI\epsilon}$ (M = moment in kg cm), $K = \frac{\bar{K}}{EI\epsilon^2}$ ($\bar{K}$ = loading force in kg), $t = \bar{t}a\epsilon^2\sqrt{\frac{I}{F}}$ (t = time in sec).

Equations (1) and (2) are derived with the aid of Laplace transformations.

Graphs of the functions $e^{-\beta\tau}\tau^{\frac{1}{4}}J_{\frac{1}{4}}(\tau)$ and $e^{-\beta\tau}\tau^{-\frac{1}{4}}J_{-\frac{1}{4}}(\tau)$ occurring in these equations are put at the disposal of the reader.

Several specializations of the general case represented by (1) and (2) are treated, viz.:

1. P = constant (up from $t = 0$ to $t = \infty$).

2. P = constant during a short duration t_1 of impact (the maxima both of Y and M, in their dependency on β and t_1 are studied and graphically represented).

3. Two important theorems, valid for all sorts of impacts are deduced:

(a) The maximum bending moment occurs within or at the end of the interval of impact.

(b) Impacts of the same intensity and of the same character (in as much the one impact can be deduced from the other one by a proportional transformation) yield maximum bending moments inversely proportional to the square roots of the impact times.

If the impact problem is put in another way, such that the force P is the unknown quantity (as may occur if a falling mass comes into contact with the beam) then again the solution is procured by integral equations of the type (1) and (2). They can be solved by using a step by step method indicated by Timoshenko.

3. *The Smallest Characteristic Number of Certain "Eigenwert" Problems.* Many problems in vibration theory and stability lead to the determination of the roots λ of the secular equation

$$\begin{vmatrix} \alpha_{11}m_1 - \frac{1}{\lambda} & \alpha_{12}\sqrt{m_1m_2} & \cdots & \alpha_{1n}\sqrt{m_1m_n} \\ \alpha_{21}\sqrt{m_2m_1} & \alpha_{22}m_2 - \frac{1}{\lambda} & \cdots & \alpha_{2n}\sqrt{m_2m_n} \\ \cdot & & & \\ \cdot & & & \\ \cdot & & & \\ \alpha_{n1}\sqrt{m_nm_1} & \cdots & \cdots & \alpha_{nn}m_{nn} - \frac{1}{\lambda} \end{vmatrix} = 0 \qquad (1)$$

in which the numbers α_{ij} represent so-called Maxwell numbers, characterized by $\alpha_{ij} = \alpha_{ji}$, $\alpha_{ii} > 0$, and in which $m_i > 0$.

In technical problems the smallest root λ_1 is in general the most important one. Following a trend of thought developed by Graeffe in solving algebraical equations and restricting himself to such problems for which all roots λ_i are different, the author derives a monotonously increasing infinite series of values, the limiting value of which is λ_1.

In defining

$$\alpha_{ij}^{(p)} = \sum_{k=1}^{n} \alpha_{ik}^{(p-1)} \alpha_{kj}^{(p-1)} \qquad \text{with} \qquad \alpha_{ij}^{(0)} = \alpha_{ij} \sqrt{m_i m_j} \tag{2}$$

he proves that

$$\lambda_1 > \frac{1}{\sqrt[2p]{\sum_{i=1}^{n} \alpha_{ii}^{(p)}}} \quad (p = 1, 2, \cdots) \qquad \text{and that}$$

$$\lambda_1 = \operatorname*{Lim}_{p \to \infty} \frac{1}{\sqrt[2p]{\sum_{i=1}^{n} \alpha_{ii}^{(p)}}} \tag{3}$$

$p = 0$ and $p = 1$ lead to well-known approximative formulas the first of which is ascribed to Dunkerley (cf., for instance, Biezeno and Grammel, *Technische Dynamik* Chapter III, **13,** 25 and Chapter III, **13,** 31).

4. *A Comparative Study About the Main Photoelastic Properties of Different Materials* (*Rept. IV of the Dept. of Photoelasticity*). Though the laboratory for applied mechanics of the Technische Hoogeschool at Delft possessed a photoelastic plant, no use was made of it for industrial purposes. During the war the Institute, mentioned in the heading of this Chapter, founded a separate department for photoelastic research, with the main aim to put its results at the disposal of the industry and other interested groups. The lack of material for models made it impossible up to now to do much work in the field of stress determination. On the other hand relatively much time could be spent on the investigation of the various properties and qualities of different materials in relation with their suitability for optical stress determination. The results of this investigation are gathered in this paper, in which attention is given to polystyrene, celluloid, phenolite. Their mechanical and optical properties are investigated at great length and for one and the same object, the stress distribution of which was known theoretically, the experimental results obtained with every one of the three materials are compared. Much

attention is given to the machining of the materials. All those who have to make their choice with respect to reliability, optical sensitiveness, durations of heat treatment, and so on will find valuable information in this report.

5. *On the Stress Concentration in the Corners of a Cross, the Rectangular Branches of Which Have Equal Width (Rept. V of the Dept. of Photoclasticity).* The stress concentration mentioned in the title is studied in regard to its dependence on the radius of the fillets of the cross when the latter is subjected to tension in the two perpendicular directions. Naturally the experiments are carried out only under one dimensional tension P. If tensions P and Q are simultaneously applied in two perpendicular directions the required results can be derived from the data obtained by the first mentioned experiment by making use of the law of superposition. The material used was xylonite, because of lack of polystyrene. A very effective method was introduced to obtain the required results in a short time. With the aid of a test strip a tensile stress σ_0 was determined, connected with a sharply perceptible change of color of the strip. This change of color was chosen such that the corresponding tensile stress was not too high (in this case $\sigma_0 = 78$ kg/cm^2). The model was charged in such a way that successively in all points in which the stress was to be measured, the change of color occurred. With every such experiment the load was registered and the mean value σ was calculated in such section of the cross as might be expected to show a uniform distribution of stress. The stress concentration factor occurring in the point under consideration evidently was given by the quotient $\sigma_0 : \sigma$. If the width of the straight parts of the cross be denoted by $2B$, the radius of the fillets by R, the ratio of the loads P and Q in the two perpendicular cross directions by μ, a graph can be designed in which for distinct values of μ, the maximum stress concentration is represented as function of R/B. As a matter of fact, this graph is put at the disposal of the reader. The stress-concentration factor appears in usual practice to vary between 1.35 and 2.10.

6. *Photoelastic Determination of the Stresses Occurring in a Tunnel Projected between the Banks of the "Noordzee Kanaal" Connecting Amsterdam with the North Sea (Rept. IX).* No special remarks are to be made. The report is mentioned just to give an idea of the work that is done by the department in question.

7. *Stress Concentrations in Corner Joints (Rept. VIII).* The data laid down in this report are the result of laborious and lengthy experiments performed on a large series of glass models, and bearing upon the stress concentration occurring in corner joints such as those appearing in innumerable technical constructions. The characteristic dimensions

of such a rectangular corner joint are the width h of the two straight sides, the direction and the length of the inner bevel, and the radii of the fillets constituting the transition from bevel to the normal border. One side of the construction was clamped, whereas the other side was loaded in succession by a bending moment, a normal force, and a shearing force. In each of these cases the stress distribution along the inner boundary of the corner joint was measured and critical examination of the results enabled the author to draw up elementary and simple directions by which henceforth all stresses at the inner boundary of a corner joint can be calculated with great accuracy, whatever the load at the end sections of the joint may be.

III. Publications of the Nationaal Luchtvaartlaboratorium at Amsterdam. (Aeronautical Research Laboratory)

1. *Stresses of the Second Order in the Skin and Ribs of Wings in Bending.* Wing structures in which the skin in the unloaded condition is not curved in the direction of the tensile stresses are considered. Bending of the wing causes a curvature of the skin in the direction of the tensile stresses; thus the wing ribs are loaded in consequence of the fact, that tensile stresses are changing their inclination; a second-order loading arises. If the structure of the wing ribs is such that their flanges are allowed to deflect in the plane of the rib (truss type and particularly open ribs), the deflection of the flanges by the second-order loads will affect the magnitude of the stresses in the skin: the extensions of the skin are allowed to decrease as the skin is situated now on a smaller radius of curvature. Flexibility of the rib flanges thus changes the distribution of tensile stresses over the width of the skin. Formulas are derived and graphs are given for the stresses in the ribs and in the skin. Usually the decrease of skin stresses is small; it becomes of more importance if the ratio of the height of the rib flange to the unsupported flange length is small, the height of the wing section is small, and the skin (longitudinal stiffeners included) is heavy. Even if the decrease of skin stresses is small, the "second-order" stresses in the ribs may be many times larger than the stresses, caused directly by local airload.

2. *Stress and Strain in Shell Wings with two Spars. a. The effect of elastic rib shear on stresses in two-spar wings with stressed skin.*

b. The stress distribution in wings with two nonparallel spars interconnected by elastically deformable ribs and skin.

c. The stress distribution in wings with two nonparallel torsionally rigid spars, interconnected by elastically deformable ribs and skin.

d. The distortions of wings with two spars.

e. Manual for the stress analysis of shell wings with two spars.

Preceding Dutch papers on the subject of stress and strain in shell wings with two main spars considered the spars to be deformable in bending and shear; the skin was allowed to shear under shear stresses, whereas the ribs were completely rigid against bending and shear in their plane. Spars and ribs had no stiffness against torque. Furthermore the rib system was a continuous system, thus the behavior of the structure could be described by differential equations holding for the whole of the wing span. Solving these equations by numerical integration the spar deflections were obtained and from these the stresses could be calculated.

Later research made it clear that in certain structures the deformation of the ribs in shear should not be neglected. In order to show the effect of rib shear, paper *a* communicates the stress distribution in 8 wings under continuously distributed and locally applied torque loads, these 8 wings differing only in the shear rigidity of their ribs. The assumption of completely rigid ribs proves to give a good approximation when the shear rigidity of the most stressed ribs surpasses certain well-defined limits.

Introduction of the deformability of the ribs showed that discontinuities in torsional rigidity of the wing shell or in torsional moment necessitates the assumption of "local" ribs apart from the system of continuous ribs. This means that the differential equations, complicated already by the fact that their order increases by two, determine the stress distribution only between consecutive local ribs and that at each of these ribs special boundary conditions have to be satisfied. This mixed system of local and continuous ribs is hardly suitable to practical analysis. With nonparallel spars the difficulties increase still more.

In order to eliminate these difficulties the assumption of continuous ribs is abandoned in paper *b*; the rib system consists of local ribs, 5 to 10 per half wing located at those points along the span, where the ribs of the actual structure will carry high shear loads. In general each rib replaces a group of ribs and its rigidity equals the total rigidity of the group.

The wing scheme is such that it may represent wings with built-up spars, in which the shear load is carried not only by the spar web but for some part too by an auxiliary spar or by the wing nose. In order to account for this the scheme allows the torsional centers of the spars to lie outside the plane through the spar caps. The torsional rigidity of these built-up spars may be accounted for by increasing the shear rigidity of the skin between the spars. This approximative consideration of the torsional rigidity of the spars has been adopted in paper *b*. Structures with built-up spars the torsional rigidity of which is not small compared with the rigidity of the tube between the spars have to be considered more

accurately; paper *c* deals with this problem in assuming torsionally rigid tubes between the ribs in front of the front spar and to the rear of the rear spar.

A more complete description of the scheme of paper *b* is the following.

There are two spars, connected by n parallel ribs per half wing. Between the ribs the spar flanges as well as the lines through the torsional centers of the spars are straight. At the ribs the flanges may change their directions and the torsional centers may shift. There is a skin between the flanges of both spars; it is connected with these flanges and with the ribs. Besides, the skin is supported by a continuous system of stiffeners running parallel to the ribs; these stiffeners are required for kinematical reasons if the skin is not exactly cylindrical.

Finite stiffness is assumed for the spars in bending and shear, for ribs and skin in shear only. The stiffeners are absolutely rigid in their own plane. With respect to moments the vectors of which lie in the planes of the spars, the ribs, the stiffeners and the skin, these structural components have no rigidity. Besides the skin has no rigidity against extension in the direction normal to the ribs.

This structure would be statically determinate if n is unity. The addition of $2(n-1)$ ribs makes the structure redundant to the $2(n-1)$th degree. By splitting the loads up in a symmetrical and an antimetrical load system, the structure is with respect to these particular load systems redundant to the $(n-1)$th degree. The statically indeterminate quantities X_i are chosen such that they are something like the bending moment in one of the spars at the junction i of the ribs and the spar. By the conditions of equilibrium all stresses can be expressed in these quantities.

Application of Castigliano's theorem of least work yields the conditions of elasticity. They are linear equations in the X_i, containing five of them at five consecutive ribs. All those equations together form a linear recurrent system. They are solved by linear combination of one solution of the complete equations, which has arbitrary starting values X_1 and X_2, and two solutions of the homogeneous equations with different but arbitrary initial values X_1 and X_2; the linear combination is such that the end conditions at the end rib are satisfied. (Compare Section C1 for this trend of thought.)

With completely rigid ribs the "equations of 5 moments" simplify to "equations of 3 moments."

The structure with torsionally stiff spars (paper *c*) contains in each bay of the wing besides the statically indeterminate quantity X, two other statically indeterminate quantities Y_f and Y_r, being the torsional moments in the spar tubes. Each condition of elasticity now contains besides five successive X_i's four successive unknown quantities Y_{fi} and five Y_{ri}'s.

There are now two other systems of recurrent equations, containing four successive X_r's and three successive Y_{fr}'s and Y_{rr}'s.

These recurrent systems of equations are solved by combining a solution of the complete equations with arbitrary initial values X_1, X_2, Y_{f1}, Y_{r1} and four mutually independent solutions of the homogeneous equations.

When the ribs can be considered to be completely stiff in their own plane the quantities Y can be eliminated; then the system of recurrent equations is formally identical with the system of equations for wings with spars without torsional stiffness.

For particular purposes in addition to the stress distribution the knowledge of the deflections may be needed. Calculating the distortion from the stresses by means of geometrical considerations is very cumbersome with this highly complex structure. Paper *d* gives the solution of this problem by means of a modification of Castigliano's theorem: the principle of virtual forces. According to Castigliano's theorem among all stress distributions satisfying the conditions of equilibrium the actual stress distribution makes $F = A - A_r$ a minimum, A being the elastic energy expressed in the stresses, A_r being the work done by the unknown surface stresses at those parts of the boundary where the deflections are prescribed. According to the rules of the calculus of variations the supplementary conditions of equilibrium $E = 0$ may be accounted for by adding their left-hand sides each multiplied by a factor μ to the function that is to be made a minimum. It can be shown that the multiplicators have the meaning of displacements. The method is given a clear mechanical interpretation.

Paper *e* gives instructions with regard to the practical application of the wing analysis given in paper *b*; much attention is given to the problem of how to replace a given wing by a mechanically equivalent wing, which fits into the adopted scheme; formulas are given for the calculation of the required stiffness factors.

3. *Effective Width. a. The effective width of flat axially loaded strips of sheet beyond the buckling stress for various edge conditions.* The theory of the effective width given by Marguerre and Trefftz is restricted to loads slightly greater than the buckling load of the sheet. Far beyond the buckling load the wave form assumed by these authors deviates too much from the actual wave form; so the effective width calculated from their formula is too large. An improvement was made by Plantema and Floor (*N.L.L. Report* S 262) who introduced one parameter more into the expression for the assumed wave form; however they too found a finite effective width for $\epsilon_k/\epsilon = 0$ (ϵ being the direct strain of the longitudinal edges of the sheet, ϵ_k = the direct strain causing buckling of the sheet), which is not to be expected. Cox introduced a new type of wave form

and made at the same time some supplementary suppositions concerning the stresses by which however the basis of his investigation becomes mechanically unsound.

In this investigation the main characteristic of the assumed wave form, introduced by Cox, has been adopted; the further method of dealing with the problem however works along the lines given by Marguerre and Trefftz.

For a given strain at the edges the displacements are such that the elastic energy is a minimum. An approximative solution is obtained by assuming displacements that, having at least the character of the wave form to be expected, can be modulated by varying the value of one or more parameters. The parameters introduced by Marguerre and Trefftz are the length and the depth of the waves. Whereas Cox assumes the wave to be of constant depth over some width in the center of the sheet (the edges being curved in two directions), the author of this paper introduces this width as a third parameter.

Various wave forms have been assumed for supported, rigidly clamped and elastically restrained edges each. The effective width proving to be not very much affected by the particular wave form, it seems plausible that the approximation is fairly good. A consequence of the approximation is that the elastic energy as well as the effective width "in the mean" is too large. However, when the approximate effective width is compared with experimental results the experimental values prove to be larger than the theoretical values. The explanation for this rather surprising result is that in an actual sheet, having finite length, the wave length is not free to change gradually in making the energy a minimum as is the case with a sheet of infinite length. This means that the theory is at the conservative side as long as the proportionality limit is not surpassed.

Another remarkable feature of the results is that the effective width of a supported, rigidly and elastically clamped sheet is practically equal for equal ϵ_k/ϵ.

If ϵ_k/ϵ approaches zero the effective width is proportional to $(\epsilon_k/\epsilon)^{\frac{1}{2}}$. This result was obtained by the transformation of Friedrichs, known from the calculus of variations. In theory this method can give a lower limit of the effective width over the *whole* range $0 < \epsilon_k/\epsilon < 1$. In view of the elaborate calculations required these calculations have not been carried out.

b. The effective width of flat sheet supported by longitudinal stiffeners with open section. The longitudinal stiffeners in aircraft-stressed skin construction present some elastical restraint to the edges of the sheet. The amount of this restraint by stiffeners having open section does not

depend merely upon the torsional stiffness of the stiffener. In the first place the torsional moment varies along the stiffener; the variation of warping of the cross section which would occur with a free stiffener is prevented and for this reason its stiffness is increased. In the second place the compression of the stiffener decreases its torsional stability and therewith its torsional stiffness. In the third place the way in which the torsional moment is applied to the stiffener by the sheet causes distortions of the cross section of the stiffener in the plane normal to the axis of the stiffener. This latter fact decreases the amount of restraint.

The first and second circumstances are dealt with in literature. This paper deals with the third effect, which proves to be of major importance. The calculation has been carried out for stiffeners having L- and Z-shaped sections and the results have been presented in graphs for various ratios of the dimensions of the cross sections.

4. *The Tension Field for Stresses Beyond the Buckling Stress.* The theory of the incomplete tension field in a sheet strip with supported edges, given by Marguerre and Kromm, is reliable for small ratios τ/τ_k (τ_k being the shear stress causing buckling). However the results of this theory for τ_k/τ approaching zero do not coincide with the results given by Wagner's theory for the complete tension field; the additional tensile stresses in S_1 and S_2 the longitudinal and lateral directions being less and the effective rigidity (G') being larger than predicted by Wagner's theory.

Along the same lines as indicated in section 2*a* this paper gives an approximative solution of the problem. The parameters governing the assumed wave form are, firstly the same as those introduced by Marguerre and Kromm: the wave length and wave depth, the angle between the edges of the sheet, and the nodal line of the waves; and secondly the width in the center of the sheet, over which the depth of the wave is constant. In this way the assumed wave form allows for the tendency of the waves to flatten out from the center towards the edges with increasing stress ratio τ/τ_k.

Sheets with clamped edges as well as sheets with supported edges have been investigated for various wave forms in the double curved-sheet region near the edges.

With equal τ/τ_k the stress ratios S_1/τ and S_2/τ and the effective rigidity are different for supported and clamped edges; the clamped sheet approaches the complete tension field more than does the supported sheet. This contrast to the behavior of the effective width may be explained by saying that the central portions of the tension field, where the influence of the edge conditions has faded out, is very active indeed in supporting the load.

For τ_k/τ approaching zero the deviations from Wagner's results for the complete tension field are presumably proportional with $(\tau_k/\tau)^{\frac{1}{3}}$.

The formula has been evaluated for the supported sheet with various stiffness of the longitudinal and lateral stiffeners under shear load and the results have been laid down in graphs, giving the mean stress ratios S_1/τ and S_2/τ and the effective rigidity G'.

These graphs may be applied too for sheet-stiffener combinations under shear and normal load in longitudinal and lateral direction (and not too large ratios between the normal loads and the shear load).

The solution being an approximative one the energy for given edge displacements will be too high and the actual stresses and rigidity will approach Wagner's results for the complete tension field more closely than do the calculated stresses and rigidity. Again experimental evidence seems to deny this conclusion; the explanation once more will be that the wave length in a sheet of finite length is not free to change gradually as the load increases. Explosive changes of wave number occur, but it may be that this change is postponed by the stability of the preceding wave form. In conclusion it may be stated that the theory for infinite long strips will give a conservative estimate of the actual conditions.

5. *The Effect of the Flexibility of Fuselage Frames on the Stress Distribution in Fuselage Shells.* The stress distribution is influenced to a large extent by the deformations of the frames, especially with large airplanes the frames of which tend to be relatively light.

The stress analysis of fuselages with four longerons can be based on the method developed for wings with two spars and ribs that are flexible in shear (see Section 2). With fuselages having more longerons the application of the analysis developed by Ebner requires extensive simplification of the structure and even then the number of longerons should not exceed twelve. Fuselages with a great many longitudinal stringers will probably be schematized better by assuming longitudinals and frames, the stiffness of which is distributed continuously over the circumference and along the axis respectively. The relations of stress and strain for these orthotropic tubes an with circular cross section have been determined. The external loads at the end sections of the homogeneous tube have been expanded in Fourier series; the stresses and the deflections caused by each component of the load have been expressed in these components by explicit formulas. These formulas may serve as the starting point for calculations on the stress distribution of shells, which have a less homogeneous structure along their longitudinal axis and which are loaded along their entire length.

6. *Qualitative Pictures of Stresses in Wings and Fuselages.* The elementary beam theory applied to wings and fuselages gives stresses com-

plying with the equilibrium conditions for the cross section as a whole. However owing to discontinuities in the structure or by local application of external loads the conditions of equilibrium of structural elements and the conditions of compatibility of deformations will not be satisfied by "elementary" stresses. These circumstances give rise to "secondary" stresses, which occasionally may be of primary importance. In many cases the knowledge of the magnitude of these stresses is not needed or may be acquired in a later stage of designing. Then it may be useful to know in which points of the structure the stresses are increased by such effects. A number of cases occurring in wing and fuselage shell structures have been considered qualitatively and the results have been laid down in diagrams of the stress distributions.

7. *General Instability of Longitudinally and Laterally Stiffened Cylindrical Shells under Axial Compression.* Fuselage shells stiffened by stringers and frames may fail at the compression side by "general instability," a type of buckling in which the frames as well as the stringers are distorted. This type of failure is more critical with weaker frames.

In order to simplify the problem the axially loaded cylinder of infinite length has been considered.

If the wave length of the buckled cylinder comprises several stringer spacings tangentially and several frame spacings axially, the action of the stiffeners upon the frames and the action of the frames upon the stiffeners will be practically the same when the system of stringers and frames is replaced by a continuous system of axial and circumferential stiffeners. Thus the structure is transformed into an orthotropic shell. The first part of the investigation deals with this.

Usually the stringers are closely spaced indeed; the frame spacing however can be of the same order of magnitude as the half-wave length. Then it is not to be expected that the orthotropic shell will yield a reliable result. Therefore the second part of the investigation deals with a cylinder stiffened by uniformly distributed longitudinals and by regularly spaced frames.

In both systems the stiffeners are assumed to possess bending and torsional stiffness. Their neutral axis has some eccentricity with respect to the plane of the skin. Stiffeners and frames are interconnected such that the material situated in the line normal to the neutral lines of stiffener and frame remains upon this normal in the distorted position of the neutral lines. The skin is supposed to carry shear stresses only; in so far as normal stresses are taken up by the skin a corresponding effective width of skin is included in the cross section of the stiffening members.

In regard to the orthotropic cylinder the conditions of equilibrium

for an arbitrary deformation adjacent to the unbuckled state have been formulated. These equations have been solved for the cylinder of infinite length. The axial stress at which buckling is possible depends upon the number of waves over the circumference (n) and the wave length in axial direction (l). The complexity of the structure necessitates the introduction of a great number of parameters; they have been defined such that they all represent nondimensional figures of the order of unity; in this way the process of eliminating high-order terms was made clearer and the buckling form, yielding the smallest critical stress, could be determined quite easily.

There are three main groups of buckling forms: (1) short waves axially and long waves circumferentially; (2) long waves axially and intermediate wave length circumferentially; (3) short waves axially and circumferentially. The critical loads for group 1 and 2 could be given in explicit formulas; the minimum critical load in the third group is to be determined implicitly out of a function of n and l. Usually the smallest buckling load falls into the third group.

It may be emphasized that the eccentricity of the stiffeners with respect to the plane of the skin is a factor of major importance for the magnitude of the critical stress in the third group. Internal stiffening lowers the critical stress, sometimes to as much as one third of the value corresponding to stiffening in the plane of the skin. Outside stiffening would increase the critical stress.

The shell with regularly spaced frames represents between two successive frames a particular case of an orthotropic cylinder: the circumferential stiffeners are missing. The conditions of equilibrium of this orthotropic shell are known from the preceding investigation; their integration yields the displacements containing eight integration constants. With each bay of the cylinder eight integration constants are introduced.

The consistency of displacements at each side of a frame and of the deflections of the frame under the loads imposed on it by the skin and stiffeners gives eight equations between the integration constants of successive bays. All these sets of equations constitute a recurrent linear system of equations in the integration constants. The general solution of these equations is given; to any combination of axial load and wave number over the circumference correspond eight longitudinal modes of buckling. For a cylinder composed of m bays the stability determinant of the $8m$th degree is reduced to a determinant of the 8th degree. Though there are no further essential difficulties the practical evaluation of the solution is highly cumbersome. Usually the cylinder will be so long that the influence of the end conditions will be negligible. Then the

buckling load of the cylinder of infinite length gives a good approximation of the actual buckling load. Therefore the solution is completed for this case. Formulas and graphs are given for the calculation of the buckling load.

It may be stated that the error caused by the uniform distribution of the frames is no more than 2 per cent if the longitudinal half-wave length exceeds 2 frame spacings; the error increases up to 10 per cent if the ratio of half wave length and frame spacing approaches 1.5. For smaller wave lengths the theory of the orthotropic cylinder does not apply and must be replaced by the theory for cylinders with regularly spaced frames.

Column failure of the longitudinals between the frames may occur, when the tensional stiffness of the frames exceeds a particular limit.

8. *The Stability of Sandwich Strips and Plates.* The investigation deals with plates composed of two thin plates and an intermediate thick layer of a much softer material than that of the plates. The soft layer has to have a stabilizing effect on the thin outer plates if the latter are loaded by compressive stresses.

A theoretical investigation of the stability of such compound strips under axial load has been carried out by Gough, Elam, and de Bruyne under the assumptions that the axial load is completely taken by the outer plates and that the extension and compression of the outer plates are negligible compared with those of the inner layer. This latter assumption proves to give faulty results if the wave length of the buckled strip is long compared with the thickness of the plate; for instance, on the basis of the second assumption the ordinary Euler load never will occur.

Therefore the above-mentioned investigation was repeated after dropping the second assumption. The soft layer in this investigation was considered to be a homogeneous isotropic elastic material loaded two-dimensionally; no simplifying assumptions have been incorporated.

The problem of the instability of plates and shells of the sandwich type of construction is more involving, as the soft layer in the buckled condition is loaded three-dimensionally. In order to simplify the mechanism the behavior of this soft layer was schematized. The soft layer was replaced by rigid elements of negligible thickness normal to the outer surface and connected to the outer plates; these members are interconnected by a two-dimensionally isotropic elastic material. In this way all displacements and stresses in the soft layer can be expressed in the displacements of the outer plates.

This scheme proved to give an extremely good approximation of the above-mentioned results of the exact theory for compound strips. So this scheme could be adopted in attacking the problem of the buckling

of plates. The general stability equation of compound plates has been deduced and its solution has been given for the case of the rectangular plate loaded by normal stresses parallel to the edges.

IV. Books

1. *Technische Dynamik by C. B. Biezeno and R. Grammel.* This book on general elasticity appeared just before the outbreak of the war. As far as the author of the present article knows, no American review of the book has appeared. The book has, however, been photo offset in the United States (in a limited number of copies) "in the public interest" on behalf of the Alien Property Custodian. The reviewer is proud indeed that in this way he and his collaborator were given the opportunity to contribute something—as modest as it may be—to the general cause of liberty and freedom that has been so pre-eminently furthered by the American nation.

As to the contents of the book it seems best to quote the English review, written by L. M. Milne-Thomson (*Nature*, Feb. 1941), the more so because this authority reproduces the views and aims of the authors, laid down in the preface of the book, in a perfect way.

"In introducing the student to technical mechanics either by lectures or textbook it is usual to lay stress on those simplified problems which illustrate the principles. The more difficult problems in the form in which they face the mechanical engineer, even if touched upon, do not receive the detailed consideration which their importance not only warrants but demands. The present book is designed to form a continuation of the introductory course and may be described as a treatise on technical applications of elastomechanics for advanced students.

"According to Kirchhoff's definition, mechanics consists of kinematics, or the study of motion and of dynamics, or the study of forces. In this sense dynamics can be divided into statics, the geometry of forces and the theory of equilibrium, and into kinetics, the theory of forces not in equilibrium and the relations between force and motion. For example, an oscillation problem is a dynamical one consisting of a statical part, namely, the investigation of certain elastic properties, and a kinetic part, the calculation of the frequencies. The looser current usage takes dynamics as a synonym of kinetics, and while still describing the oscillation problem as dynamical, neglects the statical part, which is often the more interesting.

"The authors use dynamics in the sense defined by Kirchhoff, and have accordingly investigated both the statical and kinetic parts of a variety of problems concerning rods, shafts, rings, springs, plates, shells and their combinations, keeping in view that any such problem is only

worth solving when it has a practical application, and can only be described as solved when a detailed solution in numbers is forthcoming without recourse to too prohibitive numerical calculations. It must not be inferred that the book is a wearisome list of numerical results. On the contrary, great emphasis has been laid on methods of solution: in fact a chapter of 100 pages is devoted entirely to such methods. In the applications, solutions are not merely outlined but are given in full as the engineer would have to work them, and with the choice of method which the authors consider to be the best.

"The text is divided into four sections: fundamental theory, 225 pages; single parts of mechanisms, 400 pages; the steam turbine, 220 pages; internal combustion engines, 210 pages.

"The first section contains an exposition of the mathematical theory of elasticity as applied to isotropic bodies which obey Hooke's law; indeed phenomena outside the elastic limit are not considered in the sequel. This account of the theory is well and carefully written. It is refreshing to see the authors emphasize the strict limitations of the theorem of unique solution of elastic problems, in that in actuality finite (but small) strains and finite (but not small) stresses represent only approximations to the conditions in which the classical equations are valid. A simple illustration is Euler's strut at the first critical load. Another welcome feature is the inclusion of the proof of de Saint Venant's principal based on that given by Zanaboni (*Atti Lincei*, 25; 1937). With regard to the general theorems of elasticity it is to be regretted that the authors have not given the vector formulation which makes the physical implications much easier to grasp.

"The remaining three sections consist of applications of elasto-mechanical theory with special emphasis on the needs of machine construction. Special prominence is given throughout to critical loads and values.

"The authors remark in the preface that the chapters have been arranged so far as possible so that each can be read independently. This has been achieved within limitations, but the text requires close attention on the part of the reader, who is assumed to be proficient in elementary mechanics and to have a fairly extensive knowledge of mathematics.

"The book is a mine of detailed information such as could probably not be found in collected form elsewhere (for example there are 89 pages on the loaded rod) and it should therefore prove to be of great value."

2. *Plasticiteitsleer by F. K. Th. van Iterson.* Starting from the well-known idealized (σ, ϵ) diagram for metals in which σ remains constant after having reached its yield value, and neglecting as usual the elastic

deformations with respect to the much larger plastic ones, the author restricts himself in the first half of his book to the two-dimensional problem. A survey is given of the work done by Prandtl, von Mises, Hencky, Nadai and others and several problems scattered over manifold periodicals are brought together. The other part of the book is devoted to the three-dimensional problem under assumption of the Maxwell-Huber-Hencky hypothesis. In this part the author develops personal ideas on the subject, which are put to the test of his own experiments and the opinions of others. A series of articles on the same subject by the same writer appeared in the *Proceedings of the Royal Academy of Sciences* at Amsterdam: Prof. ir. F. K. Th. van Iterson, Bijdrage tot de Plasticiteitstheorie, *Verslagen Nederland. Akad. Wetensch. Afdeel. Natuurkunde*, Vol. LII, No. 1 (1943); Les déformations plastiques près des entailles, Vol. XLV, No. 2 (1942); La Pression du toit sur le charbon près du front, dans les exploitations par tailles chassantes, Vol. XLII, No. 2 (1939); Vol. XLIII, Nos. 2, 3, 4 (1940), Vol. XLIV, Nos. 2, 3 (1941).

Bibliography

I. Publications of the Laboratory for Applied Mechanics of the Technische Hoogeschool at Delft

(Prof. Dr. ir. C. B. Biezeno, Prof. Dr. ir. J. J. Koch)

A. Elastic Stability

1. Koiter, W. T., Over de stabiliteit van het elastisch evenwicht (On the stability of elastic equilibrium), Doctor's thesis, Amsterdam, 1945.
2. Biezeno, C. B., and Koch, J. J., On the buckling of a thin-walled circular tube loaded by pure bending, I. and II., *Proc. K.N.A.W.* (*Koninklijke Nederlansche Akademie van Wetenschappen*, vol. XLIII (1940)).
3. Biezeno, C. B., and Koch, J. J., The generalized buckling problem of the circular ring, *Proc. K.N.A.W.*, vol. XLVIII (1945).
4. Biezeno, C. B., and Koch, J. J., The circular ring under the combined action of compressive and bending loads, *Proc. K.N.A.W.*, vol. XLIX (1946).
5. Biezeno, C. B., and Koch, J. J., On the nonlinear deflection of a semicircular ring, clamped at both ends, *Proc. K.N.A.W.*, vol. XLIX (1946).
6. Biezeno, C. B.; and Koch, J. J., Over het niet-lineair verband tusschen de doorbuiging ende belastende kracht van een in zign beide uiteinden ingeklemden halfcirkelvormigen ring (On the nonlinear deflection of a semicircular ring, clamped at both ends), *De Ingenieur*, 0.3, 1946.
7. Wijngaarden, A. van, Large distortions of circular rings and straight rods, *Proc. K.N.A.W.*, vol. XLIX (1946).
8. Haringx, J. A., On the buckling and the lateral rigidity of helical compression springs, *Proc. K.N.A.W.*, vol. XLV (1942).

B. Plates and Shells

1. Schulz, K. J., Over den spanningstoestand in doorboorde platen (On the state of stress in perforated plates), Doctor's thesis, Delft, 1941.
2. Schulz, K. J., On the state of stress in perforated strips and plates, *Proc. K.N.A.W.*, vol. XLV (1942), vol. XLVIII (1945).
3. Biezeno, C. B., and Koch, J. J., Some explicit formulas of use in the calculation of arbitrary loaded thin-walled cylinders, *Proc. K.N.A.W.*, vol. XLIV (1941).
4. Biezeno, C. B., and Koch, J. J., The effective width of cylinders, periodically stiffened by circular rings, *Proc. K.N.A.W.*, vol. XLVIII (1945).
5. de Beer, C., Over cirkelvormige platen aan den omtrek in de hoekpunten van een regelmatigen veelhoek ondersteund en over de oppervlakte rotatorisch symmetrisch belast (On circular plates, supported in a number of points (≥ 3) regularly distributed along its boundary and rotatory-symmetrically loaded), *De Ingenieur*, 1946.

C. Miscellaneous Papers

1. Koiter, W. T., Berekening van verrend gesteunde balken (On elastically supported beams), *De Ingenieur*, 1940.

2. BIEZENO, C. B., On a special case of bending, *Proc. K.N.A.W.*, vol. XLV (1942).
3. BIEZENO, C. B., Critical speeds of rotating shafts, *Proc. K.N.A.W.*, vol. XLIII (1940).
4. BIEZENO, C. B. and KOCH, J. J. On the elastic behaviour of the so-called "Bourdon" pressure gage, *Proc. K.N.A.W.*, vol. XLIV (1941).
5. DE BEER, C., Over de spanningstoestanden in prismatische assen met door twee paar orthogonale cirkelbogen begrensde doorsneden (On the torsion of prismatic beams the cross section of which is bounded by two pairs of orthogonal circular arcs), *Proc. K.N.A.W.*, vol. XLVIII (1945).
6. WIJNGAARDEN, A. VAN, Eenige toepassingen van *Fourier*-integralen op elastische problemen (Some applications of *Fourier*-integrals with respect to elastic problems), Doctor's thesis, Delft, 1945.
7. BIEZENO, C. B., and BOTTEMA, O., The convergence of a specialised iterative process in use in structural analysis, *Proc. K.N.A.W.*, vol. XLIX.
8. BURGERS, J. M., SAAL, R. N. J., and BIEZENO, C. B., Grondslagen voor een nomenclatuur der deformaties (A draft-nomenclature for deformations), *Proc. K.N.A.W.*, vol. XVIII.

D. Experimental Work

1. BIEZENO, C. B. and KOCH, J. J., Enkele experimenteele gegevens omtrent de gereduceerde lengte van op wringing belaste assen van niet constante middellijn (The "reduced" length of (cylindrical) twisted shafts of variable cross section), *De Ingenieur*, 1939.
2. BIEZENO, C. B. and KOCH, J. J., Enkele experimenteele gegevens omtrent flenskoppelingen van op wringing belaste assen (Some experimental data concerning flange couplings), *De Ingenieur*, 1941.
3. BOITEN, R. G., and BIEZENO, C. B., Sterkte en stijfheid van een op wringing belaste door een diepe spiegleuf verzwakte as van cirkelvormige dwarsdoorsnede (Strength and stiffness of a twisted cross section weakened by a deep keyway with sharp corners), *De Ingenieur*, 1945.
4. BIEZENO, C. B., De experimenteele bepaling van de in een scheepsschroef optredende spanningen (Experimental determination of the stresses occurring in a ship-propeller), *De Ingenieur*, 1945.
5. VAN MANSUM, A. A., KOCH, J. J., and BIEZENO, C. B., Over de optische bepaling van de spanningsconcentratie in afrondingshoeken van vlakke staven met verspringende breedte (Optical determination of stress concentrations in fillets of flat bars of constant thickness and sharp varying width), *De Ingenieur*, 1941.
6. KOCH, J. J. and BIEZENO, C. B., Het kerfgetal β bij assen met verspringende middellijn (Effect of change in section of rotating shafts on fatigue properties), *De Ingenieur*, 1945.
7. KOCH, J. J., and BIEZENO, C. B., Over een verkorte methode ter bepaling van den kerffactor β bij wisselende buig- en wringbelasting (An abbreviated method for the determination of the factor β, mentioned in the preceding section as well for bending as for torsional stress cycles), *De Ingenieur*, 1940.
8. HUYDTS, L. H. M., KOCH, J. J., BOURGONJON, L. R., and ESMEIJER, W. L., Een apparatuur van groote gevoeligheid voor het electrisch meten van mechanische grootheden (A highly sensitive electrical apparatus for the magnification, reproduction and measurement of mechanical quantities occurring with vibratory phenomena), *De Ingenieur*, 1946.

II. Publications of the "Nederlandsche Centrale Organisatie voor Toegepast Natuurwetenschappelijk Onderzoek" (T.N.O.). Afdeelingen Trillingsonderzoek en Photo-elasticiteit (Dutch Central Institute for Technical Scientific Research; Vibrations and Photoelasticity) at the Hague

1. Esmeijer, W. L., Bijdrage tot de theorie van stootmetingen met behulp van trillingsmeetinstrumenten (Experimental determination of the time-integral of an impact with the aid of a vibrating system), *Rept.* 1, of the Dept. of Vibrations 1945.
2. Esmeijer, W. L., Enkele gegevens over het dynamische gedrag van een oneindig langen elastisch ondersteunden balk onder invloed van een geconcentreerde stootende belasting (The infinite, elastically supported beam, subject to an impact load), *Rept.* 3, of the Dept. of Vibrations 1945.
3. Esmeijer, W. L., Een stelling over de laagste eigenwaarde van eenige eigenwaardeproblemen (The smallest characteristic number of certain "Eigenwert" problems), *Rept.* 5, of the Dept. of Vibrations 1946.
4. Willemze, F. G., Proefneming met polystyreen als foto-elastisch materiaal (A comparative study about the main photo-elastic properties of different materials), *Rept. of the Dept. of Photoelasticity*, IV, 1945.
5. Willemze, F. G., De invloed van de grootte van den afrondingsstraal op de spanningsconcentratie bij twee loodrecht op elkaar staande staven die axiaal belast worden (On the stress concentration in the corners of a cross, the rectangular branches of which have equal width), *Rept. of the Dept. of Photoelasticity*, V, 1945.
6. Willemze, F. G., and Boiten, R. G., Voorloopig verslag van de metingen aan het profiel van den verkeerstunnel te Velsen (Photoelastic determination of the stresses occurring in a tunnel, projected between the Banks of the "Noordzee Kanaal," connecting Amsterdam with the North Sea), *Rept. of the Dept. of Photoelasticity*, IX, 1945.
7. Willemze, F. G., Over de bepaling van het verloop der randspanning in hoekverbindingen (Stress concentrations in corner joints), *Rept. of the Dept. of Photoelasticity*, VIII, 1945.

III. Publications of the Nationaal Luchtvaartlaboratorium (N.L.L.) (Aeronautical Research Labor.) at Amsterdam

1. Van der Neut, A., and Floor, W. K. G., Stresses of the second order in the skin and ribs of wings in bending, *N.L.L. Rept.* S 217.
2. Stress and strain in shell wings with two spars.
   a. Koiter, W. T., Van der Neut, A., The effect of elastic rib-shear on stresses in two-spar-wings with stressed skin, *N.L.L. Rept.* S 275.
   b. Van der Neut, A., The stress distribution in wings with two non-parallel spars interconnected by elastically deformable ribs and skin, *N.L.L. Rept.* S 251.
   c. Plantema, F. J., and Van der Neut, A., The stress distribution in wings with two non-parallel torsionally rigid spars, interconnected by elastically deformable ribs and skin, *N.L.L. Rept.* S 279.
   d. Plantema, F. J., and Van der Neut, A., The distortions of wings with two spars, *N.L.L. Rept.* S 297.
   e. Van der Neut, A., Manual for the stress analysis of shell-wings with two spars, *N.L.L. Rept.* S 250.

3. Effective width.
   a. KOITER, W. T., The effective width of flat axially loaded strips of sheet beyond the buckling stress for various edge conditions, *N.L.L. Rept.* S 287.
   b. VAN DER NEUT, A., and FLOOR, W. K. G., The effective width of flat sheet supported by longitudinal stiffeners with open section, *N.L.L. Rept.* S 266.
4. KOITER, W. T., The tension field for stresses beyond the buckling stress, *N.L.L. Rept.* S 295.
5. VAN DER NEUT, A., The effect of the flexibility of fuselage frames on the stress distribution in fuselage shells, *N.L.L. Rept.* S 296.
6. VAN DER NEUT, A., and PLANTEMA, F. J., Qualitative pictures of stresses in wings and fuselages, *N.L. Rept.* S 282, S 293.
7. VAN DER NEUT, A., General instability of longitudinally and laterally stiffened shells under axial compression, *N.L.L. Rept.* S 255, S 256.
8. VAN DER NEUT, A., The stability of sandwich-strips and plates, *N.L.L. Rept.* S 284, S 286.

IV. Books

1. BIEZENO, C. B., and GRAMMEL, R., *Technische Dynamik*, Springer, Berlin, 1939, 1056 pp.
2. VAN ITERSON, F. K. T., *Plasticiteitsleer* (French and Dutch), H. Vaillant-Carmanne, Liege (Belgique) and N. V. Uitgeversmij. A. E. E. Kluwer, Deventer (Holland) 1945, 183 pp.

A Mathematical Model Illustrating the Theory of Turbulence

By J. M. BURGERS

Technical University, Delft, Holland

CONTENTS

I. Introduction

The application of methods of statistical analysis and statistical mechanics to the problem of turbulent fluid motion has attracted much attention in recent years. From the theoretical side we are faced with the necessity of investigating a complicated system of nonlinear equations, in order to find out enough about the properties of the solutions of these equations that insight can be obtained into the various patterns exhibited by the field and that data can be derived concerning the relative frequencies of these patterns, in the hope that in this way a basis may be found for the calculation of important values. The difficulties encountered are of a twofold nature: in part they are connected with the complicated geometrical character of the hydrodynamical equations (vectorial character of the velocity, condition imposed by the equation of continuity, properties of vortex motion); in part they are dependent upon the presence of nonlinear terms, containing derivatives of the first order of the velocity components, along with derivatives of the second order multiplied by the very small coefficient of viscosity. The latter feature in

particular is responsible for a number of important characteristics of turbulence, among which are prominent those connected with the balance of energy and with the appearance of dissipation layers. These layers (boundary layers along the walls and similar phenomena in the interior of the field) play an important part in the energy exchange, as they represent the main regions where energy is dissipated.

These features, together with the properties of the spectrum of the turbulent motion (which is obtained when the field is analyzed into a series of elementary components), the transfer of energy through the spectrum, and the appearance of a practical limit to this spectrum (responsible for the finite value of the total dissipation), all can be elucidated with the aid of a system of mathematical equations much simpler than those of hydrodynamics. It is the object of the following pages to discuss these equations, which in a sense form a mathematical model of turbulence, and to indicate the bearing of the results obtained upon the hydrodynamical problem.[1]

II. The Equations Describing the Model System

Although the quantities occurring in our equations are abstract mathematical variables and parameters, we shall indicate them by names that show their analogies to the variables of hydrodynamics. Two dependent variables, $U(t)$ and $v(y,t)$, are introduced, representing velocities. The first one will be the analogue of the primary or mean motion in the case of a liquid flowing through a channel; in the model it is a function of the time only. The other variable v represents the secondary motion; when it differs from zero we shall say that there is *turbulence* in the system, even in a case where v should be independent of the time. The independent variable y occurring in v plays the part of the coordinate in the direction of the cross dimension of the channel. In the case with which we shall be primarily concerned the domain of y extends from 0 to b, and v

[1] References: (I) J. M. Burgers, Mathematical examples illustrating relations occurring in the theory of turbulent fluid motion, *Verhandel. Kon. Nederl. Akad. Wetenschappen Amsterdam, Afdeel. Natuurkunde (1st Sect.)*, **17**, No. 2, 1–53 (1939); (II) Application of a model system to illustrate some points of the statistical theory of free turbulence, *Proc. Acad. Sci. Amsterdam*, **43**, 2–12 (1940); (III) On the application of statistical mechanics to the theory of turbulent fluid motion. A hypothesis which can serve as a basis for a statistical treatment of some mathematical model systems, *Proc. Acad. Sci. Amsterdam*, **43**, 936–945, 1153–1159 (1940); (IV) Beschouwingen over de statistische theorie der turbulente stroming, *Nederl. Tijdschr. Natuurkunde*, **8**, 5–18 (1941).

These papers will be referred to as I, II, etc.

is subjected to the boundary condition that it must vanish at both ends.[2] Later on (in Sections VIII–IX) the case of an infinite domain for y will be considered.

The equations have the form:

$$b\frac{dU}{dt} = P - \frac{\nu U}{b} - \frac{1}{b}\int_0^b dy\, v^2 \tag{1}$$

$$\frac{\partial v}{\partial t} = \frac{U}{b}v + \nu\frac{\partial^2 v}{\partial y^2} - 2v\frac{\partial v}{\partial y}. \tag{2}$$

The quantities P and ν are constant parameters. P is the analogue of an exterior force acting upon the primary motion. The terms with ν represent frictional effects, in the case of the primary motion simply proportional to U/b, and in the case of the secondary motion proportional to the second derivative of v with respect to y. It is not necessary to use the same coefficient ν for both, but nothing is gained by introducing different coefficients.

The terms of the second degree in v, which in view of what has been said in section I form an essential feature of the system, have been chosen in such a way that an equation can be formed describing the balance of energy. We multiply (1) by U and (2) by v; the latter is integrated with respect to y from 0 to b, having regard to the boundary conditions, and added to the first one. Several terms cancel and we obtain:

$$\frac{d}{dt}\left[\frac{bU^2}{2} + \int_0^b dy\,\frac{v^2}{2}\right] = PU - \frac{\nu U^2}{b} - \nu\int_0^b dy\left(\frac{\partial v}{\partial y}\right)^2. \tag{3}$$

The quantity between [ ] in the left-hand member is interpreted as the kinetic energy of the motion; the equation shows that this energy increases in consequence of work PU being performed by the exterior force P upon the principal motion U, while at the same time there is dissipation of energy as a result of the frictional effects. The term Uv/b in equation (2) introduces a transmission of energy from the primary motion to the secondary motion; this transmission, being an internal feature of the system in consequence of a compensating term in equation (1), does not appear in the total balance of energy as given by (3). In the model this transmission has been made to depend upon the value of U itself, and

[2] In the original paper, referred to as (I) in footnote 1, the breadth b of the domain had been taken equal to unity. Further the minus sign introduced into Equation (4) had not been used, which results in a difference of sign in the ξ_n (and in the γ_n of Section XIII).

not upon a gradient of the type dU/dy, as is the case with the equations of hydrodynamics. As will become evident from further developments the last term of equation (2) is responsible for an exchange of energy between the various components into which the secondary motion can be resolved; this likewise is an interior process, which does not appear in the total balance.

The equations can be brought into a different form by introducing a Fourier series for v. We put:

$$v = -\sum_{n=1}^{\infty} \xi_n \sin\left(\frac{\pi n y}{b}\right) \tag{4}$$

(the minus sign has been used in order to simplify some further expressions). The coefficients ξ_n in general will be functions of the time. This expression satisfies the boundary conditions for v. Equations (1) and (3) now take the forms:

$$b\frac{dU}{dt} = P - \frac{\nu U}{b} - \frac{1}{2}\sum \xi_n^2 \tag{5}$$

$$\frac{d\xi_n}{dt} = \left(\frac{U}{b} - \frac{\nu\pi^2 n^2}{b^2}\right)\xi_n + \frac{\pi n}{b}\left(\frac{1}{2}\sum_{k=1}^{n-1} \xi_k \xi_{n-k} - \sum_{k=1}^{\infty} \xi_k \xi_{n+k}\right). \tag{6}$$

The energy equation (3) at the same time becomes:

$$\frac{d}{dt}\left\{\frac{bU^2}{2} + \frac{b}{4}\sum \xi_n^2\right\} = PU - \frac{\nu U^2}{b} - \frac{\nu\pi^2}{2b}\sum n^2 \xi_n^2. \tag{7}$$

It is seen that each term $(b/4)\xi_n^2$ can be considered as the energy associated with a component of the spectrum, while $(\nu\pi^2 n^2/2b)\xi_n^2$ is the dissipation associated with that component. Whereas in the energy equation and also in equation (5) the terms due to the various components of the spectrum appear in simple sums and thus are separated, the presence of the terms of the second degree in (6) insures that these components are not independent of each other, so that when one has been excited all the others of necessity will come into existence as well. In the language of hydrodynamics the terms of the second degree represent the mechanism by which small eddies are produced from large ones.

A slightly more general model, in which the secondary motion is represented by two variables, will be considered in Sections XIII and XIV.

III. Laminar Solution of the System (1), (2)

The equations (1) and (2) are rigorously fulfilled by the values:

$$U = \frac{Pb}{\nu}; \qquad v = 0. \tag{8}$$

In this solution turbulence is absent. To investigate its stability small values can be given to v, U being kept fixed. The discussion is effected most easily with the aid of equation (6), in which the terms of the second degree can be neglected for infinitely small values of v, leaving:

$$\frac{d\xi_n}{dt} = \left(\frac{U}{b} - \frac{\nu\pi^2 n^2}{b^2}\right)\xi_n. \tag{9}$$

When $U < \nu\pi^2/b$ the real part of the cofactor of ξ_n in the right-hand member is negative for every value of n; hence every ξ_n will be damped, so that the laminar solution is stable. On the other hand when $U > \nu\pi^2/b$, one or more of the ξ_n will increase exponentially; the laminar solution is unstable and a new solution will appear in which v is different from zero. As mentioned before, the presence of terms of the second degree in (6), which terms cannot be neglected for finite values of v, means that not only those ξ_n for which $U > \nu\pi^2 n^2/b$ but all ξ_n will become excited.

As no density factor has been introduced, the quantity Ub/ν plays the part of Reynolds number for the system. It will be denoted by Re; its critical value is: $Re_{crit} = \pi^2$.

IV. Stationary Turbulent Solutions of Equation (2)

When U is considered as a constant, equation (2) permits solutions for v that are independent of the time. With these solutions it is possible also to satisfy equation (1), provided the proper value is given to the exterior force P. The stationary solutions of equation (2) can be expressed in exact form by means of quadratures. They form two sets, related by the formula: $v_+(y) = -v_-(b - y)$, so that the two sets are antisymmetrical with respect to each other. In each set the solutions are characterized by a number m, which runs from unity to a maximum, determined by the largest integer contained in $\sqrt{Ub/\nu\pi^2} = \sqrt{Re/Re_{crit}}$. The solution with the index m has $m - 1$ zeros between $y = 0$ and $y = b$. There is a certain resemblance to the series of eigensolutions of a linear differential equation of the second order, satisfying the condition of vanishing at both boundaries; the part of the parameter (which in that case can take an infinite series of eigenvalues) in the case of equation (2) is assigned to the amplitude of the solution, which becomes smaller and

smaller as m increases; the set of solutions in the case of (2) appears to be finite.

The full expressions of the stationary solutions, which have been given elsewhere,[3] are not necessary for our present purpose. Their most interesting property is that when Re is large and we restrict ourselves to low values of m, *e.g.*, $m = 1$ and $m = 2$, the domain $0 \leq y \leq b$ can be divided into (a) comparatively broad regions where the term $\nu(\partial^2 v/\partial y^2)$ can be neglected and equation (2) (with $\partial v/\partial t = 0$) approximately reduces to:

$$2v\frac{\partial v}{\partial y} - \frac{U}{b}v = 0, \tag{10}$$

and (b) extremely narrow regions in which the term Uv/b can be neglected in comparison with the other two, so that there remains:

$$\nu\frac{\partial^2 v}{\partial y^2} - 2v\frac{\partial v}{\partial y} = 0. \tag{11}$$

The solution of (10) is:

$$v = \frac{Uy}{2b} + C, \tag{12}$$

and that of (11):

$$v = -A \operatorname{tgh}\left\{\frac{A(y - B)}{\nu}\right\}, \tag{13}$$

A, B, and C being constants. These constants must be determined in such a way that the solutions fit together without discontinuities in v, and that the boundary conditions at $y = 0$ and $y = b$ are satisfied. Important special cases can be represented with sufficient approximation by:

$$v = \frac{U}{2}\left(\frac{y}{b} - \operatorname{tgh}\frac{Uy}{2\nu}\right) \tag{14a}$$

$$v = \frac{U}{2}\left\{\frac{y}{b} - 1 + \operatorname{tgh}\frac{U(b - y)}{2\nu}\right\} \tag{14b}$$

$$v = \frac{U}{4}\left\{\frac{2y}{b} - 1 - \operatorname{tgh}\frac{Uy}{4\nu} + \operatorname{tgh}\frac{U(b - y)}{4\nu}\right\}. \tag{14c}$$

In the first case we have a region of steep change of v, comparable to a boundary layer, in the neighborhood of $y = 0$; in the second case such a region is found in the neighborhood of $y = b$; in the third case there are boundary layers along both walls. Solutions with regions of steep

[3] See (I), pp. 18–24.

change of ν, *i.e.*, with dissipation layers, in the neighborhood of an interior point of the domain likewise can be obtained (for $m = 2$ and for a number of higher values); this will be seen also from the considerations of section VII.

V. Spectrum of the Stationary Turbulent Solutions

When the solutions (14a)–(14c) are developed into Fourier series, the following values are obtained for the coefficients:

$$\xi_n = \frac{\pi\nu}{b \sinh (\pi^2 n\nu/Ub)} \tag{15a}$$

$$\xi_n = \frac{(-1)^n \pi\nu}{b \sinh (\pi^2 n\nu/Ub)} \tag{15b}$$

$$\xi_n = \begin{cases} \dfrac{2\pi\nu}{b \sinh (2\pi^2 n\nu/Ub)} & (n \text{ even}) \\ 0 & (n \text{ odd}) \end{cases}. \tag{15c}$$

In particular taking the first case (as this is the simplest and most typical one), it is found that for $n \ll Re$:

$$\xi_n = \frac{U}{\pi n}, \tag{16a}$$

whereas for $n > Re$:

$$\xi_n = \frac{2\pi\nu}{b} e^{-\pi^2 n\nu/Ub}. \tag{16b}$$

Hence in the spectrum the *energy per component* $\frac{1}{4}b\xi_n^2$ appears to be proportional to n^{-2} so long as $n \ll Re$, while this energy decreases exponentially when $n > Re$. It follows that the total energy can be calculated with sufficient accuracy from the approximate expression (16a), as in fact the total energy depends upon the first few components only. Its amount is $bU^2/24$; this amount is not influenced by the value of the viscosity. The same applies to the value of P, which (neglecting the term $\nu U/b$) is given by:

$$P = \frac{1}{2}\sum \xi_n^2 = \frac{U^2}{12}. \tag{17}$$

The latter result shows that when turbulence has set in, the "resistance" increases proportionally to the square of U and that this resistance is dependent upon the first few components of the turbulence only.

The *dissipation per component* (or, in other terms, per degree of freedom of the system) has a constant value $\frac{1}{2}\nu U^2/b$ as long as $n \ll Re$, while it decreases nearly exponentially when $n > Re$. As the number of

degrees of freedom is unlimited the application of (16a) to all components would make the total dissipation infinite. The actual value of the total dissipation is dependent upon the extent of the spectrum before one arrives at the part to which applies formula (16b), which requires the number n to be of the order Re. The presence of a practical limit to the main part of the spectrum [as determined by (16a)] thus is of the utmost importance in fixing the total dissipation. It will be evident at the same time that the total dissipation embraces much more of the elementary components of the turbulence than does the total energy.

The magnitude of the total dissipation is calculated most easily from the integral $\nu \int_0^b dy(\partial v/\partial y)^2$, which occurs in the energy balance (3); for the case represented by formula (14a) it has the value $U^3/12$, corresponding to an effective number of components $N = Ub/6\nu = Re/6$.

Similar results can be obtained for the other cases. Formula (15c) shows that in certain cases a number of components of the spectrum will be zero.

The results obtained are an immediate consequence of the form of equation (2), in which a term of the second degree containing the product of v with its derivative of the first order is combined with a derivative of the second order multiplied by a very small constant. This will become still more clear from a discussion of the nonstationary solutions of equation (2).

VI. Additional Remarks Concerning the Spectrum of the Stationary Solutions

It is of interest to note that the expression (16a) gives an exact solution of the infinite system of equations:

$$0 = \frac{U\xi_n}{b} + \frac{\pi n}{b}\left(\frac{1}{2}\sum_{k=1}^{n-1}\xi_k\xi_{n-k} - \sum_{k=1}^{\infty}\xi_k\xi_{n+k}\right), \tag{18}$$

which is obtained from (6) (with $d\xi_n/dt = 0$) when ν is replaced by zero. The solution is not unique, as other solutions can be obtained in which the ξ_n periodically change sign, or in which, *e.g.*, the ξ_n of odd order are zero.

For large values of n the term with ν in equations (6) will be much more important than the term $U\xi_n/b$ (and presumably also than the term $d\xi_n/dt$ if this should not be rigorously zero). It is useful therefore to observe that the infinite system:

$$0 = -\frac{\nu\pi^2 n^2\xi_n}{b^2} + \frac{\pi n}{b}\left(\frac{1}{2}\sum_{k=1}^{n-1}\xi_k\xi_{n-k} - \sum_{k=1}^{\infty}\xi_k\xi_{n+k}\right) \tag{19}$$

admits an asymptotic solution which can be obtained by assuming:

$$\xi_m = \beta\lambda^m \qquad \text{for} \qquad m > M \tag{20}$$

where M is some (large) number. Upon this assumption (19), for $n > 2M$, can be transformed into;

$$\beta\left(\frac{n}{2} - M - \frac{1}{2} - \frac{\lambda^{2M+2}}{1-\lambda^2}\right) = \frac{\nu\pi n}{b} - \sum_{k=1}^{M} \xi_k(\lambda^{-k} - \lambda^k),$$

which gives:

$$\beta = \frac{2\pi\nu}{b}. \tag{20a}$$

Substitution of this result leads to:

$$\frac{2\pi\nu}{b}\left(M + \frac{\lambda^{2M}}{1-\lambda^2}\right) = \sum_{k=1}^{M} \xi_k(\lambda^{-k} - \lambda^k) \tag{*}$$

(the term $\frac{1}{2}$ has been neglected in comparison with M, while λ^{2M+2} has been replaced by λ^{2M}, as λ evidently will differ very little from unity). We cannot come further with this equation alone and attention should be given to the circumstance that the infinite system (19) is equivalent to the differential equation (11), the general solution of which, as given by (13), cannot satisfy both boundary conditions. However, when we have an approximate expression for the ξ_n of low index numbers, this expression can be substituted into (*) and the latter can be used to determine λ, provided we find a suitable value for M. We may take as such that value of the number m for which the approximation (20) and the approximation used for small index numbers are nearest each other. For instance when we substitute the values of the ξ_n given by (16a) and determine M by the condition that the ratio $(U/\pi m)/(2\pi\nu\lambda^m/b)$ shall be a minimum (which requires $M = -1/\ln\lambda$), we find:

$$-\ln\lambda \cong \frac{1.01\pi^2\nu}{Ub},$$

which makes a good approximation to (16b).

In order to investigate the part played by the nonlinear terms of (18) and (19) in the transmission of energy, we multiply (6) by $b\xi_n/2$ and form the equation of energy for a single component of the spectrum:

$$\frac{d}{dt}\left(\frac{b}{4}\xi_n^2\right) = \frac{U\xi_n^2}{b} - \frac{\nu\pi^2 n^2 \xi_n^2}{2b} + \sigma_n' - \sigma_n''. \tag{21}$$

The terms of the right-hand member have the following meaning: the first one is the energy derived by the component ξ_n from the primary motion; the second one is the energy dissipation for that component; the third one:

$$\sigma_n' = \frac{\pi n}{4} \xi_n \sum_{k=1}^{n-1} \xi_k \xi_{n-k} \tag{22a}$$

represents the energy exchange with the components of index numbers below n; the fourth one:

$$\sigma_n'' = \frac{\pi n}{2} \xi_n \sum_{k=1}^{\infty} \xi_k \xi_{n+k} \tag{22b}$$

represents the energy exchange in which components with index numbers higher than n are involved.

The total amount of energy transmitted from the part of the spectrum for the index numbers $1, \cdots n$ to the part beyond is given by the sum:

$$S_n = \sum_{m=1}^{n} (\sigma_m'' - \sigma_m') = \frac{\pi}{2} \sum_{k=n+1}^{\infty} \sum_{h=1}^{n} h \xi_h \xi_{k-h} \xi_k. \tag{22c}$$

The expressions for the exchange of energy all depend upon products of the third degree of the quantities ξ_n (which quantities themselves have the dimensions of a velocity).

When we exclude the first few values of n, in such a way that in the head of the spectrum the total energy to be derived from the primary motion $\frac{1}{2}U\Sigma\xi_n^2 = U^3/12 (= PU)$ has already been taken up, the value of S_n will be equal to:

$$S_n = \frac{U^3}{12} - \left(\frac{\nu\pi^2}{2b}\right) \sum_{m=1}^{n} m^2 \xi_m^2. \tag{22d}$$

and for $n \ll Re/6$ will be practically independent of n.

VII. Nonstationary Solutions of Equation (2)

We keep to the case where U is treated as a constant. Based upon the results of section 4 we divide the domain for y into regions where the equation

$$\frac{\partial v}{\partial t} + 2v \frac{\partial v}{\partial y} - \frac{Uv}{b} = 0 \tag{23}$$

can be applied, and others where the approximation

$$\frac{\partial v}{\partial t} + 2v\frac{\partial v}{\partial y} - \nu\frac{\partial^2 v}{\partial y^2} = 0 \tag{24}$$

will be appropriate.

Equation (23) can be solved by means of its characteristics, which are determined by the equation: $dy/dt = 2v$. When the values of v given for $t = 0$ satisfy the relation $\partial v/\partial y > 0$, the solution for large values of t asymptotically approaches to: $v = \frac{1}{2}Uy/b +$ constant. On the other hand when there are regions in which $\partial v/\partial y < 0$, the solution tends to generate discontinuities. When one should accept the presence of real discontinuities in the course of v, development into a Fourier series according to well-known theorems will lead to coefficients ultimately decreasing proportionally with n^{-1}. It is possible to calculate the total energy and the value of P with the aid of such a result; but the total dissipation will become infinite, as it has to be expected with $\partial v/\partial y$ assuming an infinite value in a discontinuity.

However, when a discontinuity threatens to appear, the approximation (23) no longer can be applied and we must use equation (24). A system of moving coordinates y', t' is introduced, defined by $y' = y - ct$; $t' = t$; equation (24) then transforms into:

$$\frac{\partial v}{\partial t'} + (2v - c)\frac{\partial v}{\partial y'} - \nu\frac{\partial^2 v}{\partial y'^2} = 0. \tag{24a}$$

We suppose that the term $\partial v/\partial t'$ will remain of the order unity when c is properly chosen, the other terms becoming of the order $1/\nu$ in the resulting solution. Hence we replace (24a) by

$$\nu\frac{\partial^2 v}{\partial y'^2} = (2v - c)\frac{\partial v}{\partial y'}, \tag{24b}$$

which gives

$$\nu\left(\frac{\partial v}{\partial y'}\right) = \left(v - \frac{1}{2}c\right)^2 - C_0,$$

C_0 being a constant. This equation must be valid through the region of steep change of v and on both sides of it, where the derivative $\partial v/\partial y'$ will return to values of the order unity so that $\nu(\partial v/\partial y')$ can be neglected. Using subscripts l and r to distinguish between points just to the left and just to the right of the discontinuity, we must have:

$$(v_l - \tfrac{1}{2}c)^2 = (v_r - \tfrac{1}{2}c)^2,$$

from which:

$$c = v_l + v_r. \tag{25}$$

The solution of (24b) now becomes:

$$v = \frac{v_l + v_r}{2} - \frac{v_l - v_r}{2} \operatorname{tgh} \frac{(v_l - v_r)(y' - y_0)}{2\nu}, \tag{26}$$

where y_0 is a second integration constant. In terms of the original coordinate y we have $y' - y_0 = y - ct - y_0$.

Summing up we see that in the case of large Reynolds numbers the nonlinear term in (2) can give rise to the appearance of discontinuities, but that the formation of a true discontinuity is prevented by the influence of the term $\nu(\partial^2 v/\partial y^2)$, in consequence of which every discontinuity is rounded off and a dissipation region is produced. The total dissipation in such a region has a finite value, for which is found $(v_l - v_r)^3/6$ (in a discontinuity always $v_l > v_r$). It is important to note that in a dissipation region the course of $v(y)$ is governed by the viscous term of the equation of motion (we may say that in the interior of this region the motion is laminar), but that nevertheless the total dissipation is independent of the viscosity and is of the third degree with respect to the velocities. The rounding off of the discontinuities also influences the asymptotic behavior of the coefficients in the Fourier development of v, which coefficients for $n > Re$ no longer are proportional to n^{-1}, but decrease exponentially in a way analogous to that described by (16b).

It will be seen that by this same process a boundary layer will be formed at $y = b$, when v is positive for values of y just smaller than b; and at $y = 0$ when v is negative for y immediately to the right of 0. Intermediate stationary dissipation regions can appear when $v_l + v_r$ takes the value 0. In a moving dissipation region v_l and v_r will be functions of the time, but we shall not enter into an investigation of their behavior.

VIII. Application of Equation (2) to an Infinite Domain

While equation (2) with the boundary conditions $v = 0$ at $y = 0$ and $y = b$ originally was meant to illustrate properties of the turbulence of a fluid moving under an exterior force through a channel, it may also be used without these boundary conditions to illustrate properties of free turbulence, by applying it to an open domain. In that case it is useful to take $U = 0$, in order to obtain results for free turbulence not activated by energy transmission from a primary motion. The equation governing the turbulence consequently becomes the same as (24):

$$\frac{\partial v}{\partial t} + 2v \frac{\partial v}{\partial y} - \nu \frac{\partial^2 v}{\partial y^2} = 0. \tag{24}$$

A typical solution of this equation, which can develop from various initial conditions, has the form:

$$v = \frac{V(\eta)}{\sqrt{t - t_0}}, \qquad \text{with} \qquad \eta = \frac{y - y_0}{\sqrt{t - t_0}}. \tag{27}$$

In the course of time this solution spreads out proportionally with the square root of time, while its amplitude decreases inversely proportionally to $\sqrt{t - t_0}$. As a function of the new variable η the quantity V must satisfy the equation:

$$\nu V'' - 2VV' + \tfrac{1}{2}\eta V' + \tfrac{1}{2}V = 0 \tag{28}$$

which can be integrated into:

$$\nu V' = V^2 - \tfrac{1}{2}\eta V. \tag{29}$$

The integration constant has been taken zero, in order to make possible solutions that for large (negative and positive) values of η decrease to zero. For infinitely small values of ν the solutions of (29) take an asymptotic form, which can be described by means of the following formulas:

$$\left.\begin{array}{c} V = 0 \quad \text{for} \quad \eta < 0 \\ V = \frac{1}{2}\eta \quad \text{for} \quad 0 < \eta < L \\ V \text{ decreases suddenly from } \frac{1}{2}L \text{ to } 0 \text{ for } \eta = L \\ V = 0 \quad \text{for} \quad L < \eta. \end{array}\right\} \tag{30}$$

Here L is a second integration constant, fixing the scale of the curve in η-measure. For small finite values of ν a correction to this asymptotic solution can be deduced [a graphical discussion of equation (29) gives much help in visualizing the resulting curve]; it is found that the true curve nowhere differs much from the broken line described by (30), while for values of η in the immediate neighborhood of L it can be approximated by the expression:

$$V \cong \frac{L}{4}\left\{1 - \operatorname{tgh}\frac{L(\eta - L)}{4\nu}\right\}. \tag{31}$$

Elsewhere it has been indicated in which way a solution of this type can arise from certain initial conditions.[4]

Returning to the y- and v-scales the linear dimension of the domain where v is appreciably different from zero, increases according to the formula:

$$l = L\sqrt{t - t_0} \tag{32a}$$

[4] See (II), pp. 8–9.

while the height of the front decreases and is equal to

$$v_{fr} = \frac{L}{2\sqrt{t - t_0}}. \tag{32b}$$

In this domain there is a momentum of amount:

$$\Omega = \int v\,dy = \tfrac{1}{4}L^2 \tag{32c}$$

which is independent of the time. It follows that L can be expressed by means of Ω: $L = 2\sqrt{\Omega}$. The kinetic energy has the value:

$$\frac{1}{2}\int v^2 dy = \frac{L^3}{24\sqrt{t - t_0}} = \frac{\Omega^{\frac{3}{2}}}{3\sqrt{t - t_0}} \tag{32d}$$

and thus decreases in the course of time; this is the consequence of the dissipation of energy in the front, which amounts to:

$$\frac{1}{6}\left(\frac{L}{2\sqrt{t - t_0}}\right)^3 = \frac{L^3}{48(t - t_0)^{\frac{3}{2}}} = \frac{\Omega^{\frac{3}{2}}}{6(t - t_0)^{\frac{3}{2}}}. \tag{32e}$$

The solution therefore represents the gradual broadening of an isolated "domain of coherence," in such a way that its momentum is preserved. It can be compared with the gradual increase of size of an eddy in the hydrodynamical case, where the same proportionality of the linear dimensions with $\sqrt{t - t_0}$ is found. It must be noted that a similar solution can be obtained in which both $y - y_0$ and v have changed sign; in that case the front moves to the left instead of to the right.

The steepness of the front is a function of its height, and decreases with decrease of the front height. There can be no steep front with a height of the order ν.

IX. Spatial Correlation in the Values of v for an Isolated Domain of Coherence

We denote by $I(r)$ the value of the correlation integral:

$$I(r) = \int_{-\infty}^{+\infty} dy_0 v(y) v(y + r) \tag{33}$$

which refers to the product of the values of v in two fixed points y and $y + r$, when the constant y_0 in the solution just found takes all values from $-\infty$ to $+\infty$, the value of l being kept unchanged. Evidently we can just as well write:

$$I(r) = \int_{-\infty}^{+\infty} dy\, v(y) v(y + r) \tag{33a}$$

where y_0 and r are kept fixed. A correlation coefficient is defined by

$$R(r) = \frac{I(r)}{I(0)}. \tag{34}$$

When r is comparable to l the calculation can be worked out by means of the asymptotic solution given in (30); we find:

$$R(r) = 1 - \frac{3}{2}\frac{r}{l} + \frac{1}{2}\frac{r^3}{l^3}. \tag{34a}$$

The value of $R(r)$ remains practically zero for values of r exceeding the length l of the domain. For very small values of r we better use the development:

$$\int dy\, v(y)v(y+r) = \int dy \left\{ v^2 + r \cdot v\frac{\partial v}{\partial y} + \frac{r^2}{2} \cdot v\frac{\partial^2 v}{\partial y^2} + \cdots \right\}$$
$$= \int dy\, v^2 - \frac{r^2}{2}\int dy \left(\frac{\partial v}{\partial y}\right)^2 + \cdots.$$

The most important contribution to the last integral comes from the steep front; making use of (31) we find:

$$R(r) = 1 - \frac{r^2}{8\nu l_1}. \tag{34b}$$

X. Application of Similarity Considerations

Following the lead given by Taylor and von Kármán with their investigations on the statistical properties of free turbulence, much attention in recent years is devoted to statistical problems, in particular in order to arrive at a theoretical expression for the correlation between velocity fluctuations in two points at a distance r apart from each other. A summary of some modern work on this subject has been given by G. K. Batchelor.[5] According to this summary the various theories proposed all start from the assumption of indefinitely high Reynolds numbers, and assume that the effect of viscosity on velocity correlations is negligible when r is large in comparison with the size of the smallest eddies; it is further supposed that the energy associated with a small range of wave numbers is received chiefly from wave numbers one order smaller (*i.e.*, eddies of larger size) and is passed on to larger wave numbers without appreciable loss through viscous dissipation; while finally the smallest existing eddies have laminar motion and are responsible for most of the

[5] G. K. Batchelor, *Nature* **158**, 883–884 (1946).

energy dissipation. It will be evident that all these features are present in our model. It is of interest therefore to consider to what extent the conclusions derived from these assumptions can be applied to the model.

In order to have a basis for the application of statistical considerations to the case of free turbulence, a supposition must be introduced concerning the way in which the field may have been generated. We can start with an arbitrary initial distribution of values for v at $t = 0$. It is to be expected that in course of time, by the generation and subsequent coalescence of discontinuities, a number of more or less clearly defined domains of coherence, of the type considered in Section VIII, will come into existence. The fronts of the domains with the larger velocities will overtake the other ones, and there will be a gradual coalescence of the domains into a smaller number. A picture of this process can be constructed without difficulty for a case in which the v-curve for $t = 0$ consists of segments where v is constant (eventually zero), with abrupt changes of v from one segment to the next one. The average size of the domains of coherence will be found to increase proportionally to $\sqrt{t - t_0}$.

Such a process could be repeated a large number of times, every time starting with an arbitrary distribution of the values of v. We then can take two fixed points, y and $y + r$, and ask for the average value of the product $v(y)v(y + r)$ referring to these points. In order to make this question definite, we either may compare the value of $v(y)v(y + r)$ each time with the value of $\{v(y)\}^2$, or something can be fixed about the initial conditions. We might require, *e.g.*, that the mean value of v^2, taken over regions of a definite length, initially shall always have the same value, and that the value of $v(y)v(y + r)$ is always observed after the same lapse of time since the process was started.

The dissipation of energy in every case is due to the circumstance that there is a continuous tendency to develop steep fronts, which are the main regions where viscosity is operative.

The introduction of an actual starting point in time, however, makes the picture less satisfactory as a description of the state to be found in an arbitrary field. In the statistical theory developed by A. N. Kolmogoroff the field, independently of its actual history, at any given instant is characterized by the mean dissipation per unit mass. This idea can be taken over in the model system.

At a given instant the following quantities describe important characteristics of the turbulent field: the mean dissipation of energy per unit length: ϵ; and the correlation function: $J(r) = \overline{v(y)v(y + r)}$, which latter embraces also the mean energy per unit length: $E = \frac{1}{2}J(0)$. Along with these we introduce an *average length l of the domains of coherence* and an *effective age T of the field*. These additional quantities can be related

to the other two in the following way: on the one hand T must be of the order of magnitude of E/ϵ; on the other hand, as the mean velocity in the field is given by $\sqrt{2E}$, it should be of the order $l/\sqrt{E}$. Comparing these results we must have, with a numerical factor α:

$$\frac{E}{\epsilon} = \frac{\alpha l}{\sqrt{E}}. \tag{A}$$

A further relation can be found by observing that the average dissipation per unit length is given by the average value of $\nu(\partial v/\partial y)^2$, and thus must be of the order $\nu E/l^2$. In this way the viscosity is brought into the picture. It now becomes possible to eliminate the mean energy E; we obtain (with another numerical factor β):

$$E = \frac{\beta \epsilon l^2}{\nu}. \tag{B}$$

From (A) and (B) we deduce:

$$\left.\begin{aligned} E &= C_1 \nu^{\frac{1}{2}} \epsilon^{\frac{1}{2}} \\ l &= C_2 \nu^{\frac{1}{2}} \epsilon^{-\frac{1}{2}} \\ T &= C_3 \nu^{\frac{1}{2}} \epsilon^{-\frac{1}{2}} \end{aligned}\right\} \tag{35}$$

where C_1, C_2, C_3 again are numerical factors. Having obtained these results it is evident that the correlation function $J(r)$ must be of the form:

$$J(r) = \sqrt{\nu\epsilon} \cdot F\left(\frac{r\epsilon^{\frac{1}{2}}}{\nu^{\frac{1}{2}}}\right).$$

When r goes to zero the function F must reduce to a constant. When on the other hand the hypothesis is accepted that for values of r large in comparison with the size of the smallest domains of coherence, the part of $J(r)$ depending on r shall become independent of ν, it is necessary that F be of the form:

$$F = A_1 - A_2\left(\frac{r\epsilon^{\frac{1}{2}}}{\nu^{\frac{1}{2}}}\right)^{\frac{1}{2}},$$

where A_1 and A_2 are numerical factors. With $A_2/A_1 = \kappa$ the correlation coefficient $R(r)$ then becomes:

$$R(r) = 1 - \kappa\epsilon^{\frac{1}{2}}\nu^{-\frac{1}{2}}r^{\frac{1}{2}}. \tag{36}$$

The dependence upon $r^{\frac{1}{2}}$ is the same result as has been obtained by Kolmogoroff for hydrodynamical turbulence, apparently along similar lines of reasoning.

The reasoning is somewhat unsatisfactory in so far as it does not give a means for determining the numerical factors involved, nor does it enable us to find the relation between the scale of the eddies of coarser type and the size of the smallest eddies present (both quantities have the dimensions of l). The gross scale of the turbulence, for which we may take the quantity l itself, can be defined in such a way that the correlation is zero for $r \geq l$; hence we shall write:

$$R(r) = 1 - \left(\frac{r}{l}\right)^{\frac{2}{3}} \qquad \text{for} \qquad r < l \tag{36a}$$

with

$$l = \kappa^{-\frac{1}{4}}(\nu^{\frac{3}{4}}\epsilon^{-\frac{1}{4}}). \tag{36b}$$

XI. Continuation

According to a formula given by Taylor it is possible from the correlation coefficient to deduce an expression for the energy distribution in the relevant part of the spectrum of the turbulent motion.[6] In the present case, where the domain for y is infinite, we must replace the Fourier series of Sections V and VI by Fourier integrals; denoting the energy between the frequencies n and $n + dn$ by $E(n)dn$, Taylor's formula gives:

$$E(n) = \text{const.} \int_0^\infty dr\, R(r) \cos \frac{\pi n r}{l} \tag{37}$$

When we introduce the expression (36a) for $R(r)$ into this formula, taking $R(r) = 0$ for $r > l$, it can be applied to find in what way $E(n)$ depends upon n for wave numbers large compared with unity, and for which nevertheless l/n is still large in comparison with the size of the smallest eddies (for values of r of the order of that size (36a) should be replaced by a parabolic expression of the type given in (34); the application of (36a) consequently cannot give reliable results for very large n). The result obtained in this way is:[7]

$$E(n) \sim n^{-\frac{2}{3}}. \tag{38}$$

A result of similar nature has been obtained by L. Onsager,[8] and, according to Batchelor's paper, also by C. F. von Weizsäcker, in both cases from dimensional considerations taking as a datum the energy dissipation per unit volume. Onsager gives a proportionality with $n^{-\frac{1}{3}}$, but I suppose that in connection with the three-dimensional character of hydrodynamical turbulence a weight factor n^2 must be introduced. Both

[6] G. T. Taylor, *Proc. Roy. Soc.* (*London*) *A* **164**, p. 479, eq. (16) (1938).

[7] In order to deduce this result use can be made of certain integrals given in G. N. Watson, *Theory of Bessel Functions* (Cambridge 1944), p. 545, section 16.56, equations (1) and (2), together with the asymptotic expansion given on p. 550, equation (3).

[8] L. Onsager, *Phys. Rev.* (II) **68**, p. 286, 1945.

authors deduce the form (36a) of the function $R(r)$ from the expression for $E(n)$ by means of the conjugate formula to (37).

The physical basis for a deduction of the statistical behavior of the amplitudes ξ_n of the components into which the turbulent motion can be resolved should be found in the properties of the function S_n defined in Section VI, which represents the transmission of energy from the part of the spectrum extending up to a definite wave number n to the part beyond. In the present case the sums of form (22c) must be replaced by integrals. The average value $\bar{S}_n$ of S_n also in the case of free turbulence will be independent of n for the range of wave numbers considered above.

The expression for S_n is a sum of terms of odd degree in the ξ_n. As the ξ_n in a case starting from arbitrary initial conditions may have negative as well as positive values, it is necessary that triple correlations exist between them, in such a way that mean values of the type $\overline{\xi_h \xi_{k-h} \xi_k}$ will be different from zero. Onsager in his (very short) note points to the circumstance that the modulation of a given Fourier component will be mostly due to those other components that belong to wave numbers of comparable magnitude. It seems appropriate to suppose that a mean value $\overline{\xi_{p+\omega} \xi_{p-\omega} \xi_{2p}}$ will be largest when $\omega = 0$ and that it will decrease quickly with increasing values of ω. If we assume that the mean amplitude of a component is proportional to (wave number)$^\sigma$, an expression of the form:

$$\overline{\xi_{p+\omega} \xi_{p-\omega} \xi_{2p}} = A (2p)^{3\sigma} e^{-\beta \omega^2 / 2p} \tag{39}$$

will satisfy these requirements; it has been chosen in such a way that the range of the wave numbers of the components with which the component ξ_{2p} is in effective coherence is of a breadth proportional to $\sqrt{2p}$.[9] The factor A in (39) has the dimensions: $(velocity)^3$; in connection with (35) we must have $A = num.\ factor \cdot \nu^3 \epsilon^3 = num.\ factor \cdot \epsilon l$ (ϵ represents the average dissipation per unit of length). β must be a pure number, of such magnitude that, say, $\beta n / 4 > 9$. Making use of (39) we obtain the following formula for $\bar{S}_n$:

$$\frac{2}{\pi} \bar{S}_n = \int_n^\infty dk \int_0^n dh\, h \overline{\xi_h \xi_{k-h} \xi_k} = \int_n^\infty dn \int_{-k/2}^{n-k/2} d\omega \left(\frac{k}{2} + \omega \right) \overline{\xi_{\frac{k}{2}+\omega} \xi_{\frac{k}{2}-\omega} \xi_k}$$

$$= A \int_n^\infty dk\, k^{3\sigma} \int_{-k/2}^{n-k/2} d\omega \left(\frac{k}{2} + \omega \right) e^{-\beta \omega^2 / k}.$$

[9] Onsager states "that the subdivision of the energy must be a stepwise process, such that an n-fold increase of the wave number is reached by a number of steps of the order $\log n$." The idea involved in the formula given in the text is in accordance with this statement, as it assumes that the component ξ_{2p} mainly derives its energy from components with wave numbers nearly equal to p, so that the principal effect is a doubling of the wave numbers in each step.

So long as k satisfies the condition $n - k/2 > 3\sqrt{k/\beta}$, the integral with respect to ω practically gives $\pi^{\frac{1}{2}}k^{\frac{3}{2}}/2\beta^{\frac{1}{2}}$. When k increases and takes the value $2sn$, the range of integration for ω extends from $-sn$ to $-(s-1)n$, and the exponential function will not exceed $e^{-\beta(s-1)^2n/2s}$, which quickly decreases to zero when $s > 4$. Hence we shall obtain an approximation to the value of $\bar{S}_n$ by restricting the range of integration for k from the lower limit n up to an upper limit $2sn$ (with a properly chosen value for s), if throughout this range we use the value $\pi^{\frac{1}{2}}k^{\frac{3}{2}}/2\beta^{\frac{1}{2}}$ as the result of the integration with respect to ω, so that:

$$\frac{2}{\pi}\bar{S}_n = \frac{A\sqrt{\pi}}{2\sqrt{\beta}}\int_n^{sn} dk\, k^{3\sigma+\frac{3}{2}}.$$

This expression will become independent of the value of n, when $3\sigma + \frac{3}{2} = -1$, which gives:

$$\sigma = -\tfrac{5}{6}. \tag{40}$$

In this way we again arrive at the expression (38) for $E(n)$. It is evident that this result is dependent upon the choice made in equation (39).

The argument is a tentative one, but it clearly shows the importance of triple correlations between the components of the spectrum.

XII. Statistical Treatment, Based upon the Energy Balance, of the System Considered in Sections II–VII

The result obtained in (40) differs from that found in Sections II–VII for the original system of equations, which referred to turbulent motion between two walls in the presence of a primary motion U differing from zero. In particular (40) is at variance with the property of equal dissipation per degree of freedom for wave numbers of average magnitude, which was obtained in the case of the original system and was intimately connected with the properties of the dissipation layers. It was deduced from an exact solution of the equations. Although this solution was independent of the time and consequently presents a simpler character than actual turbulence, the result cannot be discarded as unimportant. It was supported by the results of Section VII for nonstationary solutions; moreover in Sections XIII and XIV a system will be considered, with properties similar to those of the system (1) and (2) in every significant respect, but with turbulent solutions which cannot be independent of the time and thus come nearer to the character of actual turbulence.

There is a possibility that the statistical behavior of free turbulence is different from that of turbulence in a region of limited extent, subjected to boundary conditions at the walls and deriving its energy from a continuously present primary motion. This will be evident when we

keep in mind that the presence of a primary velocity U introduces a quantity that did not occur in the similarity considerations of Section X, so that we can no longer rely upon the expressions (35). This destroys the basis upon which equation (36) had been deduced. We cannot be certain, therefore, that in the case of turbulence connected with a primary motion the correlation will be a linear function of r^1; neither can we be certain of the applicability of formula (38). It is not to be excluded that in this case the statistical properties of turbulence must be described by relations of the type found in Section V.

The present author made an attempt in treating the statistical problem of turbulence for the motion between fixed walls in the presence of a primary motion U, assuming the equation of energy in the form (7) to represent a key condition, to which was assigned a similar part as to the condition of constant energy in the case of conservative systems. Turbulence is considered as a sequence of states, the order of which is of no importance in the calculation of mean values. It must be required that every such sequence will satisfy the condition that the mean value of the right-hand member of (7) for the sequence should be zero. To every possible sequence a statistical weight is given, determined by the number of ways in which the various states of the sequence can be arranged, using an algorithm similar to that applied in ordinary statistical mechanics. In order to express the condition implied by equation (7), every state is resolved into its elementary components, so that the expression for the dissipation can be formed without difficulty. By means of this procedure mean values can be calculated, and the result is obtained that every component of the turbulence will have the same average dissipation. This is in accordance with the approximation represented by (16a), but, as was pointed out in connection with that equation, makes the total dissipation infinite.

Evidently the procedure applied left out an important feature connected with the part played by the nonlinear terms in the equations of motion, and in order to remedy the "violet catastrophe" threatening in this way a datum must be found representing the influence of these terms. Now the results of Sections V–VII have shown that in the case of turbulence associated with a primary motion the law of decrease of the ξ_n with increasing wave number changes in form as soon as the ξ_n have fallen below an amount of the order ν/b, in such a way that values below ν/b (other than zero) can be considered as relatively improbable. By defining a "threshold value" and requiring that the ξ_n shall never take values below this threshold except zero, an element can be introduced related to the introduction of the quantum hypothesis in the statistical theory of radiation. The simplest way of doing this is to require that the

ξ_n shall take only values that are integer multiples of $\delta\nu/b$, δ being a numerical factor of order unity, zero multiple of course being included. When the statistical calculations are worked out upon this basis,[10] the result can be expressed by means of θ-functions. From these functions approximations can be obtained both for moderate n and for very large n, which have the same form as those represented by formulas (16a) and (16b), so that the total dissipation becomes finite.

One conclusion will be evident from the results obtained: the situation that is found in the well-known statistical theory of conservative systems, where the equation of energy alone is sufficient for obtaining the statistical distribution and where no special notice has to be taken of the full equations of motion, is totally different from that found in the case of nonconservative systems. It may be taken for certain that this fact is connected with the failure of Liouville's theorem for nonconservative systems. The consequence is that in the statistical treatment of nonconservative systems special regard must be given to the influence of the nonlinear terms of the equations of motion, either (as was done in Section XI) by investigating the transmission of energy through the spectrum, or (as was done in the present section) by introducing some particular result deduced from the equations of motion—in this case referring to the nature of the dissipation regions.

It is of importance to observe that in the case of hydrodynamics relations can be found concerning the dissipation in vortex systems, which are closely connected to those obtained for the model system (see the last part of Section XV).

XIII. System with Two Components in the Secondary Motion

Although all important features could be elucidated with the aid of the system governed by equations (1) and (2), for certain purposes it is of interest to consider a slightly more general system, in which the secondary motion possesses two components: $v(t,y)$ and $w(t,y)$. This system is described by the equations:

$$b\frac{dU}{dt} = P - \frac{\nu U}{b} - \frac{1}{b}\int_0^b dy(v^2 + w^2) \tag{41}$$

$$\frac{\partial v}{\partial t} = \frac{U}{b}(v - w) + \nu\frac{\partial^2 v}{\partial y^2} - \frac{\partial}{\partial y}(v^2 - w^2) \tag{42a}$$

$$\frac{\partial w}{\partial t} = \frac{U}{b}(v + w) + \nu\frac{\partial^2 w}{\partial y^2} + \frac{\partial}{\partial y}(2vw). \tag{42b}$$

[10] See (III) and (IV).

The terms of the second degree have been adjusted in such a way that for the case of a limited domain $0 \leqq y \leqq b$, with boundary conditions $v = w = 0$ at both ends, an equation of energy can be formed as before:

$$\frac{d}{dt}\left\{\frac{bU^2}{2} + \int_0^b dy\,\frac{v^2 + w^2}{2}\right\} = PU - \frac{\nu U^2}{b} - \nu \int_0^b dy\left\{\left(\frac{\partial v}{\partial y}\right)^2 + \left(\frac{\partial w}{\partial y}\right)^2\right\}. \tag{43}$$

Moreover the following equation holds:

$$\int_0^b dy\left(w\frac{\partial v}{\partial t} - v\frac{\partial w}{\partial t}\right) = -\frac{U}{b}\int_0^b dy\,(v^2 + w^2) \tag{44}$$

which is obtained when (42a) is multiplied by w, (42b) by v, after which the latter is subtracted from the former one and the result is integrated with respect to y from 0 to b, having regard to the boundary conditions. Equation (44) shows that the system has no solution independent of the time unless v and w are zero for all values of y (provided $U \neq 0$); this is a consequence of the cyclic terms $-Uw$, $+Uv$ introduced into (42a), (42b) respectively.

By introducing a complex variable $\psi = v + iw$ (using the notation $\psi^* = v - iw$ for the conjugate quantity), equations (41)–(42b) can be contracted into:

$$b\frac{dU}{dt} = P - \frac{\nu U}{b} - \frac{1}{b}\int_0^b dy\,\psi\psi^* \tag{45}$$

$$\frac{\partial \psi}{\partial t} = (1 + i)\frac{U}{b}\psi + \nu\frac{\partial^2 \psi}{\partial y^2} - \frac{\partial}{\partial y}(\psi^*)^2. \tag{46}$$

We restrict ourselves to the case where U is treated as a constant, which necessitates the replacing of equation (41) or (45) by its mean value with respect to the time:

$$P = \frac{\nu U}{b} + \frac{1}{b}\int_0^b dy\,\overline{\psi\psi^*}. \tag{47}$$

A Fourier development can be introduced by putting:

$$\psi = -\sum_{n=1}^{\infty} \zeta_n \sin\left(\frac{\pi n y}{b}\right) \tag{48}$$

where now the ζ_n are complex coefficients. Then equations (47) and (46) become:

$$P = \frac{\nu U}{b} + \frac{1}{2}\sum \overline{\zeta_n \zeta_n^*} \tag{49}$$

$$\frac{d\zeta_n}{dt} = \left\{(1+i)\frac{U}{b} - \frac{\nu\pi^2 n^2}{b^2}\right\}\zeta_n + \frac{\pi n}{b}\left(\frac{1}{2}\sum_{k=1}^{n-1}\zeta_k^*\zeta_{n-k}^* - \sum_{k=1}^{\infty}\zeta_k^*\zeta_{n+k}^*\right), \tag{50}$$

while the equation of energy assumes the form:

$$\frac{d}{dt}\left\{\frac{bU^2}{2} + \frac{b}{4}\sum \zeta_n\zeta_n^*\right\} = PU - \frac{\nu U^2}{b} - \frac{\nu\pi^2}{2b}\sum n^2\zeta_n\zeta_n^*. \tag{51}$$

The system again has the nonturbulent solution

$$U = \frac{Pb}{\nu}; \qquad v = w = 0 \tag{52}$$

which is stable when $Re = Ub/\nu < \pi^2$ and unstable when $Re > \pi^2$.

XIV. Properties of the Turbulent Solutions

In consequence of (44) no stationary turbulent solutions exist. It seems probable that periodic solutions can be found, but so far no exact result has been obtained.

In treating the system for large values of Re we again distinguish between narrow boundary layers to which applies the equation:

$$\frac{\partial\psi}{\partial t} + \frac{\partial}{\partial y}(\psi^*)^2 - \nu\frac{\partial^2\psi}{\partial y^2} = 0 \tag{53}$$

and comparatively broad regions in which we can write:

$$\frac{\partial\psi}{\partial t} + \frac{\partial}{\partial y}(\psi^*)^2 - (1+i)\frac{U\psi}{b} = 0. \tag{54}$$

Equation (53), in which for boundary-layer problems the term $\partial\psi/\partial t$ proves to be unimportant, has solutions of the two types:

$$\psi_{\mathrm{I}} = A\tilde{\omega}_{\mathrm{I}}\,\mathrm{tgh}\left(\frac{Ay}{\nu}\right); \qquad \psi_{\mathrm{II}} = A\tilde{\omega}_{\mathrm{II}}\,\mathrm{tgh}\left\{A\left(\frac{b-y}{\nu}\right)\right\} \tag{55}$$

where:

$$\tilde{\omega}_{\mathrm{I}} = e^{\pi i/3}; \qquad e^{\pi i}; \qquad e^{5\pi i/3}; \qquad \tilde{\omega}_{\mathrm{II}} = 1; \qquad e^{2\pi i/3}; \qquad e^{4\pi i/3}$$

[in the expressions (55) the coefficient A may be a function of the time].

Equation (54) can be transformed by writing

$$\psi^3 = \tfrac{1}{2}(\rho + i\sigma)^2.$$

After separation of real and imaginary parts we obtain the system:

$$\left.\begin{aligned}\frac{\partial \rho}{\partial t} &= -2z\frac{\partial \rho}{\partial y} + \frac{3}{2}\frac{U}{b}(\rho - \sigma)\\ \frac{\partial \sigma}{\partial t} &= +2z\frac{\partial \sigma}{\partial y} + \frac{3}{2}\frac{U}{b}(\rho + \sigma)\end{aligned}\right\} \tag{56}$$

where $z = \sqrt[3]{(\rho^2 + \sigma^2)/2}$. The boundary conditions that must be satisfied by ρ and σ at the ends of the interval are determined by the necessity of obtaining a proper fit with the solutions (55) without discontinuities in the value of ψ. This requires that $\rho = 0$ at $y = 0$ and that $\sigma = 0$ at $y = b$.

In equations (56) z is an (unknown) function both of y and of t. When z is replaced by its time mean value and thus is reduced to a function of y alone, a new variable can be substituted for y in such a way that a system of homogeneous linear equations with constant coefficients is obtained. A periodic solution of this simplified system, satisfying the boundary conditions for ρ and σ just mentioned, can be found; it can be used to obtain an approximate picture of a periodic solution of the system (56) and to make an estimate of the amplitude to be given to ρ and σ (again there is a connection between this amplitude and the eigenvalue of a parameter occurring in the linearized equation).[11]

When the motion starts from arbitrary initial conditions we find the same tendency toward the generation of dissipation regions as with equation (2). It is found that the dissipation in a region of steep change of v and w is given by:

$$\text{Real part of } \tfrac{1}{6}\{(v_l + iw_l) - (v_r + iw_r)\}^3.$$

This necessarily must be a positive quantity, which implies that the argument of $\{(v_l + iw_l) - (v_r + iw_r)\}$ can be situated only in certain definite sectors.

When equations (42a) and (42b), or, what comes to the same, equation (46) is applied to an unlimited domain, taking $U = 0$, a solution can be constructed similar to that given in Section VIII by writing

$$\psi = \frac{\Psi(\eta)}{\sqrt{t - t_0}}.$$

It is found that either

$$\arg \Psi = 0; \frac{2\pi}{3}; \frac{4\pi}{3}$$

[11] See (I), pp. 37–40. A minus sign ought to be introduced before A in the expression for σ, given in the second line of equation (18.13), p. 39.

the absolute value satisfying the equation:

$$\nu|\Psi|' = |\Psi|^2 - \tfrac{1}{2}\eta|\Psi|;$$

or

$$\arg \Psi = \frac{\pi}{3}; \pi; \frac{5\pi}{3}$$

the absolute value satisfying the equation:

$$\nu|\Psi|' = -|\Psi|^2 - \tfrac{1}{2}\eta|\Psi|.$$

The statistical method indicated in Section XII can be applied to the system (41)–(42b) (for the limited domain, with $U \neq 0$), as indeed was done in the original paper.[10]

XV. Concluding Remarks

The investigations described in the preceding pages can be considered in the first place from the mathematical point of view to be concerned with the properties of systems of quantities subjected to certain nonlinear differential equations.

As the quantities of interest we have taken the ξ_n (or ζ_n), *i.e.*, the amplitudes of the components that together constitute the spectrum of the system. The equations by which these amplitudes are connected are of the general type

$$\frac{d\xi_n}{dt} = \left(\frac{U}{b} - \frac{\nu\pi^2 n^2}{b^2}\right)\xi_n + f_n, \tag{57}$$

the first term of the right-hand member determining an exponential increase, the second term a damping, while a coupling between the various ξ_n is introduced through the f_n, which are quantities of the second degree in the ξ_n of such nature that

$$\sum_{n=1}^{\infty} \xi_n f_n = 0 \tag{58}$$

so that in a ξ_n-space the vector f is perpendicular to ξ. A direct investigation of the behavior of the ξ_n on the basis of these equations has not been given, but enough has been found out about them to bring into evidence highly interesting properties of the equations.

The most important question to be resolved is the mean value of $\Sigma\xi_n^2$ in function of U for large values of Ub/ν, which question involves the consideration of statistical problems.

Along with the system described by equations (6) other systems can be considered, *e.g.*, with a finite number of variables, or with more simple

expressions for the f_n, such as $f_n = \xi_{n-1}\xi_n - \xi^2_{n+1}$. For problems connected with such systems reference must be made to Section 21 of the paper quoted under (I) in footnote 1. In all cases triple correlations between the ξ_n will be obtained.

In the case of the system (6), however, the main results deduced in the preceding pages were not obtained from the equations for the ξ_n, but from the partial differential equation (2) with which the particular system (6) was equivalent. The characteristic feature of (2) is the combination of the two terms $\nu(\partial^2 v/\partial y^2)$ and $2v(\partial v/\partial y)$, which gives rise to the appearance of the dissipation layers.

That this feature has its analogy in the equations of hydrodynamics, has been mentioned already. The considerations put forward in the present paper had the object of pointing out that these terms characterize the peculiar mechanism that is operative in producing turbulence and determine the statistical relations governing the transfer of energy. In view of its importance it is useful to look somewhat more closely into the way in which a similar feature appears in hydrodynamics. The group of terms

$$\frac{\partial v}{\partial t} + 2v\frac{\partial v}{\partial y} - \nu\frac{\partial^2 v}{\partial y^2}$$

of equation (2) will find its closest analogy in the terms

$$\left(\frac{\partial u}{\partial t} + u\frac{\partial u}{\partial x}\right) - \nu\frac{\partial^2 u}{\partial x^2}$$

which are decisive in determining the appearance of shock waves in the supersonic motion of a gas. As shown by Rayleigh, and by Prandtl and others, the (theoretical) thickness of the transition layer in which kinetic energy of the mass motion is transformed into heat (internal energy) is of the order of magnitude ν/u. The ordinary problem of turbulence, however, refers to motion with velocities well below the velocity of sound, so that the moving fluid can be treated as incompressible. The condition imposed by the equation of continuity in that case prevents the appearance of shock waves, and the dissipation regions to be found in such liquids are of the nature of "quasi-slip" regions, of which boundary and vortex layers represent the typical examples. Now in all the well-known cases of boundary and vortex layers the thickness of the layer at high Reynolds numbers is found to be proportional to $\sqrt{\nu/u}$ instead of to ν/u. This implies a total dissipation (integrated over the thickness of the layer), per unit area of the layer, proportional to $\nu^{\frac{1}{2}}u^{\frac{1}{2}}$ instead of to u^3. If this result should be typical for all fluid motion, it would

appear that the resistance in turbulence would be at most proportional to the $\frac{3}{2}$-power of the velocity.

Happily there is a case in which we obtain dissipation proportional to the third power of the velocity.[12] This is found when the motion is such that vortex lines are drawn out by the field. A typical example is arrived at by considering an axially symmetric field, having the velocity components (referred to cylindrical coordinates r, ϑ, z)

$$v_r = -Ar; \qquad v_\vartheta = u(t,r); \qquad v_z = 2Az,$$

where A is a constant (of the dimensions *velocity/length*); and the pressure:

$$p = -\frac{1}{2}\rho A^2(r^2 + 4z^2) + \rho \int dr \frac{u^2}{r}.$$

These expressions satisfy the equation of continuity and the equations of motion for the r- and z-directions. The equation of motion for the ϑ-direction has the form:

$$\frac{\partial u}{\partial t} - Ar\frac{\partial u}{\partial r} - Au = \nu\left(\frac{\partial^2 u}{\partial r^2} + \frac{1}{r}\frac{\partial u}{\partial r} - \frac{u}{r^2}\right).$$

This equation has a solution that is independent of the time, *viz.*:

$$u = \frac{C}{2\pi r}(1 - e^{-Ar^2/2\nu}) \tag{59}$$

where C represents the circulation around the vortex. The vorticity $\gamma = (\partial u/\partial r + u/r)$ is given by:

$$\gamma = \frac{AC}{2\pi\nu} e^{-Ar^2/2\nu} \tag{59a}$$

and the total dissipation per unit height in the z-direction becomes:

$$\rho\nu \int_0^\infty dr 2\pi r\gamma^2 = \frac{\rho AC^2}{4\pi} \tag{60}$$

which is of the third degree with respect to the velocities, while it is independent of ν.

I have not succeeded in constructing an analogous solution for the case of a vortex sheet; in that case one falls back upon a maximum value of the vorticity of the order $\nu^{-\frac{1}{2}}$, which is not sufficient for the

[12] See (II), pp. 11–12. That the drawing out of vortices must represent a fundamental process that controls the dissipation of energy in turbulent motion had been pointed out by G. I. TAYLOR; comp. *Proc. Roy. Soc.* (*London*) *A* **164**, p. 15, 1938.

purpose in view. This indicates that in hydrodynamical turbulence, at least in the case of the flow through a tube or channel, the fate of vortices extending in the direction of the motion is of great importance. At the same time it shows that the geometrical features of incompressible fluid flow introduce specific complications into the problems, which, however, stand apart from the basic dynamical relations to which attention has been given here.

On Numerical Methods in Wave Interaction Problems

By HILDA GEIRINGER

Wheaton College

CONTENTS

This report discusses two methods for the numerical treatment of wave interaction problems both of which use Lagrange's form of the equation of motion. In 1944 Professor von Neumann[1] proposed a new approach to the hydrodynamical shock problem, which he applied to the collision of shock and rarefaction waves. This approach, based on an idea of theoretical interest, provides also a computational procedure. The same collision problem is dealt with in the present article by means of a method worked out by the author while she was connected with the Applied Mathematics Panel, New York University Group. It seemed both instructive and practical to discuss the two methods for the same (or essentially the same) gasdynamical problem. The approach is, however, an entirely different one. In sections 1–3 the problem is set forth and that part of the solution which is supplied by classical methods is indicated. In sections 4 and 5 the numerical method advanced by the author is explained under the assumption that a throughout relation between pressure and density holds even across shocks.[2] In

[1] J. v. Neumann, Proposal and analysis of a new numerical method for the treatment of hydrodynamical shock problems. A report submitted by the Applied Mathematics Group, Institute for Advanced Study, to the Applied Mathematics Panel, *N.D.R.C. Rept.* 108 (1944).

[2] See Riemann Weber, *Die partiellen Differentialgleichungen der mathematischen Physik.* 4. Aufl., 2. Bd., pp. 469-521. This exposition is based on Riemann's paper Über die Fortpflanzung ebener Luftwellen von endlicher Schwingungsweite, *Abhandlg. Göttinger Ges. Wiss.*, Bd. VIII (1860). In later editions of Riemann-Weber, *i.e.* 5th and 6th editions, the conception of entropy changes across the shock advanced by Hugoniot, Rankine, and others is discussed.

section 6 the Hugoniot case is considered where the pressure-density relation is not unaltered across shocks. In the two sections, 7 and 8, von Neumann's method is described. Section 9 contains a very condensed outline of a method proposed by R. v. Mises in a colloquium lecture at Harvard in May 1947.

I. The Problem

Consider the one-dimensional nonsteady motion of a compressible ideal gas. Denote by t, x, u, ρ, v, and p, the time, the coordinate of a particle, its velocity, the density, the reciprocal density ($v = 1/\rho$), and the pressure. The *equation of continuity* reads

$$\frac{\partial}{\partial x}(u\rho) + \frac{\partial \rho}{\partial t} = 0 \tag{1}$$

This equation is satisfied if we set

$$\rho = \frac{\partial \psi}{\partial x}, \qquad u\rho = -\frac{\partial \psi}{\partial t}. \tag{1'}$$

Then, for $dx/dt = u$

$$d\psi = \frac{\partial \psi}{\partial x}dx + \frac{\partial \psi}{\partial t}dt = \rho dx - u\rho dt = 0.$$

Hence the function ψ is constant along a particle path ("world line," a curve in the space-time plane). At a fixed moment t

$$d\psi = \rho dx, \qquad \text{or} \qquad \psi = \int_{x_0}^{x} \rho dx.$$

Hence ψ is the mass in a column of unit cross section between the planes x_0 and x. It can be used as the "label" in Lagrange's form of the equation of motion and we consider x, u, and ρ as functions of the two independent variables ψ and t.

For each particle the "material derivative" of the abscissa with respect to time is simply $\partial x/\partial t$, and the second derivative is $\partial^2 x/\partial t^2$. Newton's *equation of motion* then becomes, if friction and external forces are omitted

$$\rho \frac{\partial^2 x}{\partial t^2} = -\frac{\partial p}{\partial x} \tag{2}$$

or, using (1')

$$\frac{\partial^2 x}{\partial t^2} = -v\frac{\partial p}{\partial x} = -\frac{\partial p}{\partial \psi}. \tag{2'}$$

The pressure, p, is connected with the reciprocal density, v, and the absolute temperature, T, by the *equation of state*

$$pv = RT.$$

If the changes of state are adiabatic, heat conduction and friction are neglected, the preceding equation leads to the isentropic relation:

$$pv^\kappa = a^2 \qquad (\kappa = 1.4) \tag{3}$$

where a^2 is constant for each particle. If, in addition, at $t = 0$, all a^2 values are equal, a^2 is the same for all particles and all time, and (3) constitutes an "absolute" relation between pressure and density. According to the Rankine-Hugoniot theory equation (3) is abandoned in the case of a discontinuous motion. It is assumed that, along a world line, $\psi =$ const., a^2 remains constant as long as the changes in state are continuous, that means, as long as no "shock line" is crossed. If the world line crosses a shock, at time $\bar{t}$ the a^2 changes from a value a'^2 to another value a''^2, which remains constant on the world line up to the crossing of the next shock. In other words, at time $\bar{t}$ the value a^2 has a jump discontinuity with $a^2(\bar{t} - 0) = a'^2$ and $a^2(\bar{t} + 0) = a''^2$.

We shall start with considering the approximation, which corresponds to Riemann's original ideas where one and the same *pressure-density relation holds for all particles and all time, even across shocks.* This relation may be written in a general form:

$$p = p(v). \tag{4}$$

The existence of a throughout relation (4) is assumed by von Neumann as well. Such an equation, which implies that the pressure depends on the density only, holds approximately in certain circumstances, *e.g.*, in the adiabatic motion in case of weak shocks.[3] Our computation method will be explained first under assumption (4), then under the more general assumption mentioned above where discontinuous changes in the pressure density relation are admitted when a particle line, $\psi =$ const., crosses a shock.

If the throughout relation (4) is assumed, the equation of motion takes the form

$$\frac{\partial^2 x}{\partial t^2} = -\frac{\partial p(v)}{\partial \psi} \qquad \text{where} \qquad v = \frac{\partial x}{\partial \psi} \tag{2''}$$

[3] Supersonic flow and shock waves. A manual on the mathematical theory of non-linear wave motion. Prepared for the Applied Mathematics Panel, N.D.R.C. by the Applied Mathematics Group, New York University [*A.M.G., N.Y.U.* 62, *A.M.P. Rept.* 38.2R (1944)]. This important manual (to be quoted in the following as *Man.*) contains an extensive bibliography up to 1944. See regarding (4), *Man.* pp. 81, 92.

or

$$\frac{\partial^2 x}{\partial t^2} = -p'(v)\frac{\partial v}{\partial \psi} = -p'(v)\frac{\partial^2 x}{\partial \psi^2}. \tag{2}$$

Since p' is necessarily <0 this equation is of hyperbolic type.

Particular cases of (4) which might be considered, are:

$$p = p_0 - c^2 v \tag{a}$$
$$p = 1 - v + b^2 v^2 \tag{b}$$
$$pv = \text{const.} \tag{c}$$
$$pv^\kappa = \text{const.} = a^2. \tag{d}$$

Under these assumptions the equation of motion becomes respectively:

$$\frac{\partial^2 x}{\partial t^2} = c^2 \frac{\partial^2 x}{\partial \psi^2} \tag{a'}$$
$$\frac{\partial^2 x}{\partial t^2} = \frac{\partial^2 x}{\partial \psi^2}\left[1 - 2b^2 \frac{\partial x}{\partial \psi}\right] \tag{b'}$$
$$\frac{\partial^2 x}{\partial t^2} = \frac{\text{const.}}{(\partial x/\partial \psi)^2} \cdot \frac{\partial^2 x}{\partial \psi^2} \tag{c'}$$
$$\frac{\partial^2 x}{\partial t^2} = \frac{a^2 \kappa}{(\partial x/\partial \psi)^{\kappa+1}} \cdot \frac{\partial^2 x}{\partial \psi^2}. \tag{d'}$$

Except in the first case these equations are nonlinear. We shall consider in the first five sections the case (d) only.

The *boundary conditions* for the hyperbolic equation (2), or, more specifically, (d') are as follows:

For $t = 0$, and between $\psi = 0$ and $\psi = l$, x as well as u are given functions of ψ. 1)

For $\psi = 0$ and for $\psi = l$, the value of x (or of u) is given for all $t > 0$. 2)

In particular, we shall consider the motion between two rigid walls if the fluid has, for $t = 0$, a constant density ρ_0 and a constant velocity u_0 directed to the left. Then 1) and 2) take the form:

For $t = 0$: $x = \psi/\rho_0$, and $u = u_0 < 0$ $1^+)$

For $\psi = 0$ and $\psi = l$: $x = 0$ and $x = l$ for all $t \geqq 0$. $2^+)$

From $\rho = \rho_0$ it follows by (4) that for $t = 0$ the pressure is constant too, $p = p_0$. We may set $\rho_0 = p_0 = 1$. Then, if (d) is used, $a^2 = 1$

everywhere. Moreover, we assume $u_0 = -1$. We then have, writing u', v', ρ', p' instead of u_0, v_0, ρ_0, p_0:

$$t = 0\colon\ x = \psi,\ u = u' = -1,\ v' = \rho' = p' = 1, \text{ and in (d) } a^2 = 1 \qquad (5)$$

$$\psi = 0 \text{ and } \psi = l\colon\ u = u'' = 0 \text{ for } t > 0. \qquad (5')$$

Equation (d′) together with (5), (5′) defines the problem.

The boundary conditions (5) and (5′) are not continuous throughout. In fact at $\psi = 0$, $t = 0$ as well as at $\psi = l$, $t = 0$ the value of the velocity u is discontinuous. This is a simple way to construct a problem that gives rise to a *shock* (at $\psi = t = 0$) and to a *rarefaction wave* (at $\psi = l$, $t = 0$). It has however been pointed out repeatedly that in nonlinear problems shocks may appear without being caused by initial discontinuities. In fact, in a nonlinear problem a motion continuous at the beginning need not remain continuous.

The boundary value problem ($\bar{2}$), (5), (5′) has a well-known solution essentially due to Riemann for $t \leqq t_0$; the meaning of t_0 will be indicated presently. This solution is formed by means of several analytic expressions. From this solution, known in the rectangle $0 \leqq \psi \leqq l$, $0 \leqq t \leqq t_0$, follow the values of x and u along $t = t_0$ (Section III). These values, together with the known values of x along the vertical lines $\psi = 0$ and $\psi = l$, form again a complete set of boundary conditions for extending the solution beyond $t = t_0$. However, just as for $t \leqq t_0$, the straightforward application of Riemann's integration method is not feasible, since the shock line extends, apparently, beyond $t = t_0$. This shock line is an *unknown curve* in the x-t-plane along which the first partial derivatives of x, *i.e.*, velocity and reciprocal density (and consequently pressure) change in a discontinuous way. It acts as an unknown boundary between two domains in which the problem of finding a solution $x = x(\psi,t)$ of our boundary value problem presents very different aspects (see Section IV).

In the two sections immediately following, the solution in the rectangle mentioned above and, in particular, along $t = t_0$ will be explicitly derived. The reader sufficiently familiar with this matter may omit these two sections.

II. Solution of the Boundary Value Problem for $t \leqq t_0$

In the rectangle $0 \leqq \psi \leqq l$, $0 \leqq t \leqq t_0$ a solution $x = x(\psi,t)$ can be determined. It is continuous everywhere and has continuous first partial derivatives with the only exception of a straight line through the origin, the shock line. Along this line the solution is continuous but both partial derivatives have jump-discontinuities. The second derivatives are continuous everywhere in the rectangle, except along two straight

lines emanating at the point $\psi = l$, $t = 0$, the rarefaction lines, and, of course, along the shock line they do not exist.

The equation of the shock line as well as the values of $\partial x/\partial \psi = v$ and $\partial x/\partial t = u$ on both sides of the shock will be determined by (5), (5'), (4) and *the two "mechanical" shock conditions*, or transition conditions.

First Particular Solution. Consider in the x-t-plane (ψ being a parameter) the family of straight lines:

$$x = \frac{\psi}{\rho_0} + u_0 t + \text{const.} \tag{6}$$

This function of ψ and t satisfies the differential eq. $(\bar{2})$, for any p-v-relation, and the boundary conditions 1^+).

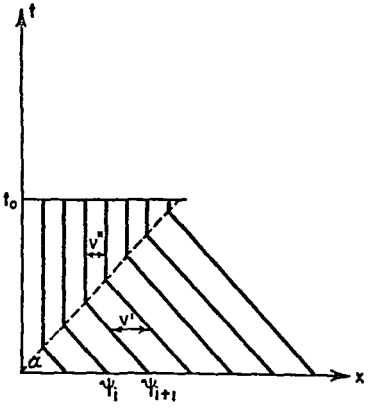

FIG. 1.—First particular solution with rectilinear shockline.

The vertical lines

$$x = a\psi + \text{const.} \tag{7}$$

satisfy $(\bar{2})$ and the condition 2^+).

By means of these two families (6) and (7) a solution of $(\bar{2})$ with discontinuous first derivatives along a straight *shock line* S is formed which satisfies 1^+), and 2^+) at $\psi = 0$ (Fig. 1). Call ρ', v', u', p' and ρ'', v'', u'', p'' the values in the two domains separated by S. ($\rho', \cdots p'$ are the values at the *"front"* side of the shock, $\rho'', \cdots p''$ these on the "back" side or behind the shock. As time goes on, the particle crosses the shock from the front towards the back.) The slope of the shock line, the *shock velocity* will be called $U = d\bar{x}/dt$.

Expressing the geometric fact that a particle line extends continuously across the shock we get (Fig. 1)

$$\frac{v''}{\sin(90 - \alpha)} = \frac{v'}{\sin\alpha + \cos\alpha}.$$

Hence with $\tan\alpha = 1/U$ and $v' = 1$

$$v'' = \frac{U}{1 + U} \qquad \text{or} \qquad U = \frac{1}{\rho'' - 1}. \tag{8}$$

Equation (8) is nothing but the *first shock condition*, the condition of *conservation of mass* across the shock:

$$\rho'(U - u') = \rho''(U - u''). \tag{8'}$$

If we put here $\rho' = 1$, $u' = -1$, $u'' = 0$ we find (8). The quantity on each side of (8) represents the *mass flux* M: $\rho'(U - u') = \rho''(U - u'') = M$.

Next, we consider the *second shock condition*, condition of *conservation of momentum* in the form:

$$(u' - u'')^2 = (p'' - p')(v' - v''). \tag{9}$$

Here $p' = v' = 1$, $u' = -1$, $u'' = 0$. Then (9) together with (4) in the form:

$$pv^\kappa = 1 \tag{4'}$$

permit us to find v''. In fact we get the equation:

$$v^{\kappa+1} - 2v^\kappa - v + 1 = 0 \qquad (\kappa = 1.4). \tag{10}$$

The function to the left equals 1 for $v = 0$ and -1 for $v = 1$, hence there is a root between 0 and 1. This root, for $\kappa = 1.4$, has been found

$$v = v'' = .46926 \qquad \text{and} \qquad \rho'' = \frac{1}{v''} = 2.1310. \tag{10'}$$

Then from (8)

$$U = .88416. \tag{10''}$$

Let us add the following remark: the shock line S (like any curve in the x-t-system) is known if at every time t one knows the corresponding label ψ, *i.e.*, the label just thrown into the shock. Then

$$\psi = \bar{\psi}(t) \qquad \text{and} \qquad x = \bar{x}(\bar{\psi}(t), t) = \bar{x}(t)$$

is the equation of the shock line in the ψ-t- and in the x-t-system respectively and:

$$U = \frac{d\bar{x}}{dt} = \frac{\partial \bar{x}}{\partial t} + \frac{\partial \bar{x}}{\partial \psi}\frac{d\bar{\psi}}{dt} = u' + v'\frac{d\bar{\psi}}{dt}$$

comparing this with (8') it follows that

$$\frac{d\bar{\psi}}{dt} = M, \tag{8''}$$

a consequence of (8') that will be used in our numerical method.

We see that, since we assumed (4) we had no use for the *third shock condition* (see Section VI) in order to determine the shock line as well as u'', v'', p''.

A *second particular solution* of $(\bar{2})$ without discontinuity in the first derivatives is also due to Riemann. Write (4) in the form:

$$p = \varphi(\rho). \tag{11}$$

Put

$$\frac{d\varphi}{d\rho} = c^2 \text{ (“local sound speed”)} \tag{11'}$$

and introduce

$$f(\rho) = \int_0^\rho c \frac{d\rho}{\rho}. \tag{11''}$$

Next, assume u to be a function of ρ alone, namely

$$u = \pm f(\rho) + C \qquad \text{or} \qquad \pm c = \rho \frac{du}{d\rho}. \tag{12}$$

Introduce

$$m = u \pm c \tag{13}$$

and consider the family of straight lines through $t = 0$, $x = l$:

$$x - mt = l \qquad \text{or} \qquad \frac{x - l}{t} = u \pm c. \tag{14}$$

It follows that along each of the lines (14) ρ and u are constant:

$$\frac{\partial \rho}{\partial t} + \frac{\partial \rho}{\partial x} \cdot m = 0 \qquad \text{and} \qquad \frac{\partial u}{\partial t} + m \frac{\partial u}{\partial x} = 0.$$

From the first of these equations we get

$$\begin{aligned} \frac{\partial \rho}{\partial t} &= -m \frac{\partial \rho}{\partial x} = (-u \mp c) \frac{\partial \rho}{\partial x} = -\left(u + \rho \frac{du}{\partial \rho}\right) \frac{\partial \rho}{\partial x} \\ &= -u \frac{\partial \rho}{\partial x} - \rho \frac{du}{d\rho} \frac{\partial \rho}{\partial x} = -u \frac{\partial \rho}{\partial x} - \rho \frac{\partial u}{\partial x} \end{aligned}$$

and this is the continuity equation (1). Also

$$\begin{aligned} \frac{\partial u}{\partial t} + u \frac{\partial u}{\partial x} &= -m \frac{\partial u}{\partial x} + u \frac{\partial u}{\partial x} = \mp c \frac{\partial u}{\partial x} \\ &= \pm \frac{\partial u}{\partial x} \frac{\varphi'(\rho)}{c} = -\frac{\partial u}{\partial x} \frac{\varphi'(\rho)}{\rho} \frac{d\rho}{du} = -\frac{\varphi'(\rho)}{\rho} \frac{\partial \rho}{\partial x} \end{aligned}$$

and this is the equation of motion (2).

The signs are to be chosen as follows

$$m = u - c = u - \sqrt{\varphi'(\rho)}$$
$$u = -f(\rho) + C, \qquad f(\rho) = \int^{\rho} c\,\frac{d\rho}{\rho} \tag{15}$$
$$x - mt = l$$

Under the law (d) with $a^2 = 1$ we then have

$$\varphi(\rho) = \rho^{\kappa}, \qquad c^2 = \kappa\rho^{\kappa-1} \qquad f(\rho) = \frac{2\sqrt{\kappa}}{\kappa - 1}\,\rho^{\frac{\kappa-1}{2}} = \frac{2c}{\kappa - 1} \tag{16}$$

Along each of the m-lines, u has a constant value. We call the m-line along which $u = u' = -1$ the *first rarefaction line* (r.l.) its slope m_1, and the density and reciprocal density along it ρ_1 and r_1. The m-line along which $u = u'' = 0$ is called *second rarefaction line* with slope m_2 density ρ_2, and reciprocal density r_2. Hence m_1 is the velocity at the front of this "rarefaction wave" or "expansion wave," m_2 the velocity at its back. This is a "centered rarefaction wave" (see *Man.* p. 53) The solution between the two rarefaction lines will be called *rarefaction solution.* If we write the equation of the problem with x and t as independent variables it takes the form

$$(c^2 - u^2)\,\frac{\partial^2\psi}{\partial x^2} - 2u\,\frac{\partial^2\psi}{\partial x\partial t} - \frac{\partial^2\psi}{\partial t^2} = 0$$

which shows that the lines (14) with slopes m, according to (13), are characteristics of the rarefaction solution. In this solution the initial discontinuity at $\psi = l$, $t = 0$ is smoothed out, immediately. (The initial discontinuity at $\psi = 0$, $t = 0$ is propagated along the shock line.)

Since $\rho = 1$ we get from (15) and (16)

$$m_1 = -1 - \sqrt{\varphi'(1)} = -1 - \sqrt{\kappa} = -2.18322$$
$$C = \frac{2\sqrt{\kappa}}{\kappa - 1} - 1$$
$$\rho_2 = \left(\frac{1 + 2\sqrt{\kappa} - \kappa}{2\sqrt{\kappa}}\right)^{\frac{2}{\kappa-1}} \tag{17}$$
$$m_2 = 0 - \sqrt{\kappa}\,\rho_2^{\frac{\kappa-1}{2}} = -\tfrac{1}{2}(1 + 2\sqrt{\kappa} - \kappa) = -.98322$$

and from (17)

$$\rho_2 = -\left(\frac{m_2}{\sqrt{\kappa}}\right)^5$$

$$v_2 = \frac{1}{\rho_2} = 2.5238 \tag{18}$$

$$m_2 - m_1 = \tfrac{1}{2}(\kappa + 1) = 1.2.$$

The values of ρ_2, v_2, and p_2 define the state behind the r. wave.

Along *any* m-line between the first and the second r.l. we get, using (15), by an easy computation

$$\rho = \left(\frac{1 + 2\sqrt{\kappa} - \kappa - m(\kappa - 1)}{\sqrt{\kappa}\,(\kappa + 1)}\right)^5$$

$$u = \frac{2m + 2\sqrt{\kappa} + 1 - \kappa}{1 + \kappa} = \frac{2}{\kappa + 1}(m_1 - m_2). \tag{19}$$

The values of u and ρ_2 in (19) reduce along the first r.l. to $u' = -1$, $\rho' = 1$ and along the second r.l. to $u'' = 0$ and the value of ρ_2 in (17).

Let us now find the *point of intersection of the shock line* $x = Ut$ and the first r.l., $x = l + m_1 t$. They intersect at the point:

$$t_0 = \frac{l}{U - m_1}, \qquad \bar{x}_0 = \frac{Ul}{U - m_1}. \tag{20}$$

For $t \leqq t_0$ and $0 \leqq \psi \leqq l$ we have now a complete solution of our boundary value problem: (1) In the trapezoid $t = 0$, $t = t_0$, $x = 0$, $t + x = t_0 + \bar{x}_0$ it consists of the family of parallel straight lines (6) with slope $-45°$ which are extended beyond the shock line by the vertical straight lines. (2) In the remainder of the rectangle $0 \leqq \psi \leqq l$, $0 \leqq t \leqq t_0$ the solution is given between the horizontal line $t = 0$ and the first r.l. by the same famly of $-45°$-lines as in (1); beyond the first r.l. and between the first and the second r.l. these same straight lines are extended (with continuous first derivatives) by the rarefaction solution, *i.e.*, a family of curves that are determined by (19) and that can easily be given explicitly (see next section). Those curves of this family that reach the second r.l. before reaching the line $t = t_0$ continue beyond the second r.l. as vertical straight lines (see Fig. 7).

Hence a solution is known as $t \leqq t_0$. The values x of this solution and of its first derivative $\partial x/\partial t = u$ at $t = t_0$ will be the initial values for the computation beyond the time t_0 of collision. Besides, the conditions (5′) hold at $\psi = 0$ and $\psi = l$.

III. The Initial Values for the Computation Beyond the Collision

We shall now determine x in terms of ψ along the line $t = t_0$. We may choose the point t_0, $\bar{x}_0$ as a new origin and use (occasionally) the coordinates $\xi = x - \bar{x}_0$, $\tau = t - t_0$. The label ψ will now be chosen in such a way that *the line* $\psi = 0$ *goes through the point* $(t_0,\bar{x}_0)$. The equations (6) and (7) then become

$$x - \bar{x}_0 = u_0(t - t_0) + \psi \qquad \text{or} \qquad \xi + \tau = \psi \tag{6'}$$

and

$$x = v''\psi + \bar{x}_0 \qquad \text{or} \qquad \xi = .46926\psi. \tag{7'}$$

The region of validity of (6') and (7) was indicated at the end of section 2. In the following we choose arbitrarily $t_0 = 12$ and determine $\bar{x}_0$ and l accordingly:

$$t_0 = 12, \qquad \bar{x}_0 = 12U = 10.6099, \qquad l = t_0(U - m_1) = 36.8086. \tag{21}$$

Let us call x_2 the point of intersection of $t = t_0$ with the second r.l.; we have because of the last equation (18):

$$x_2 - \bar{x}_0 = 14.4. \tag{21'}$$

To find $x = x(\psi,t_0)$ we may use either of expressions (19). We have *e.g.*,

$$\rho = \left(\frac{1.96644 - 0.4m}{2.83992}\right)^2 \tag{22}$$

and because of $v = \dfrac{1}{\rho} = \dfrac{\partial x}{\partial \psi}$

$$\psi = \int_{x_0}^{x} \rho dx = t_0 \int_{m_1}^{m} \rho dm. \tag{22'}$$

Integration of (22') gives ψ in terms of $m = \dfrac{x - l}{t_0}$ and inversely x in terms of ψ at $t = t_0$. We shall however rather use (19) and determine $x = x(\psi,t)$ for all $t \leqq t_0$. Thus we consider

$$u = \frac{dx}{dt} = \frac{2}{1 + \kappa}\,\frac{x - l}{t} + C \qquad \text{where} \qquad C = \frac{1 + 2\sqrt{\kappa} - \kappa}{1 + \kappa}. \tag{19'}$$

The differential equation

$$\frac{dx}{dt} = a\,\frac{x - l}{t} + b$$

has the integral

$$x = \frac{b}{1-a}t + l + Kt^a.$$

Here

$$a = \frac{2}{1+\kappa} = \frac{5}{6}, \qquad b = \frac{2\sqrt{\kappa}+1-\kappa}{1+\kappa} = \frac{-2m_2}{1+\kappa}, \qquad \frac{b}{1-a} = -5m_2.$$

Hence, with $a = \frac{5}{6}$:

$$x = l - 5m_2 t + Kt^a. \tag{23}$$

In order to find K in terms of ψ, we use the equation of the first r.l. in terms of ψ and t; this is, from (6'), $t = t_0 + \dfrac{\psi}{1+m_1}$ the curves (23) intersect the first r.l. for $t = \left(\dfrac{K}{m_1+5m_2}\right)^{\frac{1}{1-a}}$. Equating these t-values we find for K:

$$\begin{aligned} K &= (m_1 + 5m_2)\left(t_0 + \frac{\psi}{1+m_1}\right)^{\frac{1}{a}} \\ &= -6\sqrt{\kappa}\left(t_0 - \frac{\psi}{\sqrt{\kappa}}\right)^{\frac{1}{a}}. \end{aligned} \tag{24}$$

The curves between the two r.l.'s are thus given by (23), (24).

Finally the vertical lines that extend these curves beyond the second r.l. are

$$x - x_2 = v_2(\psi - \psi_2) \tag{25}$$

where $x_2 = \bar{x}_0 + 14.4$, $v_2 = 2.52387$ (see Eq. (18)) and ψ_2 is the value of ψ which in (23), (24) corresponds to $x = x_2$, $t = t_0$.

From (7'), (23), (24), (25) we get for $t = t_0$ by means of an elementary computation

$$x = \begin{cases} \bar{x}_0 + v''\psi \cdots\cdots\cdots\cdots\cdots\cdots & 0 \leqq x \leqq \bar{x}_0 \\ \bar{x}_0 + 6\sqrt{\kappa}\, t_0 \left\{1 - \left(1 - \dfrac{\psi}{t_0\sqrt{\kappa}}\right)^{\frac{1}{a}}\right\} \cdots & \bar{x}_0 \leqq x \leqq x_2 \\ x_2 + v_2(\psi - \psi_2) \cdots\cdots\cdots\cdots\cdots & x_2 \leqq x \leqq l \end{cases} \tag{26}$$

or substituting the numerical values

$$x = \begin{cases} \bar{x}_0 + .46926\psi \cdots\cdots\cdots\cdots\cdots\cdots & 0 \leqq x \leqq x_0 \\ \bar{x}_0 + 85.1916\{1 - (1 - .0704295\psi)^{\frac{1}{a}}\} \cdots & \bar{x}_0 \leqq x \leqq x_2 \\ \bar{x}_0 + 14.4 + 2.52387(\psi - \psi_2) \cdots\cdots\cdots & x_2 \leqq x \leqq l. \end{cases} \tag{26'}$$

Since we know $x = x(\psi,t)$ for $t \leqq t_0$ we know $u = \partial x/\partial t$ for $t = t_0$. This is however equivalent, in the approximation that will be used for the computations, to knowing x in terms of ψ at $t = t_0$ and at $t = t_0 - \Delta t$. This last dependence follows from (23), (24) and gives $x \equiv x^{(-1)}$ in terms of ψ, t_0, and Δt. Now call ζ the intersection $t = t_0 - \Delta t$ with the shock line, ζ_1 and ζ_2 the intersections of the same horizontal line with the two r.l.'s respectively, then:

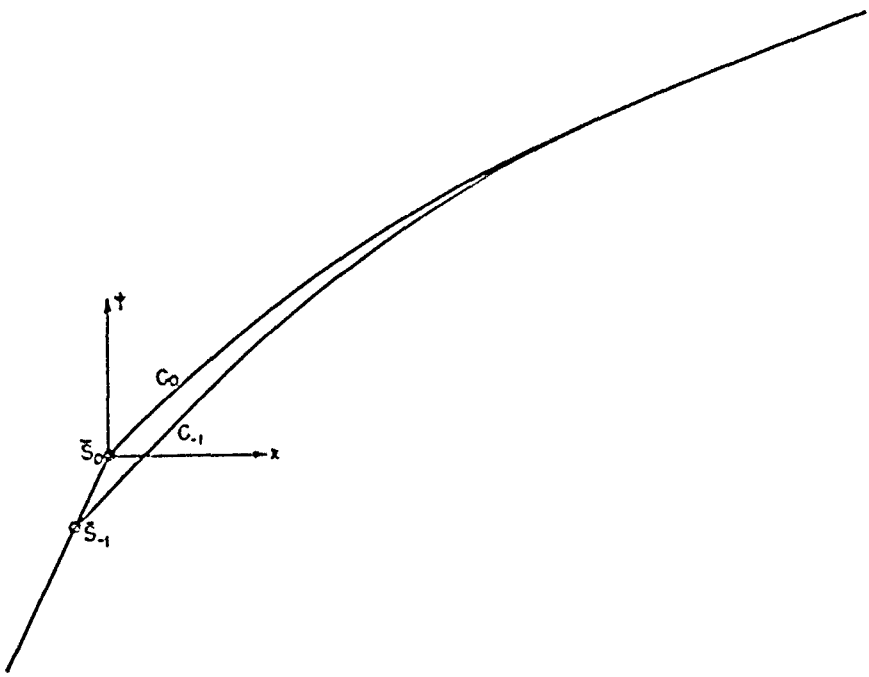

FIG. 2.—The curves C_0: $\psi = \psi(x; t_0)$ and C_{-1}: $\psi = \psi(x; t_0 - \Delta t)$.

$$\zeta = \bar{x}_0 - U\Delta t, \qquad \zeta_1 = \bar{x}_0 - m_1\Delta t, \qquad \zeta_2 = x_2 - m_2\Delta t \tag{27}$$

where m_1, m_2, $\bar{x}_0$, x_2 are given by (17), (20), (21′). We then have:

$$x = \begin{cases} \bar{x}_0 + v''\psi \cdots\cdots\cdots\cdots x \leqq \zeta \\ \bar{x}_0 + \Delta t + \psi \cdots\cdots\cdots \zeta \leqq x \leqq \zeta_1 \\ x^{(-1)} \cdots\cdots\cdots\cdots\cdots \zeta_1 \leqq x \leqq \zeta_2 \\ x_2 + 2.52387(\psi - \psi_2) \cdots \zeta_2 \leqq x \leqq l. \end{cases} \tag{28}$$

We shall see in the next section that in (26) and (28) we need, strictly speaking, each time the first (linear) dependence only. We shall however use the complete sets (26) and (28) in order to compare the results of our computational method with exact results. So far all we have done has been to adapt Riemann's solutions to our particular problem.

In order to visualize the relations (26), (28), and similar ones, let us interpret them in an (x,ψ)-coordinate system (Fig. 2). Choose x hori-

zontal, ψ vertical and consider the curve C_0, defined by (26) and the curve C_{-1} defined by (28). The curve C_0, or, as we may say, the curve $t = t_0$, is continuous everywhere and has a continuous derivative except at the point $x = \bar{x}_0$, $\psi = 0$, the shock *point*. In the x-t-diagram (Fig. 7) this is the point $\bar{x}_0$ where the line $t = t_0 = 12$ meets the first r.l. and the straight shock line S. The curve C_0 is monotonically increasing. The shock point divides it into a lower part, to the left, and a higher part, to the right. This lower (higher) part corresponds in the x-t-diagram to the part of $t = t_0$ to the left (right) of the shock point $x = \bar{x}_0$. In the x-ψ-diagram the lower part is the straight line given by the first formula

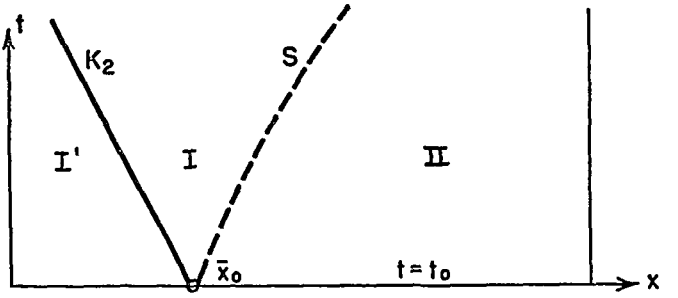

FIG. 3.—The three regions in the x-t-plane, adjacent to $t = t_0$.

(26[1]); the higher part is first curved according to (26[2]) then it continues in the straight line (26[3]), the transition being continuous and with continuous derivative ρ.

In the same way the curve $t = t_0 - \Delta t$ is given by (28). Using $\xi = x - \bar{x}_0$, the shock point is at $\xi_{-1} = -0.88416\Delta t$, $\psi_{-1} = -1.88416\Delta t$. The lower part of C_{-1} is the same straight line (26[1]) as before for C_0, but the higher part starts at $\bar{S}_{-1}(\xi_{-1},\psi_{-1})$ already and is given by the last three formulae (28); it is first, for a short distance, rectilinear, then curved, staying below the higher part of C_0; finally it meets the straight line (26[3]) [or (28[4])] at $\xi_2 = \zeta_2 - \bar{x}_0 = 14.4 + .98322\Delta t$.

IV. The Problem of Determining the Solution for $t > t_0$ and the Principle of the Proposed Numerical Method

After the collision of shock line and first r.l. we are faced with a completely different situation, which presents a difficult mathematical problem. The differential Eq. (2) is still valid and because of our assumption of a throughout relation (4) between pressure and density it will remain valid for $t > t_0$. The domain $t \geqq t_0$, $0 \leqq \psi \leqq l$ is divided into two parts I and II by the unknown shock line S (Fig. 3). In part II, which faces the front of the shock, everything is known, the solution $x = x(\psi,t)$ being given by (23), (24) and beyond the second r.l. by (7'),

which holds until a particle meets a shock line. This means in particular that if at a time t the corresponding particle $\bar{\psi}$ is known, *i.e.*, the label of the particle which at this time is thrown into the shock, then the $\bar{x}$ of this shock point can be found *exactly*. In part I we know x and u along the horizontal boundary $t = t_0$, $0 \leqq x \leqq \bar{x}_0$ and we know x along the left vertical boundary. The shock line S forms an *unknown* boundary. Along this unknown boundary however the two "mechanical" shock conditions (8′) and (9) are fulfilled and (4) holds everywhere. (The meaning of the line K_2 in Fig. 3 will be explained presently.)

On the other hand if the shock line S *were known*, *i.e.*, if we knew the relation between ψ and t that defines S, namely $\psi = \bar{\psi}(t)$ then, since S belongs to domain II as well, we should know $x = \bar{x}\,[\bar{\psi}(t),t] = \bar{x}(t)$, *i.e.*, the equation of S in the x-t-system and therefore $U = d\bar{x}/dt$ where $\frac{d\bar{x}}{dt} = \frac{\partial \bar{x}}{\partial t} + \frac{\partial \bar{x}}{\partial \psi}\frac{d\bar{\psi}}{dt} = u'' + v''\frac{d\bar{\psi}}{dt}$ [see (8′)]. Hence since $d\bar{\psi}/dt$ follows from $\psi = \bar{\psi}(t)$ we have a relation between u'' and v''; a second relation between these two values is given by (9) where u', v', p', are known and p'' follows from v'' by (4). Thus u'' and v'' could be found. But then we would obviously know too much because x alone along S is needed to determine the solution $x = x(\psi,t)$ in I and from this solution the two partial derivatives u'' and v'' *follow*. Hence, as von Neumann puts it, the super-determination along the unknown boundary should lead to its determination.

We may view the "balance" of the problem also in this way: At every point of the unknown line S we have *three* unknowns U, v'', and u'', which are linked by the *two* equations (8′), (9). Hence the necessary boundary condition along S which would, *e.g.*, consist in the knowledge of u'' along S, can *not* be determined independently of the *solution* of the differential equation (2).

The following remark is still due but does not change the essential situation: The known boundary conditions along $t = t_0$ (between $x = 0$ and $x = \bar{x}_0$) and along the vertical $x = 0$ allow the explicit determination of the solution in a part I′ of I which is unaffected by our ignorance of S. This part I′ (Fig. 3) is limited to the right by one of the two characteristics, K_2, passing through $(\bar{x}_0,t_0)$ (Fig. 3). Thus, in the rectangular triangle with the right angle at $x = 0$, $t = t_0$ and whose hypothenuse is this characteristic the solution is known and, obviously, consists of the vertical straight lines continued beyond $t = t_0$ (Fig. 7). The equation of this characteristic (see p. 208 and note that $u'' = 0$) is

$$x - \bar{x}_0 = -c(t - t_0) = -1.38(t - t_0).$$

Thus the difficulty we have been discussing exists in I, to the right of this line, only.

The problem becomes still more unusual if assumption (4) is dismissed. Then with the p-v-relation (3) we introduce along S at the back side of the shock a new unknown $a^2 = a''^2$. The third shock condition, the thermic condition, is available (see Section VI). Thus we have one more unknown and one more equation—or if we count p'' too as unknown we have to count the relation (3) between v'' and p''. The additional difficulty is however that the differential equation (d') contains a^2 explicitly. Hence not only is it impossible to indicate the necessary boundary conditions along S without solving at the same time the differential equation but, moreover, the coefficients of this differential equation depend explicitly on a^2 which, in turn, we do not know, as long as the boundary is unknown.

General methods to deal with problems of this type are unknown, Numerical methods seem to be in order. In the following we shall propose a straightforward and simple method, which we shall exemplify by means of the problem explained in the previous sections. We begin with the simpler case of an absolute relation (4) and shall consider the general case where the entropy changes across the shock in Section VI.

The Procedure of Computation. Replace the partial differential equation (d') by a difference equation. Using $\tau = t = t_0$:

$$\frac{x(\psi, \tau - \Delta t) + x(\psi, \tau + \Delta t) - 2x(\psi,\tau)}{(\Delta t)^2}$$

$$= \kappa \frac{x(\psi - \Delta\psi,\tau) + x(\psi + \Delta\psi,\tau) - 2x(\psi,\tau)}{(\Delta\psi)^2} \cdot \left[\frac{x(\psi - \Delta\psi,\tau) - x(\psi + \Delta\psi,\tau)}{2\Delta\psi}\right]^{2.4}$$

$$= \kappa \cdot 2^{2.4}(\Delta\psi)^{0.4} \cdot \frac{x(\psi - \Delta\psi, \tau) + x(\psi + \Delta\psi, \tau) - 2x(\psi,\tau)}{[x(\psi - \Delta\psi, \tau) - x(\psi + \Delta x, \tau)]^{2.4}}$$

It is more convenient to use subscripts and superscripts and to write for the now discontinuous variables τ and ψ:

$$\tau = r\Delta t, \qquad \psi = n\Delta\psi.$$

We then have, if we put $x(n\Delta\psi, r\Delta t) = x_n^{(r)}$:

$$\frac{x_n^{(r-1)} + x_n^{(r+1)} - 2x_n^{(r)}}{(\Delta t)^2} = \kappa \cdot 2^{2.4}(\Delta\psi)^{0.4} \frac{x_{n+1}^{(r)} + x_{n-1}^{(r)} - 2x_n^{(r)}}{[x_{n-1}^{(r)} - x_{n+1}^{(r)}]^{2.4}} \tag{29}$$

We shall put $\Delta\psi = 1$ and choose Δt so as to have an appropriate ratio $\Delta\psi/\Delta t$ (see next section). We then get writing

$$\kappa \cdot 2^{2.4} = 7.389 = A:$$

$$x_n^{(r+1)} = 2x_n^{(r)} - x_n^{(r-1)} + A \cdot (\Delta t)^2 \frac{x_{n+1}^{(r)} + x_{n-1}^{(r)} - 2x_n^{(r)}}{[x_{n-1}^{(r)} - x_{n+1}^{(r)}]^{2.4}} \tag{29'}$$

We then consider a fixed time τ. At this fixed time, τ, x will depend on ψ only, and we may talk of a "curve" C_τ in the x-ψ-plane (x horizontal, ψ vertical) although we know (at least for a part of C_τ) only discrete points of this curve. Instead of C_τ we prefer to write C_τ and shall explain now how a curve $C_{\tau+1}$ is derived from C_τ and $C_{\tau-1}(\tau = 0, 1, 2, \ldots)$. Let us say for the moment C_1, C_2, C_3 instead of $C_{\tau-1}$, C_τ, $C_{\tau+1}$. We assume that

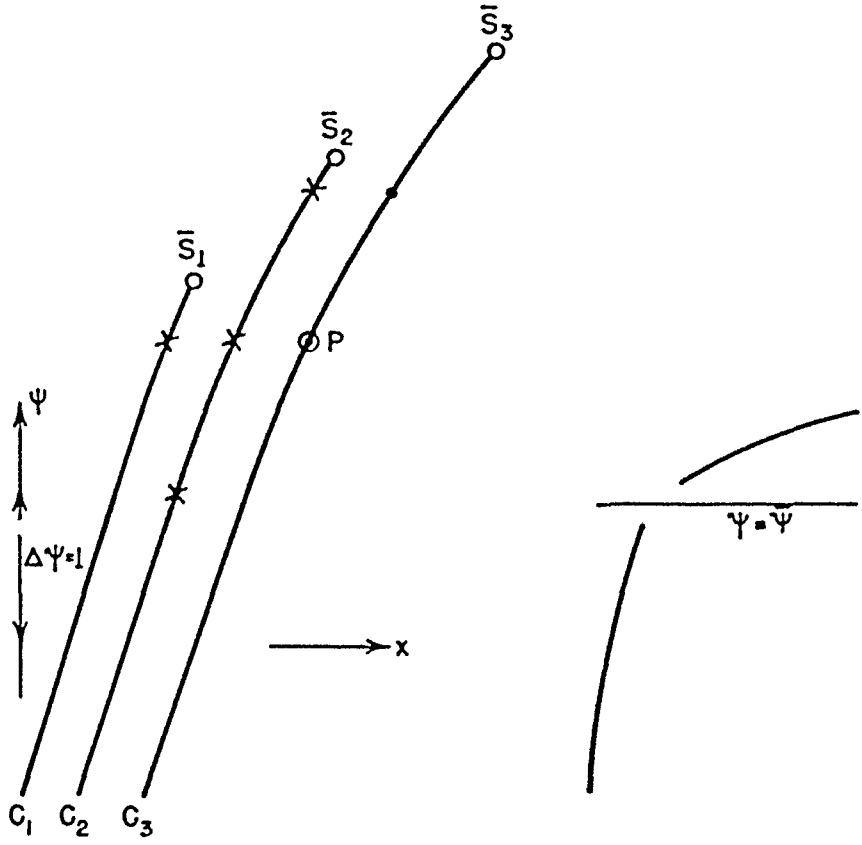

FIGS. 4 and 4a.—The computation of lattice points.

the new curve C_3 (just as C_1 and C_2), will have an upper part and a lower part separated by a shock point $\bar{S}_3$ the way it was for C_0 and C_{-1}. It is the lower part and the shock point that constitute the problem.

The Lower Part. Fig. 4 shows schematically the four points, one on C_1 and three on C_2 which are needed to compute a new point of C_3. If any of these four points are not available the new point cannot be found from (29′). First we compute from (29′) the points on C_3 that are determined by this recurrence formula. It is obvious that in order to *determine the lower part of C_3, points on the lower parts of C_1 and C_2 only are to be used.* The missing point that stops the recurrence procedure is often the highest point on the middle curve C_2, sometimes the point on C_1 or both. In our setup the lattice was chosen in such a way that the vertical distance $\Delta\psi$

between two consecutive shock points $\bar{S}_\tau$, $\bar{S}_{\tau+1}$ is always smaller than $\Delta\psi = 1$. Then, in general, one lattice point on the new curve remains undetermined and sometimes two, but never more than that. Fig. 4 illustrates these possibilities: On C_3 the last point is undetermined since one point on C_2 and one point on C_1 which would be needed are missing. On C_2 the two highest lattice points below the shock point are undetermined by the recurrence procedure. We shall discuss the problem of their determination presently.

The upper part of the new curve C_3 is exactly known because it consists of points in the rarefaction zone only which are not yet involved in the shock. Hence for any $\tau = r\Delta t$ we can compute exactly the x value as a function of ψ. Using the results (23), (24) we find in the same way as the second formula (26) was found:

$$x = \bar{x}_0 - 5\tau m_2 + 6\sqrt{\kappa}\, t_0 \left\{1 - \left(\frac{t_0 + \tau}{\tau}\right)^{\frac{1}{3}} \left(1 - \frac{\psi}{t_0\sqrt{\kappa}}\right)^{\frac{2}{3}}\right\} \tag{30}$$

or

$$x = \bar{x}_0 + 4.9161\tau + 85.1916 \left\{1 - \left(1 + \frac{\tau}{12}\right)^{\frac{1}{3}} \cdot (1 - .0704\psi)^{\frac{2}{3}}\right\} \tag{30'}$$

which for $\tau = 0$ reduces to (26). This formula holds for all x values between the shock point $\bar{S}_\tau = \bar{S}_\tau$ and the point of intersection of the line τ = constant with the second r.l. (Fig. 7). For $t = t_0$ this intersection was at $x_2 = \bar{x}_0 + 14.4$. In general the point of intersection $x_2(\tau)$ is given by

$$x_2(\tau) = \bar{x}_0 + 14.4 + \tau \cdot m_2$$

To the right of this intersection point, *i.e.*, for $x \geqq x_2(\tau)$ the x-ψ relation becomes linear with slope 2.52387 [see (26³)]. The region of validity of (30) becomes smaller and smaller as τ increases and shrinks to zero at the time T when the shock line crosses the second r.l. (It need hardly be said that this T has nothing to do with the notation used in section I for the absolute temperature.) We shall see that this happens in our problem approximately for $t = 18$, $\tau = 6$, $\psi = 7$. The relationship that then replaces (30) constitutes another accurate formula, which will be established later. At any rate, at any time τ the ψ-x-relation to the right (Fig. 7) of the shock point $\bar{S}_\tau$ is exactly known by (30) or an equivalent formula. This exact formula still holds for the shock point itself. That means: *If we know the $\bar{\psi}$ of the shock point we can compute exactly the corresponding $\bar{x}$ of $\bar{S}_\tau$ by (30) or its equivalent.*

We may differentiate (30) with respect to ψ and find the simple formula,

$$v' = \frac{\partial x}{\partial \psi} = \left(1 + \frac{\tau}{t_0}\right)^{\frac{1}{2}} \left(1 - \frac{\psi}{t_0\sqrt{\kappa}}\right)^{\frac{1}{2}} = \left(1 + \frac{\tau}{12}\right)^{\frac{1}{2}} (1 - .0704\psi)^{-\frac{1}{2}} \quad (31)$$

which we shall need presently.

The Shock Point. We assume that we know the "preceding curve" C_r with its shock point $\bar{S}_r(\bar{x}_r, \bar{\psi}_r)$. Denote by v_r', v_r'' the reciprocal densities at this point, v_r' being the slope of the exactly known upper part of C_r at the shock point $\bar{S}_r$, v_r'' that of the lower part at $\bar{S}_r$; also $\rho_r' = 1/v_r'$, $\rho_r'' = 1/v_r''$, $p_r' = (v_r')^{-\kappa}$, $p_r'' = (v_r'')^{-\kappa}$. Knowing $\bar{S}_r$ we know $\bar{x}_r$ and $\bar{\psi}_r$; next we compute v_r' from (31), and p_r' follows; as to v_r'' it has been computed in general by linear interpolation, *i.e.*, by joining the shock point $\bar{S}_r$ and the next lower lattice point; a few times an interpolation of higher order was used. From v_r'' we find p_r''. Next we compute, using the shock conditions (8′) and (9), the mass flux across the shock in the form:

$$M_r = \pm \sqrt{\frac{p_r'' - p_r'}{v_r' - v_r''}} \quad (32)$$

Denote by $\bar{\psi}_r = \bar{\psi}_r$ the ordinate of the shock point $\bar{S}_r$, by $\bar{\psi}_{r+1}$ the ordinate of the shock point at time $\tau + \Delta t = (r + 1)\Delta t$ and by

$$\Delta\bar{\psi}_r = \bar{\psi}_{r+1} - \bar{\psi}_r$$

the difference between these ordinates. Then, *the sign being positive in our problem*, we have according to (8″):

$$\Delta\bar{\psi}_r = M_r \Delta t, \qquad \bar{\psi}_{r+1} = \bar{\psi}_r + M_r \Delta t. \quad (33)$$

The right side of (33) is known by (32) as we know everything for $\bar{S}_r$, and thus $\Delta\bar{\psi}_r$ and the *ordinate* $\bar{\psi}_{r+1}$ *of the new shock point* follows. Knowing this ordinate the corresponding abscissa follows from (30) (or its equivalent for $t \geqq T$). Thus abscissa and ordinate of the new shock point $\bar{S}_{r+1}$ are found.

Finally, knowing the shock point and the whole upper part of C_{r+1} and its lower part, except one or two lattice points, these missing points can be found by interpolation. In general an interpolation of second order was used; however at the beginning, *i.e.*, for small τ-values, we used an interpolation of order three. Since for the recurrence formula (29′) a table of differences of second order of the x's with respect to ψ is needed, this interpolation works easily. Another way would have been to extrapolate the "missing points" on the lower parts of C_r and C_{r-1}.

It seemed however preferable to interpolate directly on $C_{\tau+1}$. The quadratic transition relation (9) should be identically satisfied, U, the slope of the shock line in the x-t-system, being given by $\frac{1}{\Delta t} \cdot (\bar{x}_{\tau\Delta t+\Delta t} - \bar{x}_{\tau\Delta t})$.

Reviewing the procedure it is obvious that the point open to criticism consists in the interpolation of the one or two missing lattice points on the lower part of $C_{\tau+1}$ and in the subsequent determination of $v''_{\tau+1}$ in which just these uncertain points are used. This is however in the nature of the problem since the unknown boundary depends on the solution of the differential equation and vice versa. The principle of the computation may be summarized as follows, the steps being given in the order in which they actually have been worked.

Suppose two "curves" $C_{\tau-1}$ and C_τ have been completely determined, i.e., at $\bar{S}_\tau$ we know also the first derivatives v_τ', v_τ''. In order to find $C_{\tau+1}$ we compute: (1) the coordinates of the new shock point $\bar{S}_{\tau+1}$ where $\psi_{\tau+1}$ is found by (32), (33) and $\bar{x}_{\tau+1}$ follows by (30) or its equivalent for $t \geqq T$. (2) The lower part of $C_{\tau+1}$ is found, point by point, by means of the recurrence formula (29') using the lattice points on the lower parts of C_τ and $C_{\tau-1}$. The one or two lattice points on $C_{\tau+1}$ that cannot be found in this way because of missing points in (29') are found by an interpolation applied to the new curve, in general, of second order. (3) The upper part of $C_{\tau+1}$ is computed from (30) or its equivalent for $t \geqq T$. (4) Returning to $\bar{S}_{\tau+1}$ we find $v'_{\tau+1}$ from (31), $v''_{\tau+1}$ by means of a linear interpolation between $\bar{S}_{\tau+1}$ and the next lower lattice point, and are then ready to determine $M_{\tau+1}$ and to start the procedure anew.

Let us finish this section by deriving a formula that replaces (30) for $t \geqq T$. (T, the time of intersection of the shock line and the second rarefaction line, depends of course on the shock line and cannot be found in advance, but only in the course of the computation of the shock line. This will be explained in the next section.) To T corresponds on the second r.l. an x-value $X = l + m_2 T$ and a ψ-value Ψ. The relation that holds between t and ψ along the second r.l. is found easily by differentiating (30) with respect to $t(t = t_0 + \tau)$, thus finding dx/dt, and putting $dx/dt = 0$ we get:

$$t = K(1 - .0704\psi), \qquad \text{with} \qquad K = t_0 \left(\frac{\sqrt{\kappa}}{m_2}\right)^6 = 24.4469. \quad (34)$$

Here the constant that multiplies ψ is the same as in (30), namely $1/t_0\sqrt{\kappa}$. By (34) we can compute for every particle the time when it intersects the second r.l. The corresponding x-value has been given before:

$$x_2(\tau) = \bar{x}_0 + 14.4 + \tau m_2, \qquad \text{where} \qquad \tau = t - t_0; \qquad \tau > 0. \quad (35)$$

We call *penetration region* (Fig. 7) the triangular domain between the *shock line*, the *second r.l.* and *the particle line* through the point of intersection of the shock line and the first r.l., *i.e.*, the *particle line numbered zero*. The particles whose $\psi < \Psi$ meet *first* the shock line and *then* the second r.l. whereas the particles with $\psi > \Psi$ meet the second r.l. *before* crossing the shock line. We call "final abscissa" of such a particle its abscissa at the intersection with the second r.l. because the particle will keep that abscissa all the way between the second r.l. and the shock line. These abscissae follow from (34) and, (35) by eliminating t.

$$\xi = x - \bar{x}_0 = 2.52387\psi - 9.6367. \tag{36}$$

Here $9.6367 = K - 14.4$ where K was defined in (34). We find, *e.g.*, for $\psi = 8$, $\xi = 10.554$. Now if ψ_1, ψ_2 are any two ψ-values and x_1, x_2 the corresponding x-values in (36) we see that

$$\xi_2 - \xi_1 = x_2 - x_1 = 2.524(\psi_2 - \psi_1) \tag{36'}$$

Hence the abscissa of a new shock point in the domain $t \geqq T$, $\psi \geqq \Psi$ is simply found by multiplying the $\Delta\psi$ found in (33) by 2.524 and adding this product to the abscissa of the preceding shock point. This is simpler than (30). The formula (31) for v_r' is simply replaced by

$$v_r' = v' = 2.52387 \tag{37}$$

and consequently

$$p' = .27359 \tag{37'}$$

Thus, beyond the point (X,T,Ψ) these constant values will be used.

Let us conclude with the following remark. In our problem the (unknown) shock line separates the rarefaction region II where the solution is explicitly known from a region I, where the solution is to be found (Fig. 3). Hence, if we know $\bar{\psi}_r$, the ordinate of the shock-point of the curve C_r in the x-ψ-system, the corresponding $\bar{x}_r$ can be found exactly by (30) or (36). This is a nice coincidence but may not be so in other problems; it fails, *e.g.*, in our problem for $t > T''$ where T'' is the time when the shock line meets the right vertical line, the "rigid wall" $x = l$. In general there may not be a region adjacent to S, with an *explicitly* known solution. In this case both parts of C_r, the lower and the upper part, which are separated by the shock point $\bar{S}_r$ are to be computed point by point the way it has been done so far for the lower part only. The abscissa of the shock point follows by interpolation in such a way that the two parts meet at a point of given level (see Fig. 4a). This has been done by the author successfully in the problem considered in this paper (Fig. 7) where we were able to check the results by means of the accurate rarefaction solution.

V. The Computations

We start with the remark that the curves C_r for various r are not "schlicht" but present an arrangement as shown schematically in Fig. 5. The lower (higher) part of a curve C_{r_1} intersects the higher (lower) parts of all curves with $r < r_1$, $(r > r_1)$. The lower parts without the higher parts are "schlicht" except for the fact that they all start at the same straight line (26′). The curve C_0 consists in its whole lower part of this

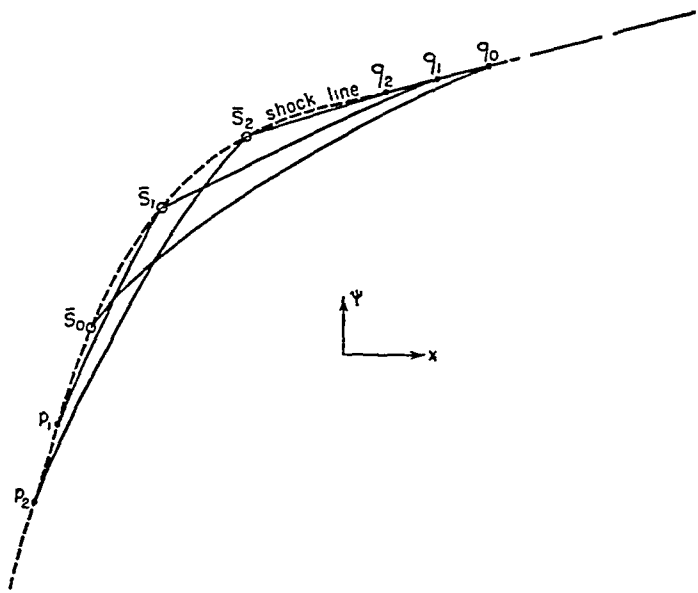

Fig. 5.—The curves C_r.

straight line; the lower part of C_1 coincides first with the same straight line, then at the point p_1, the curvilinear part begins; the curvilinear part of C_2 starts at p_2, etc. the higher parts as such are *schlicht* except for all meeting finally the straight line with slope $v' = 2.524$ at points q_0, q_1, q_2. . . .

The shock line in the x-ψ-diagram is the line joining the successive shock points (Fig. 5); our procedure furnishes corresponding to each τ (or r) one shock point $\bar{S}_\tau$. The shock line is monotonically increasing. For $t \leqq t_0$ it coincides with the straight line (26′). For $t_0 \leqq t \leqq T$ it is slightly curved. For $t \geqq T$ the shock line in the x-ψ-diagram is the straight line with slope $dx/d\psi = 2.524$.

It is not without interest to compute the higher part of the C-curves not only by the accurate formula (30) but by the recurrence formula (29′) as well and to compare the results. This has been done for a few t-values and the coincidence was good. It may be stated that, in our procedure,

the x-values of the lower part, computed by the *recurrence formula*, and those of the upper part computed, in general, by the *exact* formulas (30) or (36) are somewhat of different kinds. Consequently the small "missing" piece on the lower part that we interpolated between the exactly computed shock-point abscissa and the approximately computed lower part would look slightly different if extrapolated by means of the lower part alone.

So far no attempt has been made to estimate the error of the numerical procedure. It has, however, been observed that if for certain reasons a finer mesh was used in some interval the results and characteristic features which we shall describe became clearer and more outspoken.

Let us now investigate the bounds of the quotient $\Delta t/\Delta\psi$ to be used in the computations. If along a segment of a line $t = \text{const.}$ the values of x and $\partial x/\partial t$ are given, the solution of our hyperbolic differential equation is determined in a triangle whose sides are the segment and the characteristics passing through its end points. The equation of these characteristics for equation (d') is

$$(d\psi)^2 = \frac{a^2\kappa}{v^{\kappa+1}}(dt)^2 = \frac{c^2}{v^2}(dt)^2. \tag{38}$$

On the other hand, the solution of a numerical step-by-step procedure with steps of amount $\Delta\psi$ and Δt is determined in a triangle where the slopes of the legs are $\pm\Delta t/\Delta\psi$ (Fig. 6). It would be senseless to set up a procedure where the domain "computed" by the numerical method were not contained in the domain in which the solution is determined by the differential problem itself. Hence $\Delta t/\Delta\psi$ must not surpass the value $dt/d\psi$ defined by (38), or, since $a^2 = 1$:

$$\frac{\Delta t}{\Delta\psi} \leqq \sqrt{\frac{v^{\kappa+1}}{a^2\kappa}} = \frac{v^{1.2}}{\sqrt{\kappa}}. \tag{38'}$$

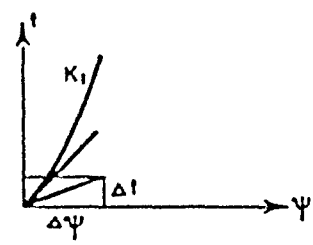

FIG. 6.—Bounds for the ratio $\Delta t/\Delta\psi$.

Now the minimum of $v = v''$ beyond $t = t_0$ is the value given by (10''), $v = .46926$. With this value we have $v^{1.2}/\sqrt{\kappa} = .34$. Hence we are safe if we take $\Delta t = \frac{1}{4}$. It would, of course, be better to carry out the computations with a smaller Δt. But since the computing, partly done to test the procedure, has been done just by means of logarithms it was tried to get results without too much bother. After several steps when the v-value had increased, an even larger $\Delta t = .4$ was used. Between $\tau = 5$ and $\tau = 6$ again $\Delta t = \frac{1}{4}$ was taken because of the nearness of T, the time of the intersection of the shock line and second r.l. With this

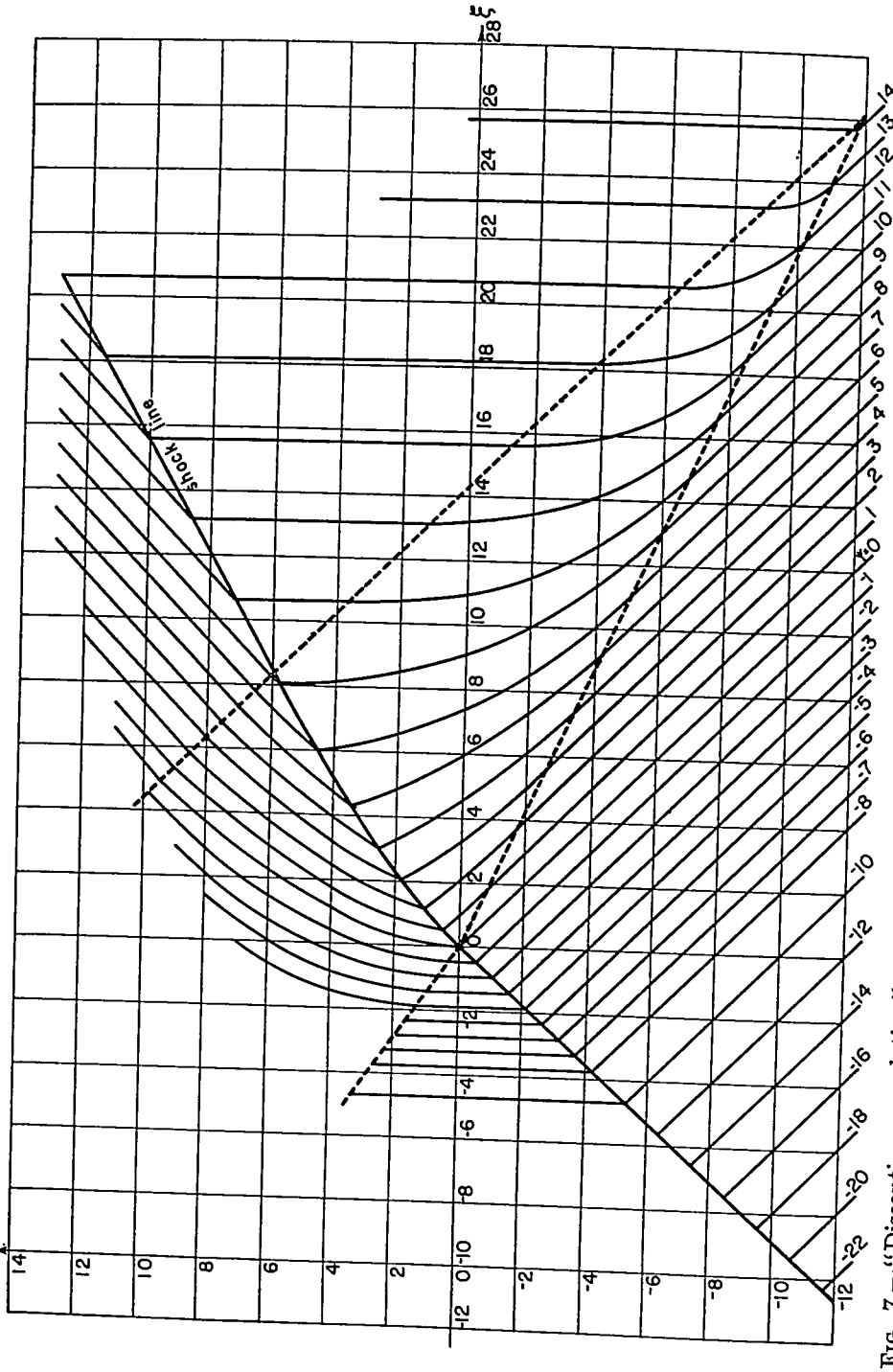

FIG. 7.—"Discontinuous solution" of the hydrodynamical problem by means of explicite expressions for $\tau \leqq 0$ and by the "step method" for $\tau > 0$.

choice of Δt and $\Delta\psi$ the vertical distance of two consecutive shock points $\bar{S}_\tau$ and $\bar{S}_{\tau+1}$ (*i.e.* $\bar{S}_{\tau\Delta t}$ and $\bar{S}_{(\tau+1)\Delta t}$) is never greater than $\Delta\psi = 1$.

In the penetration region the second differences (of x with respect to ψ) were always positive and, particularly for small τ-values, increasing with ψ. The positiveness of the second differences means that the reciprocal densities $v = 1/\rho$ increase with ψ (Fig. 7), which seems to be a characteristic feature in the penetration region. After the maximum-compression behind the shock the gas expands again under the influence of the rarefaction wave. Table 1 shows the x-values for $\tau = 0, 1, 2 \cdots$, $\psi = -8, -7, \cdots$. The values for intermediate τ's are not listed in the

TABLE 1

Coordinate $x = x(\tau,\psi)$. The Non Integer ψ-Values Denote Shock Points

ψ \ τ	0	1	2	3	4	5	6	7	8	9	10	11	12	13
−8	−3.75	−3.75	−3.75											
−7	−3.28	−3.28	−3.28											
−6	−2.82	−2.82	−2.81											
−5	−2.35	−2.35	−2.33	−2.23										
−4	−1.85	−1.85	−1.81	−1.69	−1.50	−1.13	−0.67	−0.08						
−3	−1.41	−1.41	−1.31	−1.15	−0.87	−0.50	−0.02	0.59	1.32					
−2	−0.91	−0.93	−0.81	−0.59	−0.25	0.16	0.65	1.29	2.01	2.85				
−1	−0.47	−0.42	−0.27	−0.01	0.37	0.83	1.40	2.03	2.76	3.61	4.65			
0	0.00	0.09	0.28	0.60	1.02	1.55	2.15	2.81	3.55	4.41	5.40	6.58		
1		0.62	0.87	1.23	1.70	2.28	2.92	3.62	4.40	5.25	6.26	7.37		
1.76		1.038												
2			1.47	1.89	2.42	3.02	3.71	4.47	5.28	6.19	7.18	8.27	9.46	
3			2.10	2.67	3.13	3.80	4.53	5.34	6.22	7.17	8.17	9.23	10.35	
3.25			2.25											
4				3.27	3.90	4.61	5.39	6.26	7.21	8.19	9.20	10.23	11.31	12.43
4.48				3.62										
5					4.68	5.46	6.30	7.23	8.22	9.23	10.25	11.27	12.31	13.39
5.53					5.11									
6						6.37	7.25	8.23	9.25	10.25	11.31	12.32	13.35	14.40
6.43						7.71								
7							8.25	9.23	10.25	11.31	12.34	13.38	14.41	15.43
7.15							8.41							
7.82								10.09						
8									11.31	12.35	13.39	14.42	15.45	16.48
8.50									11.81					
9										13.39	14.43	15.46	16.50	17.53
9.19										13.55				
9.91											15.39			
10												16.50	17.51	18.58
10.59												17.10		
11													18.59	19.63
11.28													18.81	
11.99														20.63

table. In this table the *vertical* differences are the $v = 1/\rho$ as presented in Table 2. They are clearly and fairly regularly increasing with ψ as well as with τ. The *horizontal* differences are the particle velocities (Table 3). They too are rather regularly increasing with ψ as well as with τ; thus the second horizontal differences, the accelerations, are positive. (The computations, at time $\tau = 0$, were started with $\psi = -10$. This range of ψ-values proved however not sufficient, as at each step one ψ-value gets lost. To help this a "lost" ψ-value was once or twice extrapolated. It would however be easy to consider from the beginning a larger range of ψ-values since for $t = t_0$ the ψ-x-relation in the lower part of C_0 is linear.)

TABLE 2

Reciprocal Densities $v_i = \dfrac{1}{\rho_i} = v_i(\psi_\kappa)$

$$v_i(\psi_\kappa) = x(\tau_i,\psi_\kappa) - x(\tau_i,\psi_{\kappa-1})$$

ψ \ τ	v_0	v_1	v_2	v_3	v_4	v_5	v_6	v_7	v_8	v_9	v_{10}	v_{11}	v_{12}	v_{13}
−7	.47̄	.47̄	.47̄											
−6	.47̄	.47̄	.48̄											
−5	.47̄	.47̄	.48̄											
−4	.47̄	.47̄	.49	.53										
−3	.47̄	.47	.50	.54	.59	.63	.66̄	.67						
−2	.47̄	.48	.52	.56	.61	.66̄	.69	.70	.69					
−1	.47̄	.50	.54̄	.58	.63̄	.68	.72	.73	.74	.74̄				
0	.47̄	.52̄	.56̄	.60	.65	.71	.75̄	.78	.79	.79	.77			
1		.53	.58	.63	.68	.73̄	.77	.81	.85̄	.85	.85	.79		
2			.61̄	.66	.71	.74	.79	.85̄	.89̄	.93̄	.93̄	.90̄		
3			.63	.68	.73	.78̄	.82	.88	.94̄	.99̄	.99	.96	.89	
4				.70	.75	.81̄	.86̄	.92̄	.99	1.02̄	1.03̄	1.00	.97̄	
5					.78	.85̄	.90	.97	1.01̄	1.04̄	1.05̄	1.04	1.00̄	.94
6						.91̄	.95	1.01̄	1.03̄	1.04̄	1.06	1.05̄	1.03	1.01̄
7							1.00	1.01̄	1.03	1.04	1.04̄	1.06̄	1.06	1.03̄
8									1.03	1.04	1.04	1.04	1.05̄	1.05
9										1 04	1.04	1.04	1.04	1.05
10												1.04	1.04	1.05
11													1.04	1.05

Table 4 applies to the shock line, and, in particular, Table 4a to the shock line in the penetration region. Here the fourth column shows the mass flux M (where $M\Delta t = \Delta\bar{\psi}$), We see that in the penetration region M is monotonically decreasing. The M are the first differences of the $\bar{\psi}$-values at the shock points, $\bar{\psi}$ being the "label" of the particle which is at a certain time thrown into the shock. The first column shows the

TABLE 3

Particle Velocities $u_i = u_i(\psi_k) = x(\tau_i,\psi_k) - x(\tau_{i-1},\psi_k)$

ψ \ τ	u_1	u_2	u_3	u_4	u_5	u_6	u_7	u_8	u_9	u_{10}	u_{11}	u_{12}	u_{13}
−6	0	.0$\bar{1}$											
−5	0	.0$\bar{2}$	.1$\bar{1}$										
−4	0	.0$\bar{4}$	.1$\bar{5}$	.2$\bar{4}$	.33	.45	.59						
−3	0	.07	.1$\bar{9}$	.28	.37	.48	.6$\bar{1}$	.7$\bar{3}$					
−2	.01	.11	.22	.33	.42	.5$\bar{2}$	.6$\bar{2}$	.7$\bar{2}$	.8$\bar{7}$				
−1	.04	.15	.2$\bar{7}$	.3$\bar{8}$	.4$\bar{8}$	.5$\bar{6}$	.6$\bar{3}$	.7$\bar{3}$	.8$\bar{6}$	1.01			
0	.09	.19	.31	.4$\bar{3}$	.53	.59	.6$\bar{6}$	.74	.8$\bar{6}$	.99	1.18		
1		.24	.36	.4$\bar{8}$	.5$\bar{8}$	.6$\bar{4}$	.70	.7$\bar{8}$	.86	1.0$\bar{0}$	1.1$\bar{2}$		
2			.4$\bar{2}$	.53	.6$\bar{1}$	.6$\bar{9}$	.75	.8$\bar{2}$	.90	1.0$\bar{0}$	1.08	1.19	
3			.4$\bar{7}$	.58	.65	.7$\bar{4}$	.8$\bar{1}$	.8$\bar{8}$	.95	1.00	1.05	1.12	
4				.6$\bar{3}$	.7$\bar{1}$	.78	.8$\bar{7}$	.95	.98	1.00	1.03	1.0$\bar{8}$	1.1$\bar{4}$
5					.7$\bar{8}$	.8$\bar{4}$	.9$\bar{4}$	.9$\bar{9}$	1.01	1.0$\bar{2}$	1.0$\bar{3}$	1.0$\bar{4}$	1.08
6						.8$\bar{8}$	.99	1.0$\bar{1}$	1.02	1.0$\bar{4}$	1.01	1.02	1.0$\bar{6}$
7							1.0$\bar{0}$	1.03	1.03	1.03	1.03	1.0$\bar{3}$	1.02
8									1.04	1.03	1.0$\bar{4}$	1.03	1.0$\bar{3}$
9										1.03	1.0$\bar{4}$	1.0$\bar{4}$	1.03
10												1.0$\bar{4}$	1.04
11													1.0$\bar{5}$

TABLE 4

The Shock Points

Table 4a

τ	$\bar{x} - \bar{x}_0$	$U = \Delta\bar{x}$	$\bar{\psi}$	$M = \Delta\bar{\psi}$
0	0		0	
		1.03		1.76
1	1.03		1.76	
		1.22		1.48
2	2.25		3.2$\bar{5}$	
		1.3$\bar{7}$		1.2$\bar{4}$
3	3.62		4.48	
		1.4$\bar{9}$		1.0$\bar{5}$
4	5.1$\bar{1}$		5.5$\bar{3}$	
		1.60		.90
5	6.7$\bar{1}$		6.43	
		1.7$\bar{0}$		.7$\bar{2}$
6	8.4$\bar{1}$		7.15	

Table 4b

τ	$\bar{x} - \bar{x}_0$	$U = \Delta\bar{x}$	$\bar{\psi}$	$M = \Delta\bar{\psi}$
7	10.09		7.8$\bar{2}$	
		1.72		.6$\bar{8}$
8	11.81		8.50	
		1.74		.3$\bar{9}$
9	13.55		9.19	
		1.83		.7$\bar{3}$
10	15.3$\bar{9}$		9.9$\bar{2}$	
		1.71		.6$\bar{8}$
11	17.10		10.59	
		1.7$\bar{4}$		.6$\bar{9}$
12	18.8$\bar{4}$		11.28	
		1.79		.71
13	20.63		11.99	

x-values of the shock point whose first differences are the shock velocities U. Again only the values for integral τ are listed; therefore the U and M in the table have the character of "average" values. These U

are monotonically increasing in the penetration region. Finally let us consider v' and v'' at the shock points: v' increases monotonically from $v' =$ at $t = t_0$ to $v' = 2.524$ for $t = T$ (the v' are exact values); v'' increases monotonically too—its initial value at $t = t_0$ was .46926; at $t = t_0 + 6$, v'' is 1.05. As v' and v'' increase (in the penetration region) p' and p'' decrease (p' varying from 1 to .27359) while M decreases and U increases monotonically. Also in the whole penetration region, the v'' at the shock point is never smaller than the preceeding v-value, *i.e.*, the last number in the respective column in Table 2.

Computation of T, the Intersection Time of the Shock Line and the Second R.L. For $\tau = 6$ the shock point $\bar{\psi}_6 = 7.15$, $\bar{x}_6 = \bar{x}_0 + 8.41 = 19.02$. This point is still in the penetration region. We can see this, *e.g.*, by computing for $t = t_0 + 6 = 18$ the abscissa x of the second r.l., $x = l + m_2 t = 36.089 - 17.739 = 19.070$ and comparing this with $\bar{x}_6 = 19.02 < 19.07$. That means that for $\tau = 6$, ($t = 18$), the second r.l. (see Fig. 7) is still to the right of the shock line; they are however very near each other. Hence we may find their intersection by linear interpolation. The mass flux M_6 at $\bar{S}_6$ equals .67. Hence we put $T = 18 + y$ and the corresponding $\Psi = 7.15 + .671y$ and have from (34) $18 + y = K[1 - .0704(7.15 + .671y)]$; from this $y = .036$ follows. Hence $T = 18.036$ and $\Psi = 7.17$, and finally from $X = l + m_2 T$, $X = \bar{x}_0 + 8.47$ follows, hence

$$T = t_0 + 6.036, \qquad \Psi = 7.17, \qquad X = \bar{x}_0 + 8.47.$$

The "Contact Zone." For $t \geqq T$ and beyond the second r.l. the picture changes. Let us first consider the shock line. The value of v' at the shock points is now constant ($= 2.524$), and of p', too. Hence $M = \sqrt{\frac{p' - p''}{v'' - v'}}$ decreases (increases) as v'' increases (decreases). U in turn is simply proportional to M [see (36′)], in contrast to the behavior in the penetration region where U was increasing while M was decreasing. The computations show that v'' (at the shock points) oscillates around values near to one. Consequently the shock line in the x-t-system (in the x-ψ-system the shock line is an exact straight line) oscillates too, though very weakly, about a straight line. It is not an exact straight line; neither is it, as in the penetration region, a line with marked positive curvature; its curvature changes sign in weak oscillations with very small amplitude. Also the v'' at a shock point is no longer always greater than all "preceding" v''-values.

As to the abscissas of the particles, what was the most striking feature in the penetration region, the *positive* second differences horizontally and vertically, no longer holds. It is as though the oscillations along the

shock line were propagated into the adjoining domain (see, *e.g.*, in Table 2 the last five numbers for $\tau = 10$ or the last six numbers for $\tau = 12$). Consequently the range of variation of the reciprocal densities is comparatively small in this domain. Considering the v's in the same horizontal row (for the same particle) (Table 2) which have been steadily increasing in the penetration region we see that this no longer holds either: here too we find weak oscillations (see, *e.g.*, $\psi = 3$ from $\tau = 7$ to $\tau = 12$, or $\psi = 5$ between $\tau = 7$ and $\tau = 13$). Similar remarks apply to the velocities u. In the penetration region they are clearly increasing in vertical as well as in horizontal direction. In the "contact zone" the range of variation of the velocities is smaller than in the penetration region. The u in the contact zone vary only slightly and not always the same way but rather in up and downs.

Since in our problem the pressure depends on the density alone it follows that if v is approximately constant the same is true for p and vice versa. Hence u, v, and p vary only slightly. The result of the preceding computations thus seem to agree with the assumption, advanced by Courant and Friedrichs,[4] of the existence of a stationary "contact zone" (in first approximation) beyond the penetration region. It is interesting to see that the solutions show these weak oscillations such that the approximately stationary values in the contact zone seem to correspond to weak waves emanating from the almost rectilinear shock line. The situation will change again when the shock line meets the right wall: $\psi = l$.

VI. Variable Entropy

We shall now consider the more adequate approach where we abandon the assumption of an all-over relation between pressure and density. We still maintain (d) but consider now the *third shock condition* which implies that the a^2 in (d) has different values across the shock, *i.e.* for each particle, $\psi = \text{const.}$, we have $a^2 = a'^2$ for the time $t < \bar{t}$ where $\bar{t}$ denotes the time when the particle gets involved in the shock and $a^2 = a''^2$ for $t > \bar{t}$ (as long as no further shock is crossed). Since for different particles the jumps in the values of a^2 neither occur at the same time nor by the same amount the values of a^2 at a given time will, in general, not be the same although at $t = 0$ the value of a^2 was *one* for all particles. The third transition condition, introduced by Rankine and Hugoniot, corresponds to a combination of the differential equation and the adiabatic condition, considered, as usual, within an (infinitesimal) transition region, whereby

[4] Courant R., and Friedrichs, K. O. Interaction of shock and rarefaction waves in one-dimensional motion. NDRC, AMP Rep. 38.1R (AMG-NYU, 1), 1943.

within this region the gas is assumed as viscous while outside viscosity is neglected. (See Sec. 9.)

Our problem, as in previous sections, is defined by the differential equation (d') the boundary conditions (5) and (5') and $a^2 = a'^2 = 1$ at $t = 0$, for all ψ. This value of a^2 will be valid in the trapezoid between the two horizontal lines $t = 0$ and $t = t_0$, the vertical line, $x = l$, and the straight shock line $x = Ut$. Hence the solution, found before for this domain, consisting of the $-45°$ straight lines which, beyond the first rl., are extended by certain curves, is still the solution in this domain. Next consider the triangle at the back of the shock $x = Ut$ between the vertical line $x = 0$ and the horizontal, $t = t_0$. The equations (8), (8'), and (9) still hold.

The third condition may, in our problem, be written in the form (completely equivalent to the usual form):

Third shock condition

$$\frac{p''}{p'} = \frac{(\kappa - 1)v'' - (\kappa + 1)v'}{(\kappa - 1)v' - (\kappa + 1)v''} \tag{39}$$

which, because of $\kappa = 1.4$ becomes

$$\frac{p''}{p'} = \frac{v'' - 6v'}{v' - 6v''} \tag{39'}$$

or for $v' = p' = 1$

$$p'' = \frac{v'' - 6}{1 - 6v''}. \tag{39''}$$

Besides we have

$$p''(v'')^\kappa = (a'')^2. \tag{40}$$

Here we can solve (9) and (39'') simultaneously with respect to v'' and p'', then U follows from (8) and a''^2 from (40). We thus get for $v'' = v$ the quadratic equation (before in the Riemann case it was a transcendental equation):

$$7v^2 - 20v + 8 = 0 \tag{41}$$

which has between zero and one a root equal to $v = v'' = .4809643$. Computing in turn the other magnitudes we find:

$$v'' = .48096, \qquad p'' = 2.9268, \qquad U = .92665, \qquad a''^2 = 1.0505 \tag{42}$$

while $v' = p' = a'^2 = 1$.

The values (42) correspond to the values (10′) and (10″) of Section I. We see that they do not greatly differ from these values. The solution in the triangle adjacent to the back side of the shock line $x = Ut$ is now formed by the vertical lines with the value v'' of (42):

$$x = v''\psi + \text{const.} \tag{7}$$

Everywhere in the aforementioned triangles the a''^2 has the value (42).

Denoting by t_0, $\bar{x}_0$ and l the same magnitudes as before we have corresponding to (21) if we assume $t_0 = 12$:

$$t_0 = 12, \qquad l = 37.3184, \qquad \bar{x}_0 = 11.1198. \tag{43}$$

In the domain $t > t_0$, at the front side of the unknown shock line we still know the solution, just as before: Everywhere $a'^2 = 1$ and solution (30) holds with the $\bar{x}_0$ of (43). To the left (back side of the unknown shock line) there is the situation described p. 215. It will be seen, however that a step-by-step method as used before will again yield numerical results.

The Principle of Computation. Equation (29′) is to be replaced by

$$x_n^{(r+1)} = 2x_n^{(r)} - x_n^{(r-1)} + \kappa a^2 \cdot 2^{2.4}(\Delta t)^2 \frac{x_{n+1}^{(r)} + x_{n-1}^{(r)} - 2x_n^{(r)}}{(x_{n+1}^{(r)} - x_{n-1}^{(r)})^{2.4}} \tag{44}$$

with the same notations as before. We also put again $\kappa.2^{2.4} = 7.389 = A$. We consider the "curves" $\tau = \text{constant}$ in the x-ψ-plane and wish to determine a curve C_{r+1} from C_r and C_{r-1}. The *upper part*, above the shock point, is known by (30) [and after the time T when the shock line crosses the second r.l. by (36)]. Let us consider the lower part. This *lower part* is determined, point by point, by (44) if we know a^2 and the four values $x_n^{(r-1)}, x_{n-1}^{(r)}, x_n^{(r)}, x_{n+1}^{(r)}$; now a^2 varies in general from particle to particle. We shall use in (44) the a^2 corresponding to $\psi = n\Delta\psi$ at $\tau = r\Delta t$. At time t_0, *i.e.* $\tau = 0$, $a^2 = 1.0505$ holds for all particles with $\psi \leqq 0$ since the above computations apply to all these particles. This value of $a^2 = a''^2$ will also hold for these particles as time goes on (at least as long as they do not cross a reflected shock again) since they have crossed the shock already. It follows, in particular, that the vertical straight lines will extend for $t > t_0$ up to the backward characteristic through the point $(t_0, \bar{x}_0)$. Since the slope dx/dt of a characteristic (see p. 208) is $dx/dt = u \pm c$ and $u = 0$ in this domain we have $dx/dt = -c$. Substituting for v the value v'' from (42) we find for the equation of this line

$$x - \bar{x}_0 = -1.40(t - t_0). \tag{45}$$

Assume now that we know a''^2 for all particles on the lower part of a curve C_r, *i.e.*, for $\psi \leqq \bar{\psi}_r$, as we do for C_0 and $\psi \leqq \bar{\psi}_0 = 0$. We then can

compute the x of all lattice points on C_{r+1}, determined by (44). Since the same a^2 holds along ψ = constant (horizontal line in the ψ-x-diagram) we now know the a''^2 for all points on C_{r+1} whose $\psi \leqq \bar{\psi}_r$, hence certainly for all points determined by (44). As before, there will be a few missing points on C_{r+1} and their x as well as their a^2 is still to be found.

Let us now consider the new *shock point* on C_{r+1}. Assume that C_r is known and on C_r the shock point $\bar{S}_r(\bar{x}_r,\bar{\psi}_r)$ and the slopes v_r' and v_r'' at $\bar{S}_r$. If this is so we also know $(a_r'')^2$, p_r'', and of course p_r'. Introducing $v''/v' = \lambda$ we have

$$\frac{a''^2}{a'^2} = \lambda^\kappa \frac{6 - \lambda}{6\lambda - 1} \tag{46}$$

and since $a'^2 = 1$

$$(a_r'')^2 = \lambda_r^k \frac{6 - \lambda_r}{6\lambda_r - 1} \tag{46'}$$

also

$$p_r' = v_r'^{-k} \tag{47}$$

and

$$p_r'' = p_r' \frac{6 - \lambda_r}{6\lambda_r - 1}. \tag{47'}$$

To find then $\bar{S}_{r+1}$ the procedure is the same as in the simplified case. By means of (32) and (33) the $\bar{\psi}_{r+1}$ is found and the corresponding abscissa follows from (30). Next we interpolate the one or two missing lattice points on C_{r+1} as before; then v'_{r+1} is found by the exact formula (31) and v''_{r+1} by interpolation between $\bar{S}_{r+1}$ and the highest lattice point below $\bar{S}_{r+1}$; finally a''^2_{r+1} follows from (46'), r being replaced by $(r + 1)$.

All that remains is to find the a''^2 for those points on C_{r+1} whose $\psi > \bar{\psi}_r$. Consider such a lattice point on C_{r+1}. If it happens to be the shock point $\bar{S}_{r+1}$ its a''^2 is given by (46') (writing $(r + 1)$ instead of r). Suppose this is not so. Then we have for the point in question

$$\bar{\psi}_r < \psi < \bar{\psi}_{r+1}.$$

Since we know $a_r''^2$ and $a_{r+1}''^2$ at $\bar{S}_r$ and $\bar{S}_{r+1}$, and the vertical distance between $\bar{\psi}_r$ and $\bar{\psi}_{r+1}$ is less than one, we can find, with sufficient accuracy, by linear interpolation the a''^2 that corresponds to ψ. Besides we are sure that, with our choice of the lattice, there is not more than one ψ between $\bar{\psi}_r$ and $\bar{\psi}_{r+1}$. For finding a''^2 we may use other values than the a''^2-values corresponding to $\bar{S}_r$ and $\bar{S}_{r+1}$ if it seems preferable. As a numerical illustration consider, *e.g.*, for $\tau = \frac{1}{4}$, $\bar{\psi}(\frac{1}{4}) = .48166$ while $\bar{\psi}(\frac{1}{2}) = .94025$ and $\bar{\psi}(\frac{3}{4}) = 1.38387$. Corresponding values of a''^2 are $a''^2(\frac{1}{4}) = 1.052$, $a''^2(\frac{3}{4}) = 1.056$. Linear interpolation gives for $\psi = 1$,

$a''^2 = 1.054$. If the values of a''^2 at $\tau = \frac{3}{4}$ and $\tau = \frac{1}{2}$ are used we get for $\psi = 1$ the same a''^2. In this way we find in the course of the computations the a''^2 for all particles.

Following up the statement on page 220 we may now describe the general method in the following way:

Suppose that two curves C_τ and $C_{\tau-1}$, i.e., $\psi = \psi(x)$ for $\tau = r\Delta t$, $\tau = (r-1)\Delta t$ have been determined, so that we know at every lattice point the corresponding x and the corresponding a^2 and at the shock point $\bar{S}_r$ we know v_r', v_r'', p_r', p_r'', $a_r'^2$, $a_r''^2$. Then in order to determine C_{r+1}: (1) The coordinates of the new shock point $\bar{S}_{r+1}$ are found, namely $\bar{\psi}_{r+1}$ by (32) and (33) and $\bar{x}_{r+1}$ by (30) or its equivalent. (2) The lower part of C_{r+1} is found from (44), point by point, using in the determination of $x_n^{(r+1)}$ the a''^2 that corresponds to $x_n^{(r)}$. The few lattice points on C_{r+1} that cannot be found in this way are found by an interpolation, in general of order two applied to this new curve. (3) The upper part of C_{r+1} is found from (30) or its equivalent for $t \geqq T$. (4) Returning to S_{r+1} we find v'_{r+1} from (31), v''_{r+1} by an interpolation (in general linear) between S_{r+1} and the next lower lattice-point; then $a_{r+1}''^2$ follows from (46'), p'_{r+1} and p''_{r+1} from (47). (5) The a''^2 of points on C_{r+1} whose $\psi \leqq \bar{\psi}_r$ are the same as for the points with same ψ on C_r. The a''^2 corresponding to a ψ where $\bar{\psi}_r < \psi < \bar{\psi}_{r+1}$ is found by linear interpolation using the a''^2-values that correspond to $\bar{\psi}_r$ and $\bar{\psi}_{r+1}$.

Thus we see that in our step-by-step method the modifications necessitated by the consideration of the "general case" do not create new difficulties but the computations remain essentially unchanged. Numerical results will be presented at another time. In the theoretical problem, the boundary conditions along an unknown boundary, the solution of the differential equation, and even the very coefficients of this equation are interwoven in an inextricable way. In the step-by-step method however we may juggle from one equation to another, using freely the results just found for an r in order to determine the result for $(r+1)$. The problematic feature is again the interpolation of the few lattice points on C_{r+1} and the interpolation of v_{r+1}'' just by means of these uncertain points. This reflects the basic difficulty in the original problem.

VII. J. von Neumann's Mechanical Model of Shock Motion

J. von Neumann has considered a mechanical model of the hydrodynamical motion that is very interesting from a theoretical point of view and at the same time seems to provide satisfactory numerical results. We consider the boundary value problem set up in Section I. Von Neumann assumes an all-over relation (4) between p and v in order to test the procedure in a case that allows important simplifications.

The Balance of Energy. The "internal energy," e, may be given as a

function of the two parameters, v, the specific volume, and η, the entropy. $e = e(v,\eta)$, where (T denoting the absolute temperature)

$$de = T\,d\eta - p\,dv, \qquad \frac{\partial e}{\partial \eta} = T(v,\eta), \qquad \frac{\partial e}{\partial v} = -p(v,\eta) \tag{48}$$

If an absolute relation (4) holds, this energy, e, splits into two parts $e = e_1 + e_2$, one part depending on v only, the other on η only. In fact from (48) we see that if p depends on v only, $p = p(v)$, then T depends on η only and the energy, e, separates into the sum of a function of specific volume, v, alone and a function of entropy alone.

$$e(v,\eta) = e_1(v) + e_2(\eta) \tag{49}$$

and

$$p = -\frac{\partial e}{\partial v} = -\frac{de_1}{dv} = p(v) \tag{50}$$

$$T = \frac{\partial e}{\partial \eta} = \frac{de_2}{\partial \eta} = T(\eta).$$

There is, as von Neumann puts it, no "interaction energy" involving both v and η. He then calls e_1 and e_2 the "potential" and the "thermal" energy respectively.

We have seen before (see Section II and beginning of Section IV) that in this case the differential equation (2′) and the two mechanical shock conditions are all that is needed to determine the shock phenomenon. The motion is determined without an additional condition. The third shock condition ("conservation of energy principle") which we used in Section VI where the Rankine Hugoniot theory was considered is not fulfilled. Its expression, however, can be used eventually to find the change in thermal energy, e_2, across the shock, after the "mechanical" quantities have been determined. We now write the third shock condition in the form (*Man.* pp. 71, 72)

$$e'' - e' = -\left[\frac{p''}{\rho''} - \frac{p'}{\rho'} + \frac{1}{2}(u'' - U)^2 - \frac{1}{2}(u' - U)^2\right] \tag{51}$$

or, with $\rho = 1/v$, we may use it in the form (von Neumann, p. 10)

$$e'' - e' = \frac{p'' + p'}{2}(v' - v''). \tag{52}$$

Because of (49), Eq. (52) gives (*Man.* p. 81, von Neumann p. 10)

$$e_2'' - e_2' = \frac{p' + p''}{2}(v' - v'') - (e_1'' - e_1') = \frac{p' + p''}{2}(v' - v'') + \int_{v'}^{v''} p\,dv. \quad (53)$$

If in the computation of $\int_{v'}^{v''} p\,dv$ it is assumed that across the shock the relation (4) holds in (53) all quantities to the right are known and the increase $e_2'' - e_2'$ can thus be found.

The total energy of the gas-dynamical system consists of the *kinetic* energy, the *potential* energy $e_1(v)$ and the *thermic* energy $e_2(\eta)$. Consider now first a *continuous* motion, *i.e.*, a motion without shocks. The total energy is conserved by the energy principle. The thermic energy is conserved too since along a particle path, ψ = constant, the entropy remains constant for a continuous motion. Hence in the absence of shocks the sum of kinetic and potential energy is conserved too. In case of shocks along each world line, ψ = constant, the specific entropy η never decreases according to the second principle of thermodynamics, *i.e.*, the difference $\eta'' - \eta'$ is positive in the direction in which the mass flux, M, introduced in (8′) is positive. Hence when the shock is crossed the thermic energy increases: $e_2'' > e_2'$ and therefore *the sum of kinetic and potential energy decreases.* Thus while for a continuous motion the sum of kinetic and potential energy is preserved this sum suffers a loss in the presence of shocks and this loss is equal in absolute value to the increase in thermic energy $e_2'' - e_2'$ across the shock front [see (68)].

The Mechanical Model. Nonlinear wave motion may be studied by considering individual particles connected by "springs," subject to a nonlinear law of attraction and repulsion. In fact, consider the differential equation

$$\frac{\partial^2 x(\psi,t)}{\partial t^2} = -\frac{\partial p(v)}{\partial \psi} \qquad \text{with} \qquad v = \frac{\partial x}{\partial \psi}. \quad (2'')$$

Make ψ a discrete variable. As von Neumann remarks, this is rather natural, since ψ, the label of the elementary volume, is, in the conception of the kinetic theory of gases, a discrete quantity. On the other hand, x and t are left continuous. Putting, as before, $\psi = n\Delta\psi$ and writing

$$x(\psi,t) = x(n\Delta\psi,t) = x_n(t) \quad (54)$$

we get

$$\frac{d^2 x_n}{dt^2} = p\left(\frac{x_n - x_{n-1}}{\Delta\psi}\right) - p\left(\frac{x_{n+1} - x_n}{\Delta\psi}\right). \quad (55)$$

If, in particular $\Delta\psi = 1$, we have

$$\frac{d^2x_n(t)}{dt^2} = p(x_n(t) - x_{n-1}(t)) - p(x_{n+1}(t) - x_n(t))$$

$$(n = 0, \pm 1, \pm 2, \cdots) \quad (55')$$

The equations (55′) are approximations of the partial differential equation (2′) but they are at the same time *the exact equations* of another physical system which is a physical approximation of the hydrodynamical motion (2′). In fact, consider a mechanical system of point particles with coordinates $\cdots x_{-3}, x_{-2}, x_{-1}, x_0, x_1, \cdots$ each with mass one and so that x_n is connected with x_{n-1} and x_{n+1} each, by a "spring" that attracts and repels the neighboring particle, say x_{n-1}, according to the law (4) $p(v) = p(x_n - x_{n-1})$ where $v = \Delta x/\Delta\psi = x_n - x_{n-1}$ is the distance between the two particles. The equations of motion of this system are obviously (55′).

The total mechanical energy of this system is given by

$$\frac{1}{2}\sum_n \left(\frac{dx_n}{dt}\right)^2 + \sum_n e_1(x_n - x_{n-1}) \qquad (56)$$

where the first term represents the kinetic, the second the potential energy. In fact, if we write for the moment $\sum_n e_1(v) = V$ and (55′) in the form

$$\frac{d^2x_n}{dt^2} = X_n \qquad \text{where} \qquad -X_n = \frac{\partial V}{\partial x_n} \qquad (55'')$$

we find, using (51):

$$-X_n = \frac{\partial V}{\partial x_n} = \frac{\partial e_1(x_n - x_{n-1})}{\partial v} \cdot 1 + \frac{\partial e_1(x_{n+1} - x_n)}{\partial v} \cdot (-1)$$

$$= -p(x_n - x_{n-1}) + p(x_{n+1} - x_n) \qquad (57)$$

and (55″) follows. This system of particles on a line connected by a nonlinear elastic law ("beads on a string") is regarded as a physical approximation or model of the continuous substance, whose motion is described in (2′). In the mechanical model a particle corresponds to a molecule, the striking difference between original and model being however, that in the original the number of particles is given by Avogadro's number, $N \sim 6 \cdot 10^{23}$, while in the model an N of the order of magnitude of $N \sim 10^2$ is used. The "intramolecular" forces, however, are increased so that on the whole the hydrodynamical situation is approximated.

If we consider the boundary value problem of the preceding sections, *i.e.*, a substance with constant velocity $u' < 0$ at $t = 0$, moving between rigid walls, it seems that the model fits the original also with respect to the emergency of shocks. In fact a shock would be a necessary consequence if particles connected by "springs" move with constant velocity between two rigid walls toward the left.

On the other hand, as von Neumann points out, in case of shocks two difficulties arise. First, while (55) is an approximation to (2′)—in the usual sense—it is hard to see what corresponds in the model to the two mechanical transition conditions that hold for the original. Besides, the comparison of the energy balance in the original and the model seems to lead to a difficulty. In fact the total energy of (55) is given by (56), the sum of the kinetic and the potential energy of the model, and there is no thermic energy in this mechanical model. Thus the mechanical energy (56) is preserved through the motion of the model while, on the other hand, as seen above, the original defined by (2′) together with (4) and with the two first shock conditions, *fails* to preserve the mechanical energy. We may also put it in the following way: Complete the system (55′) by boundary conditions that in the continuous case would produce shocks. If we start solving, step by step, this "completed" system without any attempt to locate and determine the shock, what will be in the model the equivalent of the shock in the original?

Since we know for $t \leqq t_0$ the exact solution of the gas-dynamical boundary value problem (the original) we can compare this solution (see Section II and Fig. 7) with the solution of the boundary problem (55′), (58). The boundary conditions, or rather initial conditions to be added to (55′) are as follows (see Section I)—consider positive ψ-values only:

$$\text{At } t = 0: x_\psi = \psi \text{ for } \psi = 0, 1, \cdots l \text{ and } u = \frac{dx_\psi}{dt} = u_0 < 0. \tag{58^1}$$

$$\text{For all } t > 0: x_0(t) = 0,\ x_l(t) = l \tag{58^2}$$

or, what amounts to the same: $u'' = 0$ at $\psi = 0$ and $\psi = l$.

If the system (55′), (58) is solved (see following section for the method) it turns out that the solution does not look like the smooth hydrodynamical solution found in Section II. In contrast to this the motion of the single particle shows *superposed oscillations*, varying in time of appearance and intensity (see Fig. 8). These oscillations are interpreted by von Neumann in the light of the above energy balance: The energy (56) is the total

mechanical energy of the "oscillating" particle system. This energy is conserved by (55′) while the mechanical energy of the gas-dynamical system (differential problem plus transition conditions) is diminished when shocks are present, while its thermic energy increases. Von Neumann's decisive conclusion is that the kinetic energy of these superposed oscillations appearing in the model only corresponds just to the thermic energy appearing in the hydrodynamical original. In the original the sum of the kinetic energy (of the smooth motion), of the potential energy, and of the thermic energy is preserved while in the mechanical model the total energy that is preserved can be considered as the sum of the kinetic energy of the smooth average motion, plus the kinetic energy of the superposed oscillatory motion, plus the potential energy.

Consequently it is suggested that the motion defined by (55′), (58), (63) be considered as the sum of a smooth average motion, plus superposed oscillations (Fig. 8). It is the average motion that approximates the gas-dynamical solution while the oscillations account for the change in thermic energy. (Thus in the model the "thermic" energy appears as a part of the kinetic energy.) A qualitative comparison of Figs. 7 and 8 (which are computed for numerically different boundary conditions and different p-v-relations) confirms this surmise, which forms the essential point in von Neumann's approach. Theoretically, this approach is interesting because in this way a mechanical model is furnished for a problem where thermic energy enters. (This continuous solution can however represent an approximation to the solution of the Riemann problem only, since friction forces are neglected throughout.) The practical consequence is that the system (55′), (58) can be solved *without bothering at all about shocks.* The place, form, and intensity of the oscillations will finally permit the location of the shocks *a posteriori.*

One may safely state that under appropriate conditions the "average" solution of the model converges toward the solution of the original as $\Delta\psi \to 0$. It is to be assumed that in this limiting process *the oscillations will not disappear* but period and amplitude should decrease. So far no convergence proof has been given or indicated. From the point of view of a numerical approximation, what one needs is not so much a convergence proof as an estimate of the error committed under a certain approximation. A very workable approximation need not necessarily be convergent and a convergent approximation may, under certain circumstances, be inappropriate for practical purposes. However such an estimate of the error is in general even more difficult to find than a convergence proof. Neither has been given so far for any of the methods exposed in this report.

VIII. The Computations

In order to evaluate the system (55′) numerically we make the time-variable discontinuous too by putting

$$\psi = n\Delta\psi, \qquad t = s\Delta t \qquad \begin{pmatrix} n = 0, 1, 2, \cdots \\ s = 0, 1, 2, \cdots \end{pmatrix}$$

Putting $\Delta\psi = 1$ we get from (55′)

$$\frac{x_n^{s+1} - 2x_n^s + x_n^{s-1}}{\Delta t^2} = p(x_n^s - x_{n-1}^s) - p(x_{n+1}^s - x_n^s). \tag{59}$$

[If (59) is compared with (29) for $\Delta\psi = 1$ and with the same p-v-relation they will not be found identical. The reason is that in deriving (29) the equation $(\bar{2})$ was used where the differentiation of $p(v)$ with respect to ψ had been performed before making the variables discontinuous, while in (55′) and (59) the equation (2′) was used so that in (59) the differentiation that leads from (2′) to $(\bar{2})$ is replaced by a finite difference procedure. This difference however should not be of any importance.] The essential structure of equations (29) and (59) is the same. If we now write the boundary conditions (58) in a "discontinuous" way we get, with the particles $\psi = 0$ and $\psi = l$ representing the two "walls," while $\psi = 1, 2, \cdots, l-1$ represents the substance:

$$s = 0 \qquad x_n^{(0)} = n \qquad \text{for} \qquad n = 1, 2, \cdots, l-1 \tag{60}$$

$$\frac{x_n^{(1)} - x_n^{(0)}}{\Delta t} = u_0, \qquad \text{or} \qquad x_n^{(1)} = n + u_0\Delta t$$

$$s = 1, 2, \cdots \qquad x_0^{(s)} = 0, \qquad x_l^{(s)} = l, \qquad i.e., \qquad u'' = 0.$$

The recurrence formulas (59) are of the same structure as (29). A new value $x_{n+1}^{(s)}$ is determined by the four values $x_{n-1}^{(s)}$, $x_n^{(s-1)}$, $x_n^{(s)}$, $x_n^{(s+1)}$. The ratio $\Delta t/\Delta\psi$ is to be chosen in such a way that we are sure to compute only values that are within the theoretical influence sphere defined by the slopes of the characteristics of the problem. This leads to the inequality

$$\frac{\Delta\psi}{\Delta t} \geqq \sqrt{-\frac{dp}{dv}}, \qquad \text{where} \qquad -\frac{dp}{dv} = -\frac{dp}{d\rho}\frac{d\rho}{dv} = \frac{dp}{d\rho}\frac{1}{v^2} = \frac{c^2}{v^2}$$

where notation (11′) is used. Hence von Neumann's condition:

$$\Delta t \leqq \left(\frac{v}{c}\right)_{\text{Min}} \tag{61}$$

which becomes (39) for the adiabatic relation.

The essential feature of the computations is the following. The $x_n^{(s)}$ are determined, step by step, by means of (59), (60), and that is all that is used. No transition conditions are considered, no assumption as to the nature of the shock line is made, and no explicit determination of shocks is undertaken. The idea is, and the computations made so far seem to confirm it, that "shocks" can be located *a posteriori* by means of the superposed oscillations. In fact we expect and see that after crossing a "shock" an oscillation of the particle path develops that represents thermic agitation. It can be concluded that the period of these oscillations is of order $\Delta\psi = 1$. Far from being due to an inadequacy or inaccuracy of the computational setup these oscillations represent our tools for determining the shock line. If the computation is more and more refined they will by no means disappear although their period will decrease.

As (55′) conserves the energy (56), (59) should, approximately, conserve the equivalent of (56):

$$\frac{1}{2}\sum_n \left(\frac{x_n^{(s+1)} - x_n^{(s-1)}}{2}\right)^2 + \sum_n e_1(x_n^{(s)} - x_{n-1}^{(s)}) \tag{62}$$

Since this conservation is only approximate, (62) will oscillate. Nevertheless the average statistical behavior of (62) should be fairly regular and "any excessive deviation is an indication of some error of computation." In particular, a clear trend of (62) in dependence of time, *i.e.*, of s, should raise the computor's suspicion, as (62) should oscillate rather than change monotonically.

The actual problem that underlies Fig. 8 is the boundary problem (59), (60) with the following specific assumptions: In the diagram (Fig. 8) the horizontal numbers represent $\psi = n\Delta\psi = n$, as $\Delta\psi = 1$, and because of (60), $\psi = x$. Thus we see that there are $l = 30$ particles and $x = l = 30$. The numbers on the vertical axis are the s where $s\Delta t = t$. It will be seen presently that $\Delta t = \frac{1}{2}$; hence the figure shows that the region $0 \leqq t \leqq 30.5$ has been considered. The figure also shows that, according to (60), for $t = 0$, $\rho' = v' = 1$. The all-over relation used by von Neumann is

$$p = p(v) = 1 - v + \tfrac{1}{4}v^2 = \left(1 - \frac{v}{2}\right)^2. \tag{63}$$

This is a curve, convex from below as it ought to be and it can be used in the interval

$$0 < v < 2, \qquad 1 > p > 0. \tag{63′}$$

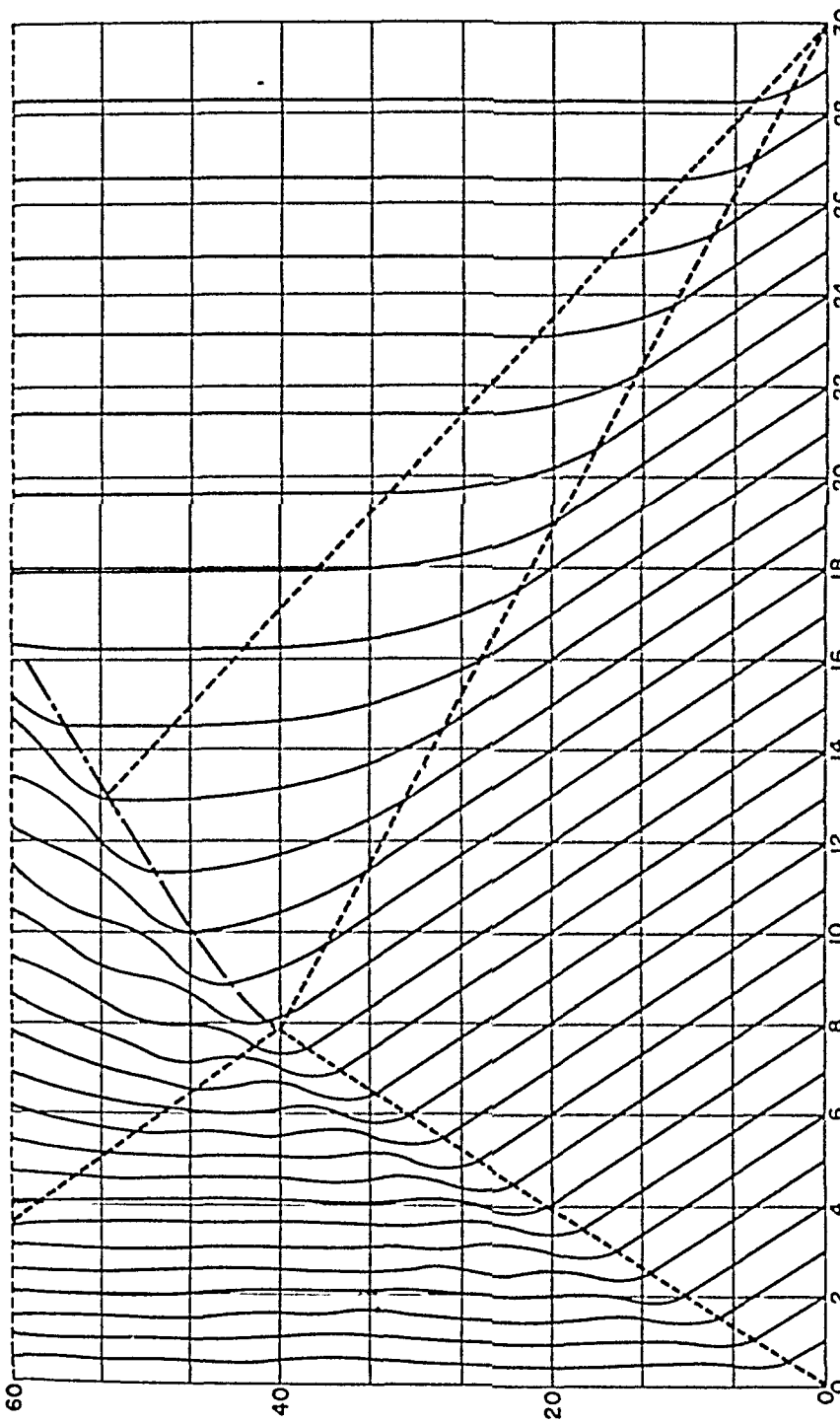

FIG. 8.—Continuous solution of the hydrodynamical problem (numerical data as in section VIII) by von Neumann's method.

Hence if at the beginning $v = v' = 1$, we have $p' = \frac{1}{4}$. The boundary conditions (60) concerning u are in particular

$$u' = u_0 = -0.4 \qquad u'' = 0. \tag{60'}$$

The exact hydrodynamical situation for the hydrodynamical boundary problem, under consideration of the two mechanical shock conditions, is for $t \leqq t_0$ completely determined (see Section II). The details however change because of (63) and (60'). We now have

$$v'' = \frac{U}{U + 0.4}, \qquad p'' = 1 - v'' + \frac{v''^2}{4}$$

and from (9)

$$.16 = (1 - v'')(1 - v'' + \tfrac{1}{4}v''^2 - 0.25).$$

This is an equation of third degree with the root (von Neumann, p. 25) $v'' = .500$. Then by means of $v'' = U/(U + 0.4)$ the velocity U of the shock follows to $U = .400$. Hence for density and pressure behind the shock: $v'' = .500$, $\rho'' = 2.000$, and $p'' = .5625$. Thus the data are:

$$u' = .400, \quad v' = 1, \quad p' = \tfrac{1}{4} \quad u'' = 0, \quad v'' = .500, \quad p'' = .5625, \quad U = .400. \tag{64}$$

At the wall, $\psi = l$, a Riemann rarefaction wave originates. We now have, regarding this wave, with the notations of Section II:

$$\begin{aligned} \varphi(\rho) &= \left(1 - \frac{1}{2\rho}\right)^2 \\ \varphi'(\rho) &= \frac{1}{\rho^2}\left(1 - \frac{1}{2\rho}\right) \\ c &= \frac{1}{\rho}\sqrt{1 - \frac{1}{2\rho}} = v\sqrt{1 - \frac{v}{2}} \\ f(\rho) &= \int c\,\frac{d\rho}{\rho} = \frac{4}{3}\left(1 - \frac{1}{2\rho}\right)^{\frac{3}{2}} = \frac{4}{3}\left(1 - \frac{v}{2}\right)^{\frac{3}{2}}. \end{aligned} \tag{65}$$

The velocity m_1 of the front of the rarefaction wave is [see (15)]:

$$m_1 = -0.4 - \frac{1}{\sqrt{2}} = -1.107$$

also

$$C = u' + f(\rho') = -0.4 + \frac{4}{3}\cdot\left(\frac{1}{2}\right)^{\frac{3}{2}} = -0.4 + \frac{\sqrt{2}}{3} = .0714$$

$$u'' = 0 = C - f(\rho_2).$$

Hence

$$C = \frac{4}{3}\left(1 - \frac{1}{2\rho_2}\right)^{\frac{1}{2}} = \frac{4}{3}\left(1 - \frac{v_2}{2}\right)^{\frac{1}{2}}, \qquad i.e., \qquad v_2 = 1.718$$

$$m_2 = u'' - \varphi'(\rho_2) = -v_2\sqrt{1 - \frac{v_2}{2}} = -0.65$$

$$p_2 = \left(1 - \frac{v_2}{2}\right)^2 = 0.020.$$

Thus with the notations of Section II:

$$\begin{aligned} m_1 &= -1.107 \qquad m_2 = -.646 \\ v_2 &= 1.718 \qquad p_2 = +0.020. \end{aligned} \tag{66}$$

Here m_1 is the velocity of the front, m_2 of the back of the rarefaction wave; v_2, p_2 are, respectively, reciprocal density and pressure behind the wave [compare (18) Sec. II].

The shock and the rarefaction front meet at the time (Fig. 8):

$$t_0 = \frac{l}{U - m_1} = \frac{30}{0.4 + 1.107} = 19.91 \tag{67}$$

$$\bar{x}_0 = U\frac{l}{U - m_1} = 7.964.$$

The vertical straight lines (Fig. 8) that originate at the back of the rectilinear shock in the region $t < t_0$ continue beyond $t = t_0$ until they meet the characteristic through $\bar{x}_0$, t_0 with slope:

$$\frac{dx}{dt} = c - u = c = v\sqrt{1 - \frac{v}{2}} = \frac{.5}{1.15} = .433.$$

This situation may be described as follows: At the instant $t = t_0$ the rarefaction wave seems to undergo a refraction on the shock and its front continues behind the shock with velocity $U = .433$.

We may finally determine the "degradation of energy" that equals the increase in thermic energy. With (64) and formula (63) we find

$$e_2'' - e_2' = \frac{1}{2} \cdot 0.8125(1 - 0.5) - \int_{0.5}^{1}\left(1 - \frac{v}{2}\right)^2 dv = .0052. \tag{68}$$

The choice of Δt is according to (61)

$$\Delta t < \left(\frac{v}{v\sqrt{1 - \frac{v}{2}}}\right)_{\text{Min}} = \left(\frac{1}{\sqrt{1 - \frac{v}{2}}}\right)_{\text{Min}} \tag{61'}$$

Here we have to introduce for v its smallest value, *i.e.*, the value right behind the shock: $v'' = .5$. Hence

$$\Delta t < \frac{2}{\sqrt{3}} = 1.15.$$

Then $\Delta t = \frac{1}{2}$ was used in the computations [which is a safer choice than in the author's setup].

Thus the hydrodynamical original for $t \leqq t_0$ is determined and can be found in detail in various ways. Von Neumann, however, computes this part, $t \leqq t_0$, too by the recurrence relations (59), (60), *i.e.*, not for the original but for the model, in order to check his method. It is, in fact, very interesting to see how right behind the theoretical shock line the oscillations start in the previously smooth picture. The continuation of the shock line beyond $t = t_0$ which is not known is then found in the same way as for $t \leqq t_0$ without bothering about finding the shock line explicitly. The shock line is drawn at the end in such a way that, roughly speaking, the smooth graph of each world line ends in front of the shock line and oscillations start at the back side. "A more detailed inspection of the numerical results allows also locating the shock across the rarefaction." (*i.e.*, for $t > t_0$.) No oscillations appear when an r.l. is crossed, in agreement with the theory.

There is, of course, no difficulty in substituting the "more realistic" relation $pv^\kappa = a^2$ for the p-v-relation (63). It is also obvious that von Neumann's method is by no means limited to the particular wave interaction problem (collision of shock and rarefaction) which has been considered here. Less obvious seems the generalization to a more general equation of state where relation (4) is abandoned.

Summarizing we may say: von Neumann's method, if considered at this moment merely as a numerical procedure, seems to be simpler *i.e.* more "automatic" than any method that undertakes to determine the shock, etc., explicitly. In fact, it succeeds in avoiding the difficulty of the problem (the "unknown boundary") and consequently the interpolations that seem to appear in one or another way in other procedures. No *a priori* assumption is made concerning the continuation of the shock line beyond $t = t_0$. On the other hand the question remains whether this *a posteriori* determination of the shock line and the state in back of the shock, exclusively based on the inspection of the oscillations (thermic agitation), is clear enough to give unique results and reliable enough in case of a moderately fine lattice. This is not a criticism but a question. It may be remarked that, as far as $t \leqq t_0$ the procedure, checked by means of the exactly known solution, deals with a situation particularly favorable for the difference method, since in this domain both particle

lines and shock line are rectilinear. At any rate it is extremely interesting to observe the spontaneous generation of "shocks."

The method, based on the mechanical model with the suggestive idea of equivalence of thermic energy and kinetic energy of the oscillations, has the great advantage of a uniform and uninterrupted computational procedure. On the other hand it seems that the computations must be done fairly accurately in order to furnish clearly enough the behavior of these oscillations that are our only means for locating the shocks.

The problem of sufficient accuracy and speediness of the approximation procedure and its adequate mechanization seems to present still a central difficulty in each of the numerical methods dealing with wave-interaction problems.

IX. Procedure for Finding a Continuous Solution by Taking Viscosity into Account

Our starting point was that the system (2′), (3), together with simple and natural boundary conditions has no solution in the usual sense. The author's method as exposed in sections IV–VI constitutes a procedure for finding, approximately, a discontinuous solution of the 'Hugoniot problem." A discontinuous solution consists of several regular solutions which are linked to each other—by the shock conditions—along sharp discontinuity lines (of u,ρ,p). Observation of the physical phenomenon does, however, not force upon us a theory which leads to a piecewise continuous solution of the ideal-gas-equations, separated by sharp discontinuity lines. Observation merely prompts us to expect regions where velocity, density, and pressure will vary rather strongly.

It is well known that, if viscosity is taken into account the same hydrodynamical problem will possess a continuous solution thanks to the smoothing effect of viscous friction. In the following we shall present a condensed outline of an analysis of our problem, due to v. Mises. His approach, which is based on the consideration of viscosity of the medium, will also suggest a procedure for actually determining a solution of the boundary value problem.

If friction is considered the only viscous force appearing in a one-dimensional motion may be denoted by π. The *continuity equation* (1) does not change at all. We shall, however, give it the new number (68). The *equation of motion* will be written now in Euler notation. We thus have the system:

$$(68) \equiv (1) \tag{68}$$

$$\rho \frac{du}{dt} + \frac{\partial(p - \pi)}{\partial x} = 0 \tag{69}$$

In this system the independent variables are x and t, the dependent variables u, ρ, and p. We thus need one more equation that holds in all points of the x-t-space. Since such an equation will specify a general type of solutions of (68), (69), v. Mises calls it "specifying equation." In its most general form it will appear as a relation between p,ρ,u,x, and t

$$F(p,\rho,u,x,t) = 0 \tag{a}$$

where F stands for a finite or infinitesimal operator. A very simple example of such a specifying equation is equation (3) of section I.

We may derive from (68) and (69) without making use of (a) a relation between p, ρ, and u, which thus represents a common feature of all p, ρ, u-distributions that satisfy the continuity equation and the equation of motion. This equation is called *the energy equation of compressible fluid flow.*

Next we consider the specifying equation. Such an equation is, *e.g.*, furnished if the usual assumption is made that the fluid motion be adiabatic, *i.e.*, that for each particle the heat input resulting from radiation plus heat conduction be zero. We neglect heat conduction, and insert the condition of adiabatic flow into the energy equation in order to express in this way the specifying equation in terms of the original variables u,ρ,p. The result is the equation which supplements (68) and (69):

$$\rho \frac{d}{dt}\left(\frac{u^2}{2} + \frac{1}{\kappa - 1}\frac{p}{\rho}\right) + \frac{\partial}{\partial x}[u(p - \pi)] = 0 \tag{70}$$

If, in (70), π is omitted, (70) can be simplified (using (68) and (69)) to yield our relation (3).

$$\frac{d}{dt}(p/\rho^\kappa) = 0 \tag{3}$$

Thus (68), (69), and (70) are the differential equations of the problem with t and x as independent, and u,ρ,p as dependent variables. Of course, the whole problem could have been set up in "Lagrange-form" as well.

From these three equations "transition conditions" are derived in the usual way. The result, with the notations of section I are the equations:

$$\rho'(u' - U) = \rho''(u'' - U) \tag{71}$$

$$\rho'(u' - U)u' + p' - \pi' = \rho''(u'' - U)u'' + p'' - \pi'' \tag{72}$$

$$\frac{(u' - U)^2}{2} + \frac{p'}{\rho'}\frac{\kappa}{\kappa - 1} - \frac{\pi'}{\rho'} = \frac{(u'' - U)^2}{2} + \frac{p''}{\rho''}\frac{\kappa}{\kappa - 1} - \frac{\pi''}{\rho''} \tag{73}$$

Here (71) is identical with (8'), while (72) and (73) reduce to our "second" and "third shock condition" if $\pi' = \pi'' = 0$. If the fluid within the transition region is considered as non-viscous it follows from (3) that:

$$\frac{p'}{\rho'^{\varkappa}} = \frac{p''}{\rho''^{\varkappa}} \tag{3'}$$

while in the general case the inequality

$$\frac{p''}{\rho''^{\varkappa}} > \frac{p'}{\rho'^{\varkappa}}$$

holds.

Now *three cases* may be distinguished:

A) The fluid is considered as non-viscous within as well as outside of the transition regions.

B) The fluid is non-viscous outside and viscous within.

C) Viscosity is assumed throughout.

In case B) one has to use (71), (72) and (73) with $\pi' = \pi'' = 0$, because π' and π'' are the viscous stresses at the end of the transition zone and must therefore be equal to the respective outside-values. *Thus B) corresponds to the Hugoniot problem.*

Assumption A) corresponds to the Riemann case, since Riemann assumed (3'). In case A) equations (71), (72), (73) hold with $\pi' = \pi'' = 0$, and, in addition (3') holds. It is easily seen that these four relations admit no other solution than $u' = u''$, $\rho' = \rho''$, $p' = p''$; this, however, would mean a "continuous" solution, while it was our starting point that such a continuous solution of the ideal-gas-problem does not exist. Hence case A) is contradictory in itself, unless some approximation is considered. In fact, when we dealt with the Riemann case, admitting (3'), we neglected the third shock condition. A solution of this modified system was bound to be an approximation. *Sharp shock fronts result only in case B), the Hugoniot case.*

We are now able to indicate quite briefly the procedure proposed by v. Mises. In fact, he suggests *to consider case C)* where viscosity is nowhere neglected; *i.e.*, he proposes to deal merely with the system (68), (69) (70),—of course supplemented by boundary conditions—and to integrate this system as well as possible, by analytical expressions or by means of a step by step procedure without bothering at all about discontinuity lines. We expect to find, in this way, a continuous solution which will however show a strong variability of the dependent variables in certain regions, which should correspond to the shocklines of the Riemann-Hugoniot theory. Great accuracy of the computations may be unavoidable when approaching these regions of rapid change. If we

apply a mechanized computation procedure this great accuracy seems to be required throughout since we do not know these critical regions in advance.

Comparing this new mathematical problem with the problem that confronts us in connection with the Riemann-Hugoniot approach, we realize that we face now a more difficult system of differential equations, but, on the whole, a problem, much more of a regular type. The Hugoniot approach which presumes sharp lines of discontinuity (of u,ρ,p) will prove of great value in cases where these discontinuity lines can be somehow determined by means of the shock conditions, or in some way, *independently* of the solution of the differential equations. (This was the case in our problem for $t \leqq t_0$, section II.) If however we do not know the shock line (as it happened in our problem for $t \leqq t_0$) and have to determine it along with the integration of the differential equations we are faced with a difficult and unusual problem (see section IV). We may be forced to use numerical methods like the one proposed by the author in sections IV–VI.

The integration of (68), (69), (70) should furnish a continuous solution of our problem just as the method outlined in sections VII, VIII. According to what precedes, this last method (as exposed here) can merely furnish an approximation to a solution of the Riemann problem where (3′) or a similar relation is assumed and the third shock condition neglected.

In both "continuous" methods the required accuracy of the computations is much greater than in the author's procedure, which corresponds to the Hugoniot approach, and where we tried to determine the discontinuity line along with the integration. The former seem, however, to be more amenable to mechanization. None of the methods exposed in this article are restricted to one-dimensional problems.

On Bergman's Integration Method in Two-Dimensional Compressible Fluid Flow

By R. v. MISES and M. SCHIFFER

Harvard University[1]

CONTENTS

Several years ago, Stefan Bergman developed a new method of using the theory of analytic functions in problems of partial differential equations of elliptic type. The application of this method to the theory of compressible fluid flow has been the subject matter of numerous papers and classified reports (see Bibliography). In the first part of the present paper a straightforward procedure for the integration of Chaplygin's equation (steady, subsonic, two-dimensional, irrotational flow), based on Bergman's general method, is presented. No previous knowledge of other papers or familiarity with more general developments is required.

[1] Research paper done under Navy Contract NOrd 8555-Task F at Harvard University. The ideas expressed in this paper represent the personal views of the authors and are not necessarily those of the Bureau of Ordnance.

The authors wish to thank Mr. Carl Cohen for his assistance in the preparation of the present paper.

The discussion is carried up to the very threshold of numerical computation. Particular attention is given to the determination of the exact limits of the domain of convergence, from the theoretical as well as from the practical point of view.

The second part of the present paper utilizes the solution given in the first part in a special way. It has been shown by Chaplygin that if the isentropic condition is approximated by a linear relation between p (pressure) and $1/\rho$ (reciprocal density) the compressible fluid equation in the hodograph plane reduces to the Laplace equation. The execution of this idea is known as the Kármán-Tsien method. Now, if the Chaplygin equation is dealt with in the manner as proposed in this paper, a particularly simple case presents itself when the p-ρ-relation is specialized in a more general way: The integrals can be given in a closed form if the precise isentropic condition is replaced by an approximation of a definite form. Since this form admits one arbitrary constant in addition to those appearing in the linear relation, a closer approximation to reality is possible in this way. This method to which the papers quoted as [6], [7], and [8], also refer is discussed in its various aspects in Part II.

Part I. General Theory

1. Chaplygin's Equation and Its Transformation

Chaplygin's equation [10][2] for the stream function ψ of a steady irrotational flow, with speed q and velocity direction θ as independent variables, reads:

$$\frac{\partial^2\psi}{\partial\theta^2} + \frac{\rho \cdot q}{1 - M^2}\frac{\partial}{\partial q}\left(\frac{q}{\rho}\frac{\partial\psi}{\partial q}\right) = 0. \tag{1}$$

Here, M is the Mach number q/a ($a = (dp/d\rho)^{\frac{1}{2}}$, the local sound velocity), p the pressure, and ρ the density. Both M and ρ are considered to be given functions of q (cf. section 2).

For subsonic flow we replace q by a new, dimensionless, variable λ, which is defined by

$$\frac{d\lambda}{dq} = \frac{(1 - M^2)^{\frac{1}{2}}}{q} = (q^{-2} - a^{-2})^{\frac{1}{2}} \qquad \text{with}$$

$$\lambda = 0 \qquad \text{for } q = a, \textit{ i.e.}, M = 1 \tag{2}$$

or

$$\lambda = -\int_q^a (1 - M^2(x))^{\frac{1}{2}} x^{-1}\, dx. \tag{2'}$$

[2] Numbers in brackets refer to the Bibliography at the end of this paper.

While q goes from zero to a, the new variable λ varies from $-\infty$ to 0.

From (2) we derive:

$$\frac{q}{\rho}\frac{\partial\psi}{\partial q} = \frac{q}{\rho}\frac{\partial\psi}{\partial\lambda}\frac{(1-M^2)^{\frac{1}{2}}}{q} = \frac{(1-M^2)^{\frac{1}{2}}}{\rho}\frac{\partial\psi}{\partial\lambda},$$

and introducing

$$z = \frac{\sqrt{1-M^2}}{\rho}, \tag{3}$$

we obtain

$$\frac{q}{\rho}\frac{\partial\psi}{\partial q} = z\frac{\partial\psi}{\partial\lambda}$$

and

$$\frac{\partial}{\partial q}\left(\frac{q}{\rho}\frac{\partial\psi}{\partial q}\right) = \frac{(1-M^2)^{\frac{1}{2}}}{q_{jl}}\frac{\partial}{\partial\lambda}\left(z\frac{\partial\psi}{\partial\lambda}\right). \tag{4}$$

If (4) is introduced into (1), the Chaplygin equation becomes:

$$\frac{\partial^2\psi}{\partial\theta^2} + \frac{1}{z}\frac{\partial}{\partial\lambda}\left(z\frac{\partial\psi}{\partial\lambda}\right) = 0 \tag{5}$$

or

$$z^{\frac{1}{2}}\frac{\partial^2\psi}{\partial\theta^2} + z^{-\frac{1}{2}}\frac{\partial}{\partial\lambda}\left(z\frac{\partial\psi}{\partial\lambda}\right) = 0. \tag{5'}$$

In (5') we replace ψ by

$$\psi^* = z^{\frac{1}{2}}\psi \tag{6}$$

so that

$$z\frac{\partial\psi}{\partial\lambda} = z\frac{\partial}{\partial\lambda}(z^{-\frac{1}{2}}\psi^*) = z^{\frac{1}{2}}\frac{\partial\psi^*}{\partial\lambda} - \psi^*\frac{d}{d\lambda}(z^{\frac{1}{2}})$$

and

$$\frac{\partial}{\partial\lambda}\left(z\frac{\partial\psi}{\partial\lambda}\right) = z^{\frac{1}{2}}\frac{\partial^2\psi^*}{\partial\lambda^2} - \frac{d^2}{d\lambda^2}(z^{\frac{1}{2}})\psi^*;$$

(5') therefore takes the form

$$\Delta\psi^* + f(\lambda)\psi^* = 0, \tag{7}$$

with

$$\Delta = \frac{\partial^2}{\partial\theta^2} + \frac{\partial^2}{\partial\lambda^2},$$

where the dimensionless quantity

$$f(\lambda) = -z^{-\frac{1}{2}}\frac{d^2(z^{\frac{1}{2}})}{d\lambda^2} = -\frac{z''}{2z} + \frac{z'^2}{4z^2} = -\left(\frac{z'}{2z}\right)^2 - \frac{d}{d\lambda}\left(\frac{z'}{2z}\right), \qquad \left(z' = \frac{dz}{d\lambda}\right) \tag{8}$$

depends on λ only.

Each function ψ^* of λ and θ that satisfies the partial differential equation (7) defines a stream function $\psi = z^{-\frac{1}{2}}\psi^*$.

2. Computation of f for Isentropic Flow

The theory so far developed applies to any fluid flow for which a definite relation between pressure and density holds. We now specify this relation by assuming that the density ρ and the pressure p satisfy the isentropic equation

$$p\rho^{-\kappa} = c, \qquad \frac{dp}{d\rho} = a^2 = \kappa p\rho^{-1} = \kappa c\rho^{\kappa-1}, \tag{1}$$

where κ is the ratio of specific heats. Then we obtain in the usual way:

$$\int \rho^{-1}dp = p\rho^{-1} + \int \rho^{-2}pd\rho = \kappa \int \rho^{-2}pd\rho = \frac{\kappa}{\kappa - 1}\, p\rho^{-1} = \frac{a^2}{\kappa - 1}.$$

Substituting this relation in the Bernoulli equation,

$$\frac{q^2}{2} + \int \rho^{-1}dp = \text{const.}, \tag{2}$$

we obtain

$$\frac{\kappa - 1}{2}\, q^2 + a^2 = a_0^2 \tag{3}$$

or

$$q^2\left[1 - \frac{\kappa - 1}{2}\, m\right] = a_0^2 m, \tag{3'}$$

where

$$m = M^2 = q^2a^{-2}, \text{ the square of the Mach number.}$$

Differentiating (3'), we obtain easily

$$\frac{d(q^2)}{dm} = q^4a_0^{-2}m^{-2}. \tag{3''}$$

Furthermore, it follows from (1) that

$$(\kappa - 1)\log\rho = \log(a^2) + \text{const.} \tag{4}$$

Using (3) and (3''), we derive from (4):

$$(\kappa - 1)\frac{d(\log \rho)}{dm} = -a^{-2}\frac{\kappa - 1}{2}\frac{d(q^2)}{dm} = -\frac{\kappa - 1}{2}q^4 m^{-2}a^{-2}a_0^{-2}$$

$$\frac{d(\log \rho)}{dm} = -\frac{1}{2}q^2 m^{-1}a_0^{-2}. \tag{4'}$$

The function f, defined in (1.8)[3] can be written:

$$f = -n^2 - \frac{dn}{d\lambda} \tag{5}$$

with

$$n = \frac{1}{2}\frac{d(\log z)}{d\lambda}. \tag{5'}$$

We defined the auxiliary variable

$$z = (1 - M^2)^{\frac{1}{2}}\rho^{-1}$$

in (1.3) and, replacing M^2 by m, we derive

$$\log z = \tfrac{1}{2}\log(1 - m) - \log \rho. \tag{6}$$

Using (4') and (3'), we obtain

$$\begin{aligned}\frac{d(\log z)}{dm} &= -\frac{1}{2}(1 - m)^{-1} + \frac{1}{2}q^2 m^{-1}a_0^{-2} \\ &= -\frac{1}{2}\left[(1 - m)^{-1} - \left(1 + \frac{1}{2}(\kappa - 1)m\right)^{-1}\right] \\ &= -\frac{1}{4}(\kappa + 1)m(1 - m)^{-1}\left(1 + \frac{1}{2}(\kappa - 1)m\right)^{-1} \\ &= -\frac{1}{4}(\kappa + 1)q^2(1 - m)^{-1}a_0^{-2}.\end{aligned} \tag{6'}$$

From the definition of λ as given in (1.2), it follows that

$$\frac{d\lambda}{d(q^2)} = (1 - m)^{\frac{1}{2}}(2q^2)^{-1} \tag{7}$$

[3] References to formulas in the same section are given by their numbers; references to formulas in previous sections are given by sections and numbers, *e.g.* "(1.2)," meaning "section 1, formula 2."

and thus, using (6′), (3″), (7):

$$n = \frac{d(\log z)}{2d\lambda} = -\frac{1}{8}(\kappa+1)q^2(1-m)^{-1}a_0^{-2}a_0^2m^2q^{-4}2q^2(1-m)^{-\frac{1}{2}}$$

$$= -\frac{1}{4}(\kappa+1)m^2(1-m)^{-\frac{1}{2}}. \quad (8)$$

By differentiation, using (3′), (3″), and (7), we obtain:

$$\frac{dn}{d\lambda} = -\frac{1}{4}(\kappa+1)\left[2m(1-m)^{-\frac{1}{2}} + \frac{3}{2}m^2(1-m)^{-\frac{3}{2}}\right] \cdot a_0^2m^2q^{-4}2q^2(1-m)^{-\frac{1}{2}}$$

$$= -\frac{1}{4}(\kappa+1)(1-m)^{-3}m^2\left[4-(3-2\kappa)m-\frac{1}{2}(\kappa-1)m^2\right]. \quad (9)$$

Then, by substituting (9) and the square of the right-hand side of (8) in (5), we obtain the result

$$f = \tfrac{1}{16}(\kappa+1)m^2(1-m)^{-3}[16-4(3-2\kappa)m-(3\kappa-1)m^2]. \quad (10)$$

This yields f in terms of m, the square of the Mach number.

The relation between λ and m is obtained by multiplying the right-hand sides of (3″) and (7), and by considering (3′):

$$\frac{d\lambda}{dm} = \frac{1}{2}(1-m)^{\frac{1}{2}}q^2a_0^{-2}m^{-2} = \frac{1}{2}(1-m)^{\frac{1}{2}}\left[m^{-1}+\frac{1}{2}(\kappa-1)\right]^{-1}m^{-2}. \quad (11)$$

Therefore, by integration,

$$\left.\begin{aligned}\lambda &= \tfrac{1}{2}\int_1^m (1-x)^{\frac{1}{2}}[x^{-1}+\tfrac{1}{2}(\kappa-1)]^{-1}x^{-2}dx \\ &= \log[1-(1-m)^{\frac{1}{2}}] - \tfrac{1}{2}\log m + h^{-1}\log[1+h(1-m)^{\frac{1}{2}}] \\ &\qquad - \tfrac{1}{2}h^{-1}\log[2(\kappa+1)^{-1}+h^2m]\end{aligned}\right\} \quad (11')$$

with

$$h = (\kappa-1)^{\frac{1}{2}}(\kappa+1)^{-\frac{1}{2}}. \quad (12)$$

The relations (10) and (11′) between λ, m, and f do not involve any integration constant (like a_0), since λ, m, and f are dimensionless. A further discussion of these relationships will follow later.

3. *Method of Generating Stream Functions*

After the determination of $f(\lambda)$, we come to the integration of the partial differential equation (1.7). Already Chaplygin determined an

infinity of solutions of this equation by the simple procedure of separating variables. One is led in this way to a set of solutions

$$C_n(\lambda,\theta) = \alpha_n(\lambda)\cos n\theta, \qquad S_n(\lambda,\theta) = \alpha_n(\lambda)\sin n\theta, \qquad n = 0, 1, 2, \cdots \quad (1)$$

where the α_n are expressed in a simple way by means of hypergeometric functions. The above particular solutions correspond to the set

$$c_n(\lambda,\theta) = \lambda^n \cos n\theta, \qquad s_n(\lambda,\theta) = \lambda^n \sin n\theta, \qquad n = 0, 1, 2, \cdots \quad (1')$$

of solutions for Laplace's equation $\Delta\psi^* = 0$. Every solution ψ^* of (1.7) which is regular in a given domain of the (λ,θ)-plane may be approximated uniformly in each closed subdomain by a series

$$\psi_N^*(\lambda,\theta) = \sum_{n=1}^{N} (a_n C_n + b_n S_n) \quad (2)$$

to an arbitrary degree of precision. It may be associated with the harmonic function

$$P_N(\lambda,\theta) = \sum_{n=1}^{N} \lambda^n (a_n \cos n\theta + b_n \sin n\theta) \quad (2')$$

and will, in fact, have many properties similar to those of the latter. Hydrodynamically, this means that $\psi_N = z^{-1}\psi_N^*$ and P_N will be stream-functions of compressible and incompressible flows, respectively, bearing more or less similarity to each other. Thus, the great experience in the theory of ideal incompressible flows may be used in order to create similar compressible flow patterns by the association (2) $\leftrightarrow$ (2'). This transition may be conceived as an operator transforming a solution of the one differential equation into a corresponding solution of the other.

Unfortunately, there appear in the theory of incompressible fluid flows functions that are neither regular nor single-valued when expressed in the hodograph plane. Consider for example a flow originating from a doublet at infinity and passing around a circle; one verifies easily that the stream function is a two-valued function possessing an infinity with branch character. In general, we may expect even in the simplest examples of flows around closed curves stream functions that are multivalued and possess algebraic and even logarithmic singularities. For these functions the above association process becomes inapplicable and the problem arises to develop another procedure in order to make harmonic functions correspond to solutions of the Chaplygin equation. This procedure has to be defined in the hodograph plane and must be applied in domains situated on Riemann surfaces over this plane. Only such

methods will permit the translation of incompressible fluid flow patterns into flow patterns for a compressible fluid in the large. Such a method has been elaborated by S. Bergman, [1] through [7], especially [6].

According to his method, we integrate the transformed Chaplygin equation (1.7) by setting

$$\psi^* = \sum_{n=0}^{\infty} g_n G_n \tag{3}$$

where each G_n depends on λ only and each g_n is a harmonic function of λ and θ. This series will be subjected to certain formal transformations. The justification of these transformations will be given in the next section by studying the uniform convergence of the series considered.

We find from the identity:

$$\Delta(AB) = A\Delta B + B\Delta A + 2\left(\frac{\partial A}{\partial \lambda}\frac{\partial B}{\partial \lambda} + \frac{\partial A}{\partial \theta}\frac{\partial B}{\partial \theta}\right)$$

and

$$\frac{\partial G_n}{\partial \theta} = 0, \qquad \Delta g_n = 0$$

that

$$\Delta(g_n G_n) = g_n G_n'' + 2G_n' \frac{\partial g_n}{\partial \lambda}.$$

Introducing the value of $\Delta(g_n G_n)$ in (3), we obtain

$$\Delta\psi^* = \sum_{n=0}^{\infty} \left[g_n G_n'' + 2G_n' \frac{\partial g_n}{\partial \lambda} \right]$$

and

$$\Delta\psi^* + f\psi^* = \sum_{n=0}^{\infty} \left[g_n(G_n'' + fG_n) + 2G_n' \frac{\partial g_n}{\partial \lambda} \right]. \tag{4}$$

In order to have the right-hand side vanish as required in (1.7), we choose:

$$G_0 = 1, \qquad G'_{n+1} = G''_n + fG_n \qquad n = 0, 1, 2, \cdots \tag{5a}$$

$$2\frac{\partial g_n}{\partial \lambda} = -g_{n-1}, \; g_0 \text{ harmonic, but otherwise arbitrary.} \tag{5b}$$

Then (4) becomes

$$\Delta\psi^* + f\psi^* = \sum_{n=0}^{\infty} [g_n(G'_{n+1} - fG_n + fG_n) - g_{n-1}G'_n]$$

$$= \sum_{n=0}^{\infty} [g_nG'_{n+1} - g_{n-1}G'_n] = 0,$$

as is seen by rearrangement of the series and in view of the fact that $G_0' = 0$. Thus, (3) with the conditions (5a) and (5b) is a solution of (1.7).

We now solve the recursion formula (5b) for the g_n in the following form: The g_n's must be harmonic functions of λ and θ. Therefore we choose analytic functions $\phi_n(\zeta)$, $\zeta = \lambda + i\theta$, such that $\phi_0(\zeta)$ is arbitrary analytic, and

$$\phi_n(\zeta) = -\tfrac{1}{2}\int_0^{\zeta} \phi_{n-1}(t)dt \tag{6}$$

and let g_0 be the real part of $\phi_0(\zeta)$ and $g_n = Re\{\phi_n(\zeta)\}$. Then we have in view of (6)

$$2\frac{\partial}{\partial\lambda} g_n(\lambda,\theta) = Re\{2\phi_n'(\zeta)\} = -Re\{\phi_{n-1}(\zeta)\} = -g_{n-1},$$

which shows that the g_n satisfy in fact the recursion formula (5b).

On the other hand, we derive from (6)

$$\phi_n(\zeta) = \frac{(-1)^n}{(n-1)!2^n}\int_0^{\zeta} \phi_0(t)(\zeta - t)^{n-1}dt, \qquad n > 0, \tag{6'}$$

whence

$$g_n(\lambda,\theta) = \frac{(-1)^n}{(n-1)!2^n} Re\left\{\int_0^{\zeta} \phi_0(t)(\zeta - t)^{n-1}dt\right\}. \tag{7}$$

4. The Domain of Convergence of the Development for ψ^*

In the representation (3.3), we expressed the stream function in the form of a series

$$\psi^*(\lambda,\theta) = \sum_{n=0}^{\infty} g_n(\lambda,\theta)G_n(\lambda) \tag{1}$$

where

$$G_0 = 1, \qquad G'_{n+1} = G''_n + fG_n. \tag{2}$$

The function f was defined in section 1 and computed in section 2,

and the $g_n(\lambda,\theta)$ are a sequence of harmonic functions satisfying the recursion formula

$$\frac{\partial}{\partial\lambda} g_n(\lambda,\theta) = -\frac{1}{2} g_{n-1}(\lambda,\theta). \tag{3}$$

We showed in the previous section, (3.6), that the $g_n(\lambda,\theta)$ may be chosen in the form

$$g_n(\lambda,\theta) = \frac{(-1)^n}{(n-1)!2^n} Re\left\{\int_0^\zeta \phi_0(t)(\zeta - t)^{n-1}dt\right\}, \qquad n > 0, \tag{4}$$
$$g_0(\lambda,\theta) = Re\{\phi_0(\zeta)\}$$

with ϕ_0 an arbitrary analytic function of the complex variable $\zeta = \lambda + i\theta$. Therefore, the development (1) takes the form

$$\psi^*(\lambda,\theta) = g_0(\lambda,\theta) + \sum_{n=1}^{\infty} G_n(\lambda) Re\left\{\int_0^\zeta \phi_0(t)\,\frac{(-1)^n(\zeta - t)^{n-1}}{2^n(n-1)!}\,dt\right\}.$$

Assuming uniform convergence in a certain domain for t, later to be determined, we obtain by interchange of the process of summation and integration

$$\psi^*(\lambda,\theta) = g_0(\lambda,\theta) + Re\left\{\int_0^\zeta \phi_0(t) U(t;\lambda,\theta)dt\right\}$$

with

$$U(t;\lambda,\theta) = \sum_{n=1}^{\infty} G_n(\lambda)\,\frac{(-1)^n(\zeta - t)^{n-1}}{2^n(n-1)!}. \tag{5}$$

This transformation of the series of $\psi^*(\lambda,\theta)$ is valid in exactly the same domain of the complex t-plane where (5) converges uniformly.

In order to find a domain of uniform convergence of $U(t;\lambda,\theta)$, we have to find a majorant of U and study its convergence. Because the development of U contains the G_n's, we have first to find functions $Q_n(\lambda)$ such that, for each n, $Q_n(\lambda)$ dominates $G_n(\lambda)$. This means that, for $-\infty < \lambda < 0$, all Q_n and their derivatives are larger than or equal to the moduli of the G_n and of their corresponding derivatives; in symbols, $G_n \ll Q_n$ shall imply:

$$|G_n| \leq Q_n \qquad \text{and} \qquad \left|\frac{d^\kappa G_n}{d\lambda^\kappa}\right| \leq \frac{d^\kappa Q_n}{d\lambda^\kappa}.$$

We shall now prove:

(A) For each partial differential equation of the type of equation (1.7),

where $f(\lambda)$ can be dominated by an expression of the form $C(\epsilon - \lambda)^{-2}$, *i.e.*,

$$f \ll F = C(\epsilon - \lambda)^{-2}, \qquad C > 0, \qquad \epsilon < 0, \tag{6}$$

the corresponding series $U(t;\lambda,\theta)$ is uniformly convergent in the domain

$$\left|\frac{\zeta - t}{2(\epsilon - \lambda)}\right| \leq a < 1. \tag{6'}$$

(B) A suitable constant C in (6) can be determined in the special case we are dealing with, namely, the function f derived from the adiabatic condition.

ad (A). We suppose that the modulus of f and of all its derivatives with respect to λ is smaller than

$$F = C(\epsilon - \lambda)^{-2}$$

and all its corresponding derivatives with respect to λ for a given $\epsilon < 0$.

Then we define functions Q_n by the recursion formula

$$\left.\begin{aligned} Q'_{n+1} &= Q''_n + C(\epsilon - \lambda)^{-2}Q_n, \\ Q_0 &= 1, \qquad Q_n(-\infty) = 0 \end{aligned}\right\} \tag{7}$$

and we have

$$G_n \ll Q_n, \tag{7'}$$

for the Q_n's are constructed of positive integrals and derivatives of F in exactly the same way as the G_n's are with respect to f, which is dominated by F.

The solution of (7) can be given in closed form:

$$Q_n = n!\mu_n(\epsilon - \lambda)^{-n} \tag{7''}$$

with the following recursion formula for the constants μ_n:

$$\mu_0 = 1, \qquad \mu_{n+1} = \mu_n(n^2 + n + C)(n + 1)^{-2} = \mu_n(n + \alpha)(n + \beta)(n + 1)^{-2} \tag{8}$$

where

$$\alpha = \tfrac{1}{2} - (\tfrac{1}{4} - C)^{\frac{1}{2}}, \qquad \beta = \tfrac{1}{2} + (\tfrac{1}{4} - C)^{\frac{1}{2}}.$$

The μ_n's obey the same recursion formula as the coefficients of the hypergeometric series

$$H(\alpha,\beta,\gamma;x) = \sum_{\nu=0}^{\infty} \mu_\nu x^\nu$$

with $\gamma = 1$.

None of the parameters α, β, γ, is zero or a negative integer. Hence, H, together with all its derivatives, is uniformly convergent for $|x| \leq a < 1$.

Substituting (7′) and (7″) in (5), we obtain

$$U(t;\lambda,\theta) \ll \sum_{n=1}^{\infty} Q_n(\lambda) 2^{-n} \frac{1}{(n-1)!} |\zeta - t|^{n-1}$$

$$= \sum_{n=1}^{\infty} \mu_n n! (\epsilon - \lambda)^{-n} 2^{-n} \frac{1}{(n-1)!} |\zeta - t|^{n-1}$$

$$= \frac{1}{2} (\epsilon - \lambda)^{-1} \sum_{n=1}^{\infty} n\mu_n \left(\frac{1}{2} \frac{1}{|\epsilon - \lambda|} |t - \zeta| \right)^{n-1}$$

But

$$\sum_{n=1}^{\infty} n\mu_n x^{n-1} = \frac{d}{dx} [H(\alpha,\beta,1;x)]$$

and consequently

$$U(t;\lambda,\theta) \ll \tfrac{1}{2}(\epsilon - \lambda)^{-1} H' \left(\alpha,\beta,1; \frac{1}{2} \frac{1}{|\epsilon - \lambda|} |\zeta - t| \right). \tag{9}$$

The uniform convergence of U and, therefore, of the development fo ψ^*, is assured for each region

$$\frac{1}{2} \frac{1}{|\epsilon - \lambda|} |\zeta - t| \leq a < 1.$$

In this domain, the series for $U(t;\lambda,\theta)$ as well as those for all derivative of this function converge uniformly and absolutely. This justifies al transformations performed in section 3 and proves that ψ^* satisfies (1.7)

ad (B). We shall now proceed to show that in equation (6) a suitabl constant C can be determined in the case of the function f that wa derived in section 2 on the basis of the adiabatic relation $p\rho^{-\kappa} = C$.

Introducing a new variable T by

$$T^2 = 1 - m, \tag{10}$$

f becomes an analytic function of T and has the development

$$f(T) = \alpha T^{-6} + \beta T^{-5} + \cdots + \kappa + \cdots, \tag{11}$$

which is regular for all complex values of T finite and different from zero

On the other hand, applying substitution (10) to equation (2.11′ we obtain:

$$\lambda = -\tfrac{1}{2}[\log(1+T) - \log(1-T)] + \tfrac{1}{2}h^{-1}[\log(1+hT) - \log(1-hT)]. \tag{12}$$

For complex values of T the variable λ assumes complex values also. From equation (12) we see that λ is a regular analytic function of T if

$$T \neq \pm 1, \pm h^{-1}$$

and that for these exceptional values of T, λ becomes infinite. For $T = \infty$ every determination of λ is purely imaginary.

From this and the equation obtained by differentiating (12),

$$\frac{d\lambda}{dT} = -(1 - h^2)T^2(1 - T^2)^{-1}(1 - h^2T^2)^{-1}, \tag{12'}$$

we find that every branch of the function $T(\lambda)$ is regular at each point λ in the half plane $Re\{\lambda - \epsilon\} < 0, \epsilon < 0$. We choose that determination of $T(\lambda)$ that is real for real λ.

Hence, by the monodromy theorem, $T(\lambda)$ is regular and uniform in the entire half plane $Re\{\lambda - \epsilon\} < 0$. Therefore for a fixed negative λ, T is bounded and different from zero on a circle $|\tau - \lambda| = (\epsilon - \lambda)$ and $f(T)$ is bounded also:

$$f(T) < K. \tag{13}$$

Let $f(T) = \varphi(\lambda)$; then Cauchy's formula yields, for the n-th derivative of any function φ:

$$\frac{d^n\varphi}{d\lambda^n} = n! \frac{1}{2\pi i} \oint_{|\tau - \lambda| = (\epsilon - \lambda)} \varphi(\tau)(\tau - \lambda)^{-(n+1)}\, d\tau$$

$$\left|\frac{d^n\varphi}{d\lambda^n}\right| \leq n!K(\epsilon - \lambda)^{-n}. \tag{14}$$

On the other hand, we have, from the definition of F in (6):

$$\frac{d^nF}{d\lambda^n} = C(n + 1)! \cdot (\epsilon - \lambda)^{-(n+2)}.$$

Hence, for real $\lambda < \epsilon$,

$$\left|\frac{d^nf(T(\lambda))}{d\lambda^n}\right| \leq KC^{-1}(n + 1)^{-1}(\epsilon - \lambda)^2 \frac{d^nF}{d\lambda^n},$$

and choosing

$$C = KA^2(n + 1)^{-1}, \qquad A \geq -\lambda,$$

we obtain

$$\left|\frac{d^nf}{d\lambda^n}\right| \leq \frac{d^nF}{d\lambda^n}$$

as required.

Let us now consider the significance of the conditions

$$\text{I. } \tfrac{1}{2}|\zeta - t||\epsilon - \lambda|^{-1} < 1 \qquad \text{and} \qquad \text{II. } \epsilon \geq \lambda \geq -A$$

which have been found sufficient for the convergence of the series (1). We have to integrate the function $U(t;\lambda,\theta)$ from 0 to ζ and we have to require at least (as may be seen by setting $t = 0$):

$$|\zeta| < 2|\epsilon - \lambda|.$$

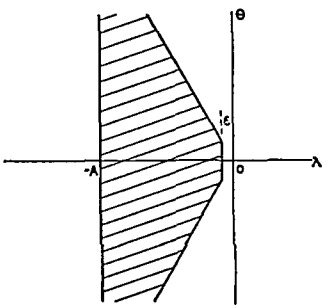

FIG. 1.—In each closed subdomain of the shaded area the series for $\psi^*(\lambda,\theta)$ converges absolutely and uniformly.

On the other hand, it is easily verified that this condition is sufficient in order to find a path of integration from 0 to ζ along which (6′) is fulfilled.

Now, $\zeta = \lambda + i\theta$, whence $\lambda^2 + \theta^2 < 4(\epsilon - \lambda)^2$. This determines the interior of a hyperbola in the ζ-plane. For $\epsilon \to 0$ this hyperbola converges to the two straight lines $\theta = \pm 3^{\frac{1}{2}} \cdot \lambda$, *i.e.*, a pair of lines through the origin forming an angle of 120° with each other. We may, therefore, finally state that the inequalities (6) with $C = KA^2(n+1)^{-1}$ and (6′) are insured in the interior of this domain and hence we may assume the absolute and uniform convergence of the series (1) in each closed subdomain of the angular domain considered, as long as $\phi_0(\zeta)$ itself is bounded in this domain (see Fig. 1).

5. Discussion of the Domain of Convergence of the Series Representing ψ^*

We have proved that the series (4.1) converges absolutely and uniformly in each closed subdomain of the angular domain $|\theta| < 3^{\frac{1}{2}}|\lambda|$. The question arises whether this series might not converge outside this domain, too.

If we introduce into the recursion formula (4.2) instead of f the comparison function $\bar{f}(\lambda) = C/\lambda^2$ we obtain instead of the G_n-factors the terms

$$Q_n(\lambda) = \mu_n n!(-\lambda)^{-n} \tag{1}$$

and the general term of our series is, therefore,

$$a_n = 2^{-n} n \mu_n \lambda^{-n} \cdot Re\left\{\int_0^\zeta \phi_0(t)(\zeta - t)^{n-1} dt\right\}. \tag{2}$$

In particular, if $\phi_0(\zeta) \equiv 1$, we obtain

$$a_n = \mu_n \cdot Re\{\zeta^n (2\lambda)^{-n}\}. \tag{3}$$

Let us now write

$$\zeta = |\zeta| e^{i\alpha}, \qquad \lambda = |\zeta| \cos \alpha. \tag{4}$$

Then we have

$$|a_n| = \mu_n |2 \cos \alpha|^{-n} \cdot |\cos n\alpha|. \tag{5}$$

We may now choose a point ζ outside our domain of proved convergence, but arbitrarily near it by taking $\alpha = \frac{2\pi}{3} - \frac{\pi}{N}$, where N is a sufficiently large integer. For all integers n' which are multiples of N we have

$$|a_{n'}| \geq \mu_{n'} |2 \cos \alpha|^{-n'} \cdot \tfrac{1}{2}. \tag{6}$$

Since $2|\cos \alpha| < 1$, and $\lim_{n=\infty} \left|\frac{\mu_{n+1}}{\mu_n}\right| = 1$, one easily sees that the sequence $|a_{n'}|$ will increase beyond every bound. Hence, in this case, the series for ψ^* does not converge outside the angular domain, $|\theta| < 3^{\frac{1}{2}}|\lambda|$. Since $\bar{f}(\lambda)$ behaves asymptotically like $f(\lambda)$ at $\lambda = 0$, there is, therefore, little chance that the conditions of convergence of (4.1) can be improved.

In general we shall need solutions of the differential equation (1.7) that are defined not only in the aforementioned domain of convergence. There are two ways to improve our previous result.

First, we remark that in every domain $Re\{\zeta\} < b < 0$ the function $f(\lambda)$ may be approximated uniformly to any degree of precision by a series of the form

$$f_m(\lambda) = \sum_{\nu=1}^{m} c_\nu e^{\lambda r_\nu}. \tag{7}$$

This series is, as an analytic function of the complex variable λ, regular in the whole finite λ-plane. Thus, as in part B of section 4, we may show that the development for a solution ψ_m of the differential equation

$$\Delta\psi_m + f_m(\lambda)\psi_m = 0 \tag{8}$$

converges absolutely in the domain

$$\tfrac{1}{2}|\zeta||\lambda - \sigma|^{-1} < 1 \tag{9}$$

for an arbitrary positive constant σ. It follows immediately that the development for ψ_m converges in the entire half plane $Re\{\zeta\} < 0$. If we replace, therefore, the function $f(\lambda)$ by an approximating $f_m(\lambda)$, we obtain a good agreement between the physical behavior of the gas described by the function $f_m(\lambda)$ and that of the real compressible gas described by $f(\lambda)$ up to a certain Mach number, as well as a series development for the solution ψ_m that converges absolutely in the whole domain $Re\{\zeta\} < 0$.

On the other hand, one should not exaggerate the importance of this result. The computation of the $G_n(\lambda)$ for the real $f(\lambda)$ is already quite a difficult task. If, for every degree m of approximation one had to carry out new computations for the corresponding $G_n^{(m)}(\lambda)$, the amount of work might be excessive. Moreover, we know that the convergence in the half plane $Re\{\zeta\} < 0$, will become worse for increasing approximation outside the sector $|\theta| < 3^{\frac{1}{2}}|\lambda|$.

We wish, therefore, to point out another way of continuing the development of ψ^* outside the original domain of convergence. Using the Borel method, we write

$$s_n(\lambda,\theta) = \sum_{\nu=0}^{n} G_n(\lambda) g_n(\lambda,\theta) \tag{10}$$

and obtain

$$\psi^*(\lambda,\theta) = \lim_{\kappa=\infty} \left\{ e^{-\kappa} \sum_{n=0}^{\infty} \frac{\kappa^{n+1}}{(n+1)!} s_n(\lambda,\theta) \right\} \tag{11}$$

This expression coincides with the original ψ^* in the whole domain of convergence. It might converge in a much wider domain. If we again replace $f(\lambda)$ by our function of comparison $\bar{f}(\lambda) = C/\lambda^2$, one sees easily that this expression (11) is defined in the entire half plane $Re\{\xi\} < 0$. It is, therefore, a useful transformation for the original function $f(\lambda)$, too, and leads, in fact, in most cases to the representation of $\psi^*(\lambda,\theta)$ throughout the required domain.

6. *Behavior of the G_n at $m = 1$*

The equations (3.5a) provide a recursion formula for the determination of the G_n. It may be written in the form

$$G_{n+1} = \frac{dG_n}{d\lambda} + \int^{\lambda} f G_n d\lambda, \qquad G_0 = 1.$$

If we compute this last integral, we obtain an integration constant each time, since the lower limit is arbitrary, *i.e.*, G_n would depend on n constants of integration. It follows, on the other hand, from equation (2.10) that $f = 0$ when $m = 0$, which is the case for $\lambda = -\infty$ [cf. equation (2.11′)]. We decide to fix the constants of integration by taking $-\infty$ as the lower limit of the integrals. It can be seen that in this case the integrals exist and the G_n are zero at $\lambda = -\infty$. However, at $\lambda = 0$, or $m = 1$, all G_n become infinite. It is therefore desirable to introduce other functions r_n in the place of the G_n which remain bounded. To find

such r_n we have to study the behavior of the G_n near $m = 1$.

For this purpose we substitute as in section 4:

$$T^2 = 1 - m \tag{1}$$

and consider $f(T)$ and $G_n(T)$ in a neighborhood of zero.

We had in (2.10):

$$f = \tfrac{1}{16}(\kappa + 1)(1 - T^2)^2 T^{-6}[5(\kappa + 1) + 2(5 - \kappa)T^2 - (3\kappa - 1)T^4]. \tag{2}$$

Assuming now that

$$G_n = c_n T^{-3n}(1 + b_n T^2 \cdots) = c_n T^{-3n} r_n(T), \tag{3}$$

we introduce into the recursion formula for the G_n the function $r_n(T)$ defined by

$$r_n(T) = 1 + b_n T^2 + \cdots. \tag{4}$$

Since $G_0 = 1$, we have $c_0 = 1, r_0 = 1$. From (4) we obtain:

$$\frac{dG_n}{dT} = c_n\left(T^{-3n}\frac{dr_n}{dT} - 3nT^{-(3n+1)}r_n\right) = c_n T^{-(3n+1)}(-3nr_n + Tr_n'), \tag{5}$$

$$r_n' = \frac{dr_n(T)}{dT} = 2b_n T + \cdots$$

According to (4.12') and using $\dfrac{\kappa - 1}{\kappa + 1} = h^2$, we have:

$$\frac{d\lambda}{dT} = T^2(h^2 - 1)(1 - T^2)^{-1}(1 - h^2T^2)^{-1}$$

$$= -2T^2[(\kappa + 1) - 2\kappa T^2 + (\kappa - 1)T^4]^{-1}. \tag{6}$$

By multiplying the right-hand sides of equations (2) and (6), we obtain

$$B = f\frac{d\lambda}{dT} = \frac{1}{16}(\kappa + 1)(1 - T^2)^2 T^{-6}[5(\kappa + 1) + 2(5 - \kappa)T^2$$

$$- (3\kappa - 1)T^4]T^2(h^2 - 1)(1 - T^2)^{-1}(1 - h^2T^2)^{-1}$$

$$= -\frac{1}{8}(1 - T^2)T^{-4}(1 - h^2T^2)^{-1}[5(\kappa + 1) + 2(5 - \kappa)T^2 - (3\kappa - 1)T^4]$$

$$= -\frac{1}{8}\cdot 5(\kappa + 1)T^{-4}[1 - 2\kappa\{5(\kappa + 1)\}^{-1}T^2 \cdots]. \tag{7}$$

From

$$G_{n+1} = \frac{dG_n}{d\lambda} + \int_{-\infty}^{\lambda} fG_n d\lambda = \frac{dG_n}{dT}A + \int_1^T BG_n dT, \tag{8}$$

where

$$A = \frac{dT}{d\lambda} = -\frac{1}{2}[(\kappa+1) - 2\kappa T^2 + (\kappa-1)T^4]T^{-2}, \tag{6'}$$

we obtain, by using (4) and (7):

$$c_{n+1}T^{-(3n+3)}(1 + b_{n+1}T^2 + \cdots) = -\tfrac{1}{2}c_nT^{-(3n+3)}$$
$$\cdot[-3n(1 + b_nT^2 + \cdots) + 2b_nT^2 + \cdots][(\kappa+1) - 2\kappa T^2 + (\kappa-1)T^4]$$
$$- \tfrac{1}{8}\cdot 5(\kappa+1)c_n\int_1^T x^{-4}\{1 - 2\kappa[5(\kappa+1)]^{-1}x^2 + \cdots\}$$
$$\cdot(1 + b_nx^2 + \cdots)x^{-3n}dx,$$

whence

$$\frac{c_{n+1}}{c_n}[T^{-(3n+3)} + b_{n+1}T^{-(3n+1)} + \cdots] = T^{-(3n+3)}$$
$$\cdot\left[\frac{1}{2}\cdot 3n(\kappa+1) + \frac{1}{8}(3n+3)^{-1}\cdot 5(\kappa+1)\right]$$
$$+ T^{-(3n+1)}\left\{(\kappa+1)\left[\frac{1}{2}(3n-2) + \frac{1}{8}\cdot 5(3n+1)^{-1}\right]b_n\right.$$
$$\left. - \kappa\left[3n + \frac{1}{4}(3n+1)^{-1}\right]\right\} + \cdots$$

Comparing the factors of equal powers of T on both sides of this last equation, we obtain

$$\frac{c_{n+1}}{c_n} = \frac{1}{2}\cdot 3n(\kappa+1) + \frac{1}{8}\cdot 5(\kappa+1)(3n+3)^{-1}$$
$$= \frac{1}{2}\cdot 3n(\kappa+1)\{1 + 5[36n(n+1)]^{-1}\}, \tag{9}$$

a recursion formula for the c_n that yields finally

$$c_{n+1} = [\tfrac{1}{2}\cdot 3(\kappa+1)]^n n!\prod_{\nu=1}^{n}\{1 + 5[36\nu(\nu+1)]^{-1}\}c_1. \tag{10}$$

Since $c_0 = 1$, we derive further from (9)

$$c_1 = \tfrac{1}{24}\cdot 5(\kappa+1),$$

which determines all c_n. Comparing now the coefficients of $T^{-(3n+1)}$, we find

$$\frac{c_{n+1}}{c_n} b_{n+1} = (\kappa + 1) \left\{ \left[\frac{1}{2} (3n - 2) + \frac{1}{8} \cdot 5(3n + 1)^{-1} \right] b_n - \left[\frac{1}{2} \cdot 3n \cdot 2\kappa(\kappa + 1)^{-1} + \frac{1}{4} \kappa(3n + 1)^{-1}(\kappa + 1)^{-1} \right] \right\},$$

$$b_{n+1}\{1 + 5[36n(n + 1)]^{-1}\} = b_n\{1 - 2(3n)^{-1} + 5[12n(3n + 1)]^{-1}\} - \{2\kappa(\kappa + 1)^{-1} + \kappa[6n(3n + 1)(\kappa + 1)]^{-1}\}, \quad (11)$$

which together with $b_0 = 1$ determines all b_n and justifies our particular choice of the functions $r_n(T)$.

If n is large, we obtain from (9)

$$\frac{c_{n+1}}{c_n} \approx \frac{1}{2} \cdot 3n(\kappa + 1),$$

and

$$b_n \approx -2n\kappa(\kappa + 1)^{-1} \quad \text{and} \quad \lim_{n \to \infty} \frac{b_{n+1}}{b_n} = 1. \quad (12)$$

Taking $\kappa = 1.4$, we obtain from (11)

$$\frac{1}{36} \cdot 5b_1 = -\frac{1}{6} \cdot \frac{1.4}{2.4}, \qquad b_1 = -.7.$$

In the same way, we derive

$$b_2 = -1.4, \qquad b_3 = -2.1, \qquad b_4 = -2.8.$$

7. *Recursion Formula for the Functions r_n*

In equation (6.4) we introduced new functions $r_n(T)$ with $r_n(0) = 1$ by setting

$$G_n(T) = c_n r_n(T) T^{-3n}. \quad (1)$$

The c_n's were determined in section 6.

By substituting (1) into the recursion formula (6.8) for the G_n's we obtain

$$\left. \begin{aligned} c_{n+1} r_{n+1}(T) T^{-(3n+3)} &= A c_n (T^{-3n} r_n' - 3n T^{-(3n+1)} r_n) \\ &\quad + c_n \int_1^T B x^{-3n} r_n(x) dx. \end{aligned} \right\} \quad (2)$$

The expressions for A and B were defined in (7) and (6′) of the previous section:

$$A = -\tfrac{1}{2}[(\kappa + 1) - 2\kappa T^2 + (\kappa - 1)T^4]T^{-2} = T^{-2} \sum_{\nu=0}^{4} \alpha_\nu T^\nu, \quad (3)$$

$$B = -\tfrac{1}{8}(1-T^2)[5(\kappa+1)+2(5-\kappa)T^2-(3\kappa-1)T^4]T^{-4}(1-h^2T^2)^{-1} = T^{-4}\sum_{\nu=0}^{\infty}\beta_\nu T^\nu. \quad (4)$$

We derive from (2), (3), and (4):

$$\frac{c_{n+1}}{c_n}r_{n+1} = \sum_{\nu=0}^{4}\alpha_\nu T^\nu(Tr_n' - 3nr_n) + T^{3n+3}\int_1^T x^{-(3n+4)}\sum_{\nu=0}^{\infty}\beta_\nu x^\nu r_n(x)dx. \quad (5)$$

In order to compute the $r_n(T)$ from this recursion formula, we have to keep in mind that $r_0 \equiv 1$ and that we obtain from (6.9) $c_1/c_0 = \frac{1}{2}$, $c_2/c_1 = \frac{77}{20}$ etc. Then we obtain

$$\tfrac{1}{2}r_1(T) = T^3\int_1^T x^{-4}\sum_{\nu=0}^{\infty}\beta_\nu x^\nu dx = T^3\int_1^T B(x)dx. \quad (6)$$

Using this result for the next recursive step, we find

$$\begin{aligned}\tfrac{77}{20}r_2(T) &= \sum_{\nu=0}^{4}\alpha_\nu T^\nu(Tr_1' - 3r_1) + T^6\int_1^T x^{-3}B(x)r_1(x)dx \\ &= \sum_{\nu=0}^{4}\alpha_\nu T^\nu(Tr_1' - 3r_1) + T^6\int_1^T 2B(x)\left(\int_1^x B(\tau)d\tau\right)dx \\ &= \sum_{\nu=0}^{4}\alpha_\nu T^\nu(Tr_1' - 3r_1) + T^6\left(\int_1^T B(\tau)d\tau\right)^2. \quad (7)\end{aligned}$$

The results (6) and (7) have one remarkable feature: since $B(T)$ contains only even powers of T, it appears that $r_1(T)$ and $r_2(T)$ are free from logarithmic terms and can be developed into power series at $T = 0$. In general, this will not be true. The power series for $r_2(T)$, when introduced into the integral in (5) in order to determine $r_3(T)$, will already produce a logarithmic term. This term, however, is multiplied by T^9 so that $r_3(T)$ has a regular development at the point $T = 0$ up to the ninth order. Further application of the recursion formula will preserve this logarithmic term and will also produce new additional terms of the type $T^\nu(\log T)^\mu$.

It is easily verified that we have in general

$$r_n(T) = P_0^{(n)}(T) + P_1^{(n)}(T)\log T + \cdots + P_{n-2}^{(n)}(T)(\log T)^{n-2}, \qquad n > 2, \quad (8)$$

where the $P_\nu^{(n)}(T)$ are regular power series of T. One may easily deduce recursion formulas for the $P_\nu^{(n)}$ by means of (5). Here, we wish to point out only that each $P_\nu^{(n)}(T)$ with $\nu > 0$ has only powers of T which are larger than 8.

We shall restrict ourselves to determining the first coefficients of $P_0^{(n)}(T)$. Let us assume the development

$$P_0^{(n)}(T) = \sum_{\nu=0}^{\infty} \rho_\nu^{(n)} T^\nu, \qquad \rho_0^{(n)} = 1. \tag{9}$$

From (5) we find for the coefficients $\rho_\nu^{(n)}$ the following recursion formula as long as $\nu \leq 8$, $\nu < 3n + 3$:

$$\frac{c_{n+1}}{c_n} \rho_\nu^{(n+1)} = \sum_{\mu=0}^{\nu} \{(\mu - 3n)\alpha_{\nu-\mu} + \beta_{\nu-\mu}[\nu - (3n + 3)]^{-1}\} \rho_\mu^{(n)}. \tag{10}$$

To obtain numerical values for the constants ρ, we introduce the value $\kappa = 1.4$ into (6.9) and obtain

$$\frac{c_{n+1}}{c_n} = \frac{36n^2 + 36n + 5}{10(n + 1)}.$$

The numerical values of the α_i and β_i are:

i	α	β
0	−1.200	−1.500
1	0	0
2	1.400	0.350
3	0	0
4	−0.200	1.358
5	0	0
.	.	.
.	.	.

From the definition and the recursion formula (10) for the $\rho_\nu^{(n)}$ we find:

$$\rho_0^{(n)} \equiv 1.000,\ \rho_1^{(n)} \equiv 0.000,\ \rho_2^{(n)} = -0.7000 \cdot n,$$
$$\rho_3^{(1)} = -2.889,\ \rho_3^{(n)} = 5n(36n^2 - 36n + 5)^{-1}\rho_3^{(1)},$$
$$\rho_3^{(n+1)} = (n + 1)n^{-1}(36n^2 - 36n + 5)(36n^2 + 36n + 5)^{-1}\rho_3^{(n)},$$

whence

$$\lim_{n=\infty} \frac{\rho_3^{(n+1)}}{\rho_3^{(n)}} = 1, \qquad \lim_{n=\infty} \rho_3^{(n)} = 0.$$

Further $\rho_4^{(1)} = 2.716$,

$$\rho_4^{(n+1)} = (n+1)(36n^2+36n+5)^{-1}(3n-1)^{-1}[88.200n^3 - 70.200n^2 + 16.050n - 13.578 + 9\rho_4^{(n)}(12n^2-20n+7)].$$

For large n,

$$\rho_4^{(n+1)} \approx \rho_4^{(n)} + 0.817n \approx \rho_4^{(1)} + \tfrac{1}{2}\cdot 0.817n(n-1).$$

Further,

$$\rho_5^{(1)} = 0, \qquad \rho_5^{(2)} = 0.263,$$

$$\rho_5^{(n+1)} = 10(n+1)(36n^2+36n+5)^{-1}\{\rho_3^{(n)}[1.4(3-3n) - 0.35(3n-2)^{-1}] + \rho_5^{(n)}[1.2(3n-5) + 1.5(3n-2)^{-1}]\}.$$

Since for large n,

$$\rho_3^{(n)} \approx 0, \qquad \text{we have} \qquad \lim_{n=\infty} \frac{\rho_5^{(n+1)}}{\rho_5^{(n)}} = 1.$$

It may further be shown that

$$\lim_{n=\infty} \rho_5^{(n)} = 0.$$

Part II. Simplified Pressure-Density Relation

1. Definition of a Series Representing a Stream Function ψ^* Regular in the Whole Half Plane

The result of section I.4[4] was that the series for ψ^* (section I.1) converges in an angular sector of the half plane $\lambda < 0$. To extend the representation for ψ^* by "analytic continuation" is possible but involves complicated computations. Moreover, the procedure employed so far has the disadvantage that the computation of the functions G_n is increasingly complicated with increasing n and that each G_n involves the previous G_m's up to $m = n-1$.

So far, we started with the adiabatic relation, based on the equation of state for a perfect gas, and developed a representation that can be carried out in practice only with a certain approximation. We shall now reverse our method. We shall begin with an approximate assumption concerning the physical function f, thus replacing it by another function $\bar{f}$, which leads to a simple mathematical representation for $\bar{\psi}^*$, instead of the stream function ψ^*, which converges absolutely and uniformly at least in the half plane $\lambda < 0$, *i.e.*, in the whole subsonic region. The computations will now be relatively easy, while we shall have to justify our choice of $\bar{f}$ by showing that the hypothetical gas thus described is sufficiently similar to a real gas.

[4] Roman numerals refer to the Part [*e.g.*, "I.4.1" means "Part I, section 4, formula (1)"].

We begin with a function

$$\tilde{f} = C\lambda^{-2}, \qquad C > 0, \tag{1}$$

instead of the function f as defined and computed in previous sections and derived from the pressure-density relation $p\rho^{-\kappa} = c$. Similarly, as in section I.4, we are now led to functions $\tilde{G}_n$, such that

$$\left.\begin{aligned} \tilde{G}'_{n+1} &= \tilde{G}''_n + C\lambda^{-2}\tilde{G}_n, \\ \tilde{G}_0 &= 1, \qquad \tilde{G}_n(-\infty) = 0, \qquad n > 0 \end{aligned}\right\} \tag{2}$$

whence

$$\tilde{G}_n = n!\mu_n(-\lambda)^{-n}. \tag{3}$$

The function U [equation (I.4.5)] now takes the form:

$$\begin{aligned} \tilde{U}(t;\lambda,\theta) &= -\sum_{n=1}^{\infty} 2^{-n} n!\mu_n(-\lambda)^{-n}(t-\zeta)^{n-1}\frac{1}{(n-1)!} \\ &= (2\lambda)^{-1}\sum_{n=1}^{\infty}\mu_n n(\zeta - t)^{n-1}(2\lambda)^{-(n-1)}. \end{aligned} \tag{4}$$

As shown in section I.4,

$$\tilde{U}(t;\lambda,\theta) = (2\lambda)^{-1}\frac{d}{dx}[H(\alpha,\beta,\gamma;x)]$$

where H is the hypergeometric function with $\alpha = \frac{1}{2} - (\frac{1}{4} - C)^{\frac{1}{2}}$, $\beta = \frac{1}{2} + (\frac{1}{4} - C)^{\frac{1}{2}}$, $\gamma = 1$; and $x = (2\lambda)^{-1}(\zeta - t)$.
Hence:

$$\tilde{U}(t;\lambda,\theta) = -\frac{d}{dt}\{H[\alpha,\beta,\gamma;\,(2\lambda)^{-1}(\zeta - t)]\}. \tag{5}$$

The series for ψ^* then takes the form

$$\tilde{\psi}^*(\lambda,\theta) = g_0(\lambda,\theta) - Re\left\{\int_0^{\zeta}\phi_0(t)\frac{d}{dt}\{H[\alpha,\beta,\gamma;\,(2\lambda)^{-1}(\zeta - t)]\}dt\right\}. \tag{6}$$

The points of singularity of the hypergeometric function H are at

$$(2\lambda)^{-1}(\zeta - t) = 0,\ 1,\ \infty.$$

The branch of H considered in our representation is even regular at the origin. If $(2\lambda)^{-1}(\zeta - t) = \infty$, then for finite ζ, one has $\lambda = 0$; that is, the Mach number equals 1.

On the other hand, $(2\lambda)^{-1}(\zeta - t) = 1$ implies $t = -(\lambda - i\theta)$. This singularity is in the half plane $\lambda > 0$, *i.e.*, outside the subsonic region.

Therefore, $\bar{U}$ and hence $\bar{\psi}^*$ are generated from the analytic function $\phi_0(\zeta)$ by means of a well-known function and are regular in the whole subsonic region.

A further simplification can be obtained by the assumption $\phi_0(0) = 0$. Since $g_0(\lambda,\theta) = Re(\phi_0(\zeta))$, equation (6) can be written

$$\bar{\psi}^*(\lambda,\theta) = Re\left\{\phi_0(\zeta) - \int_0^\zeta \phi_0(t)\frac{d}{dt}\{H[\alpha,\beta,\gamma;\ (2\lambda)^{-1}(\zeta - t)]\}dt\right\}$$

$$= Re\left\{\phi_0(\zeta) - \phi_0(\zeta)H(\alpha,\beta,\gamma;0) + \phi_0(0)H[\alpha,\beta,\gamma;\ (2\lambda)^{-1}\zeta]\right.$$

$$\left. + \int_0^\zeta \phi_0'(t)H[\alpha,\beta,\gamma;\ (2\lambda)^{-1}(\zeta - t)]dt\right\}. \quad (7)$$

Since $H(\alpha,\beta,\gamma;0) = 1$, the assumption $\phi_0(0) = 0$ leads to

$$\bar{\psi}^*(\lambda,\theta) = Re\left\{\int_0^\zeta \phi_0'(t)H[\alpha,\beta,\gamma;\ (2\lambda)^{-1}(\zeta - t)]dt\right\}. \quad (7')$$

If we start with a flow of an incompressible fluid, described by a stream function $g_0(\lambda,\theta) = Re[\phi_0(\zeta)]$, the application of the operation (6) to $\phi_0(\zeta)$ will lead to a corresponding flow pattern of the compressible fluid considered that will in general preserve the type of the original pattern. But while a change of $\phi_0(\zeta)$ by an additive constant in the incompressible flow does not change the flow described at all, the addition of every such constant will lead to a different flow pattern in the compressible fluid flow, as is easily seen from (7). Among all the flows, corresponding to the same flow of an incompressible fluid, there exists one [characterized by the assumption $\phi_0(0) = 0$] for which the particularly simple representation (7') is valid.

This remark shows that the correspondence between incompressible and compressible flow patterns is by no means uniquely defined and that the same generating procedure leads to an infinity of different compressible fluid stream functions if we start from the same incompressible fluid flow.

As remarked in section (I.3), our procedure of finding solutions for the transformed Chaplygin equation may be interpreted as follows: One starts from a known flow pattern of an incompressible fluid and corrects it for the compressible case by applying the above operation to its stream function $g_0(\lambda,\theta)$. This gives a certain distortion of this stream function g_0. It is important to get a measure for the magnitude of this distortion. We find a partial answer from (6). The particular stream function $g_0(\lambda,\theta) = c$ is transformed into

$$\bar{\psi}^*(\lambda,\theta) = c \cdot Re\{H[\alpha,\beta,\gamma;\ (2\lambda)^{-1}\zeta]\} = c \cdot Re\{H[\alpha,\beta,\gamma;\ (\tfrac{1}{2} + \tfrac{1}{2}i\theta\lambda^{-1})]\}.$$

One sees that for large values of $|\lambda|$, *i.e.*, small velocities, $\bar{\psi}^*$ does not vary too much, but that for smaller values of λ the deviation from the constancy becomes appreciable. This particular $\bar{\psi}^*$ might serve as a criterion for the distortion in dependence on λ.

2. The Physical Relations Corresponding to the Assumption $\bar{f} = C\lambda^{-2}$

In section II.1 we found that under the assumption (1) the reduced stream function $\bar{\psi}^*$ can be generated by means of a well-known function that is regular in the whole subsonic region. Now, we have to study how far our hypothetical gas approximates the real one. In other words, we have to study the physical behavior of our gas. A gas is described by a curve in the space of the four variables, q, p, ρ, and M, where q is the velocity, p the pressure, ρ the density, and M the Mach number. We aim, therefore, to obtain functions and curves describing the relations between the different variables. It is, however, sufficient to compute and plot only three of the 6 possible relations. We choose $M(\rho)$, $q(\rho)$, and $p(\rho)$.

I. The relation $M(\rho)$.

In section I.1 we defined the auxiliary variable z by

$$z = (1 - M^2)^{\frac{1}{2}}\rho^{-1}. \tag{1}$$

Based on Chaplygin's equation, we obtained for the function $f(\lambda)$ as defined in (I.1.7)

$$f(\lambda) = -z^{-\frac{1}{2}}\frac{d^2}{d\lambda^2}(z^{\frac{1}{2}}), \tag{2}$$

whence

$$(z^{\frac{1}{2}})'' + f(\lambda)z^{\frac{1}{2}} = 0.$$

Now, dealing with the hypothetical gas, we substitute $\bar{f}$ for f,

$$\bar{f} = C\lambda^{-2},$$

and therefore obtain for $z^{\frac{1}{2}}$ the following linear differential equation:

$$(z^{\frac{1}{2}})'' + C\lambda^{-2}z^{\frac{1}{2}} = 0. \tag{2'}$$

The general solution of (2') is

$$z_{\frac{1}{2}} = \gamma_1 \cdot |\lambda|^{\delta_1} + \gamma_2 \cdot |\lambda|^{\delta_2}. \tag{3}$$

The exponents δ_1, δ_2 are the solutions of the equation $\delta(\delta - 1) + C = 0$,

$$\delta_{1,2} = \tfrac{1}{2} \pm (\tfrac{1}{4} - C)^{\frac{1}{2}}.$$

Since δ_1 and δ_2 are determined by our choice of C—and we shall choose C positive, near zero so that $\delta_1 \sim 1$, $\delta_2 \sim 0$—we have at our disposal in

addition to our freedom in choosing C the two parameters γ_1 and γ_2.

In the particular case $C = 0$ we obtain $\delta_1 = 1$, $\delta_2 = 0$, *i.e.*,

$$z^{\frac{1}{2}} = \gamma_1|\lambda| + \gamma_2. \tag{3'}$$

Already Chaplygin [10] realized that the equation (I.1.1) can be transformed into Laplace's equation if the p-ρ-relation is assumed to be of the form $p = \alpha\rho^{-1} + \beta$, and that in this case the whole theory of a compressible fluid flow can be reduced to the well-developed theory of an incompressible fluid flow. This approach was considerably developed later by von Kármán [11] and Tsien [12] and the assumption of a linear p-ρ^{-1}-relation is known now as the Kármán-Tsien approximation. One finds easily in this case $z = \gamma$, *i.e.*, a particular case of (3') with $\gamma_1 = 0$. Since this approximation is very useful over a wide range of λ, we shall henceforth also assume $\gamma_1 = 0$ in our improved approximation. This will simplify our computations considerably; but it should be kept in mind that, if necessary, we have at our disposal an additional parameter in order to obtain a better agreement between the hypothetical and the real gas.

Choosing $\gamma_1 = 0$ and dropping the indices, we have in (3):

$$z^{\frac{1}{2}} = \gamma|\lambda|^{\delta}, \tag{3''}$$

whence

$$-\lambda = z^{\frac{1}{2\delta}}\gamma^{-\frac{1}{\delta}} \tag{4}$$

and

$$\frac{d\lambda}{d\rho} = -(2\delta)^{-1}\gamma^{-\frac{1}{\delta}}z^{\frac{1}{2\delta}-1} \cdot \frac{dz}{d\rho}. \tag{4'}$$

On the other hand, in (I.1.2) we defined

$$\frac{d\lambda}{dq} = (1 - M^2)^{\frac{1}{2}}q^{-1},$$

whence, using (1):

$$\frac{d\lambda}{dq} = \rho q^{-1}z. \tag{5}$$

From the Bernoulli relation

$$q\frac{dq}{d\rho} + \rho^{-1}\frac{dp}{d\rho} = 0$$

we derive

$$\frac{d\lambda}{d\rho} = \frac{d\lambda}{dq}\frac{dq}{d\rho} = -zq^{-2}\frac{dp}{d\rho},$$

and since

$$M = q\left(\frac{dp}{d\rho}\right)^{-\frac{1}{2}} = (1 - z^2\rho^2)^{\frac{1}{2}},$$

we obtain

$$\frac{d\lambda}{d\rho} = -zM^{-2} = -z(1 - z^2\rho^2)^{-1} \tag{6}$$

When we equate the right sides of (4′) and (6), the result obtained is

$$\frac{dz}{d\rho} - 2\delta\gamma^{\frac{1}{\delta}}z^{2-\frac{1}{2\delta}}(1 - z^2\rho^2)^{-1} = 0. \tag{7}$$

This differential equation yields z as a function of ρ, and because $M^2 = 1 - z^2\rho^2$, we can compute from (7) $M(\rho)$, *i.e.*, one of our desired relations between the variables of the gas. However, the differential equation (7) cannot be solved in a closed form. We have solved it numerically in the interval $0 < \rho z < 1$. At the extreme values of this interval, the Mach numbers are 1 and 0, respectively.

The integral curves $z(\rho)$, representing solutions of (7), are monotonically increasing in the subsonic region, because $1 - z^2\rho^2 > 0$, $\gamma^{\frac{1}{\delta}} > 0$, for positive z [see (4)], and $\delta > 0$.

II. The relation $q(\rho)$.

In Bernoulli's relation

$$\tfrac{1}{2}q^2 + \int_{\rho_0}^{\rho} x^{-1}dp(x) = c_1$$

we substitute

$$q^2 = M^2\frac{dp}{d\rho} = M^2p'$$

and obtain

$$\tfrac{1}{2}\rho M^2\rho^{-1}p' + \int_{\rho_0}^{\rho} x^{-1}p'(x)dx = c_1. \tag{8}$$

Writing $J(\rho)$ for $\int_{\rho_0}^{\rho} x^{-1}p'(x)dx$ we obtain the differential equation for $J(\rho)$:

$$\tfrac{1}{2}\rho M^2J'(\rho) + J(\rho) = c_1,$$

leading to

$$J(\rho) = c_1 - c_2 \cdot exp\left[-2\int_{\rho_0}^{\rho} x^{-1}M(x)^{-2}dx\right]. \tag{9}$$

Since

$$\tfrac{1}{2}q^2 = c_1 - J(\rho),$$

we obtain

$$q^2 = 2c_2 \cdot exp\left[-2\int_{\rho_0}^{\rho} x^{-1}M(x)^{-2}dx\right], \tag{10}$$

the desired relation $q(\rho)$.

III. The relation $p(\rho)$.

Since $J(\rho) = \int_{\rho_0}^{\rho} x^{-1}p'(x)dx$, we obtain from (9)

$$\frac{dJ(\rho)}{d\rho} = \rho^{-1}p' = c_2 \cdot exp\left[-2\int_{\rho_0}^{\rho} x^{-1}M(x)^{-2}dx\right] 2 \cdot M^{-2}\rho^{-1},$$

$$p' = 2c_2M^{-2} \cdot exp\left[-2\int_{\rho_0}^{\rho} x^{-1}M(x)^{-2}dx\right],$$

whence

$$p = 2c_2\int_{\rho_0}^{\rho} M(x)^{-2} \cdot exp\left[-2\int_{\rho_0}^{x} y^{-1}M(y)^{-2}dy\right]dx + c_3, \tag{11}$$

the desired relation $p(\rho)$.

It should be noted that the integration of the differential equation (7) determines $M(\rho)$ only up to a constant of integration. We may determine this constant by the requirement that the values $M = 0$ and $\rho = 1$ shall correspond, which determines the units in which ρ is measured.

In formula (10), the value $\rho_1 = 1$ of ρ for which $M = 0$, is obviously of special interest. We shall show that $\int_{\rho_0}^{1} x^{-1}M(x)^{-2}dx$ is convergent, and this will imply that q is different from zero at $M = 0$. Therefore, since $M = q(p')^{-\frac{1}{2}}$, the velocity of sound $c = (p')^{\frac{1}{2}}$, is infinite for $M = 0$, *i.e.*, at $M = 0$ the gas behaves like an incompressible fluid.

We shall study the behavior of $z(\rho)$ at $\rho = 1$. We substitute

$$z = 1 + A_1(\rho - 1)^{\epsilon_1} + A_2(\rho - 1)^{\epsilon_2} + \cdots, \qquad 0 < \epsilon_1 < \epsilon_2 \cdots \tag{12}$$

with undetermined constants A_i and ϵ_i. By an easy computation, we obtain from (7) the following condition on these constants:

$$-2\epsilon_1A_1^2(\rho - 1)^{2\epsilon_1 - 1} - 2\epsilon_1A_1(\rho - 1)^{\epsilon_1} + \cdots$$

$$= 2\delta\gamma^{\frac{1}{\delta}}[1 + A_1\{2 - (2\delta)^{-1}\}(\rho - 1)^{\epsilon_1} + \cdots]. \tag{13}$$

By comparing the smallest powers of $(\rho - 1)$ on both sides we obtain the condition

$$2\epsilon_1 - 1 = 0, \qquad \epsilon_1 = \tfrac{1}{2}. \tag{14}$$

Hence, we have

$$z = 1 + A_1(\rho - 1)^{\frac{1}{2}} + \text{higher powers of } (\rho - 1), \tag{15}$$

and, therefore, using (1):

$$M^2 = 1 - \rho^2z^2 = -2A_1(\rho - 1)^{\frac{1}{2}} + \cdots. \tag{16}$$

Finally, we find

$$\rho^{-1}M^{-2} = -(2A_1)^{-1}(\rho - 1)^{-\frac{1}{2}} + \cdots \tag{17}$$

where the dots denote a series which is finite at the point $\rho = 1$. Now we integrate (17) term by term and obtain

$$\int_{\rho_0}^{\rho} x^{-1}M(x)^{-2}dx = -A_1^{-1}[(\rho - 1)^{\frac{1}{2}} - (\rho_0 - 1)^{\frac{1}{2}}] + \cdots,$$

which proves the convergence of the integral at the point $\rho = 1$.

We come, therefore, to the result that the velocity q of our hypothetical gas is never zero, but has a minimum value $q_{\min}$ corresponding to $M = 0$.

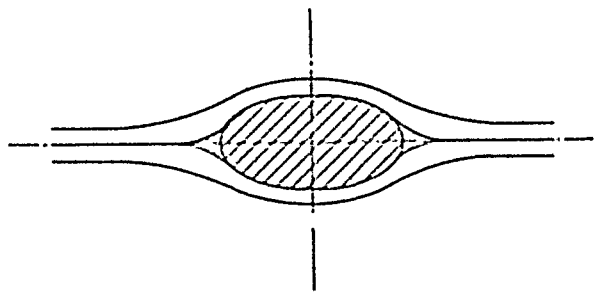

FIG. 2.—Flow around an obstacle according to the assumption $\bar{f} = C\lambda^{-2}$. No stagnation points, but wakes.

In order to understand the meaning of this fact, consider at first a real gas coming from infinity with a finite speed upon an obstacle with a smooth boundary. The streamline $\psi = 0$ which encloses this boundary will split up at a certain point of this boundary into two branches that reunite at another point of the boundary from where the streamline continues to infinity. From continuity considerations we conclude that the velocity at the two branch points must be zero. Applying the same considerations to our hypothetical fluid, which does not permit zero velocities, we arrive at an apparent contradiction. Its solution lies in the fact that the fluid fans out a little before the body and closes in a little behind it so that the branch points of the streamline are the vertices of two cusps formed by the streamline (see Fig. 2). At the cusp points the velocity may obviously remain finite. If we consider, therefore, the flow of the real gas that is approximated by our hypothetical fluid, we may say that this approximation certainly breaks down in the region where the velocity becomes smaller than the minimum velocity. Here our hypothetical flow produces wakes that are only caused by the insufficient approximation. This fact is a serious weakness of this kind of approximation. It may, however, be kept less significant if we choose

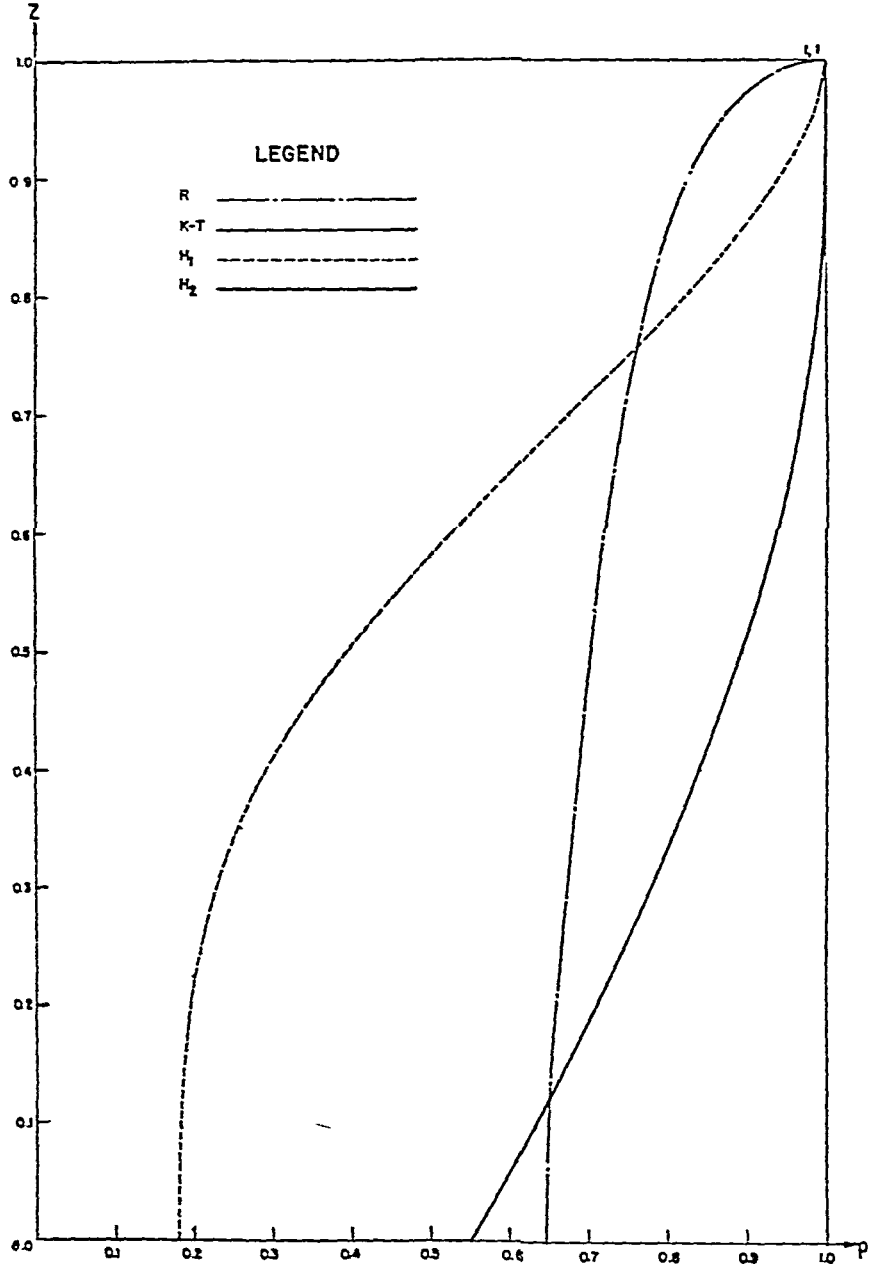

Figs. 3–6 show the relations $z(\rho)$, $M(\rho)$, $q(\rho)$, and $p(\rho)$ according to the theory of a real gas (R), to the Kármán-Tsien approximation ($K-T$), and for two gases based on the assumption $\bar{f} = C\lambda^{-2}$ (H_1 and H_2).

FIG. 3.—$z(\rho)$-curves [where $z = \rho^{-1}(1 - M^2)^{\frac{1}{2}}$].

the constant δ so small that $q_{\min}$ has a sufficiently small value. In this way we may improve the Kármán-Tsien method for higher Mach numbers without sacrificing too much in the approximation at the velocity zero.

3. *Numerical Discussion*

In order to study the approximation to the real gas yielded by our theoretical assumption

$$\tilde{f} = C\lambda^{-2}, \qquad C > 0, \tag{1}$$

we discuss the $M(\rho)$-, $q(\rho)$-, and $p(\rho)$-relations for a real gas, for a gas based on the Kármán-Tsien theory, and for two gases based on (1). Since z was an important auxiliary variable in our theory, we also include the relation $z(\rho)$. To facilitate comparison, we choose in the following graphs the scale such that we have at the point $M = 0$, $\rho_0 = 1$ and $p_0 = 1$. This assumption leads to a scale for q also, by the use of the Bernoulli relation.

For the real gas, we then obtain the following relations:

$$p = \rho^\kappa = \rho^{1.4}, \qquad (\kappa = 1.4), \tag{2}$$

$$q^2 = 2\kappa(\kappa - 1)^{-1}(1 - \rho^{\kappa-1}) = 7(1 - \rho^{0.4}), \tag{3}$$

$$M^2 = q^2(p')^{-1} = 2(\kappa - 1)^{-1}(\rho^{1-\kappa} - 1) = 5(\rho^{-0.4} - 1), \tag{4}$$

$$z^2 = (1 - M^2)\rho^{-2} = (\kappa + 1)(\kappa - 1)^{-1}\rho^{-2} - 2(\kappa - 1)^{-1}\rho^{-(\kappa+1)} = 6\rho^{-2} - 5\rho^{-2.4}. \tag{5}$$

For the Kármán-Tsien approximation, we obtain the following corresponding equations:

$$p = -A\rho^{-1} + (1 + A), \qquad A > 0, \tag{2'}$$

$$q^2 = A(\rho^{-2} - 1) \tag{3'}$$

$$M^2 = 1 - \rho^2 \tag{4'}$$

$$z = 1. \tag{5'}$$

Now, starting with

$$\tilde{f} = C\lambda^{-2} \tag{1}$$

we obtained in (II.2.3):

$$z^{\frac{1}{\delta}} = \gamma \cdot |\lambda|^{\frac{1}{\delta}}, \tag{6}$$

and eventually in (II.2.7):

$$\frac{dz}{d\rho} - 2\delta\gamma^{\frac{1}{\delta}} \cdot z^{2-\frac{1}{2\delta}}(1 - z^2\rho^2)^{-1} = 0. \tag{7}$$

In view of (I.1.3) and our choice of scale, $\rho_0 = 1$ implies $z_0 = 1$, which fixes the constant of integration. However, γ and δ are two parameters at our disposal. For the particular choice $\delta = 0$ and $\gamma = 1$ we obtain the Kármán-Tsien case considered above. It is obvious that the

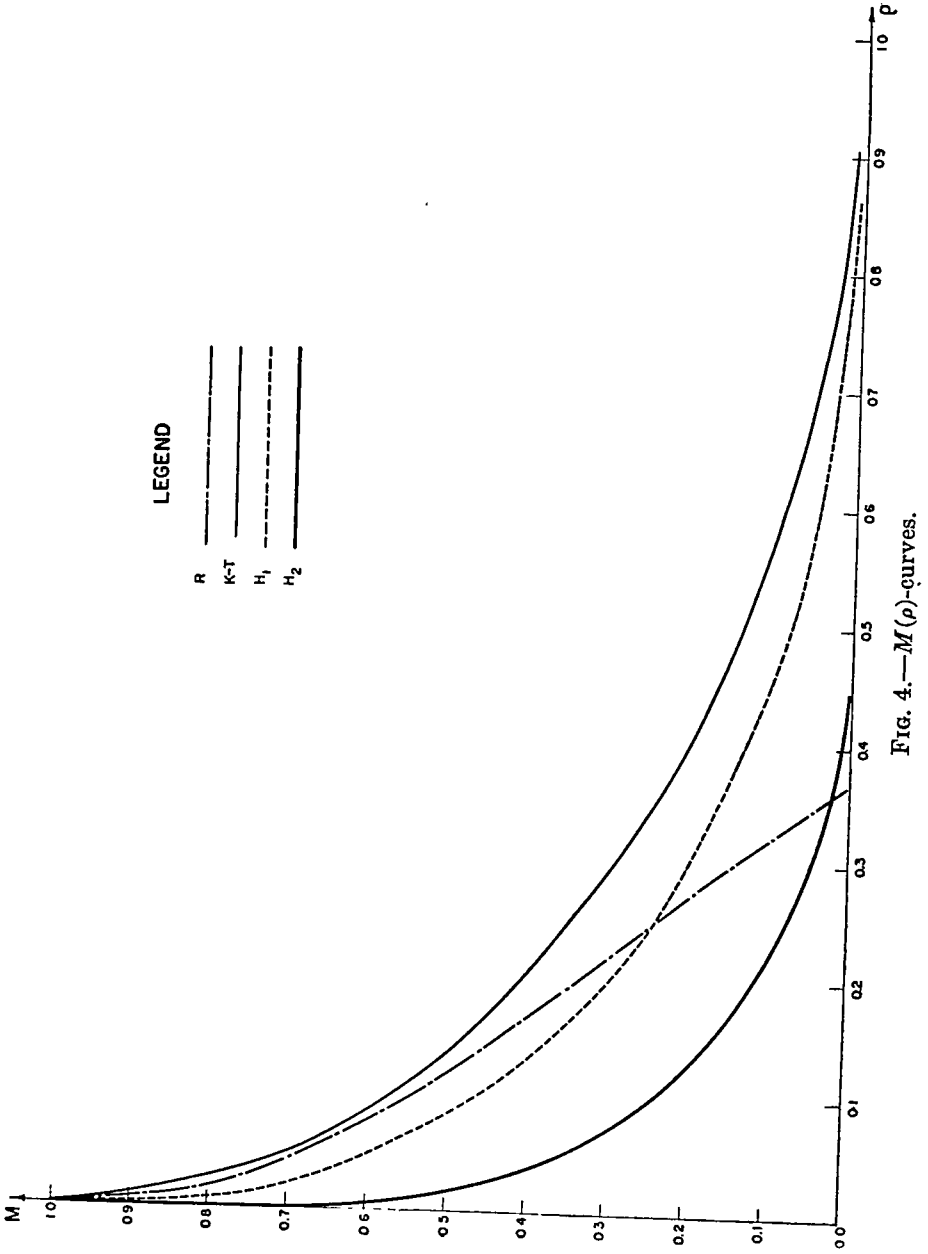

FIG. 4.—$M(\rho)$-curves.

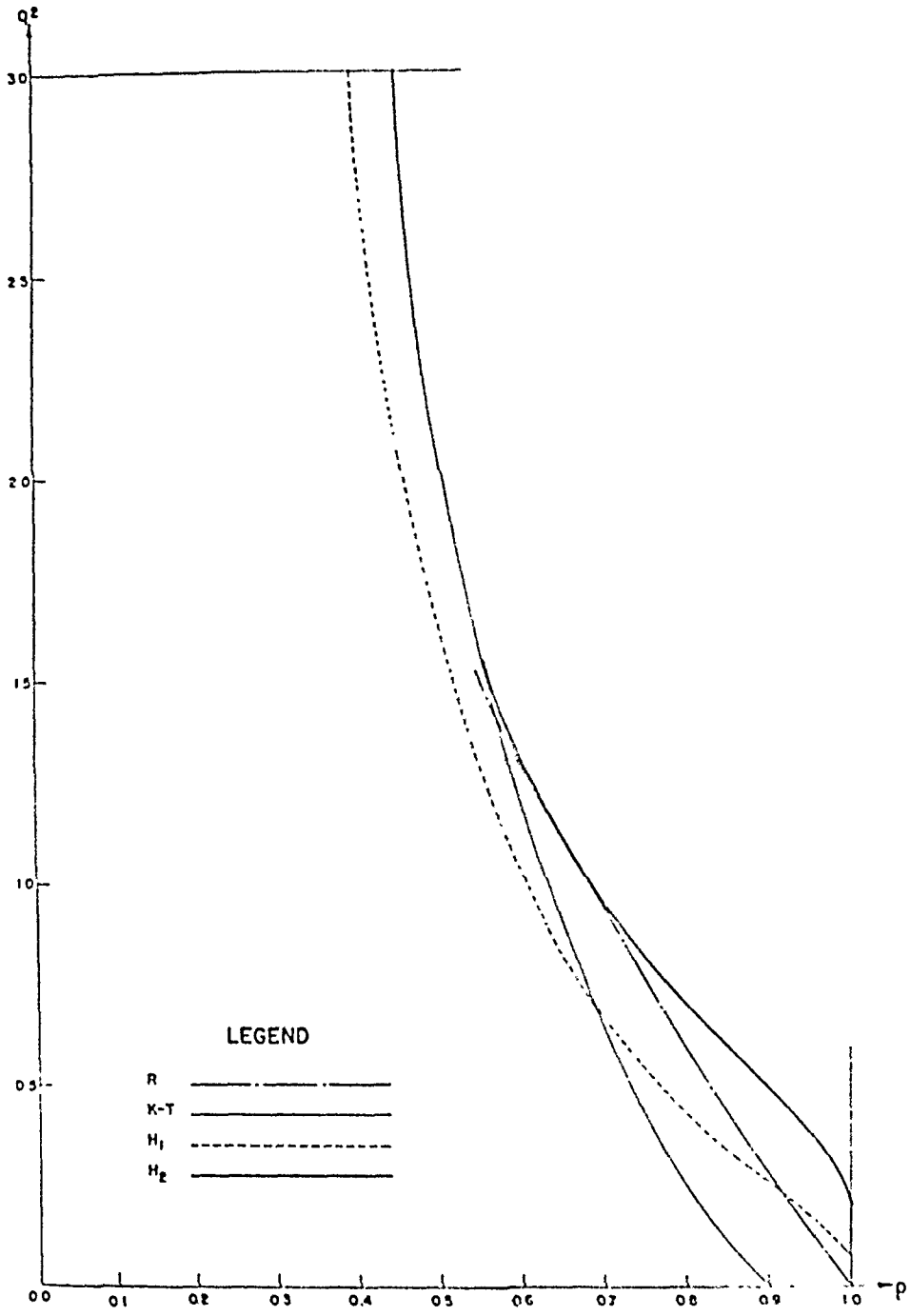

FIG. 5.—$q(\rho)$-curves.

higher degree of freedom in the general case will lead to an improvement of the approximation.

We have carried out the integration of (7) for two different choices of the parameters γ and δ. In the first case we have chosen a small δ in order to stay in the neighborhood of the Kármán-Tsien approximation. In this way, we studied the improvement of the approximation under variation of δ. In the second case, we chose the constant δ so that the asymptotic behavior of the hypothetical gas at Mach number 1 is that of a real isentropic gas.

The equations connecting p, q, M, and ρ are now the following:

$$M^2 = 1 - \rho^2 z^2, \tag{4''}$$

$$q^2 = q_0{}^2 \cdot exp\left[-2\int_1^\rho x^{-1}M(x)^{-2}dx\right], \tag{3''}$$

$$p = 1 + q_0{}^2 \int_1^\rho M(x)^{-2} \cdot exp\left[-2\int_1^x y^{-1}M(y)^{-2}dy\right]dx. \tag{2''}$$

By integrating (7), we obtain z as a function of ρ and, therefore, (2''), (3''), and (4'') give a representation of p, q, M as functions of ρ. The new arbitrary constant of integration, q_0, defines the minimum velocity of the fluid.

A. In the first case, we chose $\delta = \frac{1}{14}$. Equation (7) then becomes

$$\frac{dz}{d\rho} = Dz^{-5}(1 - z^2\rho^2)^{-1} \qquad \text{with} \qquad D = 2\rho\gamma^{\frac{1}{\delta}} = \frac{1}{7}\gamma^{14}. \tag{8}$$

Substituting $L = z^2$, we obtained

$$\frac{dL}{d\rho} = 2DL^{-2}(1 - \rho^2 L)^{-1} \tag{9}$$

and integrated this equation numerically. We chose the constant $D = 0.105$ in order to get a good agreement for smaller Mach numbers. The constant $q_0{}^2$ in (3'') was chosen more or less arbitrarily; we had only to provide for a small value of the minimal velocity q_0 and we took $q_0 = 0.265$.

B. While in our first example we tried to obtain a good approximation to a real gas for smaller Mach numbers, in our second example we wanted to give a model gas that behaves like a real one at the point $M = 1$.

Replacing, as we did in section I.4, $(1 - M^2)^{\frac{1}{2}}$ by T, we obtain from (4) and (5) in the case of a real gas

$$\rho = [\tfrac{1}{2}(\kappa + 1) - \tfrac{1}{2}(\kappa - 1)T^2]^{-\frac{1}{\kappa-1}}, \tag{10}$$

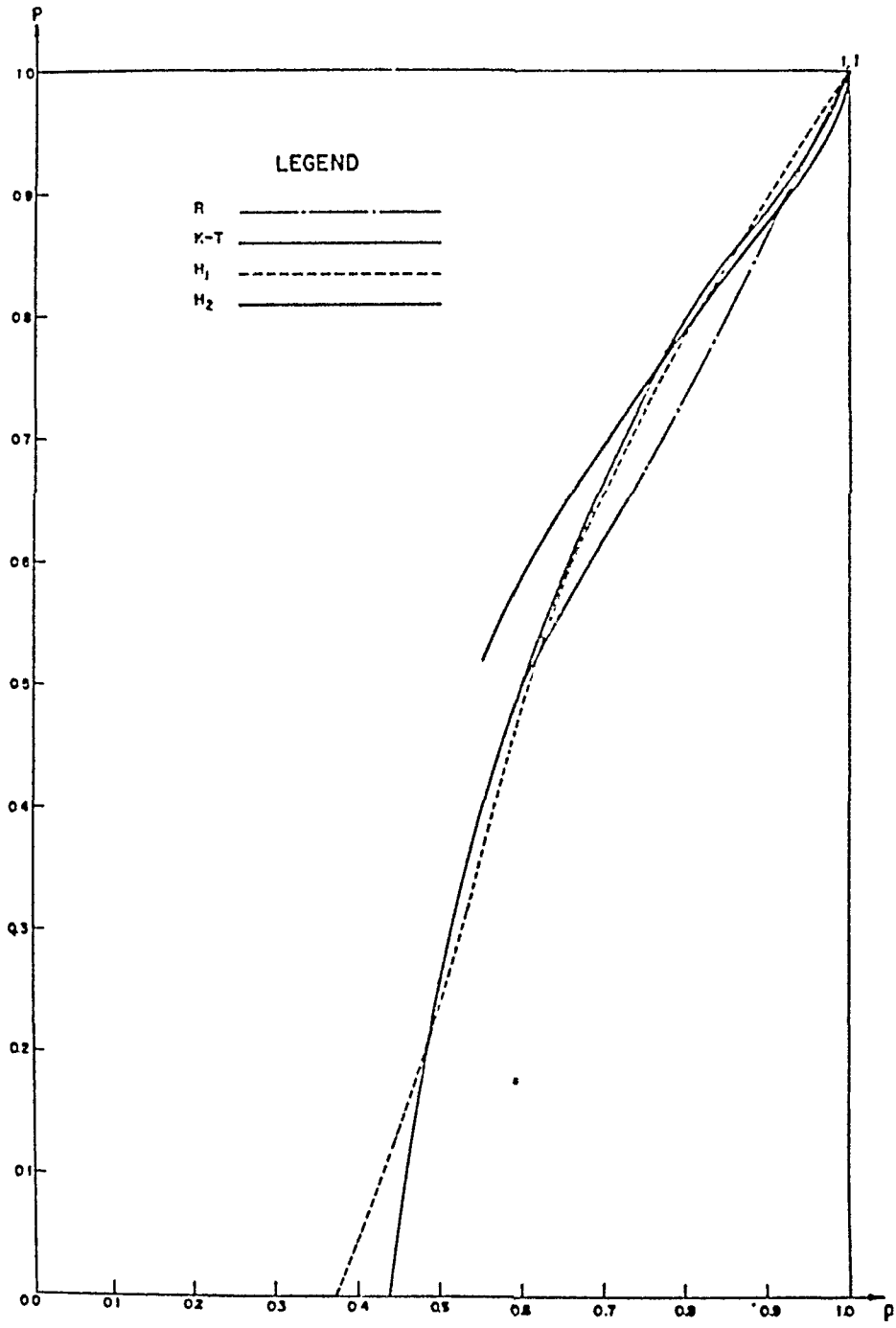

FIG. 6.—$p(\rho)$-curves.

$$z = T\rho^{-1} = T[\tfrac{1}{2}(\kappa + 1) - \tfrac{1}{2}(\kappa - 1)T^2]^{\frac{1}{\kappa-1}}. \tag{11}$$

On the other hand, we derive from (I.4.12)

$$\lambda = \tfrac{1}{3}(h^2 - 1)T^3 + \cdots \qquad h^2 = (\kappa - 1)(\kappa + 1)^{-1} = \tfrac{1}{6}. \tag{12}$$

Hence, we have for small values of λ the development

$$T = [\tfrac{1}{3}(1 - h^2)]^{-\frac{1}{3}}|\lambda|^{\frac{1}{3}} + \cdots \tag{13}$$

and, substituting this in (11), we obtain

$$z = [\tfrac{1}{3}(1 - h^2)]^{-\frac{1}{3}}|\lambda|^{\frac{1}{3}} \cdot [\tfrac{1}{2}(\kappa + 1)]^{\frac{1}{\kappa-1}} + \cdots = K|\lambda|^{\frac{1}{3}} + \cdots \tag{14}$$

If we want to obtain in (6) a choice of parameters that leads to the asymptotic behavior of the real gas for $M = 1$, *i.e.*, $\lambda = 0$, a comparison of (6) with (14) suggests the value $\delta = \frac{1}{6}$. One might even try to compute the value of γ from the known constant K; however, we found it more convenient to choose γ so as to yield a good fitting of the two curves compared.

For $\delta = \frac{1}{6}$, (7) takes the form

$$\frac{dz}{d\rho} = Dz^{-1}(1 - z^2\rho^2)^{-1},$$

or, substituting again $L = z^2$,

$$\frac{dL}{d\rho} = 2D(1 - L\rho^2)^{-1}. \tag{15}$$

We fixed γ so that $D = \frac{1}{3}\gamma^6 = 0.606$. This choice leads to curves that fit the corresponding curves for a real gas quite well for higher Mach numbers. This time, we chose the minimum velocity $q_0 = 0.471$, in order to get a good correspondence near $M = 1$. In particular, we wish to point out the behavior of the new p, ρ-curve, which runs nearly parallel to the curve for the real gas in the interval $0.93 \leq M \leq 1$.

Bibliography

1. BERGMAN, S., Zur Theorie der Funktionen, die eine lineare partielle Diffgl. befriedrigen I, *Réc. Math. Moscou*, vol. 2 Nouvelle Série (1937), pp. 1169–1198.
2. ———, Linear operators in the theory of partial diff. equations, *Trans. Am. Math. Soc.*, vol. 53, 1943, pp. 130–155.
3. ———, Certain classes of analytic functions of two real variables and their properties, *Trans. Am. Math. Soc.*, vol. 57, 1945, pp. 299–331.

4. ———, The hodograph method in the theory of compressible fluids. Supplement to *Fluid Dynamics* by von Mises and Friedrichs, Brown University, Providence, R.I., 1941–42.
5. ———, A formula for the stream function of certain flows, *Proc. Natl. Acad. Sci. U.S.*, 29, 1943, pp. 276–281.
6. ———, Two dimensional flows of compressible fluids, *Natl. Advisory Comm. Aeronaut.*, Tech. Notes: No. 972, 1945, No. 973, 1945, No. 1018, 1946, No. 1096, 1946.
7. ———, Two dimensional subsonic flows of a compressible fluid and their singularities, *Trans. Am. Math. Soc.*, vol. 61, 1947, pp. 452–498.
8. ———, Two dimensional transonic flow patterns and their properties, *Amer. J. Math.* (to appear).
9. Bergman, S., Greenstone, L., Epstein, B., Isaacs, R., Numerical Determination . . . of an Integral Operator in the Theory of Compressible Fluids, *J. Math. Phys.*, vol. 26, 1947, pp. 1–9, 165–181, 195–222 and vol. 27, 1948 (to appear).
10. Chaplygin, S. A., *On gas jets*, *Sci. Ann. Imp. Univ. Moscow, Phys.-Math. Div. Pub.* No. 21, 1904. Eng. trans. by M. H. Slud., 1944, Brown University, Providence, R.I., also *N.A.C.A. Tech. Mem.* No. 1063, 1944.
11. von Kármán, Th., Compressibility Effects in Aerodynamics, *J. Aeronaut. Sci.*, vol. 8, No. 9, July 1941, pp. 337–356.
12. Tsien, Hsue-Shen, Two-dimensional subsonic flow of compressible fluids, *J. Aeronaut. Sci.*, vol. 6, No. 10, Aug. 1939, pp. 399–407.

Author Index

Numbers in parentheses are reference numbers. They are included to assist in locating references in which the author's names are not mentioned in the text. *Example:* Bass, J., 38(96), *89*, indicates that this author's article is reference 96 on page 38. Numbers in italics refer to the page at the end of the chapter on which the reference is listed.

Numbers in bold-face type refer to the pages of the chapter written by the author mentioned. *Example:* Geiringer, H., **201–248** indicates that this author wrote the chapter included in pages 201–248.

Subject Index

V

W

Z